

**On relations of anisotropy and linear inhomogeneity using
Backus average, 1-D tomography and two-parameter
velocity inversion**

by

©Md Abu Sayed

A Dissertation submitted to the School of Graduate Studies in partial fulfillment of the
requirements for the degree of

Master of Science

Department of Earth Sciences

Memorial University of Newfoundland

July 2019

St. John's

Newfoundland

Abstract

We divide this thesis into three major parts.

In the first part, we study three velocity models and corresponding traveltimes to obtain the inhomogeneity and anisotropy of a medium by comparing them to the field data. We derive an analytical relation that relates the linear inhomogeneity of a layered medium to the anisotropy parameter in an equivalent medium. For the analytic ease, we consider the P and S wave velocity gradients to be equal. We relax this constraint in the third part of the thesis, where the velocity gradients are independent of each other. We find that the obtained value of the anisotropy in the equivalent medium is in the same order of magnitude as the inhomogeneity parameter from the linearly inhomogeneous and elliptically anisotropic medium. This statement encourages us to do further investigation on the more general relationship between the inhomogeneity and anisotropy parameters in an equivalent medium.

In the second part, we develop a 1-D travelttime tomography method to calculate the velocity of a medium. We use the results of 1-D tomography to obtain linear inhomogeneity parameters in a specific layer. To get the trustworthiness of the method, we perform several synthetic experiments. We show that the inverted model parameters are reasonably accurate and stable. To examine the results of linear inhomogeneity parameters using a different method, we also develop an inversion method based on a two-parameter velocity model.

Finally, we apply both the methods to Vertical Seismic Profile (VSP) data and do a study comparing their results.

In the third part, we derive an analytical relationship between the anisotropy, characterized by the Thomsen [1986] parameters, and the linear inhomogeneity parameters, which forms a system of three equations for nine unknowns. To obtain well-posedness, we constrain the problem by considering two seismological methods, 1-D tomography and two-parameter methods, applied to field data. Lastly, we compare the results that come from the application of each method to the analytical relationship, for a particular region of interest, to assess the validity of the theoretical relationship.

Acknowledgments

Firstly, I want to thank my supervisor Michael A. Slawinski for his guidance, encouragement, and support throughout my degree program at Memorial University.

I have also received valuable feedback from my supervisory committee member Roger Mason. I am grateful to the comments I receive from my thesis reviewer Zvi Koren. I also wish to acknowledge proofreading support of David Dalton. I also wish to thank my group members Theodore Stanoev, Izabela Kudela, Filip Adamus and Ayiaz Kaderali. I also wish to acknowledge communications with Colin Farquharson, Charles Hurich, and Alison Malcolm.

I also thank IHS Energy for donating the digital well data. I also would like to acknowledge the Canada-Newfoundland and Labrador Offshore Petroleum Board (C-NLOPB) for providing the digital VSP data. Many thanks go to Peter Bruce for his technical assistance on collecting the data.

I thank my mother, brothers and late father for their support throughout my life.

This research was performed in the context of The Geomechanics Project supported by Husky Energy. Also, this research was partially supported by the Natural Sciences and Engineering Research Council of Canada, grant 238416-2013, and by the Polish National Science Center under contract No. DEC-2013/11/B/ST10/0472.

I also gratefully thank the School of Graduate Studies for their financial support.

Table of Contents

Abstract	ii
Acknowledgments	iv
Contents	v
List of Tables	ix
List of Figures	x
List of Symbols	xi
1 Introduction and Overview	1
1.1 Introduction	1
1.2 Research overview	2
1.3 Literature review	3
1.4 Data set	5
2 On traveltime-model comparisons	7
2.1 Introduction	7
2.2 Problem description	7
2.3 Velocity models	9

2.3.1	Case one: $ab\chi$ model	9
2.3.2	Case two: Backus model	14
2.3.3	Anisotropy and inhomogeneity relation	17
2.3.4	Case three: Green-river shale model	21
2.4	Numerical results	23
2.4.1	Travelttime: Model results	23
2.4.2	Travelttime as average velocity: Analytical results	25
2.4.3	Travelttime comparisons: Numerical results	26
2.5	Normal Moveout (NMO) velocity using Backus average and Dix equation .	27
2.6	Conclusion	29
2.A	30
2.A.1	Fermat's Travelttime	30
2.A.2	Travelttime using three-parameter velocity model	35
2.A.3	Backus Travelttime	37
2.A.4	Travelttime in Shale	44
2.A.5	Anisotropy and inhomogeneity relation	51
2.A.6	Travelttime using average velocities	56
2.A.7	NMO velocity	57
3	On 1-D travelttime tomography and two-parameter velocity inversion	63
3.1	Introduction	63
3.2	Method developement	64
3.2.1	Solution of the ray equation in vertically inhomogeneous media . .	64
3.2.2	Discretizing the forward model for 1-D tomography	68
3.2.3	Development of the inversion method for 1-D tomography	69
3.2.4	A review of Levenberg-Marquardt Method	70
3.3	Synthetic experiments	74

3.3.1	Test of the noise and the number of data points	74
3.3.2	Test of the model parameters a and b	80
3.4	1-D tomography : Application in real data	86
3.5	Conclusion	90
3.A	90
3.A.1	1-D tomography : synthetic data	90
3.A.2	1-D tomography : real data	107
3.A.3	ab model inversion : real data	118
4	On relations of anisotropy and linear inhomogeneity	121
4.1	Introduction	121
4.2	Equivalent medium parametrization	122
4.2.1	Elasticity parameters in TI media	122
4.2.2	Anisotropy parameters	127
4.2.3	Total differentials of anisotropy parameters	129
4.3	Methods for well-posedness	130
4.3.1	1-D tomography	130
4.3.2	ab model	131
4.4	Numerical search	131
4.4.1	Restrictions	131
4.4.2	Calculations	133
4.5	Discussion	135
4.6	Conclusion and future work	136
4.A	Tables	137
5	Summary and conclusion	152
5.1	Summary and future work	152

5.2 Significant findings	153
Overall Bibliography	154
A Data: Mizzen O-16	159
A.1 Traveftime data [C-NLOPB]	159
A.2 Well log data [Enachescu, 2011]	161

List of Tables

1.1	Well log data	5
1.2	Checkshot data	6
2.1	Comparison of the traveltimes	24
2.2	Comparison of average traveltimes	27
3.1	Varying noise and number of data points	75
3.2	Varying model parameters	80
3.3	Comparison of inversion methods	87
4.1	VSP results	137
4.2	<i>ab</i> -model results	144

List of Figures

2.1	Relationship between anisotropy and inhomogeneity	22
3.1	Travetime inversion: variation of noise and number of data points, $v_{in} = v_{true} \pm 20$	76
3.2	Velocity inversion : variation of noise and number of data points, $v_{in} = v_{true} \pm 20$	77
3.3	Travetime inversion: variation of noise and number of data points, $v_{in} = v_{true} \pm 40$	78
3.4	Velocity inversion : variation of noise and number of data points, $v_{in} = v_{true} \pm 40$	79
3.5	Traveltime inversion for different velocity gradients, $v_{in} = v_{true} \pm 30 (ms^{-1})$	82
3.6	Velocity model for different velocity gradients, $v_{in} = v_{true} \pm 30 (ms^{-1})$	83
3.7	Traveltime inversion for different velocity gradients, $v_{in} = v_{true} \pm 60 (ms^{-1})$	84
3.8	Velocity model for different velocity gradients, $v_{in} = v_{true} \pm 60 (ms^{-1})$	85
3.9	Traveltime inversion for different velocity gradients, $v_{in} = v_{true} \pm 60 (ms^{-1})$	88
3.10	Velocity model for different velocity gradients, $v_{in} = v_{true} \pm 60 (ms^{-1})$	89
4.1	Triple point solution	132
4.2	Solutions of 1-D tomography and <i>ab</i> -model for all dataset	135
4.3	Solutions of 1-D tomography and <i>ab</i> -model for a specific range of dataset .	136

List of Symbols

Abbreviations

TI	Transversely Isotropic
VSP	Vertical Seismic Profile
KB	Kelly Bushing
TVD	Total Vertical Depth

Mathematical relations and operators

=	equality
\equiv	equivalence
$:=$	definition
\approx	approximation
\bar{f}	average of f
\times	product
$\int dx$	integration operator with respect to x
$\frac{d}{dx}$	differential operator with respect to x

Physical quantities

Greek letters

χ	Anisotropy parameter
ρ	mass density
ϑ	wavefront angle
θ	ray angle
δ	Thomsen parameter
ε	Thomsen parameter
γ	Thomsen parameter
λ	Levenberg-Marquardt damping parameter

Roman letters

t	travelttime
a_p	velocity for P-wave at top of the layer
a_s	velocity for S-wave at top of the layer
b_p	velocity gradient for P-wave
b_s	velocity gradient for S-wave
w	weight function
z	layer thickness
l'	averaging width
c_{ijkl}	density normalized elasticity tensor in \mathbb{R}^3

Chapter 1

Introduction and Overview

1.1 Introduction

To obtain information on physical properties of the matter, such as oil and gas in a sedimentary basin, we rely mostly on indirect observations of the object lying below the surface. One of the essential indirect methods is known as the seismic method, in which we gather information about the earth's interior through the use of seismic waves and the knowledge of how these waves travel. The speed of seismic waves is affected by the properties of the material; the stiffness of the material is one of the properties that affect the speed of these waves. Measuring the time it takes for individual waves to arrive at a seismometer after an earthquake or an explosion can indicate specific properties of the materials that the waves pass through. When a wave reaches a layer with a different composition, it changes its direction and speed.

To gain information on the shape of the layers, the structure of the subsurface, and the mechanical properties of the rocks, we may use different velocity models. Looking into the properties of the material allows us to detect the presence of a particular object, such

as fluid. To get an accurate measurement of the fluid location, we require a velocity model that takes into account the effects of both inhomogeneity and anisotropy of a medium. In this thesis, we have three main objectives: 1) Develop mathematical tools based on three velocity models that can be used to obtain linear inhomogeneity parameters of a medium. 2) Derive a general relationship between linear inhomogeneity and anisotropy parameters in an equivalent transversely isotropic (TI) medium. 3) Examine the solution of this analytical relationship based on field data.

1.2 Research overview

In this thesis, we present three projects that are complementary to each other.

In the first project, we consider the following three cases that describe the velocity model in terms of inhomogeneity and anisotropy parameters: 1) A medium is linearly inhomogeneous and elliptically anisotropic. 2) A medium is homogeneous and transversely isotropic (TI). 3) A medium is homogeneous and TI with scaled elasticity parameters. In case one, to obtain the model parameters, we calculate the traveltimes using *P*-wave velocity. In case two, we use both *P*- and *S*-wave velocities and obtain model parameters in an equivalent medium. Here we consider the medium to be thinly layered, and the velocity to be constant in each layer. The velocities are used from a well log that is discussed in section 1.4.

For a nearly vertical log, the Backus average can be applied to thin isotropic layers to obtain the elasticity parameters of an equivalent TI medium. We assume the wavelength is sufficiently large that we can take the average of any interval we wish, including the entire medium. We also consider the elastic behaviour of Green-River-Shale to be sufficiently similar for both field and laboratory measurements to allow a meaningful comparison. We find a significant discrepancy in values in the second and the third cases (Section 2.3.4). We

also derive an analytical relation between linear inhomogeneity and anisotropy in equivalent TI medium. Based on the analytical relation, we show that the anisotropy in the equivalent medium is a measure of the inhomogeneity of the layered medium.

In the second project, we develop a 1-D tomography method based on the Levenberg-Marquardt [Pujol, 2007] algorithm. The inversion method is tested through synthetic experiments. Application of the method to the VSP data allows us to obtain the inhomogeneity parameters of a medium, which we use to constrain the problem in the third project of this thesis.

In the third project, we derive a system of equations which relate the linear inhomogeneity to the anisotropy parameters in an equivalent TI medium. We show that the system has three independent equations and the number of unknown parameters may reduce to four. To get well-posedness, we use one of the inhomogeneity parameters from the 1-D tomography and solve the system of equations. We repeat the calculation and obtain the solution for the system of equations based on the inhomogeneity parameters from two-parameter velocity inversion.

1.3 Literature review

Our work relies on the assumption that a linear increase of velocity with depth is a reasonable model for seismic studies in sedimentary basins. One of the first people who examined that was Slotnick [1936], a Russian-born American mathematician and geophysicist. Among others, his linear model was studied by Epstein and Slawinski [1999], Slawinski and Slawinski [1999] and Slawinski et al. [2004]. Also, extended discussions and derivations of equations that we use in our work are in Slawinski [2015] and Slawinski [2018]. Slotnick's [Slotnick, 1936] unbounded linear velocity model, where he specifies the ve-

locity at the upper interface and the vertical velocity gradient, may be more suitable for a thin layer. The following works also consider the unbounded velocity model: Al-Chalabi [1997a], Al-Chalabi [1997b], Chapman and Keers [2002], Faust [1951] and Faust [1953]. Several other works consider asymptotically bounded velocity models; among others, it is worth mentioning the following works: Muskat [1937], Ravve and Koren [2006a] and Ravve and Koren [2006b].

For the concept of equivalent media, we follow the work of Backus [1962]. His article was based on the works of the following researchers: Rudzki [1911]*, Riznichenko [1949], Haskell [1953], White and Angona [1955], Postma [1955], Rytov [1956], Helbig [1958], and Anderson [1961]. Schoenberg and Muir [1989] extend the Backus work and develop a method for a medium composed of general anisotropic layers. Kumar [2013] developed the averaging technique for monoclinic layers with vertical plane of symmetry.

The Backus average has been a significant topic of study for Michael A. Slawinski and The Geomechanics Project. Their work on Backus average is exhibited in, among others, Bos et al. [2017] and Dalton and Slawinski [2016]. Another book worth mentioning is the one written by Slawinski [2018], which examines the Backus average in Chapter 4. To scale the elasticity parameters in shale, we use the Green-river shale values from Thomsen [1986].

For the development of the forward model in 1-D tomography, we follow the work of Slawinski [2015] and Červený [2001]. For the 1-D travelttime tomography, we use the approach taken by Zelt and Smith [1992] and Pujol et al. [1985]. The inversion method is based on the Levenberg-Marquardt algorithm, which is described as by Levenberg [1944] and Marquardt [1963]. The comparison between the Levenberg-Marquardt method and other least square methods is described by Pujol [2007].

*This publication, which was presented to the Academy of Sciences at Cracow in 1911, has been translated with comments by Klaus Helbig and Michael A. Slawinski; it appears as Rudzki [2003].

The relationship between inhomogeneity and anisotropy parameter for the alternating in-homogeneous layers is studied by Adamus et al. [2018]. In this thesis, we derive a general relation between linear inhomogeneity to anisotropy in equivalent TI medium.

1.4 Data set

Herein, the VSP and well log data used was obtained from the Mizzen O-16 discovery well, which is a site in the Flemish Pass basin and was drilled in 2009 by Statoil [Enachescu, 2011], as discussed in Abu Sayed and Stanoev [2019]. The well log data used is supplied by the IHS energy; the data description is supplied in Ikon Science and Nalcor Energy [2016]. We collect P - and S -wavespeed measurements for depths of at depth 1865.00 m to 2648.60 m .

The checkshot (VSP) data is provided by the Canada-Newfoundland & Labrador Offshore Petroleum Board [C-NLOPB]. Therein, the traveltimes data corresponds to a single source and multiple receivers. The source is placed at a 26.50 m offset, and the receivers are located along a the vertical axis, starting at a depth of 1865 m and ending at 2650 m . We consider our last receiver at depth 2650m so that the velocity inversion from traveltimes matches the region where the well log data are recorded. The descriptions of the data are given in Tables 1.1 and 1.2, which are collected with the permission of the Petroleum Development Section of Natural Resources, Government of Newfoundland and Labrador.

Field	Well	KB (m)	TVD (m)	Water depth (m)	Spud date	Log data
Mizzen	O-16	21.15	3797	1095	2008	✓

Table 1.1: Well log data

Field	Well	Offset (m)	TVD (m)	Water depth (m)	Spud date	Checkshot
Mizzen	O-16	26.50	3797	1095	2009	✓

Table 1.2: Checkshot data

Chapter 2

On traveltime-model comparisons

2.1 Introduction

In this chapter, we study the effects of inhomogeneity and anisotropy of a well log using three different velocity models. The first is a linearly inhomogeneous and elliptically anisotropic model, known as $ab\chi$. The second is an equivalent transversely isotropic medium obtained by the Backus average. The third accommodates the scarcity of horizontal well log information by scaling from known values of shale. To increase model reliability, we derive analytical expressions relating inhomogeneity and anisotropy of the first and second models. For each model, we calculate traveltimes for increasing offsets and compare their results.

2.2 Problem description

Here, we study the inhomogeneity and anisotropy of a well log using three different velocity models. In the first, we study a three-parameter velocity model, namely $ab\chi$, where

inhomogeneity is a linear function of depth and anisotropy is an elliptical function of the direction of propagation. Parameters a and b describe the inhomogeneity and χ describes the difference between horizontal and vertical speeds. To estimate the values of the three parameters, we minimize the misfit between the model traveltimes and the traveltimes for the P wave based on the measured velocities in a borehole. To calculate traveltimes from velocity data, we assume that the medium is multilayered and isotropic, and that the well log speeds represent the velocity of the layers.

In the second, we calculate traveltimes using a four-parameter velocity model for a homogenized medium of isotropic layers. To do so, we use the Backus [1962] average, which is an elegant method of producing equivalent parameters for a thinly layered medium. The homogenization method can be applied to random layering and random layer thicknesses. We assume that the physical properties of the individual layers are homogenous and isotropic. To obtain the elasticity parameters for the equivalent transversely isotropic (TI) medium, we use the P - and S -wave speeds from well log information. Through a derived analytical relation, we compare the effects of the linear inhomogeneity of the first model to the anisotropy parameter in the equivalent TI medium.

In the third, we scale the elasticity parameters of the equivalent TI medium to account for the scarcity of horizontal velocity information, using known values of Green-River-shale [Thomsen, 1986]. We calculate traveltimes corresponding to the scaled TI medium. In all the three cases, we calculate traveltimes only for P wave velocities. To find a relation of the velocity models to average velocities, we calculate traveltimes along vertical axis based on mean, average and root-mean-square velocities, and compare them to the model results.

2.3 Velocity models

2.3.1 Case one: $ab\chi$ model

Let us consider a model of linear inhomogeneity and elliptical velocity dependence, where a and b describe a linear increase of velocity with depth, z , and χ quantifies the difference between horizontal and vertical velocities, v_h and v_v . The traveltimes of the signal, wavefront velocity, wavefront angle, ray velocity, and ray angle are all governed by the eikonal equation [e.g., Rogister and Slawinski, 2005]. The subsequent raytracing equations are derived from Hamilton's equations, which result in a conserved quantity, which is the ray parameter, p . Consequently, using Legendre's transformation, we may explicitly express the ray angle in terms of the wavefront angle, which is a unique property of elliptical anisotropy [Slawinski, 2015, Section 14.3]. Legendre transformation allows us to replace a function by a new function that depends on partial derivatives of the original function with respect to original independent variables [Slawinski, 2015, Section 14.3]. In seismology, we replace the ray-theory Hamiltonian by the ray-theory Lagrangian through Legendre transformation

$$\mathcal{L}(\mathbf{x}, \dot{\mathbf{x}}) = \sum_{j=1}^3 p_j(\mathbf{x}, \dot{\mathbf{x}}) \dot{x}_j - \mathcal{H}(\mathbf{x}, \mathbf{p}(\mathbf{x}, \dot{\mathbf{x}})), \quad (2.1)$$

where \mathcal{L} is referred to as the ray-theory Lagrangian corresponding to a given ray-theory Hamiltonian \mathcal{H} , and $p_j(\mathbf{x}, \dot{\mathbf{x}})$ is a solution of

$$\dot{x}_j = \frac{\partial \mathcal{H}(\mathbf{x}, \mathbf{p})}{\partial p_j}, \quad j \in \{1, 2, 3\}. \quad (2.2)$$

The velocity dependence with respect to depth is

$$v = a + bz, \quad (2.3)$$

whereas anisotropy is quantified by a dimensionless parameter

$$\chi := \frac{v_h^2 - v_v^2}{2v_v^2}; \quad (2.4)$$

if $v_h = v_v$ then $\chi = 0$ and the medium is isotropic. Slawinski et al. [2004] show that χ permits a more accurate fit between the real and modelled traveltimes in comparison to the two-parameter model, consisting of just a and b .

The ray velocity in such a medium is [Slawinski, 2015, p. 523–524]

$$V(\theta, z) = (a + bz) \sqrt{\frac{1 + 2\chi}{1 + 2\chi \cos^2 \theta}}, \quad (2.5)$$

where θ is the ray angle, a and b are constants and their units are the units of velocity and the reciprocal of time, respectively. The phase velocity and phase angle relation is [Slawinski, 2015, p. 357]

$$v(\vartheta, z) = (a + bz) \sqrt{(1 + 2\chi) \sin^2 \vartheta + \cos^2 \vartheta}. \quad (2.6)$$

The relationships between the phase and ray angle for elliptical anisotropy is [Slawinski, 2015, p. 361]

$$\tan \theta = (1 + 2\chi) \tan \vartheta. \quad (2.7)$$

The traveltime of a signal between a source and a receiver for a downgoing wave is [Slawinski et al., 2004]

$$t = \frac{1}{b} \ln \left(\frac{a + bz}{a} \frac{1 + \sqrt{1 - a^2 p^2 (1 + 2\chi)}}{1 + \sqrt{1 - (a + bz)^2 p^2 (1 + 2\chi)}} \right), \quad (2.8)$$

whereas for both downgoing and upgoing directions [Slawinski, 2015, p. 367]

$$t = \frac{\tanh^{-1} \left[p b x - \sqrt{1 - p^2 a^2 (1 + 2\chi)} \right] + \tanh^{-1} \sqrt{1 - p^2 a^2 (1 + 2\chi)}}{b}. \quad (2.9)$$

In equations (2.8) and (2.9), the expression for the ray parameter, p , is

$$p = \frac{2x}{\sqrt{[x^2 + (1 + 2\chi)z^2] [(2a + bz)^2 (1 + 2\chi) + b^2 x^2]}}. \quad (2.10)$$

If we deal with a signal between a source and a receiver along the acquisition surface, then the signal is two-way. In that case, we cannot apply equation (2.8) to obtain direct traveltimes. The reason behind not getting direct travel time from equation (2.8) is that the formulation requires the ray to travel only with increasing depth. In our study, the sources are located at the surface and the receivers are located at the borehole, and for the velocity inversion we only take first arrival traveltimes which travels one-way. To calculate velocities between two depths h_1 and h_2 , we replace a by $a + bh_1$ and z by $h_2 - h_1$ in equations (2.8) and (2.9). The rays in such a medium are the arcs of ellipses [Epstein and Slawinski, 1999]. As a consequence of lateral homogeneity, the ray parameter, equation (2.10), is constant. For the traveltime calculation at zero orientation angle in Table 2.1, we use expression (2.8). Expression (2.9) cannot be used for a signal propagating along $x = 0$; in such a case the numerator of expression (2.9) is $-\infty + \infty$. However, expressions (2.8) and (2.9) produce equal traveltime results for any other source-receiver orientation angles*, up to a critical angle. The critical angle is

$$\theta_c = \arcsin(v_1/v_2), \quad (2.11)$$

where v_1 and v_2 are the signal propagation phase speeds in the upper and lower medium,

*Throughout this chapter, we refer to “source-receiver orientation angle” as “orientation angle”

respectively.

The $ab\chi$ model requires traveltime information in order to numerically fit values for a , b and χ . To satisfy this requirement, we calculate Fermat's travelttime for rays transmitted from source to receiver through isotropic layers at regularly increasing orientation-angle intervals. The speed of the ray within each of the layers, which is provided by well log information, is considered constant. Since p is constant, we invoke Snell's law, where

$$p = \frac{\sin \theta_1}{v_1} = \frac{\sin \theta_2}{v_2} = \dots = \frac{\sin \theta_n}{v_n}. \quad (2.12)$$

Using (2.12), the horizontal distance covered by a ray segment in the first layer is

$$x_1 = h_1 \tan \theta_1 = h_1 \frac{\sin \theta_1}{\cos \theta_1} = \frac{h_1 p v_1}{(1 - p^2 v_1^2)^{\frac{1}{2}}}, \quad (2.13)$$

where θ_1 is the takeoff angle. The corresponding travelttime is

$$t_1 = \frac{R_1}{v_1} = \frac{h_1}{v_1 \cos \theta_1} = \frac{h_1}{v_1 (1 - p^2 v_1^2)^{\frac{1}{2}}}. \quad (2.14)$$

Hence, the horizontal distance and the travelttime for i -th layer are

$$x_i = \frac{H_i p v_i}{(1 - p^2 v_i^2)^{\frac{1}{2}}} \quad \text{and} \quad t_i = \frac{H_i}{v_i (1 - p^2 v_i^2)^{\frac{1}{2}}}. \quad (2.15)$$

Summing over the i -th layer, total horizontal distance and travelttime are

$$x = \sum_{i=1}^n x_i = \sum_{i=1}^n \frac{H_i p v_i}{(1 - p^2 v_i^2)^{\frac{1}{2}}}, \quad (2.15)$$

$$t = \sum_{i=1}^n t_i = \sum_{i=1}^n \frac{H_i}{v_i (1 - p^2 v_i^2)^{\frac{1}{2}}}. \quad (2.16)$$

We use equation (2.15) to calculate the takeoff angle for a given orientation angle. Then, we use equation (2.16) to calculate traveltimes based on the calculated takeoff angle. It is worth mentioning that in this multilayer model, we consider the velocity to be a function of vertical depth. It is possible to apply a limiting (continuous) case, where the number of layers is infinite, and the thickness of each layer is infinitesimal only if the velocity increases along with the depth. In the case of decreasing velocity, the signal reaches the critical angle with the increase of number of layers. A similar method is applied by Pujol et al. [1985] to calculate traveltimes in a vertically inhomogeneous multilayer medium.

To calculate numerically the $ab\chi$ model parameters, we sample a random a , b and χ with which we calculate a traveltimes, $t(a, b, \chi)$, using formula (2.8), that corresponds to the Fermat's traveltimes, t_F , for some orientation angle. Here, we explain the steps we implement to calculate Fermat's traveltimes from the well log speeds. In general, the well log data contains high-frequency contents, which restricts the ray to travel from a source to a receiver with higher offset. Otherwise, the ray hits the critical angle even with a lower take-off angle. To obtain sufficient amount of traveltimes data based on the assumptions that the medium is composed of isotropic thin layers, we must remove the high-frequency contents from the data set. We apply a weighted average in every twelve consecutive data points and obtain a smoother velocity profile, which allows us to calculate Fermat's traveltimes with higher offsets. The calculation is shown in appendix 2.A.1.

Lastly, to perform minimization (2.17) between the traveltimes, we use speeds of P waves from a vertical well log. We minimize the sum of the squared difference of the j -th orientation angle, i.e.,

$$\sum_{j=1}^N (t_F - t(a, b, \chi))_j^2 \rightarrow \min. \quad (2.17)$$

We subdivide the region of interest into N layers and calculate Fermat's traveltime for one hundred sources regularly incrementing by 0.5° from 0° to 50° of orientation angle. The

estimated values are

$$a = 2.0841 \times 10^3 \text{ ms}^{-1}, \quad b = 0.3980 \text{ s}^{-1}, \quad \chi = 0.00024; \quad (2.18)$$

since the region of interest is comprised of isotropic layers, we deem the value of χ to be reasonable and, hence, the $ab\chi$ model to be valid.

2.3.2 Case two: Backus model

Since our well log information is vertical, we may perform the Backus [1962] average to deduce macroscopic information of its mechanical properties. Following the definition of Backus [1962, Section 3], the average of a function $f(x_3)$ of width ℓ' is the moving average given by

$$\bar{f}(x_3) = \int_{-\infty}^{\infty} w(\zeta - x_3) f(\zeta) d\zeta, \quad (2.19)$$

where the properties of the weighting function are

$$w(x_3) \geq 0, \quad w(\pm\infty) = 0, \quad \int_{-\infty}^{\infty} w(x_3) dx_3 = 1,$$

$$\int_{-\infty}^{\infty} x_3 w(x_3) dx_3 = 0, \quad \int_{-\infty}^{\infty} x_3^2 w(x_3) dx_3 = (\ell')^2,$$

and x_3 is the depth. The result of performing average (2.19) on isotropic layers results is a homogeneous TI medium, where

$$c_{1111}^{\overline{\text{TI}}} = \left(\frac{c_{1111} - 2c_{2323}}{c_{1111}} \right)^2 \left(\frac{1}{c_{1111}} \right)^{-1} + \left(\frac{4(c_{1111} - c_{2323})c_{2323}}{c_{1111}} \right), \quad (2.20a)$$

$$c_{1133}^{\text{TI}} = \overline{\left(\frac{c_{1111} - 2c_{2323}}{c_{1111}} \right)} \overline{\left(\frac{1}{c_{1111}} \right)}^{-1}, \quad (2.20\text{b})$$

$$c_{3333}^{\text{TI}} = \overline{\left(\frac{1}{c_{1111}} \right)}^{-1}, \quad (2.20\text{c})$$

$$c_{2323}^{\text{TI}} = \overline{\left(\frac{1}{c_{2323}} \right)}^{-1}. \quad (2.20\text{d})$$

Herein, we state only the four elasticity parameters that pertain to quasi-*P*-wave propagation; the two remaining parameters [e.g., Slawinski, 2018, Section 4.2.2] are required for *qSV*- and *qSH*-wave propagation, which is beyond the scope of this work. Within a TI medium, the *qP* wavefront velocity [e.g., Slawinski, 2015, p. 403] is

$$v_{qP}(\vartheta) = \sqrt{\frac{(c_{3333}^{\text{TI}} - c_{1111}^{\text{TI}})n_3^2 + c_{1111}^{\text{TI}} + c_{2323}^{\text{TI}} + \sqrt{\Delta}}{2\rho}}, \quad (2.21\text{a})$$

where

$$\Delta \equiv \left[(c_{1111}^{\text{TI}} - c_{2323}^{\text{TI}})(1 - n_3^2) - (c_{3333}^{\text{TI}} - c_{2323}^{\text{TI}})n_3^2 \right]^2 + 4(c_{2323}^{\text{TI}} + c_{1133}^{\text{TI}})^2 n_3^2 (1 - n_3^2), \quad (2.21\text{b})$$

$n_3 = \cos \vartheta$ and the wavefront angle, ϑ , is the angle between the wavefront normal and vertical axis. The wavefront has a radius of $1/v(\vartheta)$. However, for any given point along the wavefront, the normal is the ray velocity, $V(\vartheta)$. To calculate the traveltimes of a ray in a homogenous TI medium, we require the distance travelled, s , and the ray velocity, V , i.e., for a trajectory set by ray angle θ

$$t(\theta) = \frac{s(\theta)}{V(\theta)}. \quad (2.22)$$

Herein, the distance is a straight line between source and receiver whereas ray velocity is [Slawinski, 2015, equation (8.4.9)]

$$V(\vartheta) = \sqrt{(v(\vartheta))^2 + \left(\frac{\partial v(\vartheta)}{\partial \vartheta}\right)^2}, \quad (2.23)$$

where v is phase velocity (2.21a). To calculate both v and V , we require ϑ , however, we only know the ray angle, θ . The relation between θ and ϑ is [e.g., Slawinski, 2015, equation (8.4.12)]

$$\tan \theta = \frac{\tan \vartheta + \frac{1}{v} \frac{\partial v}{\partial \vartheta}}{1 - \frac{\tan \vartheta}{v} \frac{\partial v}{\partial \vartheta}}. \quad (2.24)$$

From relation (2.24), it is not possible to calculate analytically ϑ for any given θ , apart from cases of elliptical velocity dependence. As stated by Slawinski [2015, p. 355], for a given θ , the expression for the ϑ can be explicitly solved for θ if and only if v^2 is quadratic in the components of a vector that specifies the orientation of the wavefront. In general, the expression for ϑ of a quasi- P wave in equation (2.24) does not have the quadratic form in v .

In an analogous manner to formula (2.4), where

$$v_h = \sqrt{c_{1111}^{\overline{II}}} \quad \text{and} \quad v_v = \sqrt{c_{3333}^{\overline{II}}}, \quad (2.25)$$

the anisotropy of the Backus medium is

$$\chi_{\overline{II}} := \frac{c_{1111}^{\overline{II}} - c_{3333}^{\overline{II}}}{2 c_{3333}^{\overline{II}}}. \quad (2.26)$$

To calculate traveltimes for increasing orientation angles, we perform the Backus average

on the well log information and obtain

$$c_{1111}^{\overline{TI}} = 5.0194, \quad c_{1133}^{\overline{TI}} = 3.5239, \quad c_{3333}^{\overline{TI}} = 4.9908, \quad c_{2323}^{\overline{TI}} = 0.7188, \text{ and } \chi_{\overline{TI}} = 0.0028, \quad (2.27)$$

where the elasticity parameters are density scaled and multiplied by $10^6 \text{ m}^2 \text{ s}^{-2}$.

2.3.3 Anisotropy and inhomogeneity relation

An analytical relation of inhomogeneity and anisotropy is shown in Adamus et al. [2018] for a periodic, isotropic, two-layered medium. Herein, we derive an analytical relation between anisotropy parameter, $\chi_{\overline{TI}}$, of the Backus model, and linear inhomogeneity parameter, b , also known as vertical velocity gradient, of the $ab\chi$ model, for many layers. To do so, we recall equations (2.20a) and (2.20c), which are

$$c_{1111}^{\overline{TI}} = \left(\frac{c_{1111} - 2c_{2323}}{c_{1111}} \right)^2 \left(\frac{1}{c_{1111}} \right)^{-1} + \left(\frac{4(c_{1111} - c_{2323})c_{2323}}{c_{1111}} \right)$$

and

$$c_{3333}^{\overline{TI}} = \left(\frac{1}{c_{1111}} \right)^{-1},$$

and equation (2.26). Furthermore, we assume that our $ab\chi$ model is for isotropic layers and, hence, we recall velocity (2.3); namely, for both P and S waves,

$$v_P = a_P + b_P z \quad \text{and} \quad v_S = a_S + b_S z. \quad (2.28)$$

Thus,

$$\begin{aligned} c_{3333}^{\overline{\text{II}}} &= \overline{\left(\frac{1}{c_{1111}}\right)}^{-1} = \overline{\left(\frac{1}{v_P^2}\right)}^{-1} = \left(\frac{1}{h_2 - h_1} \int_{h_1}^{h_2} \frac{1}{(a_P + b_P z)^2} dz\right)^{-1} \\ &= (h_2 - h_1) \left(\int_{h_1}^{h_2} (a_P + b_P z)^{-2} dz \right)^{-1}. \end{aligned}$$

To perform the integration, we apply u substitution for $a_P + b_P z$, which gives $dz = \frac{du}{b_P}$, and change the limits from h_1 to $a_P + b_P h_1$ and h_2 to $a_P + b_P h_2$, which results in

$$\begin{aligned} c_{3333}^{\overline{\text{II}}} &= (h_2 - h_1) \left(\int_{a_P + b_P h_1}^{a_P + b_P h_2} u^{-2} \frac{du}{b_P} \right)^{-1} = (h_2 - h_1) \left(\frac{-u^{-1}}{b_P} \Big|_{a_P + b_P h_1}^{a_P + b_P h_2} \right)^{-1} \\ &= (h_2 - h_1) (-b_P) \left((a_P + b_P h_2)^{-1} - (a_P + b_P h_1)^{-1} \right)^{-1} \\ &= \frac{(h_2 - h_1) b_P}{(a_P + b_P h_1)^{-1} - (a_P + b_P h_2)^{-1}}. \end{aligned} \tag{2.29}$$

In a similar manner, for equation (4.3a),

$$c_{1111}^{\overline{\text{II}}} = \overline{\left(\frac{c_{1111} - 2c_{2323}}{c_{1111}}\right)}^2 \left(\frac{1}{c_{1111}}\right)^{-1} + \overline{\left(\frac{4(c_{1111} - c_{2323})c_{2323}}{c_{1111}}\right)}.$$

For the first term,

$$\begin{aligned} \overline{\left(\frac{c_{1111} - 2c_{2323}}{c_{1111}}\right)} &= \frac{1}{h_2 - h_1} \int_{h_1}^{h_2} \frac{(a_P + b_P z)^2 - 2(a_S + b_S z)^2}{(a_P + b_P z)^2} dz \\ &= \frac{1}{h_2 - h_1} (h_2 - h_1) - \frac{2}{h_2 - h_1} \int_{h_1}^{h_2} \frac{(a_S + b_S z)^2}{(a_P + b_P z)^2} dz \\ &= 1 - \frac{2I_1}{h_2 - h_1}, \end{aligned} \tag{2.30}$$

where

$$I_1 = \int_{h_1}^{h_2} \frac{(a_S + b_S z)^2}{(a_P + b_P z)^2} dz.$$

After integration,

$$\begin{aligned} I_1 &= \frac{h_2 b_S^2}{b_P^2} - \frac{h_1 b_S^2}{b_P^2} \\ &+ \frac{\ln(a_P + h_1 b_P) (2a_P b_S^2 - 2a_S b_P b_S)}{b_P^3} - \frac{\ln(a_P + h_2 b_P) (2a_P b_S^2 - 2a_S b_P b_S)}{b_P^3} \\ &+ \frac{a_P^2 b_S^2 - 2a_P a_S b_P b_S + a_S^2 b_P^2}{b_P (h_1 b_P^3 + a_P b_P^2)} - \frac{a_P^2 b_S^2 - 2a_P a_S b_P b_S + a_S^2 b_P^2}{b_P (h_2 b_P^3 + a_P b_P^2)}. \end{aligned}$$

For the last term,

$$\begin{aligned} \left(\frac{4(c_{1111} - c_{2323})c_{2323}}{c_{1111}} \right) &= \frac{4}{h_2 - h_1} \int_{h_1}^{h_2} \frac{(a_P + b_P z)^2 (a_S + b_S z)^2}{(a_P + b_P z)^2} dz - \frac{4}{h_2 - h_1} \int_{h_1}^{h_2} \frac{(a_S + b_S z)^4}{(a_P + b_P z)^2} dz \\ &= \frac{4}{h_2 - h_1} \int_{h_1}^{h_2} (a_S + b_S z)^2 dz - \frac{4}{h_2 - h_1} \int_{h_1}^{h_2} \frac{(a_S + b_S z)^4}{(a_P + b_P z)^2} dz \\ &= \frac{4I_2}{h_2 - h_1} - \frac{4I_3}{h_2 - h_1}, \end{aligned} \tag{2.31}$$

where

$$I_2 = \int_{h_1}^{h_2} (a_S + b_S z)^2 dz = -\frac{h_1^3 b_S^2}{3} - h_1^2 a_S b_S - h_1 a_S^2 + \frac{h_2^3 b_S^2}{3} + h_2^2 a_S b_S + h_2 a_S^2,$$

and

$$I_3 = \int_{h_1}^{h_2} \frac{(a_S + b_S z)^4}{(a_P + b_P z)^2} dz.$$

After integration,

$$\begin{aligned}
I_3 = & h_2 \left(\frac{2a_p \left(\frac{2a_p b_S^4}{b_P^3} - \frac{4a_S b_S^3}{b_P^2} \right)}{b_P} - \frac{a_p^2 b_S^4}{b_P^4} + \frac{6a_S^2 b_S^2}{b_P^2} \right) \\
& - h_1 \left(\frac{2a_p \left(\frac{2a_p b_S^4}{b_P^3} - \frac{4a_S b_S^3}{b_P^2} \right)}{b_P} - \frac{a_p^2 b_S^4}{b_S^4} + \frac{6a_S^2 b_S^2}{b_S^2} \right) \\
& + h_1^2 \left(\frac{a_p b_S^4}{b_P^3} - \frac{2a_S b_S^3}{b_P^2} \right) - h_2^2 \left(\frac{a_p b_S^4}{b_P^3} - \frac{2a_S b_S^3}{b_P^2} \right) \\
& + \frac{\ln(a_p + h_1 b_P) (4a_p^3 b_S^4 - 12a_p^2 a_S b_P b_S^3 + 12a_p a_S^2 b_P^2 b_S^2 - 4a_S^3 b_P^3 b_S)}{b_P^5} \\
& - \frac{\ln(a_p + h_2 b_P) (4a_p^3 b_S^4 - 12a_p^2 a_S b_P b_S^3 + h_2 12a_p a_S^2 b_P^2 b_S^2 - 4a_S^3 b_P^3 b_S)}{b_P^5} \\
& - \frac{h_1^3 b_S^4}{3b_P^2} + \frac{h_2^3 b_S^4}{3b_P^2} \\
& + \frac{a_p^4 b_S^4 - 4a_p^3 a_S b_P b_S^3 + 6a_p^2 a_S^2 b_P^2 b_S^2 - 4a_p a_S^3 b_P^3 b_S + a_S^4 b_P^4}{b_P (h_1 b_P^5 + a_p b_P^4)} \\
& - \frac{a_p^4 b_S^4 - 4a_p^3 a_S b_P b_S^3 + 6a_p^2 a_S^2 b_P^2 b_S^2 - 4a_p a_S^3 b_P^3 b_S + a_S^4 b_P^4}{b_P (h_2 b_P^5 + a_p b_P^4)}.
\end{aligned}$$

Substituting equations (4.7), (4.5) and (2.31), we obtain

$$c_{1111}^{\overline{\text{II}}} = \left(1 - \frac{2I_1}{h_2 - h_1} \right)^2 c_{3333}^{\overline{\text{II}}} + \frac{4I_2}{h_2 - h_1} - \frac{4I_3}{h_2 - h_1}. \quad (2.32)$$

Inserting equations (4.7) and (2.32) into (2.26), we get

$$\chi_{\overline{\text{II}}, b} := \frac{\left(1 - \frac{2I_1}{h_2 - h_1} \right)^2 c_{3333}^{\overline{\text{II}}} + \frac{4I_2}{h_2 - h_1} - \frac{4I_3}{h_2 - h_1} - c_{3333}^{\overline{\text{II}}}}{2c_{3333}^{\overline{\text{II}}}}. \quad (2.33)$$

Since the well log information is for shale, we assume that, with increasing depth, the

measure of inhomogeneity changes equally for P and S waves, i.e.,

$$b_P = b_S = b.$$

Therefore, b is a representative measure of inhomogeneity for both P and S waves. Further, for some depth, $h_2 - h_1$, relation (2.33) produces a value for $\chi_{\overline{\text{TI}},b}(a_P, a_S, b)$. Recalling the layer of interest in Section 2.3.1,

$$a_P = 2084.09 \text{ ms}^{-1}, \quad a_S = 752.95 \text{ ms}^{-1}, \quad b = 0.3980 \text{ s}^{-1}, \quad \text{we obtain } \chi_{\overline{\text{TI}},b} = 0.0018, \quad (2.34)$$

which is in same order of magnitude with the measure of $\chi_{\overline{\text{TI}}} = 0.0028$ in values (2.27). Thus, the theoretical measure of anisotropy derived from $ab\chi$ -model parameters, $\chi_{\overline{\text{TI}},b}$, under the assumption of linear inhomogeneity, isotropic layers and near-vertical well log information, provides a reasonable correlation between inhomogeneity among isotropic layers and anisotropy of their equivalent medium—using the Backus average.

Hence, we claim that the measure of anisotropy of the Backus average—of isotropic layers—is a solely a measure of the inhomogeneity among its constituent layers. Figure 2.1 illustrates the relationship, wherein a steady change in anisotropy in equivalent TI medium occurs with the increase of linear inhomogeneity.

However, we conjecture that relation (2.33) might lose its validity for well log information deviating away from the vertical.

2.3.4 Case three: Green-river shale model

The anisotropy of our equivalent TI medium is, in values (2.27), $\chi_{\overline{\text{TI}}} = 0.0028$. This value, however, corresponds to well log information, which is measured solely along the vertical

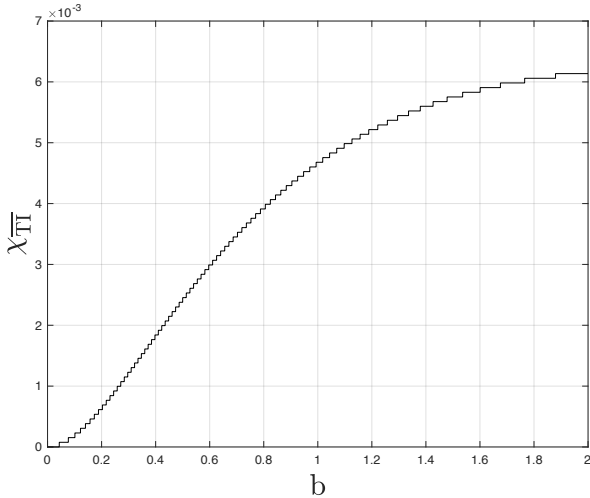


Figure 2.1: Relationship between anisotropy parameter, $\chi_{\overline{\text{TI}}}$, in equivalent TI media and inhomogeneity parameter, b , in linearly inhomogeneous media

axis. Knowing that $\chi_{\overline{\text{TI}}}$ is proportional to the difference of horizontal and vertical velocities, we deduce that $\chi_{\overline{\text{TI}}}$, which is valid within the equivalent Backus model, is, in fact, too small to be a representative measure of the anisotropy of shale.

To accommodate this discrepancy, we use known values of Green River shale [Thomsen, 1986], which are representative of a typical shale, to scale the elasticity parameters corresponding to horizontal wavespeeds within the equivalent TI medium. Recalling Slawinski [2015, Exercise 9.2], the elasticity parameters, therein, are

$$c_{1111}^{\text{TI}} = 3.13, \quad c_{1133}^{\text{TI}} = 0.34, \quad c_{3333}^{\text{TI}} = 2.25, \quad c_{2323}^{\text{TI}} = 0.65, \quad c_{1212}^{\text{TI}} = 0.88; \quad (2.35)$$

the elasticity parameters are not density scaled and multiplied by 10^{10} N m^{-2} . Using values (2.35), and maintaining consistent ratios, we calculate

$$c_{1111}^{\overline{\text{TI}}^*} = c_{3333}^{\overline{\text{TI}}} \frac{c_{1111}^{\text{TI}}}{c_{3333}^{\text{TI}}} = 6.9427 \quad \text{and} \quad c_{1133}^{\overline{\text{TI}}^*} = c_{3333}^{\overline{\text{TI}}} \frac{c_{1133}^{\text{TI}}}{c_{3333}^{\text{TI}}} = 0.75417, \quad (2.36)$$

where both are multiplied by $10^6 \text{ m}^2 \text{ s}^{-2}$. In equation (2.36), the numerical value for $c_{3333}^{\overline{\text{TI}}^*}$ is calculated using equation (2.20c). We use well log data to calculate this parameter. We calculate

$$\chi_{\overline{\text{TI}}}^* = \frac{c_{1111}^{\overline{\text{TI}}^*} - c_{3333}^{\overline{\text{TI}}}}{2 c_{3333}^{\overline{\text{TI}}}} = 0.1956.$$

Although $\chi_{\overline{\text{TI}}}^*$ is a contrived value, it increases the trustworthiness of the measure of anisotropy in the equivalent Backus medium by providing a “realistic” difference between horizontal and vertical P wave velocities.

2.4 Numerical results

2.4.1 Traveltime: Model results

Let us compare traveltimes for increasing orientation angles within the $ab\chi$, Backus and Green River shale models, whose relevant parameters are given by (2.18), (2.27) and (2.36).

For the first model, we consider velocity for which inhomogeneity is linear with depth, a and b , and anisotropy, χ , is elliptical. For the second model, we consider velocity in an equivalent medium resulting from the Backus average of isotropic layers. For the third model, we consider velocity in a medium whose horizontal velocities are scaled in accordance with known Green River shale values.

There are certain limitations that we impose on our model by putting different assumptions in each case which, as a result, do not allow us to extract certain information from the real media. For instance, when a ray travels from a source to a receiver with a greater orientation angle, the lateral inhomogeneities along the horizontal direction affect the traveltimes in a real medium. As a result, we cannot measure the lateral inhomogeneities of the medium in our models.

θ (in $^\circ$)	t_F	$t_{ab\chi}$	$t_{\overline{TI}}$	t_{TI}^*
0	0.3504	0.3504	0.3508	0.3508
15	0.3627	0.3627	0.3631	0.3454
30	0.4045	0.4045	0.4050	0.4025
45	0.4951	0.4950	0.4960	0.4938
60	0.6990	0.6989	0.7015	0.6693

Table 2.1: Comparison of the traveltimes for the same source-receiver configuration for the four models. Herein, the angle is calculated from the source-receiver geometry, such as $\theta = \arctan(x/z)$, where x is offset and z is depth. For $t_{\overline{TI}}$ and t_{TI}^* , it is the ray angle due to the straightness of rays in homogeneous models. For t_F and $t_{ab\chi}$, it is not the ray angle, since the orientation, and hence the angle, change along the ray. All the traveltimes are presented in seconds. The Matlab codes are provided in 2.A.

Also, in terms of comparing traveltimes between the first and other cases, we must keep in mind that, in the last two cases, the use of well log speeds for thin layers in the velocity model takes into account the fact that the inhomogeneities with depth could be in any order. On the other hand, in the first case, the medium is considered linearly inhomogeneous with depth. Therefore, should the medium possess a strong inhomogeneity with depth, the calculated traveltimes are expected to produce different results.

We recall the layer of interest and calculate traveltimes from the top of the layer, for increasing orientation angles, to the receiver. In Table 2.1, we cannot display an orientation angle of 75° since it is beyond the critical angle, which, up to the first decimal place, is $\theta_c = 70.4^\circ$. This value is obtained numerically using Fermat's traveltime formulation with a range of takeoff angles. For $\theta > \theta_c$, the receiver cannot be reached, therefore, θ_c restricts t_F .

$t_{ab\chi}$ is restricted by the limit of the downgoing signal. As indicated in Section 2.3.1, we search for a takeoff angle for which the traveltimes from expressions (2.8) and (2.9) begin to diverge. We calculate that this angle corresponds to $\theta > 74.9$, which means that beyond this angle a ray cannot reach the receiver without an upward segment.

$t_{\overline{\text{TI}}}$ and t_{TI}^* are not restricted, since they correspond to homogeneous media, wherein rays are straight. As shown in Table 2.1, $t_{\overline{\text{TI}}}$ and t_{TI}^* differ from one another due to the strength of anisotropy.

2.4.2 Traveltime as average velocity: Analytical results

Let us compare the traveltimes of Section 2.4.1 to average velocity. Herein, we conjecture that the traveltimes obtained using expression (2.8) or (2.9) correspond to [e.g., Slawinski and Slawinski, 1999, Appendix 1],

$$v_{\text{avg}} = \frac{\int_0^T V dt}{\int_0^T dt} = \frac{\int_0^z dz}{\int_0^z \frac{dz}{V}}.$$

In the case of a medium with the constant vertical velocity gradient, the average velocity is

$$v_{\text{avg}} = \frac{bz}{\ln \left| \frac{a+bz}{a} \right|}. \quad (2.37)$$

To calculate velocities between depth h_1 and h_2 , we replace a by $a + bh_1$ and z by $h_2 - h_1$ in equation (2.37). The traveltimes are

$$t_{\text{avg}} = \frac{h_2 - h_1}{v_{\text{avg}}}. \quad (2.38)$$

Using expression (2.37) in (2.38),

$$t_{\text{avg}} = \frac{1}{b} \ln \left| \frac{a + b h_2}{a + b h_1} \right|. \quad (2.39)$$

Along $x = 0$, between two depths h_1 and h_2 , the traveltime expression (2.8) for three-parameter model becomes

$$t = \frac{1}{b} \ln \left| \frac{a + b h_2}{a + b h_1} \right|. \quad (2.40)$$

Thus, we find that traveltimes expressions (2.38) and (2.40) are identical.

2.4.3 Traveltime comparisons: Numerical results

Let us compare the traveltimes to other measures of velocity. The definitions of mean and root-mean-square velocities are [e.g., Slawinski and Slawinski, 1999, Appendix 1]

$$v_{\text{mean}} = \frac{\int_0^z V dz}{\int_0^z dz} \quad \text{and} \quad v_{\text{rms}} = \sqrt{\frac{\int_0^T V^2 dt}{\int_0^T dt}} = \sqrt{\frac{\int_0^z V dz}{\int_0^z \frac{dz}{V}}}.$$

In the case of linearly inhomogeneous medium, these velocities, at depths 0 and z , are

$$v_{\text{mean}} = 1 + \frac{b}{a} z \quad \text{and} \quad v_{\text{rms}} = \sqrt{\frac{2abz + b^2z^2}{2 \ln \left| \frac{a + bz}{a} \right|}}. \quad (2.41)$$

To calculate the velocities between two depths, h_1 and h_2 , we replace a by $a + bh_1$ and z by $h_2 - h_1$ in equation (2.37). It is worth mentioning that there is a fundamental distinction between physical velocities (phase, group velocities, etc.) and velocity measures (mean, rms

velocities, etc.) [Margrave and Lamoureux, 2019]. The velocity measures are the quantities that are derived from the data analysis. They have the physical dimension of velocity, but they are related to physical velocities in some indirect fashion. It cannot be expected that a physical wave propagates at the speed of one of the velocity measures. However, using these measures facilitates the analysis of the velocity, which is fundamental to seismic processing. The corresponding traveltime measures are

$$t_{\text{mean}} = \frac{h_2 - h_1}{v_{\text{mean}}} \quad \text{and} \quad t_{\text{rms}} = \frac{h_2 - h_1}{v_{\text{rms}}}. \quad (2.42)$$

θ (in $^\circ$)	$t_{ab\chi}$	t_{mean}	t_{avg}	t_{rms}
0	0.3504	0.3498	0.3504	0.3501

Table 2.2: Traveltimes, in seconds, for wave propagation along vertical axis for depths 1865.00m to 2648.60m .

Table 2.2 illustrates numerically that $t_{ab\chi} = t_{\text{avg}}$ along $x = 0$, which is demonstrated analytically in expressions (2.39) and (2.40).

2.5 Normal Moveout (NMO) velocity using Backus average and Dix equation

By applying Backus average, we compute the vertical transverse anisotropy parameters corresponding to a stack of homogeneous layers. In this section we present the numerical results of the normal (compressional) moveout velocity of this effective medium [Tsvankin, 2001],

$$v_{nmo, \text{Backus}} = v_P \sqrt{1 + 2\delta}, \quad (2.43)$$

where $v_P = \sqrt{C_{3333}/\rho}$ is the vertical compressional velocity, C_{3333} is the stiffness tensor component, ρ is the medium density, and δ is the Thomsen anisotropy parameter. However, we consider the density normalized elasticity parameter to compute v_P . Thomsen anisotropy parameter is [Thomsen, 1986],

$$\delta = \frac{(C_{1133} + C_{2323})^2 - (C_{3333} - C_{2323})^2}{2C_{3333}(C_{3333} - C_{2323})}. \quad (2.44)$$

The effective normal moveout velocity [Dix, 1955] is,

$$v_{nmo,Dix} = \sqrt{\sum_{i=1}^n v_i^2 t_{0,i} / \sum_{i=1}^n t_{0,i}}, \quad (2.45)$$

where v_i is the velocity of the layer, known as interval velocity, $t_{0,i} = 2\Delta z_i/v_{0,i}$ is the two way vertical time, and Δz_i is the layer thickness. The Dix equation for interval velocity of n -th layer is,

$$v_n^2 = \frac{(v_{rms,n}^2 \sum_1^n t_{0,i} - v_{rms,n-1}^2 \sum_1^{n-1} t_{0,i})}{t_{0,n}}. \quad (2.46)$$

By applying equation (2.44) in equation (2.43) and using the well log data from Mizzen O-16, we obtain $v_{nmo,Backus} = 2220.97 \text{ ms}^{-1}$. Using equation (2.45), we obtain $v_{nmo,Dix} = 2238.55 \text{ ms}^{-1}$. The difference between the velocities from the two methods is 17.58 ms^{-1} .

To calculate NMO velocity using the Backus average for a linearly inhomogeneous medium, we need analytical expressions relating elasticity parameters of the Backus medium to linear inhomogeneity parameters of the linear medium. In this thesis, we derive analytical relations for $c_{1111}^{\overline{\text{TI}}}$ and $c_{3333}^{\overline{\text{TI}}}$ to obtain anisotropy parameter $\chi_B^{\overline{\text{TI}}}$. Similar approach can be taken to find the expressions for $c_{2323}^{\overline{\text{TI}}}$ and $c_{1313}^{\overline{\text{TI}}}$, which will allow us to obtain the Thomsen parameter δ in the Backus medium. As future work, we plan to work on the derivations

and retrieve values for NMO velocity for a linearly inhomogeneous medium using both the Backus average and Dix equation.

2.6 Conclusion

The inhomogeneity and anisotropy of a well log is examined using three different velocity models.

In Table 2.1, we tabulate the traveltimes from different velocity models and find that they are similar, which implies that, collectively, they effectively model geological phenomena. In addition, in Table 2.1, Fermat’s traveltimes are less than the Backus traveltimes, which supports the conjecture of Chapman [2014, Module 2]. Therein, he states that the resultant traveltimes through a TI medium that is long-wave-equivalent to a thinly layered isotropic medium—obtained by the Backus [1962] average—is, amazingly, the same result from high-frequency, multiple scattering theory.

In Table 2.2, we illustrate that the traveltimes for the $ab\chi$ model, $t_{ab\chi}$, is equal to the average traveltimes, t_{avg} , along $x = 0$, where the average traveltimes is defined by the average velocity. We conjecture that traveltimes from both velocities are equal for $x \neq 0$.

In Section 2.3.3, we relate analytically the anisotropy parameter of Section 2.3.2, $\chi_{\overline{\text{TI}}}$, and the inhomogeneity parameter, b , of Section 2.3.1. For the former, we calculate $\chi_{\overline{\text{TI}}} = 0.0028$. For the latter, we use Figure 2.1 to correlate $b = 0.40 \text{ s}^{-1}$ to the anisotropy value $\chi_{\overline{\text{TI}},b} = 0.0018$, which is closure to $\chi_{\overline{\text{TI}}}$. Based on these results, we conclude that the anisotropy of the Backus average of isotropic layers is possibly a measure of inhomogeneity.

Throughout our study, the borehole is nearly vertical and, thus, the well log speeds do not

contain horizontal information. In view of such scarcity of well log information, and that the anisotropy parameter is defined in terms of both horizontal and vertical speeds, we do not expect to obtain a reliable measure of anisotropy from the considered velocity models. To accommodate our restriction, we use known values from Green River shale to calculate $\chi_{\text{TI}}^* = 0.1956$, which is an anisotropy parameter for an equivalent TI medium with scaled elasticity parameters. The result indicates that, indeed, χ_{TI} does not represent a reliable measure of anisotropy.

In future work, to account for the discrepancy of anisotropy, we would require the velocity from cross well or traveltimes from walkaway VSP with higher offsets. In either case, the data consists of both horizontal and vertical information.

2.A

2.A.1 Fermat's Traveltime

```

1 %% Calculation of Fermat's Traveltime
2 close all; clear all ;clc
3 syms theta
4 [num1 ,txt1 ,raw1] = xlsread('mizzen_o_16_wl.xlsm'); % Well
   log data
5
6 d_in = num1(1035:8887, 1); % Provided in A.2 column 2
7
8 data_s_p = num1(1035:8887, 7); % slowness in us/m
9 v_p = (1./data_s_p).*1e6; % Provided in A.2 column 3
10

```

```

11 data_s_s = num1(1035:8887, 6); % slowness in us/m
12 v_s = (1./data_s_s).*1e6; % Provided in A.2 column 4
13 n = 12;
14 d = arrayfun(@(i) d_in(i), 1:n:length(d_in)-n+1)';
15 data_v_p = arrayfun(@(i) sum(d_in(i:i+n-1).'*v_p(i:i+n-1))/
    sum(d_in(i:i+n-1)), 1:n:length(v_p)-n+1)';
16
17 % the weighted averaged vector
18
19 n_p = length(data_v_p)-1;
20
21 %% Geometry
22 Depth_of_layer = d(1); % in m
23 Depth_of_receiver = d(end);
24 layer_thickness = (d(end) - d(1));
25 in_ang = (5)*pi/180;
26 S_N =length(in_ang);
27 M = 1;
28 offset = layer_thickness*tan(in_ang);
29
30 %% Variables from travel time data
31 rec_depth = d(end);
32 N = n_p; % Number of Layers
33
34 %%%%%%Similar_to_previous%%%%%
35 z_p = d;

```

```

36  for i = 1:N
37  d_z_p(i)= d(i+1)-d(i); % layer thickness
38  end
39  z_p = z_p.';
40  d_z_p = d_z_p.';
41  H = d_z_p;
42
43 %% Variables for initial velocity and ray parameter for P
        wave
44  v_o_true = data_v_p(1:(end-1),1);
45  x_obs = offset;
46
47
48  for i=1:S_N
49      for k=1:M
50          ray_p_o_i_true(k,i) = sin(theta)./ v_o_true(1,1);
51      end
52  end
53
54
55
56  for i=1:S_N
57      for k=1:M
58          for j = 1:N
59              x_jki_i_true(j,k,i) = (H(j)).*(sin(theta)./
v_o_true(1,1)).*v_o_true(j,1))./ ...

```

```

60          (1-(sin(theta)./ v_o_true(1,1)).^2.*v_o_true
61          (j,1).^2).^(.5); % in m
62      end
63  end
64
65 for i = 1:S_N
66     for k = 1:M
67         x_ki_true(k,i)=sum(x_jki_i_true(1:N,k,i)); % in m
68     end
69 end
70 dx_true = (x_obs - x_ki_true);
71 %%%%%%%%%%%%%%%%%%%%%%%%%%%%%%%%%%%%%%
72 for i = 1:S_N
73     theta_1(i) = vpasolve(dx_true(1,i) == 0, theta);
74 end
75 theta = theta_1;
76 %%%%%%%%%%%%%%%%%%%%%%%%%%%%%%%%%%%%%%here
77 for i=1:S_N
78     for k=1:M
79         ray_p_o_i_true(k,i) = sin(theta(k,i))./ v_o_true
80         (1,1);
81     end
82 end
83 for i=1:S_N

```

```

84     for k=1:M
85         for j = 1:N
86             t_jki_true(j,k,i) = H(j)./( v_o_true(j,1).* (1-
87                                         ray_p_o_i_true(k,i).* v_o_true(j,1)).^2 ).^(.5)
88             ); % in s
89         end
90     end
91     %%%%%% Calculation of T_true %%%%%%
92     for i = 1:S_N
93         for k = 1:M
94             t_ki_true(k,i)=sum( t_jki_true (1:N,k,i)); % in s
95         end
96     end
97     t_t = double(t_ki_true)

```

2.A.2 Traveltime using three-parameter velocity model

```
1 close all; clear all ;clc  
2  
3 offset = load('offset.mat'); % offset data obtained from  
Fermat_tt.m code  
4 offset = offset.offset;  
5  
6 t_data = load('t_t.mat'); % traveltime data obtained from  
Fermat_tt.m code  
7 t_data = t_data.t_t;  
8  
9 Depth_of_layer = 1865; % in m  
10 Depth_of_receiver = 2648.6; % in m  
11 z = Depth_of_receiver - Depth_of_layer;  
12 x = offset;  
13 t_d = t_data;  
14  
15 %% Application of Matlab built in Least Square algorithm  
16  
17 % Startup Values  
18 lb=[eps eps eps];  
19 ub=[inf inf inf];  
20 x0=[2e3 .4 1e-10];  
21  
22 fun = @(X) abchi_fn_1(X(1),X(2),X(3), z, x, t_d);
```

```

23
24 x = lsqnonlin(fun,x0,lb,ub)
25
26 a_p = x(1);
27 b_p = x(2);
28 chi = x(3);
29
30
31 function fun=abchi_fn_1(a_2, b_2, chi_2, z, x, t_d)
32
33 term_1 = 1+2.*chi_2;
34 term_2 = ((2.*a_2)+((b_2).*z)).^2;
35
36 p_d = sqrt((x.^2 + ((term_1).*z.^2)).*((term_2).* (term_1)+((b_2.^2).* (x.^2)) ));
37 p = (2.*x)./(p_d);
38
39 term_3 = a_2 + (b_2.*z);
40 term_4 = sqrt(1-(a_2.^2).* (p.^2).* (term_1));
41 term_5 = sqrt(1-(term_3.^2).* (p.^2).* (term_1));
42 t_time = (1./b_2).*log(((term_3).* (1+term_4))./(a_2.* (1+
term_5)));
43 fun = t_time - t_d;
44 end

```

2.A.3 Backus Traveltime

```
1 %% Calculation of Traveltime in equivalent TI media
2 close all; clear all ;clc
3 syms nu
4 [num1,txt1,raw1] = xlsread('mizzen_o_16_wl.xlsm'); % Well
   log data
5
6 % This is the layer we pick (depth 1865.00 m to 2648.60 m);
7
8 data_s_s = num1(1035:8871, 6); % slowness in us/m
9 data_v_s = (1./data_s_s).*1e6;
10 v_s = data_v_s;
11
12 err_free = v_s>-1;
13 err_free_n = find(err_free==1);
14 v_s = v_s(err_free_n(:)); % Provided in A.2 column 4
15
16
17 data_s_p = num1(1035:8871, 7); % slowness in us/m
18 data_v_p = (1./data_s_p).*1e6;
19 v_p = data_v_p;
20 v_p = v_p(err_free_n(:)); % Provided in A.2 column 3
21
22 z_p = num1(1035:8871, 1); %
23 z_p = z_p(err_free_n(:));
```

```

24 d = z_p; % Provided in A.2 column 2

25

26 n_p = size(v_p);
27 data_v_p_for_mid = v_p(2:(end-1),1);
28 C_1111 = data_v_p_for_mid.^2;

29

30 data_v_s_for_mid = v_s(2:(end-1),1);
31 C_2323 = data_v_s_for_mid.^2;

32

33

34 for i = 1:n_p-1
35 m_p(i) = d(i) + ((d(i+1)-d(i))/2);
36 end
37 t_t = m_p(end) - m_p(1);

38

39 for i = 1:n_p-2
40 d_d(i) = m_p(i+1)-m_p(i);
41 end

42

43 for i = 1:n_p-2
44 w_d(i) = d_d(i)/t_t;
45 term_1(i) = w_d(i).*((C_1111(i)-2.*C_2323(i))./C_1111(i));
46 term_2(i) = w_d(i).*(1./C_1111(i));
47 term_3(i) = w_d(i).*(4.*((C_1111(i)-C_2323(i)).*C_2323(i));
48 ./C_1111(i));

```

```

48 term_4 ( i ) = w_d( i ).*C_2323( i );
49 term_5 ( i ) = w_d( i ).*( 1 ./ C_2323( i )) ;
50 end
51 term_1 = sum( term_1 );
52 term_2 = sum( term_2 );
53 term_3 = sum( term_3 );
54 term_4 = sum( term_4 );
55 term_5 = sum( term_5 );
56
57 C_3333_TI = ( term_2 ).^(-1);
58 C_1111_TI = ( term_1 ).^2 .* ( term_2 ).^(-1) + term_3 ;
59 C_1133_TI = term_1 .* ( term_2 ).^(-1);
60 C_1212_TI = term_4 ;
61 C_2323_TI = ( term_5 ).^(-1);
62
63 C11 = C_1111_TI;
64 C13 = C_1133_TI;
65 C44 = C_2323_TI;
66 C33 = C_3333_TI;
67 C66 = C_1212_TI;
68
69 Chi_data = (C11 - C33)/(2*C33);
70
71 %% Geometry
72 Depth_of_layer = d(1); % in m
73 Depth_of_receiver = z_p(end); % in m

```

```

74 layer_thickness = Depth_of_receiver - Depth_of_layer;
75 theta = 30*pi/180;
76 X_cross = layer_thickness*tan(theta);
77 diag_dist = sqrt(layer_thickness^2 + X_cross^2);
78
79 %% Geometry ends
80
81 %% Calculation : ray angle to phase angle
82 c_1 = C33 - C11;
83 c_2 = C11 + C44;
84 c_3 = 2; % in nondensity scale , it becomes 2*rho
85 c_4 = C11 - C44;
86 c_5 = C33 - C44;
87 c_6 = 4*(C44 + C13)^2;
88
89 f_4 = (cos(nu))^2; % cos^2(nu)
90 f_4_prime = -sin(2*nu);
91
92 f_5_t1 = c_4*(1-f_4) - c_5*f_4;
93 f_5_t2 = c_6*f_4*(1-f_4);
94 f_5 = f_5_t1^2+f_5_t2; % Delta
95
96 f_1 = sqrt((c_1*f_4 + c_2 + sqrt(f_5))/c_3); %Phase velocity
. %%One error found in here f_4^2 was wrong
97 v = f_1;
98

```

```

99 % calculation of v_prime with respect to nu
100 sec_5 = c_6*f_4_prime - 2*c_6*f_4*f_4_prime;      % sec means
101 sections of an equation like terms in the equation
102 sec_4 = (2*(c_4*(1-f_4)-c_5*f_4))*(-c_4*f_4_prime - c_5*
103 f_4_prime);
104 sec_3 = (f_5^(-.5)/2)*(sec_4+sec_5);
105 sec_2 = 2*c_1*c_3^(-1)*f_4*f_4_prime;
106 sec_1 = ((c_1*f_4^2+c_2+sqrt(f_5))/c_3)^(-.5)*.5;
107 v_prime = sec_1*(sec_2+sec_3);

108
109
110 f_theta = tan(theta);
111 f_nu = tan(nu);
112 bottom = 1 - (f_nu*v_prime)/v;
113 top = (v_prime/v)+f_nu;

114 nu_res = vpasolve(f_theta*bottom - top == 0, nu)
115 nu_res = double(nu_res);
116
117 nu = nu_res;
118 f_nu = tan(nu);

119
120
121 f_4 = (cos(nu))^2; % cos^2(nu)
122 f_4_prime = -sin(2*nu);

```

```

123
124 f_5_t1 = c_4*(1-f_4) - c_5*f_4;
125 f_5_t2 = c_6*f_4*(1-f_4);
126 f_5 = f_5_t1^2+f_5_t2; % Delta

127
128 f_1 = sqrt((c_1*f_4 + c_2 + sqrt(f_5))/c_3); %Phase velocity
129 v = sqrt(C33);

130
131 % Getting ray velocity in in first way
132 V_ray_1 = v/(cos(theta-nu));
133 V_ray_1 = double(V_ray_1);

134
135
136 % Getting ray velocity in second way
137 sec_5 = c_6*f_4_prime - 2*c_6*f_4*f_4_prime; % sec means
           sections of an equation like terms in the equation
138 sec_4 = (2*(c_4*(1-f_4)-c_5*f_4))*(-c_4*f_4_prime-c_5*
           f_4_prime);
139 sec_3 = (f_5^(-.5)/2)*(sec_4+sec_5);
140 sec_2 = 2*c_1*c_3^(-1)*f_4*f_4_prime;
141 sec_1 = ((c_1*f_4^2+c_2+sqrt(f_5))/c_3)^(-.5)*.5;
142 v_prime = sec_1*(sec_2+sec_3);

143
144 V_ray_2 = sqrt(v^2+v_prime^2);
145 V_ray_2 = double(V_ray_2);

```

```
147 % Comparison  
148 delta_v_ray = V_ray_2 - V_ray_1  
149 delta_v_ray_to_v_p = V_ray_2 - v  
150  
151 % Calculation of traveltime in TI medium  
152 t_time = diag_dist/V_ray_2
```

2.A.4 Traveltime in Shale

```
1 %% Calculation of Traveltime for green river shale  
2  
3 close all; clear all ;clc  
4 syms nu  
5 [num1,txt1,raw1] = xlsread('mizzen_o_16_w1.xlsm'); % Well  
log data  
6  
7 % this is the layer we pick (depth 1865.00 m to 2648.60 m);  
8  
9 data_s_s = num1(1035:8871, 6); % slowness in us/m  
10 data_v_s = (1./data_s_s).*1e6;  
11 v_s = data_v_s;  
12  
13 err_free = v_s>-1;  
14 err_free_n = find(err_free==1);  
15 v_s = v_s(err_free_n(:));  
16  
17  
18 data_s_p = num1(1035:8871, 7); % slowness in us/m  
19 data_v_p = (1./data_s_p).*1e6;  
20 v_p = data_v_p;  
21 v_p = v_p(err_free_n(:));  
22  
23 z_p = num1(1035:8871, 1); %
```

```

24 z_p = z_p( err_free_n(:));
25 d = z_p;
26
27 n_p = size(v_p);
28 data_v_p_for_mid = v_p(2:(end-1),1);
29 C_1111 = data_v_p_for_mid.^2;
30
31 data_v_s_for_mid = v_s(2:(end-1),1);
32 C_2323 = data_v_s_for_mid.^2;
33
34
35 for i = 1:n_p-1
36 m_p(i) = d(i) + ((d(i+1)-d(i))./2);
37 end
38 t_t = m_p(end) - m_p(1);
39
40 for i = 1:n_p-2
41 d_d(i) = m_p(i+1)-m_p(i);
42 end
43
44 for i = 1:n_p-2
45 w_d(i) = d_d(i)./t_t;
46 term_1(i) = w_d(i).*((C_1111(i)-2.*C_2323(i))./C_1111(i));
47 term_2(i) = w_d(i).*(1./C_1111(i));
48 term_3(i) = w_d(i).*(4.*((C_1111(i)-C_2323(i)).*C_2323(i))

```

```

./ C_1111(i));

49 term_4 ( i ) = w_d(i).*C_2323(i);
50 term_5 ( i ) = w_d(i).*(1./C_2323(i));
51 end
52 term_1 = sum(term_1);
53 term_2 = sum(term_2);
54 term_3 = sum(term_3);
55 term_4 = sum(term_4);
56 term_5 = sum(term_5);

57
58 C_3333_TI = (term_2).^(-1);
59 C_2323_TI = (term_5).^(-1);
60 C_1111_TI = (3.13./2.25).*C_3333_TI; % Using ratio from
    Green-river shale
61 C_1133_TI = (0.34./2.25).*C_3333_TI; % Using ratio from
    Green-river shale
62 C_1212_TI = (0.88./0.65).*C_2323_TI; % Using ratio from
    Green-river shale

63
64 C11 = C_1111_TI;
65 C13 = C_1133_TI;
66 C44 = C_2323_TI;
67 C33 = C_3333_TI;
68 C66 = C_1212_TI;

69
70 Chi_data = (C11 - C33)/(2*C33);

```

```

71
72 %% Geometry
73 Depth_of_layer = d(1); % in m
74 Depth_of_receiver = z_p(end); % in m
75 layer_thickness = Depth_of_receiver - Depth_of_layer;
76 theta = 60*pi/180;
77 X_cross = layer_thickness*tan(theta);
78 diag_dist = sqrt(layer_thickness^2 + X_cross^2);

79
80 %% Geometry ends

81
82 %% Calculation : ray angle to phase angle
83 c_1 = C33 - C11;
84 c_2 = C11 + C44;
85 c_3 = 2; % in nondensity scale , it becomes 2*rho
86 c_4 = C11 - C44;
87 c_5 = C33 - C44;
88 c_6 = 4*(C44 + C13)^2;

89
90 f_4 = (cos(nu))^2; % cos^2(nu)
91 f_4_prime = -sin(2*nu);

92
93 f_5_t1 = c_4*(1-f_4) - c_5*f_4;
94 f_5_t2 = c_6*f_4*(1-f_4);
95 f_5 = f_5_t1^2+f_5_t2; % Delta

96

```

```

97 f_1 = sqrt((c_1*f_4 + c_2 + sqrt(f_5))/c_3); %Phase velocity
98 v = f_1;
99
100 % calculation of v_prime with respect to nu
101 sec_5 = c_6*f_4_prime - 2*c_6*f_4*f_4_prime;      % sec means
102 sections of an equation like terms in the equation
103 sec_4 = (2*(c_4*(1-f_4)-c_5*f_4))*(-c_4*f_4_prime-c_5*
104 f_4_prime);
105 sec_3 = (f_5^(-.5)/2)*(sec_4+sec_5);
106 sec_2 = 2*c_1*c_3^(-1)*f_4*f_4_prime;
107 sec_1 = ((c_1*f_4^2+c_2+sqrt(f_5))/c_3)^(-.5)*.5;
108 v_prime = sec_1*(sec_2+sec_3);
109
110
111 f_theta = tan(theta);
112 f_nu = tan(nu);
113 bottom = 1 - ((f_nu*v_prime)/v);
114 top =(v_prime/v)+f_nu;
115
116 nu_res = vpasolve(f_theta*bottom - top == 0, nu)
117 nu_res = double(nu_res);
118 nu = nu_res;
119 %f_theta = tan(theta);
120 f_nu = tan(nu);

```

```

121 % bottom = 1 - ((f_nu*v_prime)/v);
122 % top =(v_prime/v)+f_nu ;
123
124
125 f_4 = (cos(nu))^2; % cos^2(nu)
126 f_4_prime = -sin(2*nu);
127
128 f_5_t1 = c_4*(1-f_4) - c_5*f_4;
129 f_5_t2 = c_6*f_4*(1-f_4);
130 f_5 = f_5_t1^2+f_5_t2; % Delta
131
132 f_1 = sqrt((c_1*f_4 + c_2 + sqrt(f_5))/c_3); %Phase velocity
133 v = sqrt(C33);
134
135 % Getting ray velocity in in first way
136 V_ray_1 = v/(cos(theta-nu));
137 V_ray_1 = double(V_ray_1);
138
139
140 % Getting ray velocity in second way .
141 sec_5 = c_6*f_4_prime - 2*c_6*f_4*f_4_prime;
142 sec_4 = (2*(c_4*(1-f_4)-c_5*f_4))*(-c_4*f_4_prime- c_5*f_4_prime);
143 sec_3 = (f_5^(-.5)/2)*(sec_4+sec_5);
144 sec_2 = 2*c_1*c_3^(-1)*f_4*f_4_prime;
145 sec_1 = ((c_1*f_4^2+c_2+sqrt(f_5))/c_3)^(-.5)*.5;

```

```

146 v_prime = sec_1*(sec_2+sec_3);

147

148 V_ray_2 = sqrt(v^2+v_prime^2);

149 V_ray_2 = double(V_ray_2);

150

151 %Compare their results

152 delta_v_ray = V_ray_2 - V_ray_1

153 delta_v_ray_to_v_p = V_ray_2 - v

154 % Calculation of traveltime in TI medium

155 t_time = diag_dist/V_ray_2

```

2.A.5 Anisotropy and inhomogeneity relation

```
1 %% Calculation of the Anisotropy vs. Inhomogeneity plot
2 close all; clear all ;clc
3
4 lb=[ -1];
5 ub=[ 1];
6 x0=[0.00000001];
7
8 H_1 = 1865.00;
9 H_2 = 2648.60;
10 H = H_2 - H_1;
11
12 %% Make a set of values for b_p and b_s
13 b_p_t = 0:0.0001:2; % Set a range of values for b_p
14 b_p_t = b_p_t .';
15 b_s_t = 0:0.0001:2; % Set a range of values for b_s
16 b_s_t = b_s_t .';
17
18 pp = length(b_p_t);
19
20 a_p = 2084.09; % value is obtained from equation (2.11)
21 a_s = 752.95; % value is obtained from equation (4.18)
22
23 for i = 1:length(b_p_t)
24     [x(i ,:) ,val(i)] = fminsearchbnd(@(X)c_b_fn_1p(X(1) ,a_p ,
```

```

    a_s , b_p_t(i) , b_s_t(i) , H, H_1, H_2),x0,lb,ub);

25 end

26 chi_b_t = x(:,1);

27

28 figure(1)

29 plot(b_p_t, chi_b_t, 'k')

30 xlabel('{\rm b}')

31 set(xlabel('{\rm b}'), 'Interpreter', 'latex', 'fontsize', 24)

32 ylabel('$$\chi_{\overline{{\rm TI}}}$$')

33 set(ylabel('$$\chi_{\overline{{\rm TI}}}$$'), 'Interpreter', 'latex', 'fontsize', 24)

34 grid on

35

36 chi_b = x(end,1);

37

38 b_p = b_p_t(end);

39 b_s = b_s_t(end);

40

41

42

43 %% check the values

44

45 v_p_1 = a_p + b_p.*H_1;

46 v_p_2 = a_p + b_p.*H_2;

47 v_s_1 = a_s + b_s.*H_1;

48 v_s_2 = a_s + b_s.*H_2;

```

```

49 C_3333 = (H.*b_p)./((v_p_1).^(-1)-(v_p_2).^(-1));

50

51 c_3333_t1 = -(H_1 - H_2)/(1/(b_p*(a_p + H_1*b_p)) - 1/(b_p*(

a_p + H_2*b_p)));;

52

53 c_1111_t2a = - (H_1^3*b_s^2)/3 - H_1^2*a_s*b_s - H_1*a_s^2 +

(H_2^3*b_s^2)/3 + H_2^2*a_s*b_s + H_2*a_s^2;

54

55 P_0 = (H_2*b_s^2)/b_p^2 - (H_1*b_s^2)/b_p^2 + (log(a_p + H_1

*b_p)*(2*a_p*b_s^2 - 2*a_s*b_p*b_s))/b_p^3 - (log(a_p +

H_2*b_p)*(2*a_p*b_s^2 - 2*a_s*b_p*b_s))/b_p^3 + (a_p^2*


b_s^2 - 2*a_p*a_s*b_p*b_s + a_s^2*b_p^2)/(b_p*(H_1*b_p^3

+ a_p*b_p^2)) - (a_p^2*b_s^2 - 2*a_p*a_s*b_p*b_s + a_s^2*


b_p^2)/(b_p*(H_2*b_p^3 + a_p*b_p^2));

56 P_1 = H_2*((2*a_p*((2*a_p*b_s^4)/b_p^3 - (4*a_s*b_s^3)/b_p

^2))/b_p - (a_p^2*b_s^4)/b_p^4 + (6*a_s^2*b_s^2)/b_p^2) -


H_1*((2*a_p*((2*a_p*b_s^4)/b_p^3 - (4*a_s*b_s^3)/b_p^2))

/b_p - (a_p^2*b_s^4)/b_p^4 + (6*a_s^2*b_s^2)/b_p^2) + H_1

^2*((a_p*b_s^4)/b_p^3 - (2*a_s*b_s^3)/b_p^2) - H_2^2*((

a_p*b_s^4)/b_p^3 - (2*a_s*b_s^3)/b_p^2) + (log(a_p + H_1*b_p)

*(4*a_p^3*b_s^4 - 12*a_p^2*a_s*b_p*b_s^3 + 12*a_p*a_s

^2*b_p^2*b_s^2 - 4*a_s^3*b_p^3*b_s))/b_p^5 - (log(a_p + H_2*b_p)

*(4*a_p^3*b_s^4 - 12*a_p^2*a_s*b_p*b_s^3 + 12*a_p

*a_s^2*b_p^2*b_s^2 - 4*a_s^3*b_p^3*b_s))/b_p^5 - (H_1^3*b_s^4)/

(3*b_p^2) + (H_2^3*b_s^4)/(3*b_p^2) + (a_p^4*b_s^4 - 4*a_p^3*a_s*b_p*b_s^3 + 6*a_p^2*a_s^2*b_p^2*b_s^2 - 4*
```

```

a_p*a_s^3*b_p^3*b_s + a_s^4*b_p^4)/(b_p*(H_1*b_p^5 + a_p*
b_p^4)) - (a_p^4*b_s^4 - 4*a_p^3*a_s*b_p*b_s^3 + 6*a_p^2*
a_s^2*b_p^2*b_s^2 - 4*a_p*a_s^3*b_p^3*b_s + a_s^4*b_p^4)
/(b_p*(H_2*b_p^5 + a_p*b_p^4));
```

57

```

58 c_1111_t1 = (1-(2*P_0/H))^2*c_3333_t1 + (4/H)*(c_1111_t2a-
P_1);
```

59

```

60 function fun=c_b_fn_1p(chi_b, a_p, a_s, b_p, b_s, H, H_1,
H_2)
```

61

```

62 c_3333_t1 = -(H_1 - H_2)/(1/(b_p*(a_p + H_1*b_p)) - 1/(b_p*(
a_p + H_2*b_p)));
```

```

63 P_1 = - (H_1^3*b_s^2)/3 - H_1^2*a_s*b_s - H_1*a_s^2 + (H_2
^3*b_s^2)/3 + H_2^2*a_s*b_s + H_2*a_s^2;
```

64

```

65 P_0 = (H_2*b_s^2)/b_p^2 - (H_1*b_s^2)/b_p^2 + (log(a_p + H_1
*b_p)*(2*a_p*b_s^2 - 2*a_s*b_p*b_s))/b_p^3 - (log(a_p +
H_2*b_p)*(2*a_p*b_s^2 - 2*a_s*b_p*b_s))/b_p^3 + (a_p^2*
b_s^2 - 2*a_p*a_s*b_p*b_s + a_s^2*b_p^2)/(b_p*(H_1*b_p^3
+ a_p*b_p^2)) - (a_p^2*b_s^2 - 2*a_p*a_s*b_p*b_s + a_s^2*
b_p^2)/(b_p*(H_2*b_p^3 + a_p*b_p^2));
```

```

66 P_2 = H_2*((2*a_p*((2*a_p*b_s^4)/b_p^3 - (4*a_s*b_s^3)/b_p
^2))/b_p - (a_p^2*b_s^4)/b_p^4 + (6*a_s^2*b_s^2)/b_p^2) -
H_1*((2*a_p*((2*a_p*b_s^4)/b_p^3 - (4*a_s*b_s^3)/b_p^2))
/b_p - (a_p^2*b_s^4)/b_p^4 + (6*a_s^2*b_s^2)/b_p^2) + H_1
```

$$\begin{aligned}
& ^2*((a_p * b_s^4) / b_p^3 - (2 * a_s * b_s^3) / b_p^2) - H_2^2 * ((\\
& a_p * b_s^4) / b_p^3 - (2 * a_s * b_s^3) / b_p^2) + (\log(a_p + H_1 * \\
& b_p) * (4 * a_p^3 * b_s^4 - 12 * a_p^2 * a_s * b_p * b_s^3 + 12 * a_p * a_s \\
& ^2 * b_p^2 * b_s^2 - 4 * a_s^3 * b_p^3 * b_s)) / b_p^5 - (\log(a_p + \\
& H_2 * b_p) * (4 * a_p^3 * b_s^4 - 12 * a_p^2 * a_s * b_p * b_s^3 + 12 * a_p \\
& * a_s^2 * b_p^2 * b_s^2 - 4 * a_s^3 * b_p^3 * b_s)) / b_p^5 - (H_1^3 * \\
& b_s^4) / (3 * b_p^2) + (H_2^3 * b_s^4) / (3 * b_p^2) + (a_p^4 * b_s^4 \\
& - 4 * a_p^3 * a_s * b_p * b_s^3 + 6 * a_p^2 * a_s^2 * b_p^2 * b_s^2 - 4 * \\
& a_p * a_s^3 * b_p^3 * b_s + a_s^4 * b_p^4) / (b_p * (H_1 * b_p^5 + a_p * \\
& b_p^4)) - (a_p^4 * b_s^4 - 4 * a_p^3 * a_s * b_p * b_s^3 + 6 * a_p^2 * \\
& a_s^2 * b_p^2 * b_s^2 - 4 * a_p * a_s^3 * b_p^3 * b_s + a_s^4 * b_p^4) \\
& / (b_p * (H_2 * b_p^5 + a_p * b_p^4));
\end{aligned}$$

67

68 c_1111_ti = (1 - (2 * P_0 / H))^2 * c_3333_ti + (4 / H) * (P_1 - P_2);

69

70

71 %% chi_b

72 chi_b_cal_from_ab = ((c_1111_ti - c_3333_ti) / (2 * c_3333_ti));

73

74 %% fun

75 fun = abs(chi_b - chi_b_cal_from_ab);

76 end

2.A.6 Traveltime using average velocities

```
1 close all; clear all ;clc  
2  
3 a = 2.084086163931543e+03;  
4 b = 0.397960845768006;  
5 chi = 2.404424815631195e-04;  
6  
7 H_1 = 1865.00;  
8 H_2 = 2648.60;  
9 z = H_2 - H_1;  
10 a_p = a - b*H_1;  
11  
12 theta = 0*pi/180;  
13 x = z*tan(theta);  
14 t_1 = log(a_p + H_2*b)/b - log(a_p + H_1*b)/b  
15  
16 v_mean = a+(b.*z./2);  
17 v_avg = b.*z./log(abs(1+(b.*z./a)));  
18 v_rms = sqrt((2.*a.*b.*z + b^2.*z^2)./(2.*log(abs(1+(b.*z./a))))));  
19 t_mean = z./v_mean  
20 t_avg = z./v_avg  
21 t_rms = z./v_rms  
22  
23 a_2 = a;
```

```

24 b_2 = b;
25 chi_2 = chi;
26
27 term_1 = 1+2*chi_2;
28 term_2 = ((2*(a_2))+((b_2)*z)).^2;
29
30 p_d = sqrt((x.^2 + ((term_1)*z.^2))*((term_2)*(term_1)+((b_2
.^2)*(x.^2)))); 
31 p = (2*x)/(p_d);
32
33 term_3n = 1 - (p.^2.*a_2.^2.*(1+2.*chi_2));
34
35 t_time_hyp = (1/b_2).* (atanh(p.*b_2.*x-sqrt(term_3n)) +
atanh(sqrt(term_3n)));
36
37 term_3 = a_2 + (b_2*z);
38 term_4 = sqrt(1-(a_2.^2)*(p.^2)*(term_1));
39 term_5 = sqrt(1-(term_3.^2)*(p.^2)*(term_1));
40
41 t_time_log = (1/b_2)*log(((term_3)*(1+term_4))/(a_2*(1+
term_5)))

```

2.A.7 NMO velocity

```

1 %% Calculation of NMO velocity in equivalent TI media
2 close all; clear all ;clc
3 syms nu

```

```

4 [num1,txt1,raw1] = xlsread('mizzen_o_16_w1.xlsm'); % Well
5 log data
6 % This is the layer we pick (depth 1865.00 m to 2648.60 m);
7
8 data_s_s = num1(1035:8871, 6); % slowness in us/m
9 data_v_s = (1./data_s_s).*1e6;
10 v_s = data_v_s;
11
12 err_free = v_s>-1;
13 err_free_n = find(err_free==1);
14 v_s = v_s(err_free_n(:)); % Provided in A.2 column 4
15
16
17 data_s_p = num1(1035:8871, 7); % slowness in us/m
18 data_v_p = (1./data_s_p).*1e6;
19 v_p = data_v_p;
20 v_p = v_p(err_free_n(:)); % Provided in A.2 column 3
21
22 z_p = num1(1035:8871, 1); %
23 z_p = z_p(err_free_n(:));
24 d = z_p; % Provided in A.2 column 2
25
26 n_p = size(v_p);
27 data_v_p_for_mid = v_p(2:(end-1),1);
28 C_1111 = data_v_p_for_mid.^2;

```

```

29
30 data_v_s_for_mid = v_s(2:(end-1),1);
31 C_2323 = data_v_s_for_mid.^2;
32
33
34 for i = 1:n_p-1
35 m_p(i) = d(i) + ((d(i+1)-d(i))./2);
36 end
37 t_t = m_p(end) - m_p(1);
38
39 for i = 1:n_p-2
40 d_d(i) = m_p(i+1)-m_p(i);
41 end
42
43 for i = 1:n_p-2
44 w_d(i) = d_d(i)./t_t;
45 term_1(i) = w_d(i).*((C_1111(i)-2.*C_2323(i))./C_1111(i));
46 term_2(i) = w_d(i).*(1./C_1111(i));
47 term_3(i) = w_d(i).*(4.*((C_1111(i)-C_2323(i)).*C_2323(i));
48 term_4(i) = w_d(i).*C_2323(i);
49 term_5(i) = w_d(i).*(1./C_2323(i));
50 end
51 term_1 = sum(term_1);
52 term_2 = sum(term_2);

```

```

53 term_3 = sum(term_3);
54 term_4 = sum(term_4);
55 term_5 = sum(term_5);

56
57 C_3333_TI = (term_2).^( -1);
58 C_1111_TI = (term_1).^2 .* (term_2).^( -1) + term_3;
59 C_1133_TI = term_1 .* (term_2).^( -1);
60 C_1212_TI = term_4;
61 C_2323_TI = (term_5).^( -1);

62
63 C11 = C_1111_TI;
64 C13 = C_1133_TI;
65 C44 = C_2323_TI;
66 C33 = C_3333_TI;
67 C66 = C_1212_TI;

68
69 Chi_data = (C11 - C33)/(2*C33);
70 delta_cal = ((C13 + C44).^2 - (C33 - C44).^2)./((2.*C33).*(
    C33 - C44));
71 rt_term = 1+(2.*delta_cal);
72 v_nmo_B = sqrt(C33).*sqrt(rt_term);

73
74 %% Calculation of NMO velocity in effective Dix medium
75 d_z_p_new = d_d.';
76 v_p_new = data_v_p_for_mid;

77

```

78

```

79  for i = 1:(n_p-2)
80      term_1(i) = d_z_p_new(i).*v_p_new(i);
81      term_2(i) = d_z_p_new(i)./v_p_new(i);
82      term_3(i) = d_z_p_new(i);
83      v_avg(i) = sum(term_3(1:i))./sum(term_2(1:i));
84      v_mean(i) = sum(term_1(1:i))./sum(term_3(1:i));
85      v_rms_in(i) = sum(term_1(1:i))./sum(term_2(1:i));
86      v_rms(i) = sqrt(v_rms_in(i));
87  end
88
89  time_t = (2.*d_z_p_new)./v_p_new ;
90  for i = 1:(n_p-2)
91      time_t_sum(i) = sum(time_t(1:i));
92  end
93  for i = 1:(n_p-3)
94      v_int_upt(i) = (v_rms(i+1).^2.*time_t_sum(i+1)) - (v_rms(
95          i).^2.*time_t_sum(i));
96      v_int_downt(i) = time_t_sum(i+1) - time_t_sum(i);
97      v_int(i) = sqrt(v_int_upt(i)./v_int_downt(i));
98      time_nmo(i) = 2.*time_t(i);
99      v_nmo_upt(i) = v_int(i).^2 .* time_nmo(i);
100 end
101
102 v_nmo_Dix = sqrt( sum(v_nmo_upt(1:end))./sum(time_nmo(1:end))

```

```
) );  
103 diif_methods = v_nmo_B - v_nmo_Dix;
```

Chapter 3

On 1-D traveltime tomography and two-parameter velocity inversion

3.1 Introduction

In this chapter, we examine linear inhomogeneity of a medium by applying two inversion methods on seismic traveltimes. In the first method, we derive an analytical expression for the solution of Hamilton's ray equation in vertically inhomogeneous and isotropic media. Considering the analytical solution as a forward model, we construct an inversion method based on the Levenberg-Marquardt damped least square solution. In the second inversion method, we use the traveltimes expression based on a two-parameter velocity model as the forward model. We perform several synthetic experiments on the first method based on a linear velocity model. While we study the linear velocity in synthetic studies to reduce the model parameters to two, the inversion method can be used to construct a velocity model that varies with depth in any order. The synthetic experiments show that the traveltime convergence occurs even with a significant change in the start-up values; however, as the

discrepancy gets higher, the inverted velocity diverges more from the reference velocity model. In comparison to the startup values, the inversion method is less sensitive to the number of data points and the noise. We apply the inversion methods on real data to study the linear inhomogeneity and find the two-parameter velocity model estimates higher inhomogeneity in compare to the 1-D tomography.

3.2 Method development

3.2.1 Solution of the ray equation in vertically inhomogeneous media

In general, the velocity of seismic waves can vary in any direction. Assuming the velocity only a function of vertical depth, we present an analytical solution for Hamilton's ray equation. In the derivation, we apply the method of characteristics, similar to the approach described by Slawinski [2015] and Červený [2001]. However, to parameterize the ray equation, Slawinski [2015] used arc length as opposed to travelttime, and Červený [2001] used the level set equation $p^2 - v^{-2} = 0$ as opposed to $p^2 v^2 = 1$, where p is the slowness parameter, and v is the wave velocity. In our derivation, we use travelttime for the parametrization and $p^2 v^2 = 1$ as the level set equation.

In this section, we present the solution of Hamilton's ray equation for a vertically inhomogeneous and isotropic medium. We start with a 3-D inhomogeneous medium and then move into a 1-D medium by considering velocity as a function of depth. In a smoothly inhomogeneous isotropic medium, the high-frequency seismic wave field can be separated into two independent waves, P and S [Slawinski, 2015, p. 277]. Both waves satisfy the eikonal equation

$$p^2 = \frac{1}{v^2(\mathbf{x}, \mathbf{p})}, \quad (3.1)$$

where, $p^2 = \mathbf{p} \cdot \mathbf{p}$, \mathbf{p} is the slowness and $p_i := \frac{\partial \psi}{\partial x_i}$, $i \in \{1, 2, 3\}$, ψ is the phase function. Equation (3.1) is a set of first order partial differential equations that depends on the variables \mathbf{x} and $\mathbf{p}(\mathbf{x})$. It relates the magnitude of phase slowness of the wave to the medium properties [Slawinski, 2015]. The method of characteristics is commonly applied in the eikonal equation to get a system of six first-order ordinary differential equations [Slawinski, 2015, p. 343]

$$\begin{aligned}\frac{dx_i}{ds} &= \zeta \frac{\partial F}{\partial p_i} \\ \frac{dp_i}{ds} &= -\zeta \frac{\partial F}{\partial x_i}\end{aligned}, \quad i \in \{1, 2, 3\}, \quad (3.2)$$

where ζ is a scaling factor and s is the parameter along the curve. The choice of s determines the parametrization. As discussed in Slawinski [2015, p. 343], the solution of the eikonal equation is a surface in the \mathbf{xp} -space. This surface can be described as level sets of a function, which we denote by $F(\mathbf{x}, \mathbf{p})$. It is a Hamiltonian with a factor of $\frac{1}{2}$. A relationship for the scaling factor ζ in equation (3.2) to the flow parameter s are provided in Červený [2001]. They consider three cases of s along the curve: the arclength, the travelttime and the parameter σ .

For a vertically inhomogeneous isotropic medium, we solve Hamilton's ray equation by parametrizing the characteristic equations in terms of time and scaling factor as a constant number, so that expression (3.2) becomes

$$\begin{aligned}\dot{x}_i &= \frac{\partial}{\partial p_i} \left(\frac{F}{2} \right) = \frac{\partial \mathcal{H}}{\partial p_i} \\ \dot{p}_i &= -\frac{\partial}{\partial x_i} \left(\frac{F}{2} \right) = -\frac{\partial \mathcal{H}}{\partial x_i}\end{aligned}, \quad i \in \{1, 2, 3\}, \quad (3.3)$$

where $\mathcal{H} := \frac{F}{2}$, known as the ray-theory Hamiltonian. We choose $F(\mathbf{x}, \mathbf{p}) = p^2 v^2(\mathbf{x}, \mathbf{p})$ as

the level sets, which leads to a Hamiltonian

$$\mathcal{H}(\mathbf{x}, \mathbf{p}) = \frac{1}{2} p_1^2 v^2(\mathbf{x}) = \frac{1}{2} [p_1, p_3] \cdot [p_1, p_3] v^2(x_1, x_3), \quad (3.4)$$

and the corresponding ray equations

$$\frac{dx_1}{dt} = p_1 v^2, \quad (3.5a)$$

$$\frac{dx_3}{dt} = p_3 v^2, \quad (3.5b)$$

$$\frac{dp_1}{dt} = -p^2 v \frac{\partial v}{\partial x_1} = 0, \quad (3.5c)$$

$$\frac{dp_3}{dt} = -p^2 v \frac{\partial v}{\partial x_3}. \quad (3.5d)$$

Dividing expression (3.5a) by (3.5b)

$$\frac{dx_1}{dx_3} = \frac{p_1}{p_3}. \quad (3.6)$$

Using the eikonal equation $p_1^2 + p_3^2 = v^{-2}$ in expression (3.6)

$$\frac{dx_1}{dx_3} = \frac{p_1}{\sqrt{v^{-2} - p_1^2}} = \frac{p_1 v}{\sqrt{1 - p_1^2 v^2}}. \quad (3.7)$$

Using expression (3.7) in expression (3.5a)

$$dt = \frac{dx_1}{p_1 v^2} = \frac{\frac{p_1 v}{\sqrt{1 - p_1^2 v^2}} dx_3}{p_1 v^2} = \frac{dx_3}{v \sqrt{1 - p_1^2 v^2}}. \quad (3.8)$$

Expression (3.5c) shows that the slowness parameter, p_1 , is constant along the whole ray path. For a vertically inhomogeneous medium p_1 is a conserved quantity, which is known as the ray parameter. We express the ray parameter by \mathfrak{p} . We obtain the solution of ray equation by integrating expressions (3.6) and (3.8) for x_3 to get

$$x_1(x_3) = \int_{z_0}^z \frac{\mathfrak{p}v(x_3)}{\sqrt{1 - \mathfrak{p}^2 v^2(x_3)}} dx_3, \quad (3.9)$$

and

$$t(x_3) = \int_{z_0}^z \frac{1}{v\sqrt{1 - \mathfrak{p}^2 v^2(x_3)}} dx_3, \quad (3.10)$$

where x_3 is the vertical depth. Equations (3.9) and (3.10) are in agreement with Červený [2001]. To trace a ray, we need to solve expressions (3.9) and (3.10) simultaneously.

If the velocity changes linearly with depth, i.e., $v(x_3) = a + bx_3$, using expressions (3.9) and (3.10), the ray parameter and the traveltimes can be written as [Slawinski and Slawinski, 1999]

$$\mathfrak{p} = \frac{2bx_3}{\sqrt{(b^2x_3^2 + a^2 + (a + bx_3)^2)^2 - 4a^2(a + bx_3)^2}}, \quad (3.11)$$

$$t = \frac{1}{b} \left| \log \left(\frac{a + bx_3}{a} \frac{1 + \sqrt{1 - a^2 \mathfrak{p}^2}}{1 + \sqrt{1 - \mathfrak{p}^2(a + bx_3)^2}} \right) \right|. \quad (3.12)$$

We use expression (3.12) as the forward model to the *ab*-model inversion.

3.2.2 Discretizing the forward model for 1-D tomography

In this section, we discretize the expressions (3.9) and (3.10) to solve the ray equation numerically. To perform the integration for multiple source-receiver pairs, we consider the medium to be composed of N layers; H is the layer thickness, where the layers are equally thin, homogeneous, and isotropic. Using expressions (3.9) and (3.10), the ray tracing equations from the i -th source to the k -th receiver are

$$x_{k,i} = x_{1k,i} + x_{2k,i} + \dots + x_{jk,i} = \sum_{j=1}^m \frac{H_j B_{kj,i}}{\sqrt{1 - B_{kj,i}^2}}, \quad j \in \{1, 2, 3, \dots, m\}, \quad (3.13)$$

$$t_{k,i} = t_{1k,i} + t_{2k,i} + \dots + t_{jk,i} = \sum_{j=1}^m \frac{H_j}{v_j \sqrt{1 - B_{kj,i}^2}}, \quad j \in \{1, 2, 3, \dots, m\}, \quad (3.14)$$

where θ_{1k} is the take-off angle, $B_{kj,i} = p_{k,i} v_j$, i and k denote the indices of sources and receivers. Traveltime in the j -th segment is t_{jk} . The total number of model parameters is m , which is equal to the number of layers. We consider the sources to be located at the surface and the receivers to be set along the vertical axis. To calculate the total traveltimes and the offset for a given source-receiver pair, we modify the upper limit of the summation by replacing m to $L(k)$. For a given source-receiver pair, we modify the upper limit of the summation by replacing m by $L(k)$ to calculate the total traveltimes and the offset. This is because, the Geophone locations may not be related to the layering, therefore, an index $L(k)$ is introduced that indicates in which layer the k -th geophone is located. If the geophone locations k and $k+1$ are in the same layer, then $L(k) = L(k+1)$.

3.2.3 Development of the inversion method for 1-D tomography

Using the analytical solution as a forward model, we develop an inversion method based on Levenberg-Marquardt (L-M) damped least-squares solution. The L-M method is a powerful tool for the iterative solution for both linear and nonlinear problems [Pujol, 2007]. Levenberg [1944] used the technique for the first time, and about twenty years later, Marquardt [1963] independently rediscovered the method utilizing an independent approach.

In this section, we develop the L-M method for a vertically inhomogeneous and isotropic medium. As the forward model, we use expressions (3.13) and (3.14) from section 3.2.2. In the case of $t = t(v_j)$, the traveltime residual can be written as

$$dt_k = \sum_{j=1}^{L(k)} \frac{\partial t_k}{\partial v_j} dv_j, \quad j \in \{1, 2, 3, \dots, L(k)\}. \quad (3.15)$$

Where, we neglect the higher order terms in Taylor series expansion. Taking the derivative of expression (3.14) with respect to v_j ,

$$\frac{\partial t_k}{\partial v_j} = \frac{p_k^2 h_j}{\sqrt{1 - B_{kj}^2}} - \frac{h_j}{v_j^2 \sqrt{1 - B_{kj}^2}}, \quad j \in \{1, 2, 3, \dots, L(k)\}. \quad (3.16)$$

Also, the system of linear equations (3.15) may be written in the matrix form,

$$\mathbf{C} = \mathbf{t}_{\text{obs}} - \mathbf{t}_{\text{mod}} = \mathbf{AX}, \quad (3.17)$$

where *

$$\mathbf{C} = (dt_1, dt_2, \dots, dt_M)^T \quad \text{and} \quad \mathbf{X} = (dv_1, dv_2, \dots, dt_N)^T. \quad (3.18)$$

*Throughout the Chapter 3, we present vectors and matrices in bold letters.

In expression (3.17), \mathbf{A} is an $(M \times N)$ matrix of partial derivatives, M and N are the total number of receivers and layers, respectively. \mathbf{X} represents the model parameter adjustment vector, and \mathbf{C} is the traveltime residual vector. We calculate both the traveltime residual vector and the partial derivative matrix in each iteration.

For a particular source-receiver pair, the basic algorithm is as follows—we apply the Newton-Raphson method to calculate the take-off angle from equation (3.13) by assuming we have the velocities in each layer. The corrected take-off angle is used to calculate the model traveltime. The parameter adjustment vector is calculated from expression (3.17), which allows us to update the velocity in each iteration. We repeat the process until we achieve a satisfactory agreement between the model and observed data.

To solve equation (3.17) for \mathbf{X} , Pujol [2007] stated that the convergence is not assured when \mathbf{X} is computed using ordinary least squares. The assumption behind linearizing the problem no longer remains valid if the initial model is far from the real solution. One of the ways to overcome this problem is the application of Levenberg-Marquardt method.

3.2.4 A review of Levenberg-Marquardt Method

In this section, we review the basic steps of Levenberg-Marquardt iteration scheme. We follow the description of Pujol [2007]. Let us consider the higher order terms in Taylor series expansion that we ignored in equation (3.17)

$$\mathbf{R} = \mathbf{C} - \mathbf{AX}. \quad (3.19)$$

The elements of \mathbf{C} represent the residuals of traveltime for each source-receiver pair. The problem is to calculate the elements of \mathbf{X} 's which minimize \mathbf{R} . The misfit function is

defined as follows,

$$S = \sum_{i=1}^n R_i^2 = \mathbf{R}^T \mathbf{R} \quad \{1, 2, 3, \dots, n\}, \quad (3.20)$$

where n is the number of data points. Substituting equation (3.19) into (3.20), we get

$$S = (\mathbf{C}^T - \mathbf{X}^T \mathbf{A}^T)(\mathbf{C} - \mathbf{A}\mathbf{X}) = \mathbf{C}^T \mathbf{C} - 2\mathbf{C}^T \mathbf{A}\mathbf{X} + \mathbf{X}^T \mathbf{A}^T \mathbf{A}\mathbf{X}. \quad (3.21)$$

Instead of minimizing the misfit function S , Levenberg [1944] proposes to minimize the following function

$$\bar{S} = wS + Q, \quad (3.22)$$

where w is known as Levenberg damping parameter, $Q = \mathbf{X}^T \mathbf{D} \mathbf{X}$ with $\mathbf{D} = \mathbf{I}$, the identity matrix. Using equation (3.21) in equation (3.22)

$$\bar{S} = w \left(\mathbf{C}^T \mathbf{C} - 2\mathbf{C}^T \mathbf{A}\mathbf{X} + \mathbf{X}^T (\mathbf{A}^T \mathbf{A} + \frac{1}{w} \mathbf{I}) \mathbf{X} \right). \quad (3.23)$$

Minimizing Equation (3.23)

$$\frac{d\bar{S}}{d\mathbf{X}} = \left(\frac{d\bar{S}}{dX_1}, \frac{d\bar{S}}{dX_2}, \dots, \frac{d\bar{S}}{dX_N} \right)^T = \mathbf{0},$$

The iteration scheme becomes

$$(\mathbf{A}^T \mathbf{A} + \lambda \mathbf{I}) \mathbf{X} = \mathbf{A}^T \mathbf{c}, \quad (3.24)$$

where $\lambda = \frac{1}{w}$. Using the method of Pujol et al. [1985], we assign a constant value to λ and

in each iteration we reduce it by a factor of 10. At p -th iteration, we solve

$$\left((\mathbf{A}^T \mathbf{A})^{(p)} + \lambda^{(p)} \mathbf{I} \right) (\mathbf{X})^{(p)} = (\mathbf{A}^T \mathbf{c})^{(p)}. \quad (3.25)$$

To otherwise improve the numerical aspects of the method, we use the scaled version of equation (3.25), which is suggested by Marquardt [1963]. Instead of using $\mathbf{A}^T \mathbf{A}$ and $\mathbf{A}^T \mathbf{c}$ in expression (3.25), we use the scaled forms $[\mathbf{A}^T \mathbf{A}]^*$ and $[\mathbf{A}^T \mathbf{c}]^*$. The components of the scaled matrix are [Pujol, 2007]

$$([\mathbf{A}^T \mathbf{A}]^*)_{ij} = S_{ii} S_{jj} (\mathbf{A}^T \mathbf{A})_{ij} \quad (3.26)$$

and

$$([\mathbf{A}^T \mathbf{c}]^*)_i = S_{ii} (\mathbf{A}^T \mathbf{c})_i, \quad (3.27)$$

where

$$S_{ii} = \frac{1}{\sqrt{([\mathbf{A}^T \mathbf{A}]^*)_{ii}}}. \quad (3.28)$$

The scaled Levenberg-Marquardt equation is

$$([\mathbf{A}^T \mathbf{A}]^{*(p)} + \lambda^{(p)} \mathbf{I}) \mathbf{X}^{*(p)} = [\mathbf{A}^T \mathbf{c}]^{*(p)}. \quad (3.29)$$

In each iteration step, we solve equation (3.29) for \mathbf{X}^* and then calculate the components of \mathbf{X}^* based on \mathbf{X} ,

$$X_i = S_{ii} X_i^*. \quad (3.30)$$

The vector form of expression (3.30) is

$$\mathbf{X} = \mathbf{S}\mathbf{X}^*, \quad (3.31)$$

where \mathbf{S} is a diagonal matrix with diagonal elements S_{ii} . In each iteration, we update the velocity as

$$\mathbf{V}^{(p+1)} = \mathbf{V}^{(p)} + \mathbf{X}^{(p)}. \quad (3.32)$$

The iteration process continues until we reach a specific value of the misfit functional. Under the assumption of uncorrelated data with equal variances, σ_0^2 , at p -th iteration, the misfit functional is defined as [Zhdanov, 2002, p. 73]

$$f(\mathbf{X}^{(p)}) = \frac{1}{\sigma_0^2} \left(t_{obs} - t_{mod}^{(p)} \right)^2. \quad (3.33)$$

In synthetic cases, we add normally distributed noise to the traveltime data, and following equation (3.33), we set the iteration to stop while $f(\mathbf{X}^{(p)}) \approx N$, where N is the number of data points.

In each iteration of the Levenberg-Marquardt method, for a given set of velocities in layers, we use equation (3.13) to update the take-off angle. We apply a root-finding algorithm known as the Newton-Raphson method [Heath, 2002] to calculate $p_{k,i}$. It produces successively better approximations to the roots of a real-valued function. To optimize the computation time, we terminate the iteration once we reach to the value of 10^{-6} for the dx_1 , which is the difference between the horizontal distance of the shooting ray and the offset given from the data.

The updated take-off angle is used to calculate the velocity in the next iteration of the Levenberg-Marquardt method. The process of calculation makes the method two-step as

opposed to the one-step approach described by Pujol et al. [1985]. The two-step approach provides us with a better initial model for the traveltimes since it calculates only the take-off angle in first and the velocity in the second. It also allows us to use a single unit for model parameters, which reduces the work of nondimensionalization to define misfit functional.

In contrast to the other local optimization method, such as Gauss-Newton or steepest descent method, the Levenberg-Marquardt method minimizes both model parameters and the data residuals [Pujol, 2007]. As a result, the chances of convergence increases.

3.3 Synthetic experiments

In the synthetic experiments, we consider multiple sources at the surface, many receivers along the vertical depth and assign a reference velocity which changes linearly with depth. The linear velocity is described by two parameters, i.e., the velocity at the surface and the velocity gradient. The variations of both parameters in the startup model allow us to observe the influence of the initial model to the inversion result. We also study the effects of the noise on the data and the number of data points. In the synthetic study, the forward traveltimes is calculated based on the analytic solution, the observed traveltimes is calculated based on the variations in the reference velocity model by changing the startup model and the amount of noise in the data.

3.3.1 Test of the noise and the number of data points

In Table 3.1, we consider the reference velocity model as a linear function of depth, $v = a + bz$, with $a = 1000 \text{ ms}^{-1}$ and $b = 0.12 \text{ s}^{-1}$. We choose a based on the typical value of the P -wave velocity at the surface in the offshore. To have more options in choosing the

number of layers in the synthetic experiments, we decide to consider the velocity gradient in the lower side, such as 0.12. If the velocity gradient is higher, with the increase of layers, the ray hits the critical angle in a relatively lower take-off angle. For the first six cases, the startup velocity for inversion is considered as $v_{ref} \pm 20\text{ms}^{-1}$ and for the last six cases, the startup velocity is considered as $v_{ref} \pm 40\text{ms}^{-1}$. Following Pujol et al. [1985], we choose the value of the parameter λ in the Levenberg-Marquardt algorithm. We start at 10^4 , and in each iteration, it reduces by a factor of 10. We consider the number of traveltime data and the number of model parameters to be equal. However, the inversion method can be applied to both underdetermined and overdetermined cases.

Test	Noise (%)	Source	Geophone	Layer	$f(\mathbf{M})$	a_{inv}	b_{inv}	Figure
1	1	101	1	101	97.74	1002.15	0.1179	3.1a,3.2a
2	1	101	2	202	199.90	1001.46	0.1184	3.1b,3.2b
3	5	101	1	101	100.70	1002.17	0.1173	3.1c,3.2c
4	5	101	2	202	200.95	1001.73	0.1187	3.1d,3.2d
5	10	101	1	101	100.53	1002.40	0.1178	3.1e,3.2e
6	10	101	2	202	199.87	1002.22	0.1171	3.1f,3.2f
7	1	101	1	101	99.91	1003.42	0.1157	3.3a,3.4a
8	1	101	2	202	201.90	1003.15	0.1166	3.3b,3.4b
9	5	101	1	101	100.23	1002.62	0.1159	3.3c,3.4c
10	5	101	2	202	201.32	1001.91	0.1166	3.3d,3.4d
11	10	101	1	101	100.23	1004.20	0.1153	3.3e,3.4e
12	10	101	2	202	200.12	1002.48	0.1170	3.3f,3.4f

Table 3.1: Model set-up : test of the first six, $a_{true} = 1000\text{ms}^{-1}$, $b_{true} = 0.12\text{s}^{-1}$, $a_{in} = a_{true} \pm 20\text{ms}^{-1}$, $b_{in} = b_{true}$; test of the last six, $a_{true} = 1000\text{ms}^{-1}$, $b_{true} = 0.12\text{s}^{-1}$, $a_{in} = a_{true} \pm 40\text{ms}^{-1}$, $b_{in} = b_{true}$

In Table 3.1, $f(\mathbf{M})$ provides the misfit functional, a_{inv} and b_{inv} present the model parameters after fitting a line to the inverted velocity. The traveltime convergence results are shown in Figures 3.1 and 3.3. The misfits of the inverted velocity to the reference velocity are shown in Figures 3.2 and 3.4. To examine the effect of noise and the number of data points, we add 1%, 5% and 10% of random noises and 101 and 202 number of data points.

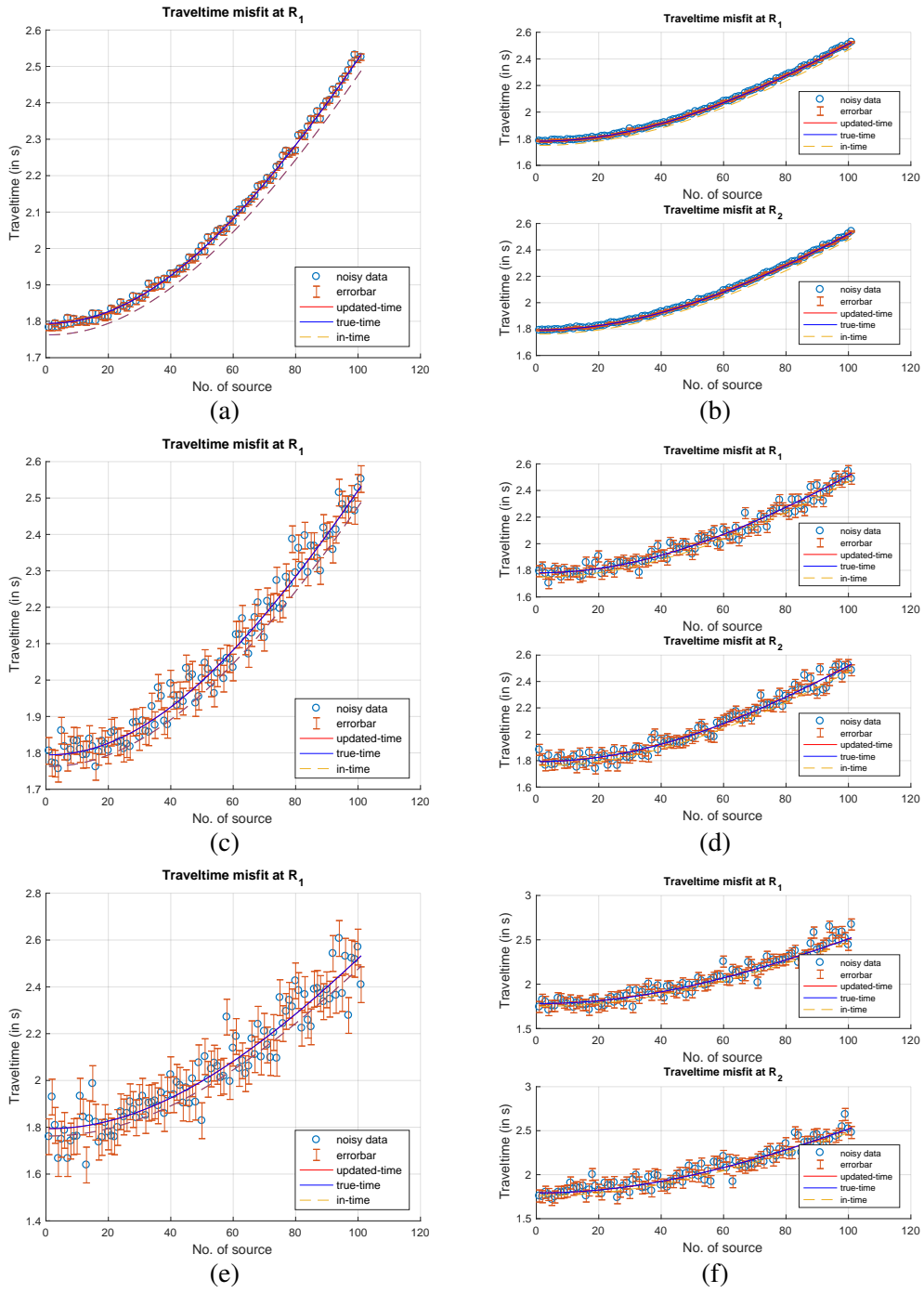


Figure 3.1: Travetime inversion: variation of noise and number of data points, $v_{in} = v_{true} \pm 20$

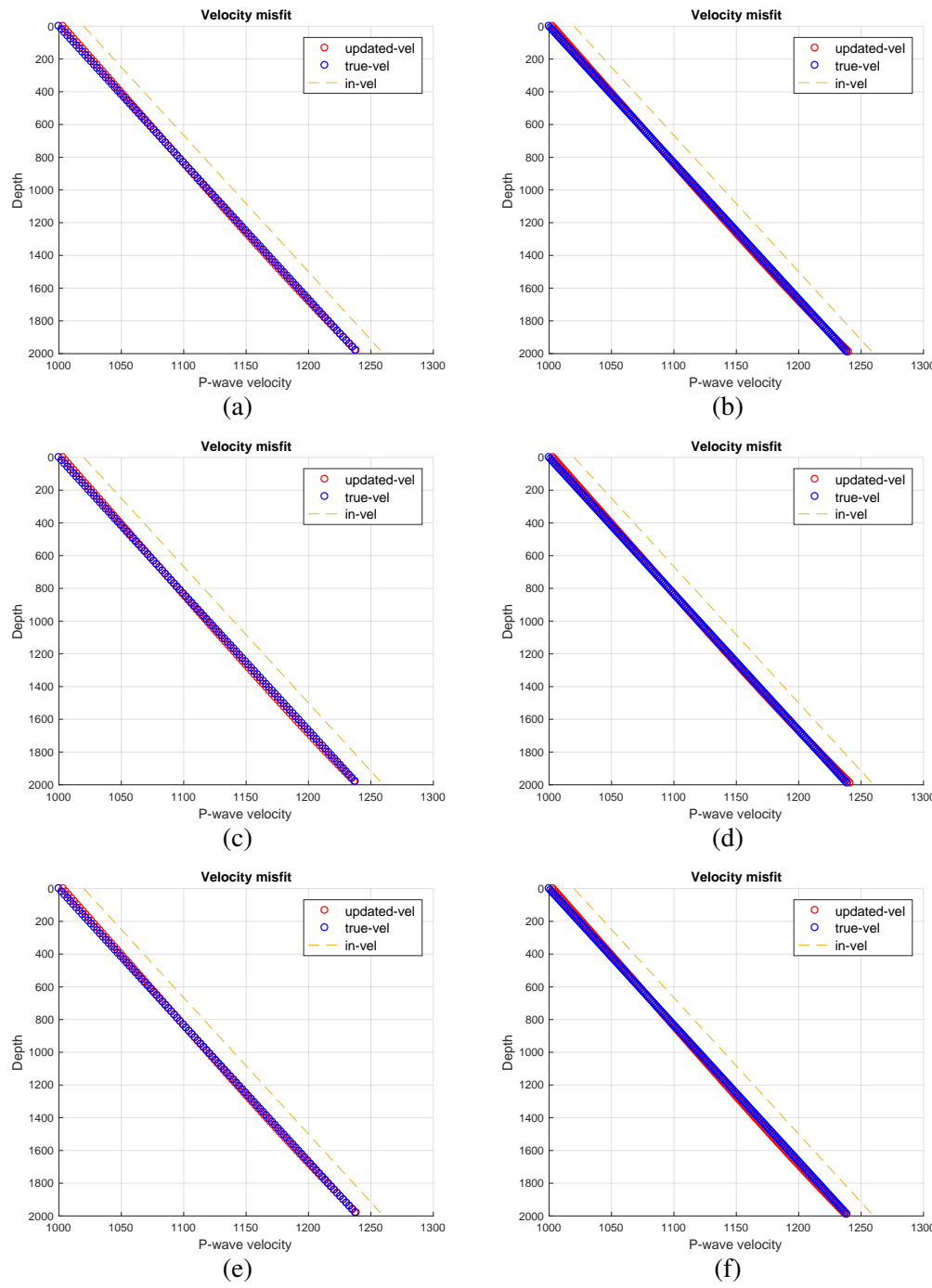


Figure 3.2: Velocity inversion : variation of noise and number of data points, $v_{in} = v_{true} \pm 20$

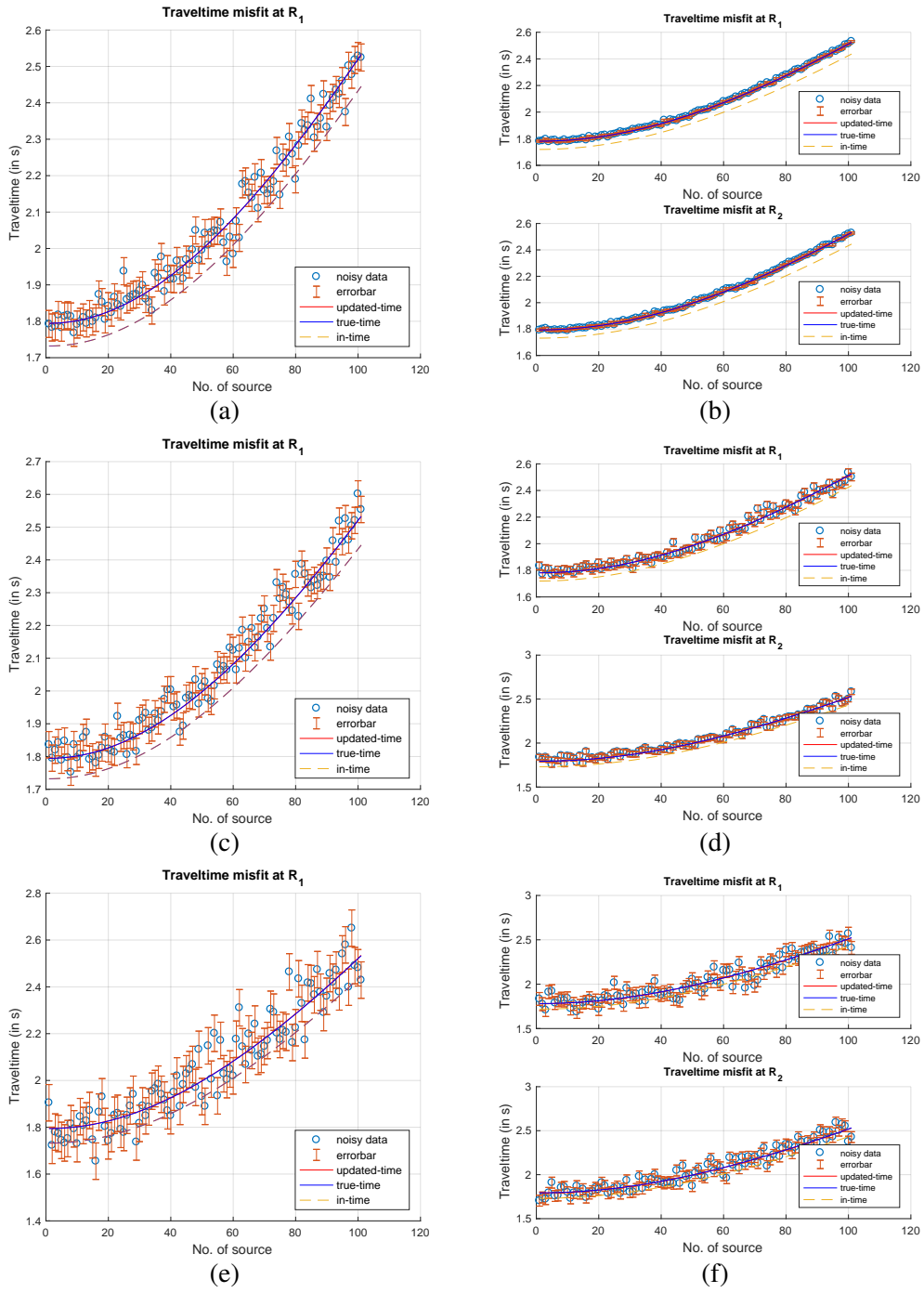


Figure 3.3: Travetime inversion: variation of noise and number of data points, $v_{in} = v_{true} \pm 40$

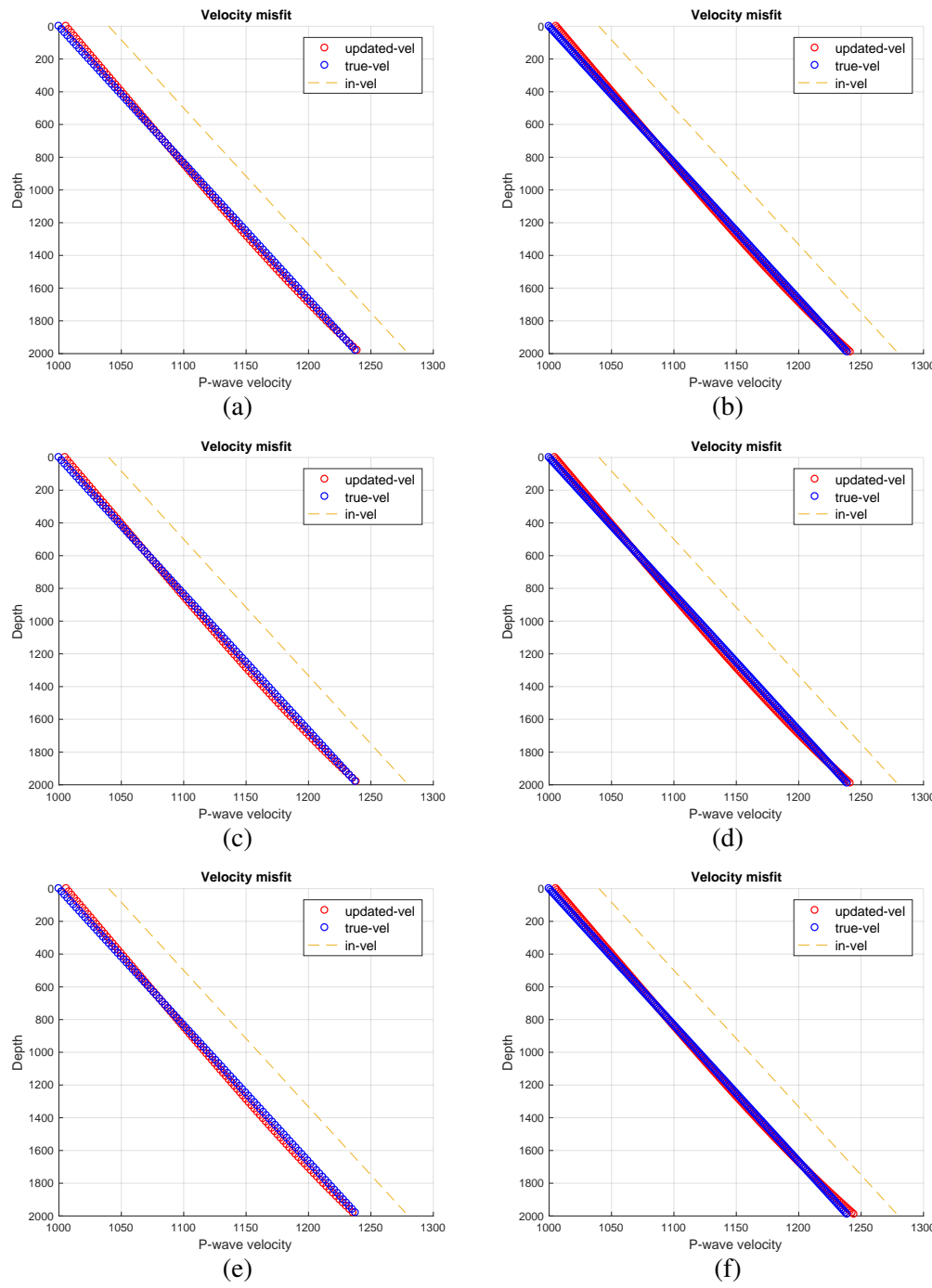


Figure 3.4: Velocity inversion : variation of noise and number of data points, $v_{in} = v_{true} \pm 40$

3.3.2 Test of the model parameters a and b

In Table 3.2, we consider the reference velocity model to be a linear function of depth, where parameters $a = 1000 \text{ ms}^{-1}$ and $b = 0.12 \text{ s}^{-1}$. In contrast to Table 3.1, here we change the model parameter b . For the first six tests, the startup velocity for the inverse model is $v_{ref} + \pm 30 \text{ ms}^{-1}$, and for the last six tests, the startup velocity is $v_{ref} \pm 60 \text{ ms}^{-1}$. We set the noise to 1%, the number of data points to 202 and the total number of model parameters to 202.

The purpose of this section to show, for a given noise and data points, the effects of the startup model parameters a_{in} and b_{in} on the inversion. For b_{in} , we change it from $b_{true} \rightarrow b_{true} \pm 0.01$.

The traveltime convergence results are shown in Figures 3.5 and 3.7. The velocity misfits are shown in Figures 3.6 and 3.8.

Test	a_{in}	b_{in}	a_{inv}	b_{inv}	$f(\mathbf{M})$	Figure
1	970	0.1200	997.77	0.1225	201.07	3.5a,3.6a
2	970	0.1150	1002.05	0.1178	200.53	3.5b,3.6b
3	970	0.1100	1006.44	0.1130	201.56	3.5c,3.6c
4	1030	0.1200	1002.11	0.1178	199.09	3.5d,3.6d
5	1030	0.1250	998.19	0.1220	199.71	3.5e,3.6e
6	1030	0.1300	993.00	0.1275	198.04	3.5f,3.6f
7	940	0.1200	994.58	0.1257	201.30	3.7a,3.8a
8	940	0.1150	999.20	0.1209	196.79	3.7b,3.8b
9	940	0.1100	1003.75	0.1160	201.69	3.7c,3.8c
10	1060	0.1200	1005.02	0.1145	201.03	3.7d,3.8d
11	1060	0.1250	1000.29	0.1199	199.32	3.7e,3.8e
12	1060	0.1300	994.62	0.1259	198.07	3.7f,3.8f

Table 3.2: Model set-up: number of data points = 202, added noise up to 1%. test of the first six, $a_{in} = a_{true} \pm 30$ and test of the last six, $a_{in} = a_{true} \pm 60$ (units of a and b are ms^{-1} and s^{-1})

Table 3.2 shows the inversion results to be more sensitive to the parameter b compared to the parameter a . However, the synthetic experiments show that the inversion method produces the reference velocity consistently within a small range of error. If we apply a good startup model and sufficient data points, the synthetic results show that the inversion method can produce a reasonable velocity model of a medium.

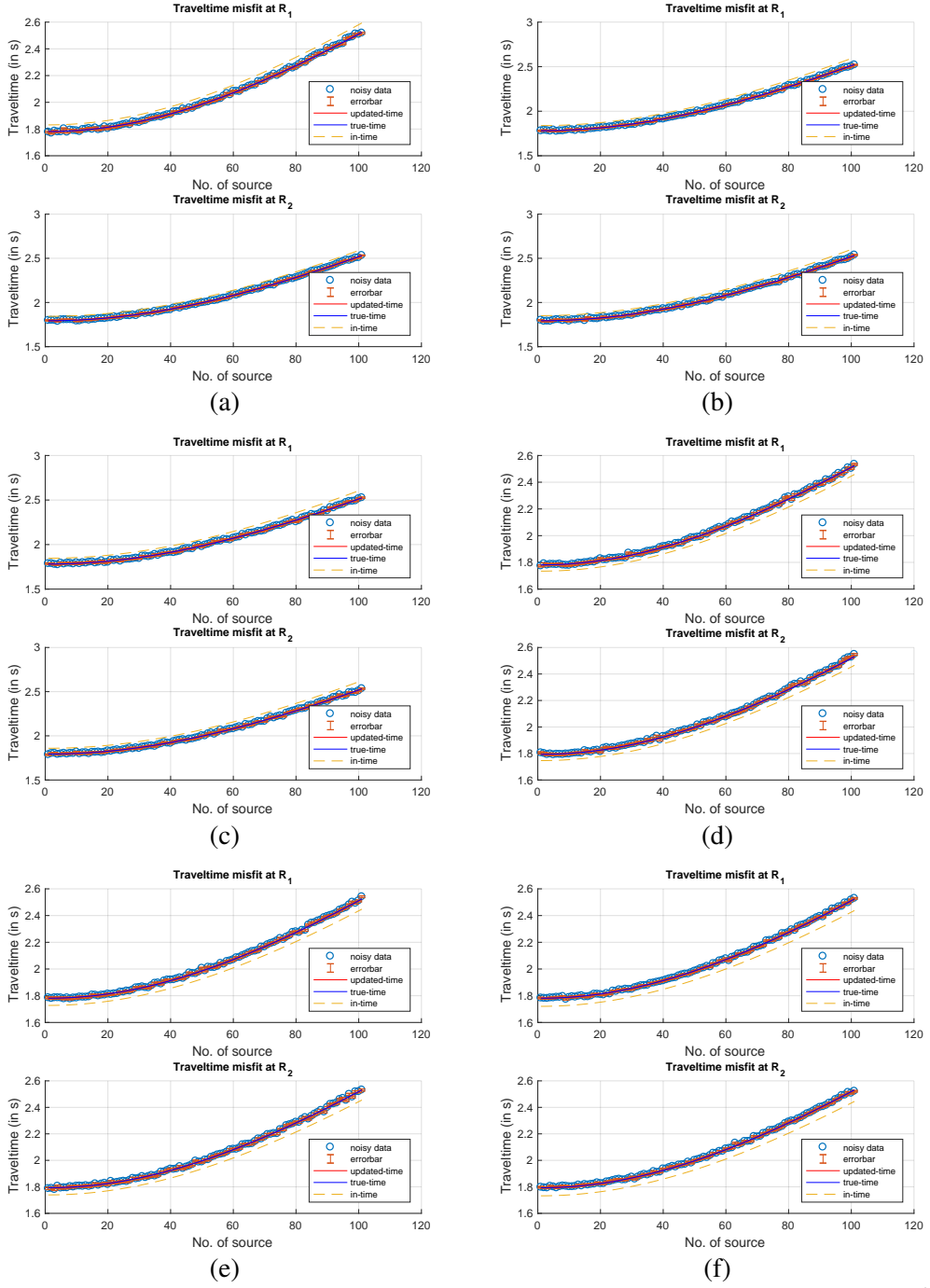


Figure 3.5: Traveltime inversion for different velocity gradients, $v_{in} = v_{true} \pm 30 (ms^{-1})$.

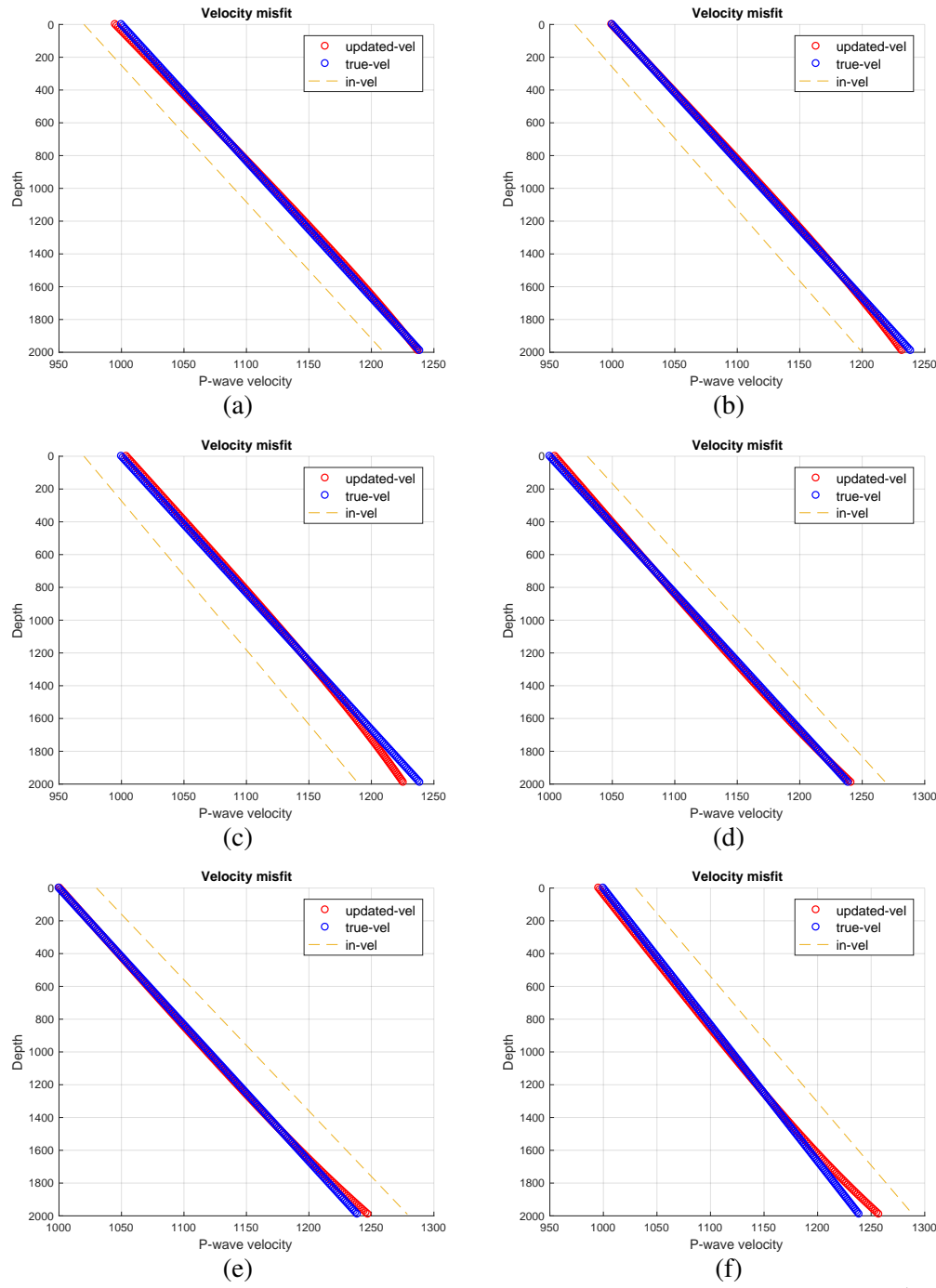


Figure 3.6: Velocity model for different velocity gradients, $v_{in} = v_{true} \pm 30 \text{ (ms}^{-1}\text{)}.$

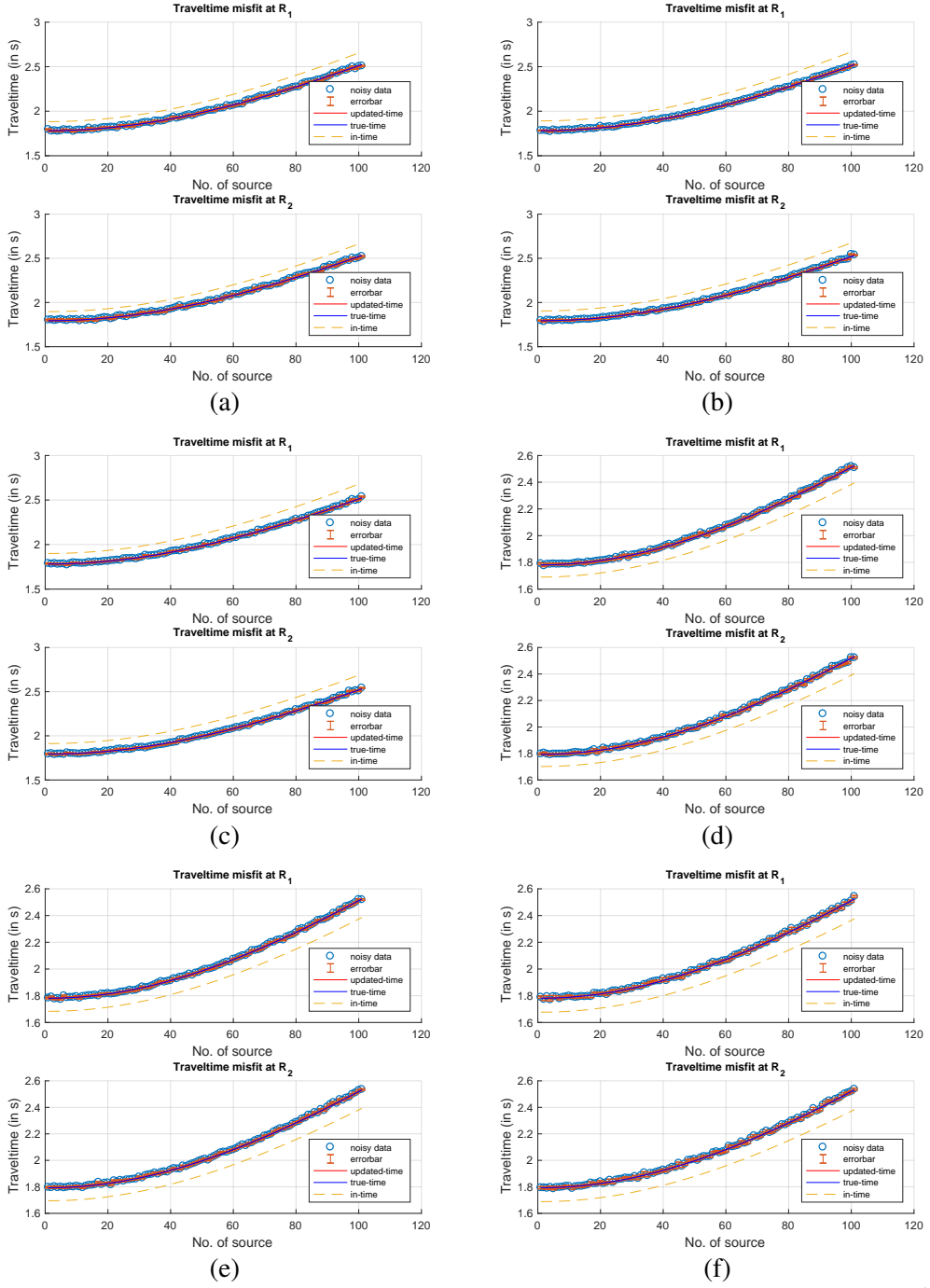


Figure 3.7: Traveltime inversion for different velocity gradients, $v_{in} = v_{true} \pm 60 (ms^{-1})$.

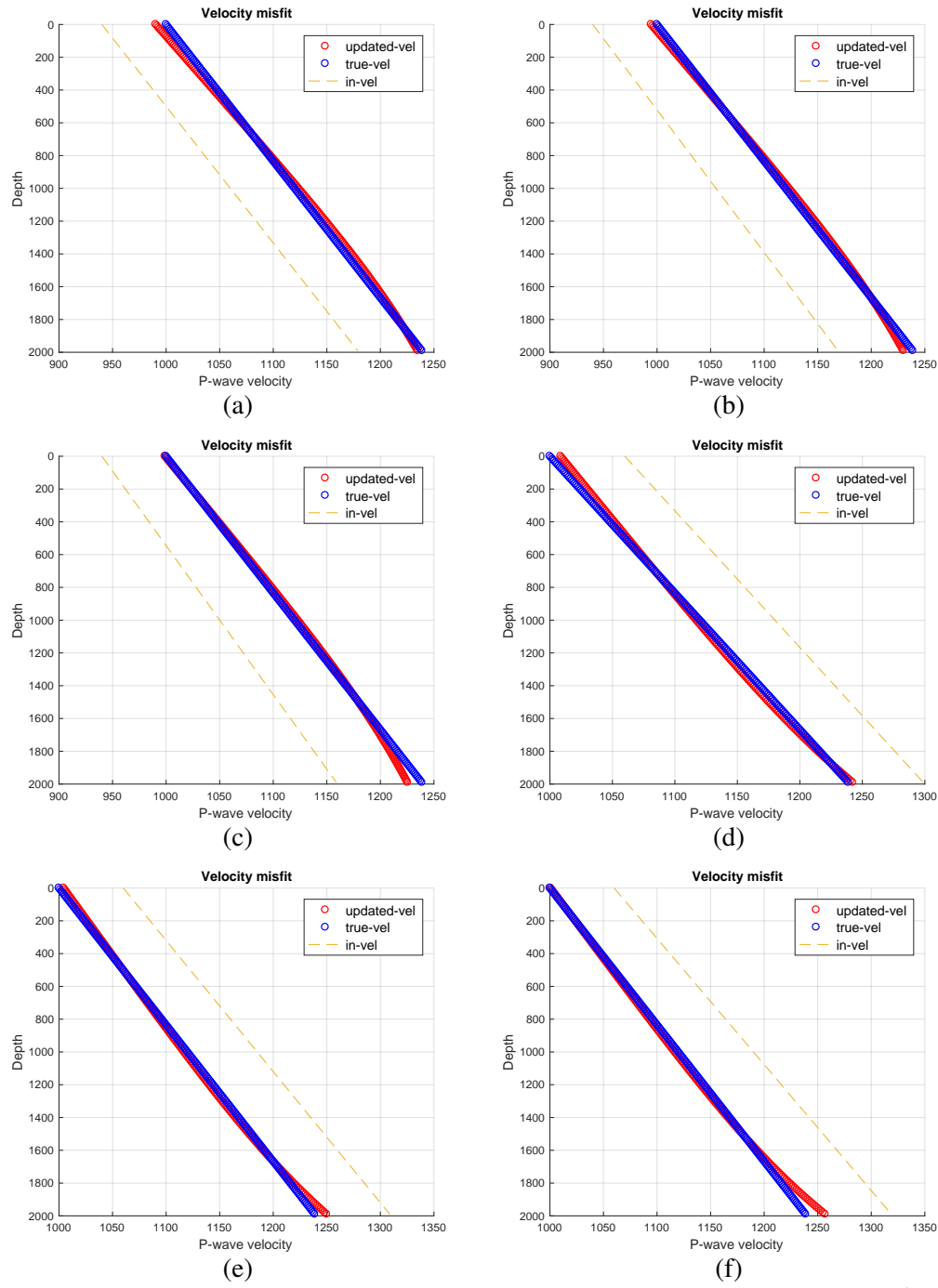


Figure 3.8: Velocity model for different velocity gradients, $v_{in} = v_{true} \pm 60 \text{ (ms}^{-1}\text{)}).$

3.4 1-D tomography : Application in real data

In this section, we apply the 1-D tomography and two-parameter inversion methods to a field data (1.4). In the two-parameter inversion, the traveltime expression is used from Slawinski and Slawinski [1999]. We develop the codes for both methods in Matlab and provide the source codes in the appendices 3.A.1, 3.A.2, and 3.A.3.

In Table 3.3, we use the traveltime data from Appendix A.1. The total number of data points is 54, and the receivers are located up to the depth of 2650.20 m. In a real case study, the velocity results from 1-D traveltime tomography can be in any order with depth. To get the linear inhomogeneity parameters, we use linear regression on the inverted velocity.

We also apply the real data on the ab model to calculate a global a and b . In Table 3.3, for the range of startup values, the two-parameter velocity inversion results do not change. The values of a and b are 1247.07 ms^{-1} and 0.4384 s^{-1} . However, the inversion results of the tomography are sensitive to the startup values. The low number of data points makes the inversion problem more sensitive to startup values.

The traveltime convergence results are shown in Figure 3.9. The velocity misfits of the inverted velocity to the reference velocity are shown in Figure 3.10. Based on the synthetic experiments, we know that the inverted velocity reproduces the reference velocity with less error if the traveltime convergence occurs faster. Therefore, we perform several tests with a range of startup values and show that tests 3 and 4 have the best startup values out of the six tests. Based on the results of experiments 3 and 4, we intuit that the inhomogeneity of the medium ranges from 0.3960 s^{-1} to 0.4037 s^{-1} . The inhomogeneity results can be improved by increasing the number of data points.

Test	a_{in}	b_{in}	a_{inv}	b_{inv}	$a_{t_{ab}}$	$b_{t_{ab}}$	$f(\mathbf{M})$	Figure
1	1225	0.40	1258.66	0.4373	1247.07	0.4384	52.01	3.9a,3.10b
2	1250	0.40	1271.63	0.4228	1247.07	0.4384	52.72	3.9b,3.10a
3	1285	0.40	1288.79	0.4037	1247.07	0.4384	51.55	3.9c,3.10c
4	1300	0.40	1295.85	0.3960	1247.07	0.4384	49.48	3.9d,3.10d
5	1315	0.40	1302.69	0.3885	1247.07	0.4384	53.79	3.9e,3.10e
6	1340	0.40	1313.67	0.3765	1247.07	0.4384	50.59	3.9f,3.10f

Table 3.3: Results of 1-D tomography and two-parameter method using real data (units of a and b are ms^{-1} and s^{-1})

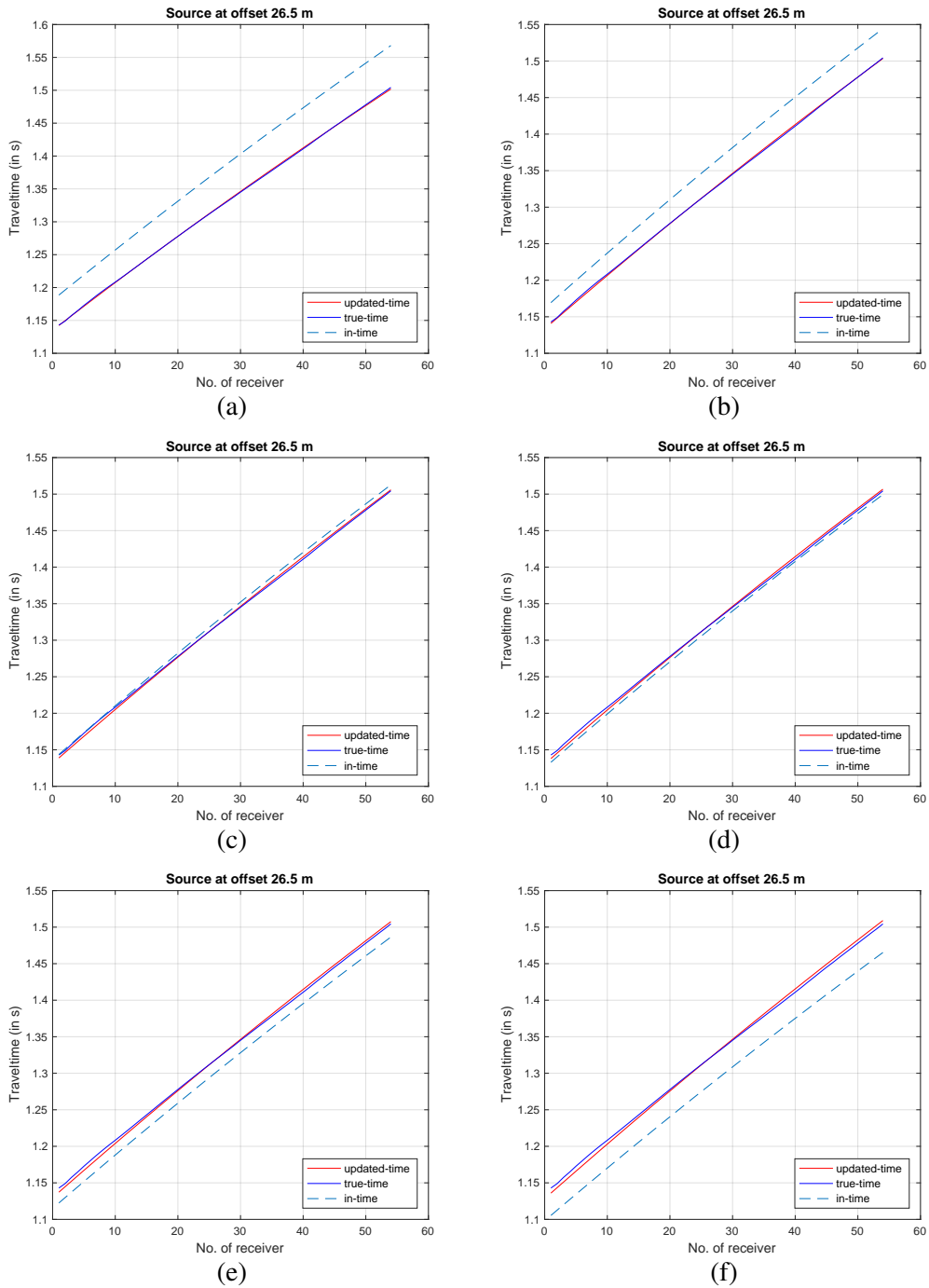


Figure 3.9: Traveltime inversion for different velocity gradients, $v_{in} = v_{true} \pm 60 (ms^{-1})$.

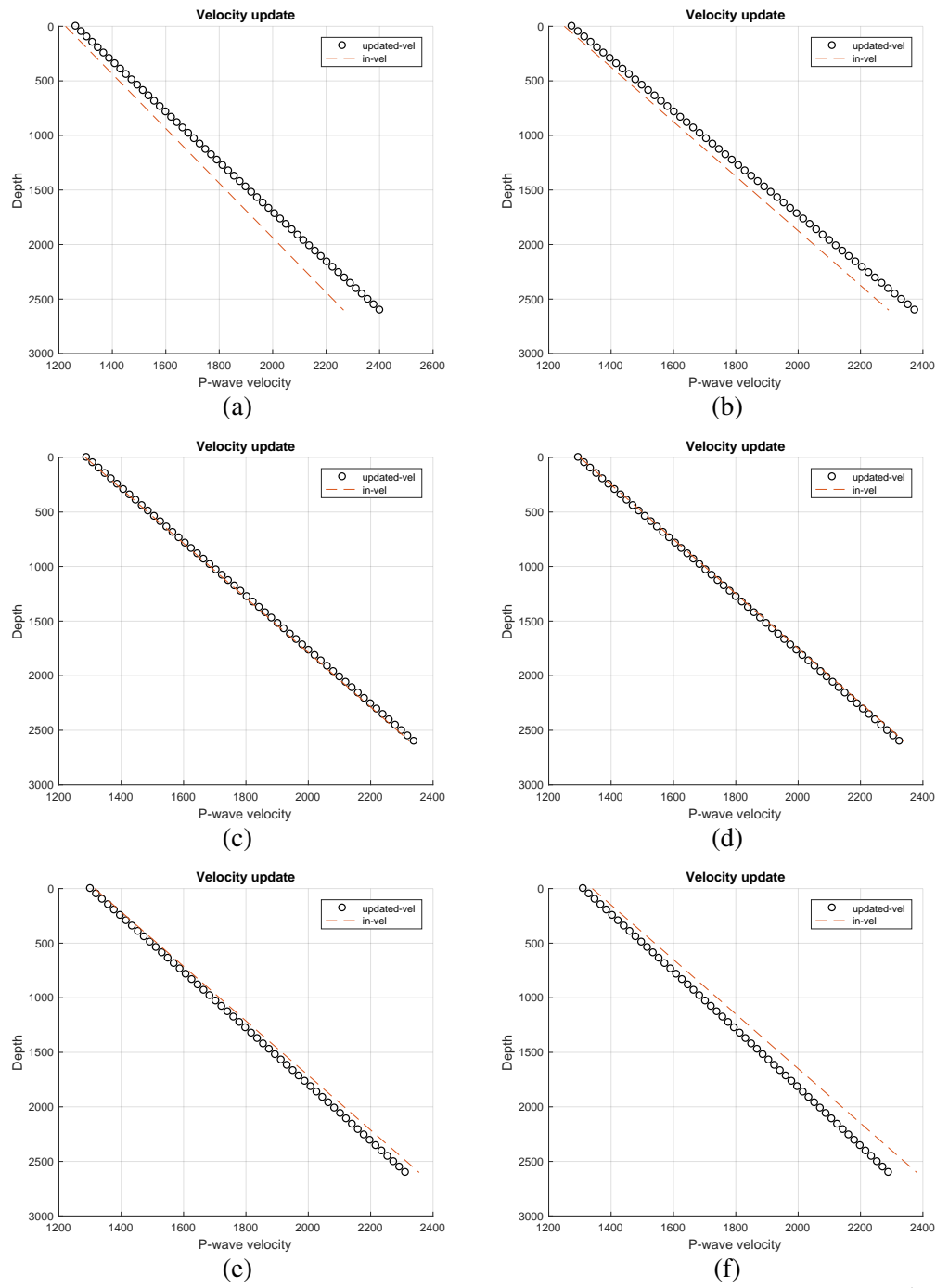


Figure 3.10: Velocity model for different velocity gradients, $v_{in} = v_{true} \pm 60\text{ (ms}^{-1}\text{)}.$

3.5 Conclusion

The synthetic experiments show that the tomography method can reproduce the reference velocity with some misfits. The misfit gets higher when there is more noise, and fewer data points.

From the two-parameter method, we find that the inhomogeneity parameter, b , is higher in comparison to the 1-D tomography.

Since, from the traveltimes data, the 1-D tomography calculates m parameters and the ab method computes only two parameters to obtain velocity, therefore, we intuit that, for finding the local inhomogeneity of a segment, the 1-D tomography method is more reliable.

In practical seismology, the velocities are measured in the well log after a few hundred meters of depth from the surface. The VSP method can be used as a proxy to obtain the inhomogeneity parameters above the well log region.

For a common region of interest, we state that the study allows us to obtain linear inhomogeneity of a medium using two different seismic methods. To examine that statement, as a future project, we plan to do a comparison study by applying the developed methods on different sites.

3.A

3.A.1 1-D tomography : synthetic data

```
1 close all; clear all ;clc  
2  
3 %% Variables from travel time data
```

```

4 rec_depth = 1985:15:2000; % Creating data array for
5 offset_fict = 0:20:2000; % Creating data array for Sources
6 % 201 sources at the surface with
7 % 20m apart from
8 N = length(rec_depth)*length(offset_fict);% Number of Layers
9 (= Number of model parameters)
10 z_p = 0:(rec_depth(end)/N):rec_depth(end);
11 M = length(rec_depth); % Number of Geophone
12 S_N = length(offset_fict); % Number of sources
13
14 for i=1:S_N
15     for k=1:M
16         x_obs(k,i) = offset_fict(i);
17     end
18 end
19 %% Similar_to_previous %%
20 for i = 1:N
21 d_z_p(i)= z_p(i+1)-z_p(i); % layer thickness
22 end
23
24
25 for k = 1:M
26     for j = 1:N

```

```

27      H_n(k,j)=d_z_p(1);
28      end
29  end
30
31 for k = 1:M
32   for j = 1:N-1
33     H_n(k,j)=d_z_p(1);
34     if sum(d_z_p(1:(j))) <= rec_depth(k)
35       H(k,j)=d_z_p(j);
36       H(k,j+1)= rec_depth(k)-sum(d_z_p(1:(j)));
37     end
38   end
39 end
40
41
42 %% Variables for initial velocity and ray parameter
43 a = 1000;
44 b = .12;
45
46 %% From here complication starts
47 for j=1:N
48   v_o_true(j) = a+(b.*z_p(j));
49   v_o(j) = (a+20)+((b).*z_p(j));
50 end
51
52

```

```

53 v_true = v_o_true;
54 v_in = v_o;
55
56
57 %% Newton's Gradient %%
58 % Initial guess for theta_in to use in Newton method
59 for i=1:S_N
60     for k=1:M
61         theta_true(k,i) = atan(x_obs(k,i)./ rec_depth(k));
62     end
63 end
64
65 % Initialize the iteration for Newton-Raphson method
66 for i=1:S_N
67     for k=1:M
68         dx_true(k,i) = 2500; % Initialize the iteration with
69             higher values
70     end
71 end
72 myCoordList_true=[]; Ite_true = 0;
73 lim_dx_true = 1e-6;
74 while (abs(dx_true(:,end)) > lim_dx_true)
75
76 for i=1:S_N
77     for k=1:M

```

```

78 ray_p_o_i_true(k,i) = sin(theta_true(k,i))./
79 v_o_true(1);
80 end
81
82 for i=1:S_N
83 for k=1:M
84 for j = 1:N
85 B_kji_i_true(k,j,i) = ray_p_o_i_true(k,i)*
86 v_o_true(j);
87 x_jki_true(j,k,i) = H(k,j).* B_kji_i_true(k,j,i)
88 ) ./ (1 - B_kji_i_true(k,j,i).^2).^(.5);
89
90 dx_prime_t1_true(j,k,i) = (H(k,j).* v_o_true(j)
91 .* cos(theta_true(k,i)))...
92 ./( v_o_true(1).*(1-B_kji_i_true(k,j,i).^2)
93 .^(.5));
94 dx_prime_t2_true(j,k,i) = (H(k,j).* v_o_true(j)
95 .* cos(theta_true(k,i)).* B_kji_i_true(k,j,i))
96 ...
97 ./ ( v_o_true(1).*(1-B_kji_i_true(k,j,i).^2)
98 .^(1.5));

```

```

96      dx_true_all_prime(j,k,i) = dx_prime_t1_true(j,k,
97                                i)+dx_prime_t2_true(j,k,i);
98
99  end
100
101 for i = 1:S_N
102   for k = 1:M
103     x_ki_true(k,i)=sum( x_jki_true(1:N,k,i)); % in m
104     dx_true_prime(k,i)= sum(dx_true_all_prime(1:N,k,i));
105   end
106 end
107 dx_true = abs(x_obs - x_ki_true);
108 theta_true = theta_true - (dx_true ./ dx_true_prime);
109 Ite_true = Ite_true+1;
110 myCoordList_true=[myCoordList_true; [Ite_true]];
111 end
112
113 for i=1:S_N
114   for k=1:M
115     ray_p_true(k,i) = sin(theta_true(k,i))./ v_o_true(1)
116     ;
117   end
118
119 for i=1:S_N

```

```

120    for k=1:M
121        for j = 1:N
122            t_jki_true(j,k,i) = H(k,j)./( v_o_true(j).*((1-
123                ray_p_true(k,i).*v_o_true(j)).^2).^(.5)); % in s
124        end
125    end
126
127    for i = 1:S_N
128        for k = 1:M
129            t_ki_true(k,i)=sum(t_jki_true(1:N,k,i)); % in s
130        end
131    end
132
133 %% Optimization Starts %%
134
135 lambda = 1; misfit_fn = 10^4; Ite_m = 0; myCoordList_m=[];
136 myCoordList_t_ki = [];
137 while (misfit_fn >= 202)
138
139 %% Newton-Raphson method %%
140 % Initial guess for theta_in to use in Newton-Raphson method
141 for i=1:S_N
142     for k=1:M
143         theta_in(k,i) = atan(x_obs(k,i)./ rec_depth(k));

```

```

144      end
145  end
146 % Initialize the iteration for Newton method
147 myCoordList_in=[]; Ite_in = 0;
148 for i=1:S_N
149   for k=1:M
150     dx_in(k,i) = 2500; % Initialize the iteration with
151       higher values
152   end
153
154
155 myCoordList_in=[]; Ite_in = 0;
156 lim_dx_in = 1e-6;
157 while (abs(dx_in(:,end)) > lim_dx_in)
158
159 for i=1:S_N
160   for k=1:M
161     ray_p_o_i_in(k,i) = sin(theta_in(k,i))./ v_o(1);
162   end
163 end
164
165 for i=1:S_N
166   for k=1:M
167     for j = 1:N
168       B_kji_i_in(k,j,i) = ray_p_o_i_in(k,i)*v_o(j);

```

```

169
170      x_jki_in(j,k,i) = H(k,j) .* B_kji_i_in(k,j,i) ./
171          (1 - B_kji_i_in(k,j,i).^2).^(.5);
172
173      dx_prime_t1_in(j,k,i) = (H(k,j).*v_o(j).*cos(
174          theta_in(k,i)))...
175              ./ (v_o(1).*(1-B_kji_i_in(k,j,i).^2).^(.5));
176
177      dx_prime_t2_in(j,k,i) = (H(k,j).*v_o(j).*cos(
178          theta_in(k,i)).*B_kji_i_in(k,j,i))...
179              ./ (v_o(1).*(1-B_kji_i_in(k,j,i).^2).^(.5));
180
181      end
182  end
183
184  for i = 1:S_N
185      for k = 1:M
186          x_ki_in(k,i)=sum(x_jki_in(1:N,k,i)); % in m
187          dx_in_prime(k,i)= sum(dx_in_all_prime(1:N,k,i));
188      end
189  end
190  dx_in = abs(x_obs - x_ki_in);

```

```

191 theta_in = theta_in - (dx_in ./ dx_in_prime);
192 Ite_in = Ite_in + 1;
193 myCoordList_true=[myCoordList_in; [Ite_in]];
194 end
195
196 for i=1:S_N
197     for k=1:M
198         ray_p_in(k,i) = sin(theta_in(k,i)) ./ v_o(1);
199     end
200 end
201
202 for i=1:S_N
203     for k=1:M
204         for j = 1:N
205             B_kji(k,j,i) = ray_p_in(k,i).*v_o(j);
206             t_jki_in(j,k,i) = H(k,j)./(v_o(j).*((1-(B_kji(k,j,i)).^2).^(.5)); % in s
207         end
208     end
209 end
210
211 for i = 1:S_N
212     for k = 1:M
213         t_ki_in(k,i)=sum(t_jki_in(1:N,k,i)); % in s
214     end
215 end

```

```

216
217
218 %Calculation of the derivatives from initial estimates
219 for i=1:S_N
220     for k=1:M
221         for j = 1:N
222             ddvj_tk(k,j,i) = -H_n(k,j)./(v_o(j).^2.*((1-B_kji
223                                         (k,j,i).^2).^(.5))...
224                                         +(ray_p_in(k,i).^2.*H_n(k,j))./(1-B_kji(k,j
225                                         ,i).^2).^(1.5));
226         end
227     end
228 end
229 %%%%%% Adding_Noise %%%%%%
230 t = t_ki_in(:);
231 t_true = t_ki_true(:);
232 noiseSigma = 0.01 * t_true; % standard deviation =
233 noise = noiseSigma .* randn(length(t_true),1); % considering
234 mean = 0
235 noisySignal = t_true + noise;
236 Y_c = noisySignal;
237 dt = (Y_c - t);
238 dt = reshape(dt,[M,S_N]);

```

```

238 noise = reshape( noise ,[M,S_N]) ;
239 Y_c = reshape( Y_c ,[M,S_N]) ;
240 %%%%%% Adding_Noise %%%%%%
241
242 for i=1:S_N
243     for k=1:M
244         for j = 1:N
245             term_A1(k,j,i) = ddvj_tk(k,j,i);
246         end
247     end
248 end
249
250 term_A = [term_A1];
251 %
252 %

253 %%%%%% Conversion to vectors and
254 %matrix%%%%%
255 C = dt(:);
256
257 A_c_terms = [];
258 for ll = 1:size(term_A,3)
259     A_c_terms = cat(1,A_c_terms,term_A(:,:,ll));
260 end

```

```

261 A = A_c_terms;

262

263 A_T_A = transpose(A)*A;

264 A_T_C = transpose(A)*C;

265

266 for i = 1:(N)

267 for j = 1:(N)

268     if i==j

269         s_ij(i,j)=1./sqrt(A_T_A(i,j));

270     elseif i ~= j

271         s_ij(i,j)=0;

272 end

273 end

274 end

275 S = s_ij;

276 A_T_A_ast = S.'*A_T_A*S;

277 A_T_C_ast = S.'*A_T_C;

278

279 I = eye(N,N);

280 lembda = I*1000;

281

282 inv_t_ast = A_T_A_ast+lembda;

283 X_ast = inv(inv_t_ast)*A_T_C_ast;

284 X = S.* X_ast;

285

286

```

```

287 dt_up = dt(:);
288 misfit_fn = (sum((dt_up(:)./noise(:)).^2));
289
290 dv = X. ';
291 v_o = v_o + dv;
292 v_f = v_o;
293 lembda = lembda * 0.1;
294 Ite_m = Ite_m+1;
295 myCoordList_m=[myCoordList_m; [Ite_m , misfit_fn]];
296 myCoordList_t_ki=[myCoordList_t_ki; [t_ki_in]];
297 %%%%%%%%%%%%%%%%%%%%%%%%%%%%%%%%%%%%%%
298 end
299
300 %%%%%%%%%%%%%%%%%%%%%%%%%%%%%%%%%%%%%%
301 figure(1) % Travelttime plot
302 %%%%%%%%%%%%%%%%%%%%%%%%%%%%%%%%%%%%%%
303 subplot(2,1,1)
304 time_k1_in = myCoordList_t_ki(1,:);
305 time_k1_true = t_ki_true(1,:);
306 time_k1_f = t_ki_in(1,:);
307 NT = Y_c(1,:); %Noisy Travelttime
308 err = noise(1,:);
309 err = std(err).*ones(size(err));
310
311 indx = 1:1:length(NT);
312 scatter(indx,NT);

```

```

313 hold on;
314 errorbar(indx, NT, err, 'LineStyle', 'none');
315 hold on;
316
317 plot(time_k1_f, 'r')
318 hold on
319
320 plot(time_k1_true, 'b')
321 hold on
322
323 plot(time_k1_in, '--')
324 legend({'noisy data', 'errorbar', 'updated-time', 'true-time',
325         'in-time'}, 'Location', 'southeast', 'FontSize', 8)
326 xlabel('No. of source', 'FontSize', 12)
327 ylabel('Travelttime (in s)', 'FontSize', 12)
328 title('Travelttime misfit_fn at R_{1}', 'FontSize', 10)
329 grid on
330
331 % When more than one receiver
332 subplot(2,1,2)
333 time_k1_in = myCoordList_t_ki(2,:);
334 time_k1_true = t_ki_true(2,:);
335 time_k1_f = t_ki_in(2,:);
336 NT = Y_c(2,:); %Noisy Travelttime
337 err = noise(2,:);

```

```

338 err = std(err).*ones(size(err));

339

340 indx = 1:1:length(NT);

341 scatter(indx,NT);

342 hold on;

343 errorbar(indx, NT, err, 'LineStyle', 'none');

344 hold on;

345

346 plot(time_k1_f, 'r')

347 hold on

348

349 plot(time_k1_true, 'b')

350 hold on

351

352 plot(time_k1_in, '--')

353 legend({'noisy data', 'errorbar', 'updated-time', 'true-time',
          'in-time'}, 'Location', 'southeast', 'FontSize', 8)

354 xlabel('No. of source', 'FontSize', 12)

355 ylabel('Traveltime (in s)', 'FontSize', 12)

356 title('Traveltime misfit_fn at R_{2}', 'FontSize', 10)

357 grid on

358

359

360

361 %%%%%%
362 figure(2) % Velocity plot

```

```

363 %
364
365
366 z_p_plot = z_p(1:end-1);
367 scatter(v_f, z_p_plot, 'r')
368 hold on
369 scatter(v_true, z_p_plot, 'b')
370 hold on
371 plot(v_in, z_p_plot, '--')
372 legend({'updated-vel', 'true-vel', 'in-vel'}, 'Location',
373         'northeast', 'FontSize', 12)
374 set(gca, 'Ydir', 'reverse')
375 xlabel('P-wave velocity', 'FontSize', 12)
376 ylabel('Depth', 'FontSize', 12)
377 title('Velocity misfit_fn', 'FontSize', 12)
378 grid on

```

3.A.2 1-D tomography : real data

```
1 close all; clear all ;clc
2 %% Data upload
3 [num,txt,raw] = xlsread('mizzen_o_16_cs.xlsm'); % Checkshot
4 data
5 vert_depth = num(:,2);
6 vert_depth = rmmissing(vert_depth)-5; % True vertical depth
7 from source)
8 travelttime = num(:,3);
9 travelttime = rmmissing(travelttime); % Measured travelttime
10 from source to receivers
11 travelttime = travelttime(1:54);
12 offset = 26.5; % Source offset 26.5 m
13 sigma = .0003; % from time picking
14
15 %% Variables from travel time data
16 rec_depth = vert_depth(1:54).';
17 z_p = 0:(rec_depth(end)/54):rec_depth(end);
18 N = length(z_p)-1;
19 M = length(rec_depth); % Number of Geophone
20 S_N = length(offset); % Number of sources
21
22 for i=1:S_N
23     for k=1:M
```

```

22      x_obs(k,i) = offset(i);
23      end
24  end
25 %
26
27 %%%%%%%%%%%%%%%%%%%%%%%%%%%%%%%%% Similar_to_previous %%%%%%%%%%%%%%%%%%%%%%%%%%%%%%%%%
28 for i = 1:N
29 d_z_p(i)= z_p(i+1)-z_p(i); % layer thickness
30 end
31
32
33 % Not working this H?
34 for k = 1:M
35     for j = 1:N
36         H_n(k,j)=d_z_p(1);
37     end
38 end
39
40 for k = 1:M
41     for j = 1:N-1
42         H_n(k,j)=d_z_p(1);
43         if sum(d_z_p(1:(j))) <= rec_depth(k)
44             H(k,j)=d_z_p(j);
45             H(k,j+1)= rec_depth(k)-sum(d_z_p(1:(j)));
46         end
47     end

```

```

48 end

49

50

51 %% Variables for initial velocity and ray parameter

52 a_in = 1250;

53 b_in = 0.40;

54

55 %% Initial Velocity

56 for j=1:N

57     v_o(j) = a_in+(b_in.*z_p(j));

58 end

59 v_in = v_o;

60

61

62

63 %%%%%% Optimization Starts %%%%%%

64 %%%%%% Initialize Levenberg–Marquardt Method %%%%%%

65 lembda = 1e3; misfit_fn = 10^4; Ite_m = 0; myCoordList_m=[];

66 myCoordList_t_ki = [];

67 while (misfit_fn >= 54)

68

69 %%%%%% Newton's Gradient %%%%%%5%%

70 % Initial guess for theta_in to use in Newton method

71 for i=1:S_N

72     for k=1:M

73         theta_in(k,i) = atan(x_obs(k,i)./ rec_depth(k));

```

```

74      end

75  end

76 % Initialize the iteration for Newton method

77 myCoordList_in=[]; Ite_in = 0;

78 for i=1:S_N

79     for k=1:M

80         dx_in(k,i) = 2500;

81     end

82 end

83

84

85 myCoordList_in=[]; Ite_in = 0;

86 lim_dx_in = 1e-10;

87 while (abs(dx_in(:,end)) > lim_dx_in)

88

89 for i=1:S_N

90     for k=1:M

91         ray_p_o_i_in(k,i) = sin(theta_in(k,i))./ v_o(1);

92     end

93 end

94

95 for i=1:S_N

96     for k=1:M

97         for j = 1:N

98             B_kji_i_in(k,j,i) = ray_p_o_i_in(k,i)*v_o(j);

99

```

```

100      x_jki_in(j,k,i) = H(k,j) .* B_kji_i_in(k,j,i) ./
101          (1 - B_kji_i_in(k,j,i).^2).^(.5);
102
103      dx_prime_t1_in(j,k,i) = (H(k,j).*v_o(j).*cos(
104          theta_in(k,i)))...
105          ./ (v_o(1).*(1-B_kji_i_in(k,j,i).^2).^(.5));
106      dx_prime_t2_in(j,k,i) = (H(k,j).*v_o(j).*cos(
107          theta_in(k,i)).*B_kji_i_in(k,j,i))...
108          ./ (v_o(1).*(1-B_kji_i_in(k,j,i).^2).^(.5));
109      dx_in_all_prime(j,k,i) = dx_prime_t1_in(j,k,i) +
110          dx_prime_t2_in(j,k,i);
111      end
112  end
113
114  for i = 1:S_N
115      for k = 1:M
116          x_ki_in(k,i)=sum(x_jki_in(1:N,k,i)); % in m
117          dx_in_prime(k,i)= sum(dx_in_all_prime(1:N,k,i));
118      end
119  end
120  dx_in = abs(x_obs - x_ki_in);
121  theta_in = theta_in - (dx_in./dx_in_prime);

```

```

122 Ite_in = Ite_in+1;
123 myCoordList_true=[myCoordList_in; [Ite_in]];
124 end
125
126 for i=1:S_N
127     for k=1:M
128         ray_p_in(k,i) = sin(theta_in(k,i))./ v_o(1);
129     end
130 end
131
132 for i=1:S_N
133     for k=1:M
134         for j = 1:N
135             B_kji(k,j,i) = ray_p_in(k,i).*v_o(j);
136             t_jki_in(j,k,i) = H(k,j)./(v_o(j).*((1-(B_kji(k,j
137 ,i)).^2).^(.5)); % in s
138         end
139     end
140
141 for i = 1:S_N
142     for k = 1:M
143         t_ki_in(k,i)=sum(t_jki_in(1:N,k,i)); % in s
144     end
145 end
146

```

```

147
148 %Calculation of the derivatives from initial estimates
149 for i=1:S_N
150     for k=1:M
151         for j = 1:N
152             ddvj_tk(k,j,i) = -H_n(k,j)./(v_o(j).^2.*((1-B_kji
153                                         (k,j,i).^2).^(.5))...
154                                         + (ray_p_in(k,i).^2.*H_n(k,j))./(1-B_kji(k,j
155                                         ,i).^2).^(1.5));
156         end
157     end
158 end
159 %% Adding_Noise %%
160 t = t_ki_in(:);
161 t_true = traveltime(:);
162 dt = (t_true - t);
163 dt = reshape(dt,[M,S_N]);
164 t_true = reshape(t_true,[M,S_N]);
165 %% Adding_Noise %%
166
167 for i=1:S_N
168     for k=1:M
169         for j = 1:N
170             term_A1(k,j,i) = ddvj_tk(k,j,i);

```

```

171      end
172      end
173  end
174
175 term_A = [term_A1];
176 %
177 %%%%%%%%%%%%%%%%%%%%%%%%%%%%%%%%%%%%%%%%%%%%%%%%%%%%%% Conversion to vectors and
178 %matrix%%%%%%%%%%%%%%%%%%%%%%%%%%%%%%%%%%%%%%%%%%%%%
179 C = dt(:);
180
181 A_c_terms = [];
182 for ll = 1:size(term_A,3)
183     A_c_terms = cat(1,A_c_terms,term_A(:,:,ll));
184 end
185 A = A_c_terms;
186
187 A_T_A = transpose(A)*A;
188 A_T_C = transpose(A)*C;
189
190 for i = 1:(N)
191     for j = 1:(N)
192         if i==j
193             s_ij(i,j)=1./sqrt(A_T_A(i,j));
194         elseif i ~= j
195             s_ij(i,j)=0;

```

```

196      end
197  end
198 end
199 S = s_ij ;
200 A_TA_ast = S.' * A_TA*S ;
201 A_TC_ast = S.' * A_TC;
202
203 I = eye(N,N);
204 lembda = I*1000;
205
206 inv_t_ast = A_TA_ast+lembda;
207 X_ast = inv(inv_t_ast)*A_TC_ast;
208 X = S.' * X_ast;
209
210
211 dt_up = dt(:);
212 misfit_fn = sum(dt_up(:)./ sigma).^2;
213
214 dv = X. ';
215 v_o = v_o + dv;
216 v_f = v_o;
217 lembda = lembda * 0.1;
218 Ite_m = Ite_m+1;
219 myCoordList_m=[myCoordList_m; [Ite_m , misfit_fn]];
220 myCoordList_t_ki=[myCoordList_t_ki ; [t_ki_in]];
221 end

```

```

222
223 %%%
224 figure(1)
225 %%%
226 time_k1_in = myCoordList_t_ki(1:54,1);
227 time_k1_true = t_true;
228 time_k1_f = t_ki_in;
229 time_k1_f = myCoordList_t_ki((end-53):end,1);

230
231 plot(time_k1_f, 'r')
232 hold on
233 plot(time_k1_true, 'b')
234 hold on
235 plot(time_k1_in, '--')
236 legend({'updated-time', 'true-time', 'in-time'}, 'Location', 'southeast', 'FontSize', 10)
237 xlabel('No. of receiver', 'FontSize', 12)
238 ylabel('Traveltime (in s)', 'FontSize', 12)
239 title('Source at offset 26.5 m', 'FontSize', 12)
240 grid on

241
242 z_p_plot = z_p(1:end-1);
243 p_n = polyfit(z_p_plot, v_f, 1);
244 yfit = polyval(p_n, z_p_plot);
245 p_nn = polyfit(z_p_plot(39:end), v_f(39:end), 1);
246 yfitn = polyval(p_nn, z_p_plot(39:end));

```

```

247
248
249 %%%%%%%%%%%%%%%%%%%%%%%%%%%%%%%%%%%%%%
250 figure(2)
251 %%%%%%%%%%%%%%%%%%%%%%%%%%%%%%%%%%%%%%
252 scatter(v_f,z_p_plot,'k')
253 hold on
254 plot(v_in,z_p_plot,'--')
255 legend('updated-vel','in-vel')
256 set(gca,'Ydir','reverse')
257 xlabel('P-wave velocity','FontSize',12)
258 ylabel('Depth','FontSize',12)
259 title('Velocity update','FontSize',12)
260 grid on
261
262 upd = [a_in b_in p_n(1,2) p_n(1,1) p_nn(1,2) p_nn(1,1)
263 misfit_fn]
264
265 rec_depth_t = rec_depth.';
266 ind_t = 1:length(rec_depth_t);
267 ind_t = ind_t.';
268
269 upd_t = [ind_t rec_depth_t traveltime];

```

3.A.3 *ab* model inversion : real data

```
1 close all; clear all ;clc
2 [num,txt,raw] = xlsread('mizzen_o_16_cs.xlsm'); % Checkshot
3 data
4 vert_depth = num(:,2);
5 vert_depth = rmmissing(vert_depth)-5; % True vertical depth
   from source (-5 because MSL-SP=5m)
6 traveltimes = num(:,3);
7 traveltimes = rmmissing(traveltimes); % Measured travetime
   from source to receiver
8 traveltimes = traveltimes(1:54);
9 offset = 26.5; % Source offset 26.5 m
10
11 %% Variables from travel time data
12 rec_depth = vert_depth(1:54);
13 d_p = length(rec_depth);
14
15
16
17 Depth_of_layer = 0; % in m
18 Depth_of_receiver = rec_depth; % in m
19 z = Depth_of_receiver - Depth_of_layer;
20 x_o = offset;
21 t_d = traveltimes(1:d_p,1);
```

```

22 a_in = 1285;
23 b_in = .40;
24
25 lb=[eps eps];
26 ub=[inf inf];
27 x0=[a_in b_in];
28
29
30 fun = @(X) fn_ab(X(1),X(2), z, x_o, t_d);
31 x = lsqnonlin(fun,x0,lb,ub)
32
33 a_p = x(1);
34 b_p = x(2);
35
36 t_test = fn_ab(a_p,b_p, z, x_o, t_d);
37 mis_fit = sqrt(t_test.^2);
38 t_mean = mean(t_test)

39
40
41 function fun=fn_ab(a, b, z, x, t_d)
42 p_b_1 = (b.^2.*x.^2) + a.^2 + (a+b.*z).^2;
43 p_b_2 = 2.*a.* (a+b.*z);
44 p = (2.*b.*x). / sqrt(p_b_1.^2-p_b_2.^2);
45
46 term_3 = (a + (b.*z)) ./ a;
47 term_4 = sqrt(1-(a.^2).* (p.^2));

```

```
48 term_5 = sqrt(1 - ((term_3 .* a).^2) .* (p.^2));  
49  
50 t_time = (1./b).*log( (term_3).*((1+term_4)./(1+term_5)));  
51  
52 fun = abs(t_time - t_d);  
53 end
```

Chapter 4

On relations of anisotropy and linear inhomogeneity

4.1 Introduction

In this chapter *, we parametrize an equivalent medium, resulting from the Backus [1962] average, concerning linear inhomogeneity parameters of its constituent isotropic layers. The parametrization allows us to make a relationship between the anisotropy and layer inhomogeneity, which is, in the seismological context, a meaningful relationship. We derive an analytical relationship between the anisotropy and the linear inhomogeneity parameters, which forms a system of three equations for nine unknowns. The anisotropy parameters are characterized by the Thomsen [1986] parameters.

To obtain well-posedness, we reduce the number of unknown parameters by considering two seismological methods. The methods, 1-D tomography and two-parameter velocity inversion, are developed in Chapter 3. We use the inversion results from the two methods,

*The contents of this chapter is a modification of the work shown by Abu Sayed and Stanoev [2019].

for a particular region of interest, to assess the validity of the analytical relation.

Since the outcomes of the seismological methods are a pair of inhomogeneity parameters and using one of the parameters from each method allows us to obtain the solution of the analytical relation, therefore, the resultant solution from the analytical relation can also be examined by comparing it with the results of the seismological methods.

4.2 Equivalent medium parametrization

As discussed in Abu Sayed and Stanev [2019], we parametrize a transversely isotropic equivalent medium resulting from the Backus average of thin, intrinsically homogeneous, isotropic layers, which we refer to as the *Backus medium*. We assume that a stack of such constituent layers is inhomogeneous and possesses a constant-velocity gradient that increases linearly with depth [see, e.g., Slawinski and Slawinski, 1999]. Specifically, for both P and S waves,

$$v_P(z) = a_P + b_P z \quad \text{and} \quad v_S(z) = a_S + b_S z, \quad (4.1)$$

where $a_{P,S}$ are the wavespeeds at the top of the medium, $b_{P,S}$ are positive velocity-gradient constants, and z is the depth.

4.2.1 Elasticity parameters in TI media

Following the definition of Backus [1962, Section 3], the average of a function $f(z)$ of width ℓ' is the moving average given by

$$\bar{f}(z) = \int_{-\infty}^{\infty} w(\zeta - z) f(\zeta) d\zeta, \quad (4.2)$$

As discussed in chapter 2, the result of performing average (4.2) on isotropic layers results is a homogeneous TI medium, where the corresponding elasticity parameters, which are referred to as *Backus parameters*, are

$$c_{1111}^{\overline{\text{TI}}} = \left(\frac{c_{1111} - 2c_{2323}}{c_{1111}} \right)^2 \left(\frac{1}{c_{1111}} \right)^{-1} + \left(\frac{4(c_{1111} - c_{2323})c_{2323}}{c_{1111}} \right), \quad (4.3\text{a})$$

$$c_{1122}^{\overline{\text{TI}}} = \left(\frac{c_{1111} - 2c_{2323}}{c_{1111}} \right)^2 \left(\frac{1}{c_{1111}} \right)^{-1} + \left(\frac{2(c_{1111} - 2c_{2323})c_{2323}}{c_{1111}} \right), \quad (4.3\text{b})$$

$$c_{1133}^{\overline{\text{TI}}} = \left(\frac{c_{1111} - 2c_{2323}}{c_{1111}} \right) \left(\frac{1}{c_{1111}} \right)^{-1}, \quad (4.3\text{c})$$

$$c_{1212}^{\overline{\text{TI}}} = \overline{c_{2323}}, \quad (4.3\text{d})$$

$$c_{2323}^{\overline{\text{TI}}} = \left(\frac{1}{c_{2323}} \right)^{-1}, \quad (4.3\text{e})$$

$$c_{3333}^{\overline{\text{TI}}} = \left(\frac{1}{c_{1111}} \right)^{-1}. \quad (4.3\text{f})$$

Since the weighting function, w , in integral (4.2), is continuous and symmetric, the Backus average may be written as a weighted average [e.g., Slawinski, 2018, Section 4.2.2]. Herein, the Backus average is weighted by layer thickness. For density-scaled VSP measurements, $v_P = \sqrt{c_{1111}}$ and $v_S = \sqrt{c_{2323}}$; this allows for a reparametrization of parameters (4.3a)–(4.3f) in terms of linear-inhomogeneity parameters (4.1). For example, Backus parameter (4.3d) may be rewritten as [Abu Sayed and Stanoev, 2019]

$$\begin{aligned} c_{1212}^{\overline{\text{TI}}} = \overline{c_{2323}} &= \frac{1}{h_2 - h_1} \int_{h_1}^{h_2} c_{2323} dz = \frac{1}{h_2 - h_1} \int_{h_1}^{h_2} (a_S + b_S z)^2 dz \\ &= \frac{1}{3} (3a_S^2 + 3a_S b_S (h_1 + h_2) + b_S^2 (h_1^2 + h_1 h_2 + h_2^2)). \end{aligned} \quad (4.4)$$

For Backus parameter (4.3a), we commence with the first term, where

$$\left(\frac{c_{1111} - 2c_{2323}}{c_{1111}} \right) = \frac{1}{h_2 - h_1} \int_{h_1}^{h_2} \left(1 - 2 \frac{v_S^2}{v_P^2} \right) dz = \frac{1}{h_2 - h_1} \int_{h_1}^{h_2} \left(1 - 2 \frac{(a_S + b_S z)^2}{(a_P + b_P z)^2} \right) dz = 1 - \frac{2I_1}{h_2 - h_1} \quad (4.5)$$

and

$$I_1 = \int_{h_1}^{h_2} \frac{(a_S + b_S z)^2}{(a_P + b_P z)^2} dz = \frac{h_2 b_S^2}{b_P^2} - \frac{h_1 b_S^2}{b_P^2} + \frac{\ln(a_P + h_1 b_P) (2a_P b_S^2 - 2a_S b_P b_S)}{b_P^3} - \frac{\ln(a_P + h_2 b_P) (2a_P b_S^2 - 2a_S b_P b_S)}{b_P^3} + \frac{a_P^2 b_S^2 - 2a_P a_S b_P b_S + a_S^2 b_P^2}{b_P (h_1 b_P^3 + a_P b_P^2)} - \frac{a_P^2 b_S^2 - 2a_P a_S b_P b_S + a_S^2 b_P^2}{b_P (h_2 b_P^3 + a_P b_P^2)}. \quad (4.6)$$

And for the second term in parameter (4.3a),

$$\left(\frac{1}{c_{1111}} \right)^{-1} = \left(\frac{1}{v_P^2} \right)^{-1} = \left(\frac{1}{h_2 - h_1} \int_{h_1}^{h_2} \frac{1}{(a_P + b_P z)^2} dz \right)^{-1} = (h_2 - h_1) \left(\int_{h_1}^{h_2} (a_P + b_P z)^{-2} dz \right)^{-1}.$$

Replacing u for $a_P + b_P z$, which gives $dz = \frac{du}{b_P}$, and adjusting the limits, $h_1 \rightarrow a_P + b_P h_1$ and $h_2 \rightarrow a_P + b_P h_2$, we attain

$$\begin{aligned} \left(\frac{1}{c_{1111}} \right)^{-1} &= (h_2 - h_1) \left(\int_{a_P + b_P h_1}^{a_P + b_P h_2} u^{-2} \frac{du}{b_P} \right)^{-1} = (h_2 - h_1) \left(\frac{-u^{-1}}{b_P} \Big|_{a_P + b_P h_1}^{a_P + b_P h_2} \right)^{-1} \\ &= (h_2 - h_1) (-b_P) \left((a_P + b_P h_2)^{-1} - (a_P + b_P h_1)^{-1} \right)^{-1} \\ &= (a_P + b_P h_1) (a_P + b_P h_2). \end{aligned} \quad (4.7)$$

Similarly, for the last term in parameter (4.3a),

$$\begin{aligned} \overline{\left(\frac{4(c_{1111} - c_{2323})c_{2323}}{c_{1111}} \right)} &= \frac{4}{h_2 - h_1} \left(\int_{h_1}^{h_2} (a_S + b_S z)^2 dz - \int_{h_1}^{h_2} \frac{(a_S + b_S z)^4}{(a_P + b_P z)^2} dz \right), \\ \overline{\left(\frac{4(c_{1111} - c_{2323})c_{2323}}{c_{1111}} \right)} &= \frac{4}{h_2 - h_1} (I_2 - I_3), \end{aligned} \quad (4.8)$$

where

$$I_2 = \int_{h_1}^{h_2} (a_S + b_S z)^2 dz = \frac{1}{3} (h_2 - h_1) (3a_S^2 + 3a_S b_S (h_1 + h_2) + b_S^2 (h_1^2 + h_1 h_2 + h_2^2)), \quad (4.9)$$

and

$$\begin{aligned} I_3 &= \int_{h_1}^{h_2} \frac{(a_S + b_S z)^4}{(a_P + b_P z)^2} dz = h_2 \left(\frac{2a_P \left(\frac{2a_P b_S^4}{b_P^3} - \frac{4a_S b_S^3}{b_P^2} \right)}{b_P} - \frac{a_P^2 b_S^4}{b_P^4} + \frac{6a_S^2 b_S^2}{b_P^2} \right) \\ &\quad - h_1 \left(\frac{2a_P \left(\frac{2a_P b_S^4}{b_P^3} - \frac{4a_S b_S^3}{b_P^2} \right)}{b_P} - \frac{a_P^2 b_S^4}{b_P^4} + \frac{6a_S^2 b_S^2}{b_P^2} \right) \\ &\quad + h_1^2 \left(\frac{a_P b_S^4}{b_P^3} - \frac{2a_S b_S^3}{b_P^2} \right) - h_2^2 \left(\frac{a_P b_S^4}{b_P^3} - \frac{2a_S b_S^3}{b_P^2} \right) \\ &\quad + \frac{\ln(a_P + h_1 b_P) (4a_P^3 b_S^4 - 12a_P^2 a_S b_P b_S^3 + 12a_P a_S^2 b_P^2 b_S^2 - 4a_S^3 b_P^3 b_S)}{b_P^5} \\ &\quad - \frac{\ln(a_P + h_2 b_P) (4a_P^3 b_S^4 - 12a_P^2 a_S b_P b_S^3 + 12a_P a_S^2 b_P^2 b_S^2 - 4a_S^3 b_P^3 b_S)}{b_P^5} \\ &\quad - \frac{h_1^3 b_S^4}{3b_P^2} + \frac{h_2^3 b_S^4}{3b_P^2} \\ &\quad + \frac{a_P^4 b_S^4 - 4a_P^3 a_S b_P b_S^3 + 6a_P^2 a_S^2 b_P^2 b_S^2 - 4a_P a_S^3 b_P^3 b_S + a_S^4 b_P^4}{b_P (h_1 b_P^5 + a_P b_P^4)} \\ &\quad - \frac{a_P^4 b_S^4 - 4a_P^3 a_S b_P b_S^3 + 6a_P^2 a_S^2 b_P^2 b_S^2 - 4a_P a_S^3 b_P^3 b_S + a_S^4 b_P^4}{b_P (h_2 b_P^5 + a_P b_P^4)}. \end{aligned} \quad (4.10)$$

The first two terms in parameter (4.3b) are given by formulæ (4.5) and (4.7), since the third term is

$$\overline{\left(\frac{2(c_{1111} - 2c_{2323})c_{2323}}{c_{1111}} \right)} = \frac{2}{h_2 - h_1} \left(\int_{h_1}^{h_2} (a_S + b_S z)^2 dz - 2 \int_{h_1}^{h_2} \frac{(a_S + b_S z)^4}{(a_P + b_P z)^2} dz \right) = \frac{2(I_2 - 2I_3)}{h_2 - h_1}, \quad (4.11)$$

where I_2 and I_3 are provided by integration constants (4.9) and (4.10). Finally, in a manner similar to obtaining the second term in parameter (4.3a), we use u substitution and change limits of integration to obtain the term in parameter (4.3e), where

$$\begin{aligned} \overline{\left(\frac{1}{c_{2323}} \right)}^{-1} &= \left(\frac{1}{h_2 - h_1} \int_{h_1}^{h_2} \frac{1}{(a_S + b_S z)^2} dz \right)^{-1} = (h_2 - h_1) \left(\int_{h_1}^{h_2} (a_S + b_S z)^{-2} dz \right)^{-1} \\ &= (a_S + b_S h_1)(a_S + b_S h_2). \end{aligned} \quad (4.12)$$

Hence, using formulæ (4.4), (4.5), (4.7), (4.8), (4.11), (4.12), along with integration con-

stants (4.6), (4.9), (4.10), the Backus parameters (4.3a)–(4.3f) may be restated as

$$c_{1111}^{\overline{\text{TI}}}(h_1, h_2, a_S, b_S, a_P, b_P) = \left(1 - \frac{2I_1}{h_2 - h_1}\right)^2 (a_P + b_P h_1)(a_P + b_P h_2) + \frac{4(I_2 - I_3)}{h_2 - h_1}, \quad (4.13\text{a})$$

$$c_{1122}^{\overline{\text{TI}}}(h_1, h_2, a_S, b_S, a_P, b_P) = \left(1 - \frac{2I_1}{h_2 - h_1}\right)^2 (a_P + b_P h_1)(a_P + b_P h_2) + \frac{2(I_2 - 2I_3)}{h_2 - h_1}, \quad (4.13\text{b})$$

$$c_{1133}^{\overline{\text{TI}}}(h_1, h_2, a_S, b_S, a_P, b_P) = \left(1 - \frac{2I_1}{h_2 - h_1}\right)(a_P + b_P h_1)(a_P + b_P h_2), \quad (4.13\text{c})$$

$$c_{1212}^{\overline{\text{TI}}}(h_1, h_2, a_S, b_S) = \frac{1}{3} (3a_S^2 + 3a_S b_S(h_1 + h_2) + b_S^2(h_1^2 + h_1 h_2 + h_2^2)), \quad (4.13\text{d})$$

$$c_{2323}^{\overline{\text{TI}}}(h_1, h_2, a_S, b_S) = (a_S + b_S h_1)(a_S + b_S h_2), \quad (4.13\text{e})$$

$$c_{3333}^{\overline{\text{TI}}}(h_1, h_2, a_P, b_P) = (a_P + b_P h_1)(a_P + b_P h_2). \quad (4.13\text{f})$$

4.2.2 Anisotropy parameters

The anisotropy of any TI medium may be described by the Thomsen [1986] parameters. Following that, using Backus parameters (4.13), we define

$$\gamma = \gamma(h_1, h_2, a_S, b_S) := \frac{c_{1212}^{\overline{\text{TI}}} - c_{2323}^{\overline{\text{TI}}}}{2c_{2323}^{\overline{\text{TI}}}}, \quad (4.14\text{a})$$

$$\delta = \delta(h_1, h_2, a_S, b_S, a_P, b_P) := \frac{\left(c_{1133}^{\overline{\text{TI}}} + c_{2323}^{\overline{\text{TI}}}\right)^2 - \left(c_{3333}^{\overline{\text{TI}}} - c_{2323}^{\overline{\text{TI}}}\right)^2}{2c_{3333}^{\overline{\text{TI}}} \left(c_{3333}^{\overline{\text{TI}}} - c_{2323}^{\overline{\text{TI}}}\right)}, \quad (4.14\text{b})$$

$$\epsilon = \epsilon(h_1, h_2, a_S, b_S, a_P, b_P) := \frac{c_{1111}^{\overline{\text{TI}}} - c_{3333}^{\overline{\text{TI}}}}{2c_{3333}^{\overline{\text{TI}}}}. \quad (4.14\text{c})$$

Explicitly, parameter (4.14a) is

$$\gamma = \gamma(h_1, h_2, a_S, b_S) = \frac{b_S^2(h_1 - h_2)^2}{6(a_S + b_S h_1)(a_S + b_S h_2)}. \quad (4.15\text{a})$$

For parameter (4.14b),

$$\begin{aligned}\delta &= \delta(h_1, h_2, a_S, b_S, a_P, b_P) \\ &= \frac{2\delta_{k1}(-b_P(h_1-h_2)(2a_P+b_P(h_1+h_2))+\delta_{k2})(b_P(h_1-h_2)\delta_{k3}+\delta_{k1}\delta_{k2})}{b_P^6(a_P+b_Ph_1)(h_1-h_2)^2(a_P+b_Ph_2)(a_P^2+\delta_{k4}+a_Pb_P(h_1+h_2)-a_Sb_S(h_1+h_2))},\end{aligned}\quad (4.15b)$$

where

$$\begin{aligned}\delta_{k1} &= b_S(-a_Sb_P+a_Pb_S), \\ \delta_{k2} &= 2(a_P+b_Ph_1)(a_P+b_Ph_2)\ln\left(\frac{a_P+b_Ph_1}{a_P+b_Ph_2}\right), \\ \delta_{k3} &= (a_P^2(b_P^2-2b_S^2)+b_P^2(\delta_{k4})+a_Pb_P(2a_Sb_S+(b_P-b_S)(b_P+b_S)(h_1+h_2))), \\ \delta_{k4} &= -a_S^2+(b_P-b_S)(b_P+b_S)h_1h_2.\end{aligned}$$

For parameter (4.14c),

$$\varepsilon = \varepsilon(h_1, h_2, a_S, b_S, a_P, b_P) = \frac{2b_S\left(b_P^3(h_1-h_2)^2(-6a_P^2b_Pb_S+b_P(\varepsilon_{k1})+3a_P(\varepsilon_{k2}))+(\varepsilon_{k3})(\varepsilon_{k4})\right)}{3b_P^6(a_P+b_Ph_1)(h_1-h_2)^2(a_P+b_Ph_2)}\quad (4.16)$$

where

$$\begin{aligned}\varepsilon_{k1} &= -12a_S^2b_S+(b_P-b_S)b_S(b_P+b_S)(h_1-h_2)^2+3a_S(b_P^2-2b_S^2)(h_1+h_2), \\ \varepsilon_{k2} &= 2a_S(b_P^2+2b_S^2)+b_S(-b_P^2+2b_S^2)(h_1+h_2), \\ \varepsilon_{k3} &= 6(a_Sb_P-a_Pb_S)(a_P+b_Ph_1)(a_P+b_Ph_2)\ln\left(\frac{a_P+b_Ph_1}{a_P+b_Ph_2}\right), \\ \varepsilon_{k4} &= -b_P(b_P^2-2b_S^2)(h_1-h_2)+2b_S(-a_Sb_P+a_Pb_S)\ln\left(\frac{a_P+b_Ph_2}{a_P+b_Ph_1}\right).\end{aligned}$$

4.2.3 Total differentials of anisotropy parameters

We quantify the uncertainty of expressions (4.15a)–(4.16), i.e., the sensitivity to changes in model parameters, and to do that, we require the total differential. To establish this, we take the differentiation of γ with respect to each of its coordinates directions to obtain its linear functional

$$d\gamma = \left(\frac{\partial \gamma}{\partial h_1} \right) dh_1 + \left(\frac{\partial \gamma}{\partial h_2} \right) dh_2 + \left(\frac{\partial \gamma}{\partial a_S} \right) da_S + \left(\frac{\partial \gamma}{\partial b_S} \right) db_S, \quad (4.17a)$$

where

$$\begin{aligned} \frac{\partial \gamma}{\partial h_1} &= \frac{b_S^2 (h_1 - h_2) (2a_S + b_S(h_1 + h_2))}{6(a_S + b_S h_1)^2 (a_S + b_S h_2)}, \\ \frac{\partial \gamma}{\partial h_2} &= -\frac{b_S^2 (h_1 - h_2) (2a_S + b_S(h_1 + h_2))}{6(a_S + b_S h_1) (a_S + b_S h_2)^2}, \\ \frac{\partial \gamma}{\partial a_S} &= -\frac{b_S^2 (h_1 - h_2)^2 (2a_S + b_S(h_1 + h_2))}{6(a_S + b_S h_1)^2 (a_S + b_S h_2)^2}, \\ \frac{\partial \gamma}{\partial b_S} &= \frac{a_S b_S (h_1 - h_2)^2 (2a_S + b_S(h_1 + h_2))}{6(a_S + b_S h_1)^2 (a_S + b_S h_2)^2}. \end{aligned}$$

We may perform similar operations on δ and ε to obtain

$$d\delta = \left(\frac{\partial \delta}{\partial h_1} \right) dh_1 + \left(\frac{\partial \delta}{\partial h_2} \right) dh_2 + \left(\frac{\partial \delta}{\partial a_S} \right) da_S + \left(\frac{\partial \delta}{\partial b_S} \right) db_S + \left(\frac{\partial \delta}{\partial a_P} \right) da_P + \left(\frac{\partial \delta}{\partial b_P} \right) db_P \quad (4.17b)$$

and

$$d\varepsilon = \left(\frac{\partial \varepsilon}{\partial h_1} \right) dh_1 + \left(\frac{\partial \varepsilon}{\partial h_2} \right) dh_2 + \left(\frac{\partial \varepsilon}{\partial a_S} \right) da_S + \left(\frac{\partial \varepsilon}{\partial b_S} \right) db_S + \left(\frac{\partial \varepsilon}{\partial a_P} \right) da_P + \left(\frac{\partial \varepsilon}{\partial b_P} \right) db_P. \quad (4.17c)$$

In this thesis, we do not list the resultant expressions since they would require half-a-dozen pages. However, the expressions for the partial derivatives of differentials (4.17b)

and (4.17c) may be obtained using a symbolic software, such as Matlab.

4.3 Methods for well-posedness

As discussed in Abu Sayed and Stanoev [2019], expressions (4.15a)–(4.16) form an ill-posed system of three equations with nine unknowns, where

$$\begin{cases} \gamma = \gamma(h_1, h_2, a_S, b_S) \\ \delta = \delta(h_1, h_2, a_S, b_S, a_P, b_P) \\ \varepsilon = \varepsilon(h_1, h_2, a_S, b_S, a_P, b_P) \end{cases} . \quad (4.18)$$

We use differentials (4.17a)–(4.17c) to form a measure of error. To obtain solutions, we require well-posedness, which necessitates information for six of the nine unknown parameters. Applying the Backus average on a region of interest of a well log, we reduce the number of unknowns to four. In particular, we specify h_1 and h_2 , and calculate values for $\gamma =: \bar{\gamma}^{\text{TI}}$, $\delta =: \bar{\delta}^{\text{TI}}$, $\varepsilon =: \bar{\varepsilon}^{\text{TI}}$, where TI denotes a quantity obtained using the Backus average.

For well-posedness, information for any of a_S, b_S, a_P, b_P must be obtained using additional methods. To obtain information for the remaining model parameters, we use the 1-D tomography and the *ab* model.

4.3.1 1-D tomography

To obtain linear inhomogeneity parameters from VSP data, we use a 1-D tomography method, which is described in Chapter 3. The inversion algorithm, therein, is based on the Levenberg-Marquardt least-square solution. As a result of inversion, we obtain velocities

at discrete depths, where the inverted velocity profile represents the velocity of a vertically inhomogeneous medium. We apply the linear regression to the resultant velocities to obtain the linear inhomogeneity parameters. The quality of the results of 1-D tomography mostly depends on the initial model and the number of data points, as discussed in chapter 3.

4.3.2 *ab* model

The *ab* model is a traveltime inversion method, which is also described in Chapter 3. In this method, the velocity model is a linear function of depth. To obtain the traveltime in a depth segment from the well log, we assume the medium is composed of thin isotropic layers. Based on that assumption, we calculate Fermat's traveltime. To obtain linear inhomogeneity parameters from the inversion method, we minimize the difference between the Fermat's traveltime and the model traveltime based on the expression provided by Slawinski and Slawinski [1999]. The steps we follow to calculate Fermat's traveltime are described in section 2.3.1.

4.4 Numerical search

4.4.1 Restrictions

We have two restrictions in our numerical search. Firstly, the stability conditions of isotropy constrain the values for a_S and a_P such that

$$a_P > 2a_S/\sqrt{3}.$$

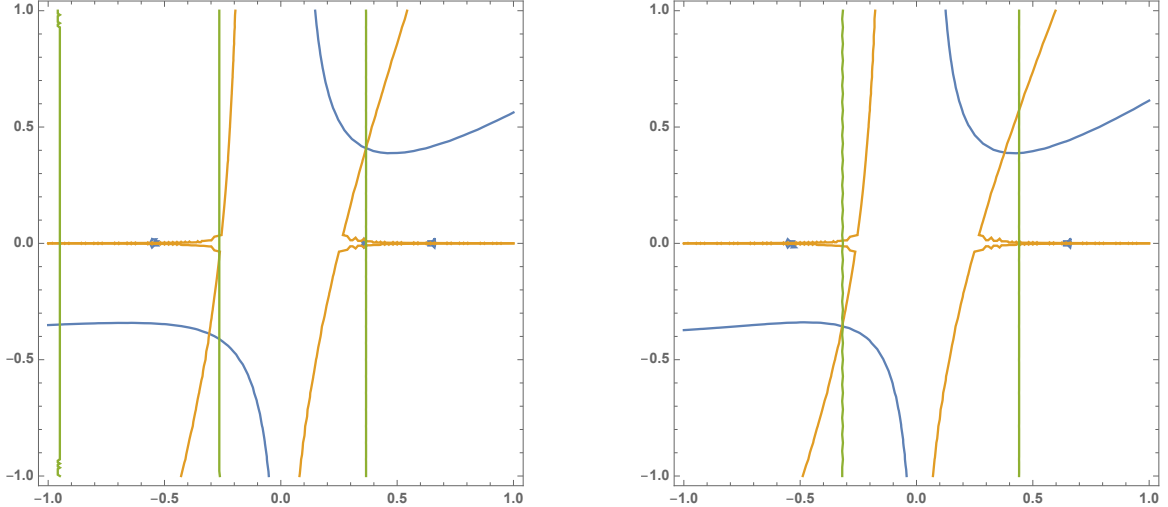


Figure 4.1: Contour plot of anisotropy values (4.19), where b_P is along the vertical axis and b_S is along the horizontal axis. Green lines represent $\gamma = \gamma^{\bar{T}}$; orange lines represent $\delta = \delta^{\bar{T}}$, blue lines represent $\epsilon = \epsilon^{\bar{T}}$.

Secondly, to remain consistent with the assumption of constantly increasing velocity gradient with depth of Slawinski and Slawinski [1999], we do restrict our solutions to positive values of b_P and b_S . However, there do exist solutions for negative values of b_P and b_S as shown in Figure 4.1 .

We may demonstrate this with a numerical example as discussed in Abu Sayed and Stanoev [2019]. For, say, an input of $a_P = 2040.36 \text{ ms}^{-1}$, there exist two solutions, as illustrated by the two instances of triple-point intersection in the left- and right-hand plots of Figure 4.1. Therein, the left-hand plot corresponds to a solution of positive b_P and b_S , where

$$a_S = 752.95 \text{ ms}^{-1}, \quad b_S = 0.3666 \text{ s}^{-1}, \quad a_P = 2164.68 \text{ ms}^{-1}, \quad b_P = 0.4081 \text{ s}^{-1}.$$

However, the right-hand plot represents to a solution of negative b_P and b_S , where

$$a_S = 906.32 \text{ ms}^{-1}, \quad b_S = -0.3194 \text{ s}^{-1}, \quad a_P = 2164.68 \text{ ms}^{-1}, \quad b_P = -0.3556 \text{ s}^{-1}.$$

Throughout the section of the numerical results, we consider positive solutions only.

4.4.2 Calculations

In this section, we obtain a solution to system (4.18) using the methodology of Section 4.3.1 with the VSP data of Mizzen O-16. Using results from 1-D tomography on traveltime data, we construct a velocity profile as a function of depth. For a region of interest, whose depth ranges from 1865 m to 2648.60 m, we recover two parameters, namely a_P and b_P . We may use either parameter as input to system (4.18) to obtain values for the remaining three unknowns.

For instance, we use $a_{P_{\text{VSP,in}}} = 1415 \text{ ms}^{-1}$ and $b_{P_{\text{VSP,in}}} = 0.70 \text{ s}^{-1}$ as startup values for the tomography. For the region of interest, we recover $a_{P_{\text{VSP,out}}} = 1354.9 \text{ ms}^{-1}$ and $b_{P_{\text{VSP,out}}} = 0.3933 \text{ s}^{-1}$, where, at the top of the region, $a_{P_{\text{layer}}} = a_{P_{\text{VSP,out}}} + b_{P_{\text{VSP,out}}} \cdot 1865 \text{ m} = 2088.38 \text{ ms}^{-1}$. Then, we input $b_P = b_{P_{\text{VSP,out}}}$ into system (4.18), for

$$h_1 = 0 \text{ m}, \quad h_2 = (2648.60 - 1865.00) \text{ m} = 783.60 \text{ m},$$

$$\gamma^{\overline{\text{TI}}} = 0.017561151400350, \quad \delta^{\overline{\text{TI}}} = -0.005822848520484, \quad \varepsilon^{\overline{\text{TI}}} = 0.002868244418444, \quad (4.19)$$

and obtain

$$a_S = 725.55 \text{ ms}^{-1}, \quad b_S = 0.3533 \text{ s}^{-1}, \quad a_P = 2085.91 \text{ ms}^{-1}, \quad b_P = 0.3933 \text{ s}^{-1}. \quad (4.20)$$

It is obvious that $a_{P_{\text{layer}}} \neq a_P$ but we may perform an error analysis to assess the “closeness” of our solution. To do that, we recall expressions (4.17a), (4.17b), (4.17c), which are total differentials $d\gamma, d\delta, d\varepsilon$. Using uncertainty measures for parameters (4.20), where

$$dh_1 = dh_2 = 0.05 \text{ m}, \quad da_S = da_P = 2 \text{ ms}^{-1}, \quad db_S = db_P = 0.01 \text{ s}^{-1}, \quad (4.21)$$

we get

$$d\gamma = 0.000790010132156, \quad d\delta = -0.000299948944243, \quad d\varepsilon = 0.000143889902574. \quad (4.22)$$

We calculate a new set of solutions for the lower limit of anisotropy by subtracting values (4.22) from the left-hand sides of system (4.18), which are

$$a_{S_-} = 742.47 \text{ ms}^{-1}, \quad b_{S_-} = 0.3522 \text{ s}^{-1}, \quad a_{P_-} = 2138.75 \text{ ms}^{-1}, \quad b_P = 0.3933 \text{ s}^{-1}. \quad (4.23)$$

In a similar fashion, the upper limit of anisotropy is obtained by adding values (4.22), which results in

$$a_{S_+} = 709.58 \text{ ms}^{-1}, \quad b_{S_+} = 0.354246 \text{ s}^{-1}, \quad a_{P_+} = 2036.58 \text{ ms}^{-1}, \quad b_P = 0.3933 \text{ s}^{-1}. \quad (4.24)$$

Thus, we see that $a_{P_{\text{layer}}}$ falls within the range determined by a_{P_-} and a_{P_+} . In particular, such initial values provide results that are within 0.12% and 0.13%, respectively, of the theoretical predictions. This entire process we may repeat using $a_P = a_{P_{\text{VSP,out}}}$ as input. Also, this process may be repeated for a range of VSP startup values, in order to find the combination of startup values that are closest to the predicted model parameters indicated by the analytical relation. We perform the experiments and tabulate the results of such a process, for values of $a_{P_{\text{VSP,in}}}$ ranging from 1325 ms^{-1} to 1515 ms^{-1} , with increments of 20 ms^{-1} , and $b_{P_{\text{VSP,in}}}$ ranging from 0.57 s^{-1} to 0.7 s^{-1} , with increments of 0.01 s^{-1} , in Table 4.1 of Appendix 4.A.

To compare the results from VSP with the *ab* model, we repeat this process for the same range of values of $a_{P_{\text{ab,in}}}$ and $b_{P_{\text{ab,in}}}$. Similarly, the results are tabulated in Table 4.2 of Appendix 4.A. We find, in comparison, the startup values of $a_{P_{\text{ab,in}}} = 1625 \text{ ms}^{-1}$ and $b_{P_{\text{ab,in}}} =$

0.6s^{-1} , provide results that are within 0.03% and 0.03%, respectively, of the theoretical predictions.

We clarify the entirety of the results of Tables 4.1 and 4.2 in Figures 4.2a and 4.2b. In those Figures, the solid red line represents the solution to system (4.18) corresponding to the value on the horizontal axis, and the solid black lines represent solutions for the lower and upper limits of anisotropy, corresponding to uncertainty parameters (4.21). Orange diamonds represent the solutions from 1-D tomography and blue dots represent solutions from the *ab* model.

4.5 Discussion

For every solution method, we obtain some $a_{P_{\text{VSP}},ab}$ and $b_{P_{\text{VSP}},ab}$ parameters. Taking the output $a_{P_{\text{VSP}},ab}$ as input to system (4.18), we calculate b_P , b_{P_-} , b_{P_+} , and compare them to the output $b_{P_{\text{VSP}},ab}$. These results are shown in Figure 4.2a; also the opposite operation is performed and those results are shown in Figure 4.2b.

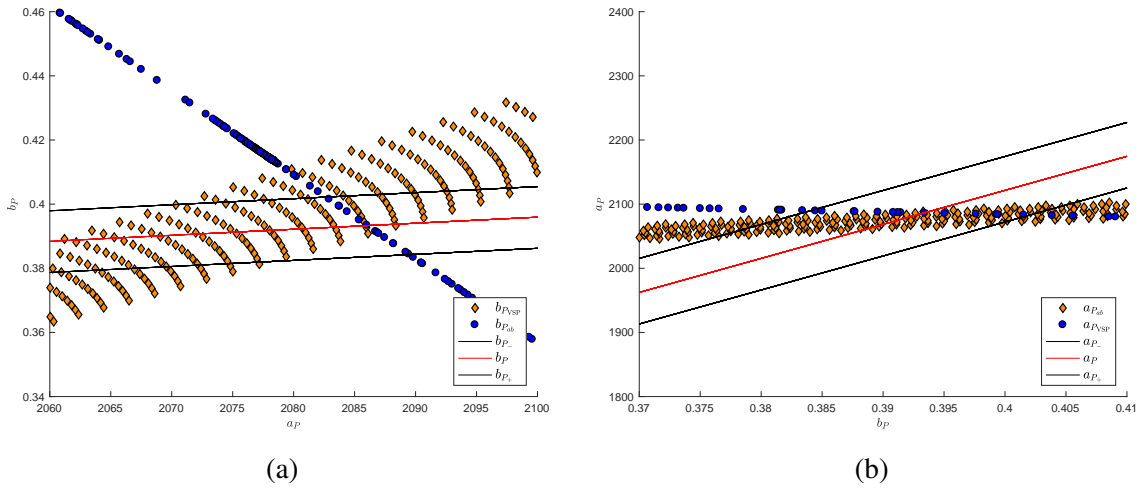


Figure 4.2: Solutions of 1-D tomography and *ab*-model for startup values of $a_{P_{\text{VSP,in}}}$ and $b_{P_{\text{VSP,in}}}$ in Table with VSP results and $a_{P_{ab,in}}$ and $b_{P_{ab,in}}$ in Table with *ab* results.

In both subplots of Figure 4.2, we see that the area of solutions for 1-D tomography overlaps

the line of *ab*-model solutions. To recognize which startup values lead to common outputs, we turn our attention to Figure 4.3. Therein, initial values of $a_{P_{VSP,in}} = 1415 \text{ ms}^{-1}$ and $b_{P_{VSP,in}} = 0.70 \text{ s}^{-1}$ result in $a_{P_{VSP,out}} = 2088.38 \text{ ms}^{-1}$ and $b_{P_{VSP,out}} = 0.39 \text{ s}^{-1}$. These results, as stated in Section 4.4.2, are within 0.12% and 0.13%, respectively, of the theoretical predictions. Similarly, initial values of $a_{P_{ab,in}} = 1625 \text{ ms}^{-1}$ and $b_{P_{ab,in}} = 0.60 \text{ s}^{-1}$ result in outputs that are within 0.03% of the theoretical predictions.

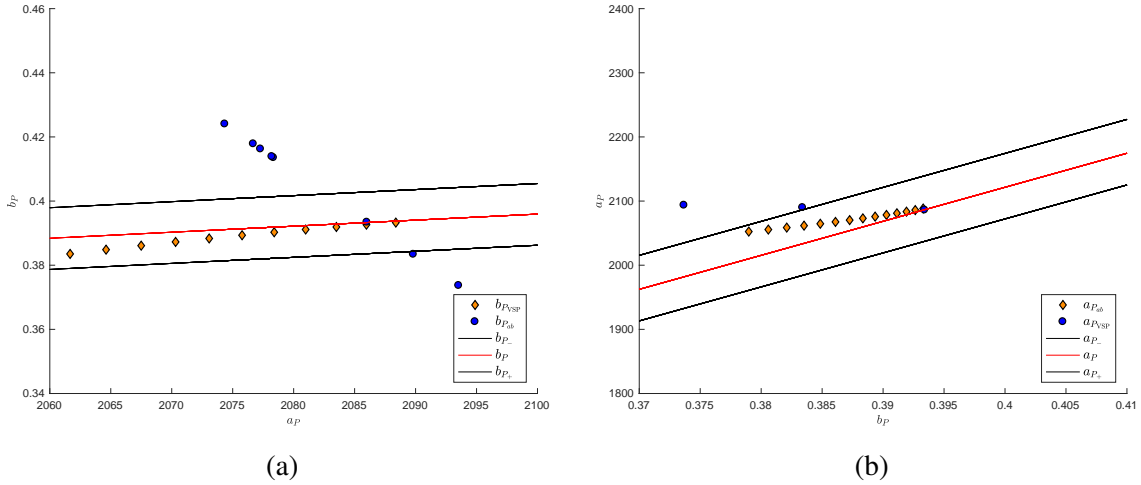


Figure 4.3: Solutions of 1-D tomography and *ab*-model for startup values of $a_{P_{VSP,in}} = 1415 \text{ ms}^{-1}$ and $b_{P_{VSP,in}}$ incrementing by 0.01 s^{-1} from 0.57 s^{-1} to 0.7 s^{-1} , and $a_{P_{ab,in}} = 1625 \text{ ms}^{-1}$ and $b_{P_{ab,in}}$ incrementing by 0.05 s^{-1} from 0.25 s^{-1} to 0.65 s^{-1} .

4.6 Conclusion and future work

In this chapter, we show that there exist multiple solutions from VSP and *ab* methods that do not lie in the theoretical range of analytical relation. However, we also show that there exist some common solutions.

Based on the initial model, we find that some initial values lead to that common solution, which may allow us to conclude that, by tuning initial model parameters, we can obtain the desired solution set.

The number of traveltime data from the field measurement plays a vital role in the VSP method. As an extension of the work, we plan to repeat our calculation for different sites with having more data points.

By far, we consider a smother velocity region and find that the relationship between inhomogeneity and anisotropy provides a reasonable solution in comparison to the solution of VSP and *ab* methods. To examine further, as a future work, we wish to apply the analytical relationship to scattered field data.

4.A Tables

Table 4.1: VSP results

Startup values		VSP results				Using $b_{P_{VSP,out}}$ as input				Using $a_{P_{layer}}$ as input		
$a_{P_{VSP,in}}$	$b_{P_{VSP,in}}$	$a_{P_{VSP,out}}$	$b_{P_{VSP,out}}$	$a_{P_{layer}}$	a_{P_+}	a_P	a_{P_-}	$b_{P_{VSP,out}}$	b_{P_-}	b_P	b_{P_+}	
1320.0	0.57	1292.3	0.4317	2097.42	2240.18	2289.65	2342.32	0.4317	0.3857	0.3955	0.405	
1325.0	0.57	1295.46	0.4286	2094.83	2223.84	2273.3	2325.98	0.4286	0.3853	0.395	0.4045	
1330.0	0.57	1298.58	0.4256	2092.27	2207.69	2257.14	2309.83	0.4256	0.3848	0.3945	0.404	
1335.0	0.57	1301.65	0.4226	2089.73	2191.74	2241.18	2293.89	0.4226	0.3843	0.394	0.4035	
1340.0	0.57	1304.68	0.4196	2087.22	2175.98	2225.41	2278.13	0.4196	0.3838	0.3935	0.4031	
1345.0	0.57	1307.68	0.4167	2084.74	2160.42	2209.84	2262.57	0.4167	0.3834	0.3931	0.4026	
1350.0	0.57	1310.63	0.4138	2082.28	2145.04	2194.45	2247.19	0.4138	0.3829	0.3926	0.4021	
1355.0	0.57	1313.54	0.4109	2079.84	2129.85	2179.25	2232.0	0.4109	0.3824	0.3921	0.4017	
1360.0	0.57	1316.41	0.4081	2077.43	2114.83	2164.22	2216.99	0.4081	0.382	0.3917	0.4012	
1365.0	0.57	1319.24	0.4053	2075.04	2100.0	2149.37	2202.16	0.4053	0.3815	0.3912	0.4008	
1370.0	0.57	1322.04	0.4025	2072.68	2085.33	2134.7	2187.49	0.4025	0.3811	0.3908	0.4003	
1375.0	0.57	1324.8	0.3998	2070.34	2070.85	2120.2	2173.01	0.3998	0.3806	0.3904	0.3999	
1380.0	0.57	1327.52	0.3971	2068.02	2056.53	2105.87	2158.69	0.3971	0.3802	0.3899	0.3994	
1385.0	0.57	1330.21	0.3944	2065.73	2042.37	2091.7	2144.54	0.3944	0.3798	0.3895	0.399	
1390.0	0.57	1332.86	0.3917	2063.45	2028.38	2077.7	2130.55	0.3917	0.3793	0.3891	0.3986	
1395.0	0.57	1335.48	0.3891	2061.2	2014.54	2063.85	2116.71	0.3891	0.3789	0.3886	0.3982	
1400.0	0.57	1338.06	0.3866	2058.98	2000.87	2050.17	2103.04	0.3866	0.3785	0.3882	0.3977	
1405.0	0.57	1340.61	0.384	2056.77	1987.35	2036.64	2089.53	0.384	0.3781	0.3878	0.3973	
1410.0	0.57	1343.13	0.3815	2054.58	1973.98	2023.26	2076.16	0.3815	0.3777	0.3874	0.3969	
1415.0	0.57	1345.62	0.3779	2052.42	1960.77	2010.04	2062.95	0.3779	0.3773	0.387	0.3965	
1420.0	0.57	1348.07	0.3765	2050.28	1947.7	1996.96	2049.88	0.3765	0.3769	0.3866	0.3961	
1425.0	0.57	1350.5	0.3741	2048.15	1934.77	1984.02	2036.96	0.3741	0.3765	0.3862	0.3957	
1430.0	0.57	1352.89	0.3717	2046.05	1921.99	1971.23	2024.18	0.3717	0.3761	0.3858	0.3953	
1435.0	0.57	1355.26	0.3693	2043.97	1909.36	1958.58	2011.55	0.3693	0.3757	0.3854	0.3949	
1440.0	0.57	1357.59	0.3669	2041.9	1896.85	1946.06	1999.04	0.3669	0.3753	0.385	0.3945	
1445.0	0.57	1359.9	0.3646	2039.86	1884.49	1933.69	1986.68	0.3646	0.3749	0.3846	0.3941	
1450.0	0.57	1362.18	0.3623	2037.83	1872.26	1921.45	1974.45	0.3623	0.3745	0.3842	0.3937	

1325.0	0.58	1295.8	0.4303	2098.24	2232.52	2281.99	2334.67	0.4303	0.3859	0.3956	0.4051
1330.0	0.58	1298.91	0.4272	2095.66	2216.37	2265.82	2318.51	0.4272	0.3854	0.3951	0.4047
1335.0	0.58	1301.97	0.4242	2093.11	2200.41	2249.86	2302.56	0.4242	0.3849	0.3946	0.4042
1340.0	0.58	1304.99	0.4212	2090.58	2184.64	2234.08	2286.79	0.4212	0.3845	0.3942	0.4037
1345.0	0.58	1307.97	0.4183	2088.08	2169.07	2218.5	2271.22	0.4183	0.384	0.3937	0.4032
1350.0	0.58	1310.91	0.4154	2085.6	2153.68	2203.1	2255.83	0.4154	0.3835	0.3932	0.4028
1355.0	0.58	1313.81	0.4125	2083.15	2138.48	2187.88	2240.64	0.4125	0.3831	0.3928	0.4023
1360.0	0.58	1316.67	0.4097	2080.73	2123.46	2172.85	2225.62	0.4097	0.3826	0.3923	0.4018
1365.0	0.58	1319.5	0.4069	2078.33	2108.61	2157.99	2210.77	0.4069	0.3821	0.3919	0.4014
1370.0	0.58	1322.28	0.4041	2075.95	2093.94	2143.31	2196.1	0.4041	0.3817	0.3914	0.4009
1375.0	0.58	1325.03	0.4014	2073.59	2079.44	2128.8	2181.6	0.4014	0.3812	0.391	0.4005
1380.0	0.58	1327.74	0.3987	2071.27	2065.11	2114.46	2167.27	0.3987	0.3808	0.3905	0.4001
1385.0	0.58	1330.42	0.396	2068.96	2050.94	2100.28	2153.1	0.396	0.3804	0.3901	0.3996
1390.0	0.58	1333.06	0.3934	2066.67	2036.94	2086.27	2139.11	0.3934	0.3799	0.3897	0.3992
1395.0	0.58	1335.67	0.3907	2064.41	2023.1	2072.41	2125.27	0.3907	0.3795	0.3892	0.3988
1400.0	0.58	1338.25	0.3882	2062.16	2009.41	2058.71	2111.58	0.3882	0.3791	0.3888	0.3983
1405.0	0.58	1340.79	0.3856	2059.95	1995.88	2045.17	2098.05	0.3856	0.3787	0.3884	0.3979
1410.0	0.58	1343.3	0.3831	2057.75	1982.5	2031.79	2084.68	0.3831	0.3783	0.388	0.3975
1415.0	0.58	1345.78	0.3806	2055.57	1969.27	2018.54	2071.45	0.3806	0.3778	0.3876	0.3971
1420.0	0.58	1348.22	0.3781	2053.41	1956.19	2005.45	2058.37	0.3781	0.3774	0.3872	0.3967
1425.0	0.58	1350.64	0.3757	2051.28	1943.25	1992.51	2045.44	0.3757	0.377	0.3868	0.3963
1430.0	0.58	1353.02	0.3733	2049.16	1930.46	1979.7	2032.64	0.3733	0.3766	0.3864	0.3959
1435.0	0.58	1355.38	0.3709	2047.06	1917.8	1967.04	2019.99	0.3709	0.3762	0.386	0.3955
1440.0	0.58	1357.71	0.3685	2044.99	1905.29	1954.51	2007.48	0.3685	0.3759	0.3856	0.3951
1445.0	0.58	1360.01	0.3662	2042.93	1892.91	1942.12	1995.1	0.3662	0.3755	0.3852	0.3947
1450.0	0.58	1362.28	0.3639	2040.89	1880.66	1929.86	1982.86	0.3639	0.3751	0.3848	0.3943
1455.0	0.58	1364.53	0.3616	2038.87	1868.55	1917.74	1970.75	0.3616	0.3747	0.3844	0.3939
1330.0	0.59	1299.36	0.4287	2098.97	2224.48	2273.94	2326.63	0.4287	0.386	0.3958	0.4053
1335.0	0.59	1302.41	0.4257	2096.4	2208.52	2257.97	2310.66	0.4257	0.3856	0.3953	0.4048
1340.0	0.59	1305.42	0.4228	2093.86	2192.75	2242.19	2294.9	0.4228	0.3851	0.3948	0.4043
1345.0	0.59	1308.39	0.4198	2091.35	2177.17	2226.6	2279.32	0.4198	0.3846	0.3943	0.4038
1350.0	0.59	1311.32	0.4169	2088.86	2161.78	2211.2	2263.93	0.4169	0.3841	0.3938	0.4034
1355.0	0.59	1314.21	0.4114	2086.39	2146.57	2195.98	2248.72	0.4114	0.3837	0.3934	0.4029
1360.0	0.59	1317.06	0.4112	2083.96	2131.54	2180.94	2233.7	0.4112	0.3832	0.3929	0.4024
1365.0	0.59	1319.87	0.4084	2081.54	2116.69	2166.07	2218.84	0.4084	0.3827	0.3925	0.402
1370.0	0.59	1322.64	0.4056	2079.15	2102.01	2151.39	2204.17	0.4056	0.3823	0.392	0.4015
1375.0	0.59	1325.38	0.4029	2076.78	2087.51	2136.87	2189.67	0.4029	0.3819	0.3916	0.4011
1380.0	0.59	1328.08	0.4002	2074.44	2073.16	2122.52	2175.33	0.4002	0.3814	0.3911	0.4007
1385.0	0.59	1330.75	0.3975	2072.12	2058.99	2108.34	2161.16	0.3975	0.381	0.3907	0.4002
1390.0	0.59	1333.38	0.3949	2069.82	2044.98	2094.31	2147.15	0.3949	0.3805	0.3903	0.3998
1395.0	0.59	1335.98	0.3923	2067.54	2031.13	2080.45	2133.3	0.3923	0.3801	0.3898	0.3994
1400.0	0.59	1338.54	0.3897	2065.29	2017.44	2066.75	2119.61	0.3897	0.3797	0.3894	0.3989
1405.0	0.59	1341.07	0.3871	2063.05	2003.9	2053.2	2106.07	0.3871	0.3793	0.389	0.3985
1410.0	0.59	1343.57	0.3846	2060.84	1990.51	2039.8	2092.69	0.3846	0.3788	0.3886	0.3981
1415.0	0.59	1346.04	0.3821	2058.65	1977.28	2026.56	2079.45	0.3821	0.3784	0.3881	0.3977
1420.0	0.59	1348.48	0.3796	2056.48	1964.18	2013.45	2066.36	0.3796	0.378	0.3877	0.3973
1425.0	0.59	1350.88	0.3772	2054.33	1951.24	2000.5	2053.42	0.3772	0.3776	0.3873	0.3969
1430.0	0.59	1353.26	0.3748	2052.21	1938.44	1987.69	2040.62	0.3748	0.3772	0.3869	0.3965
1435.0	0.59	1355.61	0.3724	2050.09	1925.77	1975.01	2027.96	0.3724	0.3768	0.3865	0.3961
1440.0	0.59	1357.93	0.37	2048.01	1913.25	1962.47	2015.44	0.37	0.3764	0.3861	0.3957
1445.0	0.59	1360.22	0.3677	2045.94	1900.86	1950.08	2003.05	0.3677	0.376	0.3858	0.3953
1450.0	0.59	1362.48	0.3654	2043.89	1888.61	1937.81	1990.8	0.3654	0.3756	0.3854	0.3949
1455.0	0.59	1364.72	0.3631	2041.86	1876.48	1925.67	1978.67	0.3631	0.3753	0.385	0.3945

1460.0	0.59	1366.93	0.3608	2039.84	1864.49	1913.67	1966.68	0.3608	0.3749	0.3846	0.3941
1335.0	0.6	1302.97	0.4272	2099.62	2216.08	2265.53	2318.22	0.4272	0.3862	0.3959	0.4054
1340.0	0.6	1305.97	0.4242	2097.07	2200.31	2249.76	2302.46	0.4242	0.3857	0.3954	0.4049
1345.0	0.6	1308.92	0.4212	2094.54	2184.73	2234.17	2286.88	0.4212	0.3852	0.3949	0.4044
1350.0	0.6	1311.84	0.4183	2092.04	2169.34	2218.77	2271.49	0.4183	0.3847	0.3944	0.404
1355.0	0.6	1314.71	0.4155	2089.56	2154.13	2203.55	2256.29	0.4155	0.3843	0.394	0.4035
1360.0	0.6	1317.55	0.4126	2087.11	2139.1	2188.5	2241.25	0.4126	0.3838	0.3935	0.403
1365.0	0.6	1320.35	0.4098	2084.68	2124.25	2173.64	2226.41	0.4098	0.3833	0.3931	0.4026
1370.0	0.6	1323.11	0.4071	2082.27	2109.57	2158.95	2211.72	0.4071	0.3829	0.3926	0.4021
1375.0	0.6	1325.83	0.4043	2079.9	2095.06	2144.43	2197.22	0.4043	0.3824	0.3922	0.4017
1380.0	0.6	1328.52	0.4016	2077.54	2080.72	2130.08	2182.88	0.4016	0.382	0.3917	0.4012
1385.0	0.6	1331.18	0.3989	2075.2	2066.54	2115.89	2168.7	0.3989	0.3816	0.3913	0.4008
1390.0	0.6	1333.8	0.3963	2072.89	2052.53	2101.87	2154.69	0.3963	0.3811	0.3908	0.4004
1395.0	0.6	1336.38	0.3937	2070.6	2038.67	2088.0	2140.84	0.3937	0.3807	0.3904	0.3999
1400.0	0.6	1338.94	0.3911	2068.34	2024.97	2074.29	2127.14	0.3911	0.3803	0.39	0.3995
1405.0	0.6	1341.46	0.3885	2066.09	2011.43	2060.74	2113.6	0.3885	0.3798	0.3896	0.3991
1410.0	0.6	1343.95	0.386	2063.87	1998.04	2047.33	2100.21	0.386	0.3794	0.3891	0.3987
1415.0	0.6	1346.41	0.3835	2061.66	1984.8	2034.08	2086.97	0.3835	0.379	0.3887	0.3982
1420.0	0.6	1348.83	0.381	2059.48	1971.7	2020.98	2073.88	0.381	0.3786	0.3883	0.3978
1425.0	0.6	1351.23	0.3786	2057.32	1958.75	2008.02	2060.94	0.3786	0.3782	0.3879	0.3974
1430.0	0.6	1353.6	0.3762	2055.18	1945.94	1995.2	2048.12	0.3762	0.3778	0.3875	0.397
1435.0	0.6	1355.93	0.3738	2053.06	1933.28	1982.52	2035.46	0.3738	0.3774	0.3871	0.3966
1440.0	0.6	1358.24	0.3714	2050.96	1920.75	1969.98	2022.93	0.3714	0.377	0.3867	0.3962
1445.0	0.6	1360.52	0.3691	2048.88	1908.35	1957.57	2010.54	0.3691	0.3766	0.3863	0.3958
1450.0	0.6	1362.78	0.3668	2046.82	1896.09	1945.3	1998.28	0.3668	0.3762	0.3859	0.3954
1455.0	0.6	1365.0	0.3645	2044.78	1883.96	1933.16	1986.15	0.3645	0.3758	0.3855	0.3951
1460.0	0.6	1367.2	0.3622	2042.75	1871.95	1921.14	1974.15	0.3622	0.3754	0.3852	0.3947
1465.0	0.6	1369.38	0.36	2040.74	1860.08	1909.26	1962.28	0.36	0.3751	0.3848	0.3943
1340.0	0.61	1306.62	0.4255	2100.2	2207.35	2256.8	2309.5	0.4255	0.3863	0.396	0.4055
1345.0	0.61	1309.56	0.4226	2097.66	2191.78	2241.22	2293.93	0.4226	0.3858	0.3955	0.405
1350.0	0.61	1312.46	0.4197	2095.14	2176.39	2225.81	2278.53	0.4197	0.3853	0.395	0.4046
1355.0	0.61	1315.33	0.4168	2092.65	2161.18	2210.6	2263.33	0.4168	0.3848	0.3946	0.4041
1360.0	0.61	1318.15	0.414	2090.19	2146.15	2195.56	2248.3	0.414	0.3844	0.3941	0.4036
1365.0	0.61	1320.93	0.4112	2087.75	2131.3	2180.7	2233.46	0.4112	0.3839	0.3936	0.4032
1370.0	0.61	1323.68	0.4084	2085.33	2116.63	2166.01	2218.78	0.4084	0.3835	0.3932	0.4027
1375.0	0.61	1326.39	0.4057	2082.94	2102.11	2151.49	2204.27	0.4057	0.383	0.3927	0.4023
1380.0	0.61	1329.07	0.4029	2080.57	2087.78	2137.14	2189.94	0.4029	0.3826	0.3923	0.4018
1385.0	0.61	1331.71	0.4003	2078.22	2073.6	2122.96	2175.77	0.4003	0.3821	0.3918	0.4014
1390.0	0.61	1334.32	0.3976	2075.9	2059.58	2108.93	2161.75	0.3976	0.3817	0.3914	0.4009
1395.0	0.61	1336.9	0.395	2073.6	2045.73	2095.07	2147.9	0.395	0.3813	0.391	0.4005
1400.0	0.61	1339.44	0.3924	2071.32	2032.04	2081.36	2134.21	0.3924	0.3808	0.3905	0.4001
1405.0	0.61	1341.95	0.3899	2069.06	2018.49	2067.8	2120.66	0.3899	0.3804	0.3901	0.3996
1410.0	0.61	1344.42	0.3873	2066.83	2005.1	2054.4	2107.27	0.3873	0.38	0.3897	0.3992
1415.0	0.61	1346.87	0.3848	2064.61	1991.86	2041.15	2094.03	0.3848	0.3796	0.3893	0.3988
1420.0	0.61	1349.29	0.3824	2062.42	1978.75	2028.04	2080.93	0.3824	0.3791	0.3889	0.3984
1425.0	0.61	1351.67	0.3799	2060.25	1965.8	2015.08	2067.98	0.3799	0.3787	0.3884	0.398
1430.0	0.61	1354.03	0.3775	2058.1	1953.0	2002.26	2055.18	0.3775	0.3783	0.388	0.3976
1435.0	0.61	1356.35	0.3751	2055.96	1940.32	1989.57	2042.5	0.3751	0.3779	0.3876	0.3972
1440.0	0.61	1358.65	0.3728	2053.85	1927.79	1977.03	2029.97	0.3728	0.3775	0.3872	0.3968
1445.0	0.61	1360.92	0.3704	2051.76	1915.39	1964.62	2017.58	0.3704	0.3771	0.3868	0.3964
1450.0	0.61	1363.17	0.3681	2049.69	1903.13	1952.35	2005.32	0.3681	0.3767	0.3865	0.396
1455.0	0.61	1365.38	0.3658	2047.63	1890.99	1940.2	1993.18	0.3658	0.3764	0.3861	0.3956
1460.0	0.61	1367.57	0.3636	2045.6	1878.99	1928.19	1981.18	0.3636	0.376	0.3857	0.3952

1465.0	0.61	1369.74	0.3613	2043.58	1867.11	1916.3	1969.31	0.3613	0.3756	0.3853	0.3948
1470.0	0.61	1371.88	0.3591	2041.58	1855.36	1904.54	1957.56	0.3591	0.3752	0.3849	0.3945
1345.0	0.62	1310.31	0.4238	2100.71	2198.32	2247.76	2300.46	0.4238	0.3864	0.3961	0.4056
1350.0	0.62	1313.2	0.4209	2098.18	2182.94	2232.37	2285.09	0.4209	0.3859	0.3956	0.4051
1355.0	0.62	1316.04	0.418	2095.68	2167.73	2217.16	2269.88	0.418	0.3854	0.3951	0.4047
1360.0	0.62	1318.85	0.4152	2093.2	2152.71	2202.13	2254.87	0.4152	0.3849	0.3947	0.4042
1365.0	0.62	1321.62	0.4124	2090.75	2137.86	2187.27	2240.02	0.4124	0.3845	0.3942	0.4037
1370.0	0.62	1324.36	0.4096	2088.32	2123.19	2172.59	2225.35	0.4096	0.384	0.3937	0.4033
1375.0	0.62	1327.06	0.4069	2085.92	2108.7	2158.08	2210.85	0.4069	0.3836	0.3933	0.4028
1380.0	0.62	1329.72	0.4042	2083.53	2094.35	2143.73	2196.52	0.4042	0.3831	0.3928	0.4024
1385.0	0.62	1332.35	0.4015	2081.17	2080.19	2129.55	2182.35	0.4015	0.3827	0.3924	0.4019
1390.0	0.62	1334.94	0.3989	2078.84	2066.18	2115.53	2168.34	0.3989	0.3822	0.392	0.4015
1395.0	0.62	1337.5	0.3963	2076.53	2052.32	2101.66	2154.49	0.3963	0.3818	0.3915	0.401
1400.0	0.62	1340.03	0.3937	2074.24	2038.63	2087.96	2140.8	0.3937	0.3814	0.3911	0.4006
1405.0	0.62	1342.53	0.3911	2071.97	2025.09	2074.41	2127.26	0.3911	0.3809	0.3907	0.4002
1410.0	0.62	1344.99	0.3886	2069.72	2011.7	2061.0	2113.87	0.3886	0.3805	0.3902	0.3998
1415.0	0.62	1347.43	0.3861	2067.5	1998.46	2047.75	2100.63	0.3861	0.3801	0.3898	0.3993
1420.0	0.62	1349.83	0.3836	2065.29	1985.36	2034.65	2087.54	0.3836	0.3797	0.3894	0.3989
1425.0	0.62	1352.21	0.3812	2063.11	1972.41	2021.69	2074.59	0.3812	0.3793	0.389	0.3985
1430.0	0.62	1354.55	0.3788	2060.94	1959.6	2008.87	2061.78	0.3788	0.3789	0.3886	0.3981
1435.0	0.62	1356.87	0.3764	2058.8	1946.93	1996.19	2049.11	0.3764	0.3785	0.3882	0.3977
1440.0	0.62	1359.16	0.374	2056.68	1934.4	1983.65	2036.59	0.374	0.3781	0.3878	0.3973
1445.0	0.62	1361.41	0.3717	2054.57	1922.0	1971.23	2024.18	0.3717	0.3777	0.3874	0.3969
1450.0	0.62	1363.65	0.3694	2052.49	1909.73	1958.96	2011.92	0.3694	0.3773	0.387	0.3965
1455.0	0.62	1365.85	0.3671	2050.43	1897.6	1946.82	1999.79	0.3671	0.3769	0.3866	0.3961
1460.0	0.62	1368.03	0.3648	2048.38	1885.6	1934.8	1987.79	0.3648	0.3765	0.3862	0.3957
1465.0	0.62	1370.19	0.3626	2046.35	1873.72	1922.91	1975.91	0.3626	0.3761	0.3858	0.3954
1470.0	0.62	1372.31	0.3603	2044.34	1861.96	1911.15	1964.16	0.3603	0.3757	0.3855	0.395
1475.0	0.62	1374.42	0.3581	2042.35	1850.34	1899.51	1952.53	0.3581	0.3754	0.3851	0.3946
1350.0	0.63	1314.03	0.422	2101.14	2189.0	2238.43	2291.15	0.422	0.3864	0.3962	0.4057
1355.0	0.63	1316.86	0.4192	2098.63	2173.81	2223.24	2275.96	0.4192	0.386	0.3957	0.4052
1360.0	0.63	1319.65	0.4163	2096.14	2158.8	2208.21	2260.95	0.4163	0.3855	0.3952	0.4047
1365.0	0.63	1322.41	0.4135	2093.68	2143.96	2193.37	2246.12	0.4135	0.385	0.3948	0.4043
1370.0	0.63	1325.13	0.4108	2091.24	2129.29	2178.69	2231.45	0.4108	0.3846	0.3943	0.4038
1375.0	0.63	1327.81	0.408	2088.82	2114.8	2164.19	2216.96	0.408	0.3841	0.3938	0.4034
1380.0	0.63	1330.46	0.4053	2086.43	2100.48	2149.85	2202.64	0.4053	0.3837	0.3934	0.4029
1385.0	0.63	1333.08	0.4027	2084.06	2086.31	2135.68	2188.47	0.4027	0.3832	0.3929	0.4025
1390.0	0.63	1335.66	0.4	2081.71	2072.31	2121.66	2174.47	0.4	0.3828	0.3925	0.402
1395.0	0.63	1338.21	0.3974	2079.39	2058.47	2107.81	2160.63	0.3974	0.3823	0.3921	0.4016
1400.0	0.63	1340.72	0.3948	2077.09	2044.77	2094.11	2146.94	0.3948	0.3819	0.3916	0.4012
1405.0	0.63	1343.21	0.3923	2074.81	2031.24	2080.57	2133.41	0.3923	0.3815	0.3912	0.4007
1410.0	0.63	1345.66	0.3898	2072.55	2017.86	2067.17	2120.03	0.3898	0.3811	0.3908	0.4003
1415.0	0.63	1348.08	0.3873	2070.32	2004.62	2053.93	2106.8	0.3873	0.3806	0.3903	0.3999
1420.0	0.63	1350.47	0.3848	2068.1	1991.53	2040.82	2093.71	0.3848	0.3802	0.3899	0.3995
1425.0	0.63	1352.83	0.3823	2065.91	1978.59	2027.87	2080.76	0.3823	0.3798	0.3895	0.399
1430.0	0.63	1355.17	0.3799	2063.73	1965.78	2015.05	2067.96	0.3799	0.3794	0.3891	0.3986
1435.0	0.63	1357.47	0.3775	2061.58	1953.11	2002.37	2055.29	0.3775	0.379	0.3887	0.3982
1440.0	0.63	1359.74	0.3752	2059.44	1940.58	1989.83	2042.77	0.3752	0.3786	0.3883	0.3978
1445.0	0.63	1361.99	0.3728	2057.33	1928.19	1977.43	2030.38	0.3728	0.3782	0.3879	0.3974
1450.0	0.63	1364.21	0.3705	2055.24	1915.93	1965.16	2018.12	0.3705	0.3778	0.3875	0.397
1455.0	0.63	1366.41	0.3682	2053.16	1903.79	1953.01	2005.98	0.3682	0.3774	0.3871	0.3966
1460.0	0.63	1368.58	0.366	2051.1	1891.79	1941.0	1993.98	0.366	0.377	0.3867	0.3963
1465.0	0.63	1370.72	0.3637	2049.07	1879.92	1929.11	1982.11	0.3637	0.3766	0.3863	0.3959

1470.0	0.63	1372.84	0.3615	2047.05	1868.17	1917.35	1970.36	0.3615	0.3762	0.386	0.3955
1475.0	0.63	1374.93	0.3593	2045.05	1856.53	1905.71	1958.73	0.3593	0.3759	0.3856	0.3951
1480.0	0.63	1377.0	0.3571	2043.06	1845.03	1894.19	1947.23	0.3571	0.3755	0.3852	0.3947
1355.0	0.64	1317.77	0.4202	2101.52	2179.42	2228.85	2281.57	0.4202	0.3865	0.3962	0.4058
1360.0	0.64	1320.55	0.4174	2099.02	2164.42	2213.84	2266.57	0.4174	0.386	0.3958	0.4053
1365.0	0.64	1323.29	0.4146	2096.54	2149.59	2199.01	2251.75	0.4146	0.3856	0.3953	0.4048
1370.0	0.64	1325.99	0.4118	2094.09	2134.95	2184.35	2237.1	0.4118	0.3851	0.3948	0.4044
1375.0	0.64	1328.66	0.4091	2091.67	2120.47	2169.86	2222.62	0.4091	0.3847	0.3944	0.4039
1380.0	0.64	1331.3	0.4064	2089.26	2106.15	2155.53	2208.31	0.4064	0.3842	0.3939	0.4034
1385.0	0.64	1333.9	0.4037	2086.88	2092.0	2141.37	2194.16	0.4037	0.3838	0.3935	0.403
1390.0	0.64	1336.46	0.4011	2084.53	2078.01	2127.37	2180.17	0.4011	0.3833	0.393	0.4026
1395.0	0.64	1339.0	0.3985	2082.19	2064.17	2113.52	2166.33	0.3985	0.3829	0.3926	0.4021
1400.0	0.64	1341.5	0.3959	2079.88	2050.49	2099.83	2152.66	0.3959	0.3824	0.3922	0.4017
1405.0	0.64	1343.97	0.3934	2077.59	2036.97	2086.3	2139.14	0.3934	0.382	0.3917	0.4012
1410.0	0.64	1346.41	0.3908	2075.32	2023.59	2072.91	2125.76	0.3908	0.3816	0.3913	0.4008
1415.0	0.64	1348.82	0.3883	2073.07	2010.36	2059.67	2112.53	0.3883	0.3812	0.3909	0.4004
1420.0	0.64	1351.19	0.3859	2070.85	1997.28	2046.58	2099.46	0.3859	0.3807	0.3904	0.4
1425.0	0.64	1353.54	0.3834	2068.64	1984.34	2033.63	2086.52	0.3834	0.3803	0.39	0.3996
1430.0	0.64	1355.86	0.381	2066.46	1971.54	2020.82	2073.72	0.381	0.3799	0.3896	0.3991
1435.0	0.64	1358.15	0.3786	2064.29	1958.88	2008.15	2061.06	0.3786	0.3795	0.3892	0.3987
1440.0	0.64	1360.42	0.3763	2062.15	1946.36	1995.62	2048.54	0.3763	0.3791	0.3888	0.3983
1445.0	0.64	1362.65	0.3739	2060.03	1933.97	1983.22	2036.16	0.3739	0.3787	0.3884	0.3979
1450.0	0.64	1364.86	0.3716	2057.92	1921.71	1970.95	2023.9	0.3716	0.3783	0.388	0.3975
1455.0	0.64	1367.05	0.3693	2055.84	1909.59	1958.81	2011.78	0.3693	0.3779	0.3876	0.3971
1460.0	0.64	1369.2	0.3671	2053.77	1897.59	1946.8	1999.78	0.3671	0.3775	0.3872	0.3968
1465.0	0.64	1371.33	0.3648	2051.72	1885.72	1934.92	1987.91	0.3648	0.3771	0.3868	0.3964
1470.0	0.64	1373.44	0.3626	2049.69	1873.97	1923.16	1976.16	0.3626	0.3767	0.3865	0.396
1475.0	0.64	1375.52	0.3604	2047.68	1862.34	1911.53	1964.54	0.3604	0.3764	0.3861	0.3956
1480.0	0.64	1377.58	0.3582	2045.69	1850.84	1900.01	1953.04	0.3582	0.376	0.3857	0.3952
1485.0	0.64	1379.61	0.3561	2043.72	1839.46	1888.62	1941.66	0.3561	0.3756	0.3853	0.3949
1360.0	0.65	1321.54	0.4184	2101.83	2169.59	2219.02	2271.75	0.4184	0.3866	0.3963	0.4058
1365.0	0.65	1324.26	0.4156	2099.34	2154.79	2204.21	2256.94	0.4156	0.3861	0.3958	0.4053
1370.0	0.65	1326.95	0.4128	2096.88	2140.15	2189.56	2242.31	0.4128	0.3856	0.3954	0.4049
1375.0	0.65	1329.6	0.4101	2094.44	2125.69	2175.08	2227.84	0.4101	0.3852	0.3949	0.4044
1380.0	0.65	1332.22	0.4074	2092.03	2111.39	2160.77	2213.55	0.4074	0.3847	0.3944	0.404
1385.0	0.65	1334.81	0.4047	2089.64	2097.25	2146.62	2199.41	0.4047	0.3843	0.394	0.4035
1390.0	0.65	1337.36	0.4021	2087.27	2083.27	2132.63	2185.43	0.4021	0.3838	0.3935	0.4031
1395.0	0.65	1339.88	0.3995	2084.93	2069.45	2118.8	2171.62	0.3995	0.3834	0.3931	0.4026
1400.0	0.65	1342.36	0.3969	2082.61	2055.79	2105.13	2157.95	0.3969	0.3829	0.3927	0.4022
1405.0	0.65	1344.82	0.3944	2080.3	2042.27	2091.6	2144.44	0.3944	0.3825	0.3922	0.4018
1410.0	0.65	1347.24	0.3918	2078.03	2028.91	2078.23	2131.08	0.3918	0.3821	0.3918	0.4013
1415.0	0.65	1349.64	0.3893	2075.77	2015.69	2065.0	2117.86	0.3893	0.3817	0.3914	0.4009
1420.0	0.65	1352.0	0.3869	2073.53	2002.62	2051.92	2104.79	0.3869	0.3812	0.391	0.4005
1425.0	0.65	1354.34	0.3844	2071.32	1989.69	2038.98	2091.86	0.3844	0.3808	0.3905	0.4001
1430.0	0.65	1356.64	0.382	2069.13	1976.9	2026.18	2079.08	0.382	0.3804	0.3901	0.3996
1435.0	0.65	1358.92	0.3796	2066.95	1964.25	2013.52	2066.43	0.3796	0.38	0.3897	0.3992
1440.0	0.65	1361.17	0.3773	2064.8	1951.73	2000.99	2053.92	0.3773	0.3796	0.3893	0.3988
1445.0	0.65	1363.4	0.3749	2062.66	1939.36	1988.61	2041.54	0.3749	0.3792	0.3889	0.3984
1450.0	0.65	1365.59	0.3726	2060.55	1927.11	1976.35	2029.3	0.3726	0.3788	0.3885	0.398
1455.0	0.65	1367.76	0.3703	2058.46	1914.99	1964.22	2017.18	0.3703	0.3784	0.3881	0.3976
1460.0	0.65	1369.91	0.3681	2056.38	1903.0	1952.22	2005.19	0.3681	0.378	0.3877	0.3972
1465.0	0.65	1372.03	0.3658	2054.32	1891.13	1940.34	1993.33	0.3658	0.3776	0.3873	0.3969
1470.0	0.65	1374.12	0.3636	2052.28	1879.4	1928.59	1981.59	0.3636	0.3772	0.3869	0.3965

1475.0	0.65	1376.19	0.3614	2050.27	1867.78	1916.96	1969.97	0.3614	0.3768	0.3866	0.3961
1480.0	0.65	1378.23	0.3593	2048.26	1856.27	1905.45	1958.47	0.3593	0.3765	0.3862	0.3957
1485.0	0.65	1380.26	0.3571	2046.28	1844.9	1894.06	1947.1	0.3571	0.3761	0.3858	0.3953
1490.0	0.65	1382.25	0.355	2044.31	1833.63	1882.79	1935.84	0.355	0.3757	0.3854	0.395
1365.0	0.66	1325.32	0.4165	2102.08	2159.55	2208.97	2261.7	0.4165	0.3866	0.3963	0.4059
1370.0	0.66	1327.99	0.4137	2099.61	2144.94	2194.35	2247.09	0.4137	0.3862	0.3959	0.4054
1375.0	0.66	1330.63	0.411	2097.16	2130.49	2179.89	2232.65	0.411	0.3857	0.3954	0.4049
1380.0	0.66	1333.23	0.4083	2094.73	2116.2	2165.59	2218.36	0.4083	0.3852	0.395	0.4045
1385.0	0.66	1335.8	0.4056	2092.33	2102.09	2151.46	2204.24	0.4056	0.3848	0.3945	0.404
1390.0	0.66	1338.34	0.403	2089.96	2088.13	2137.49	2190.29	0.403	0.3843	0.3941	0.4036
1395.0	0.66	1340.84	0.4004	2087.6	2074.32	2123.67	2176.48	0.4004	0.3839	0.3936	0.4031
1400.0	0.66	1343.31	0.3978	2085.27	2060.67	2110.01	2162.83	0.3978	0.3835	0.3932	0.4027
1405.0	0.66	1345.75	0.3953	2082.96	2047.17	2096.51	2149.34	0.3953	0.383	0.3927	0.4023
1410.0	0.66	1348.16	0.3928	2080.67	2033.82	2083.14	2135.99	0.3928	0.3826	0.3923	0.4018
1415.0	0.66	1350.54	0.3903	2078.41	2020.62	2069.93	2122.79	0.3903	0.3822	0.3919	0.4014
1420.0	0.66	1352.89	0.3878	2076.16	2007.56	2056.87	2109.73	0.3878	0.3817	0.3915	0.401
1425.0	0.66	1355.21	0.3854	2073.94	1994.65	2043.94	2096.82	0.3854	0.3813	0.391	0.4006
1430.0	0.66	1357.5	0.383	2071.73	1981.87	2031.15	2084.04	0.383	0.3809	0.3906	0.4001
1435.0	0.66	1359.77	0.3806	2069.55	1969.23	2018.5	2071.41	0.3806	0.3805	0.3902	0.3997
1440.0	0.66	1362.01	0.3782	2067.39	1956.73	2005.99	2058.91	0.3782	0.3801	0.3898	0.3993
1445.0	0.66	1364.22	0.3759	2065.24	1944.36	1993.62	2046.55	0.3759	0.3797	0.3894	0.3989
1450.0	0.66	1366.4	0.3736	2063.12	1932.12	1981.36	2034.3	0.3736	0.3793	0.389	0.3985
1455.0	0.66	1368.56	0.3713	2061.02	1920.01	1969.25	2022.2	0.3713	0.3789	0.3886	0.3981
1460.0	0.66	1370.69	0.369	2058.93	1908.03	1957.26	2010.22	0.369	0.3785	0.3882	0.3977
1465.0	0.66	1372.79	0.3668	2056.87	1896.18	1945.39	1998.37	0.3668	0.3781	0.3878	0.3973
1470.0	0.66	1374.88	0.3646	2054.82	1884.45	1933.65	1986.64	0.3646	0.3777	0.3874	0.397
1475.0	0.66	1376.93	0.3624	2052.79	1872.84	1922.03	1975.03	0.3624	0.3773	0.387	0.3966
1480.0	0.66	1378.97	0.3602	2050.78	1861.35	1910.53	1963.55	0.3602	0.3769	0.3867	0.3962
1485.0	0.66	1380.98	0.3581	2048.79	1849.98	1899.15	1952.18	0.3581	0.3766	0.3863	0.3958
1490.0	0.66	1382.96	0.356	2046.81	1838.72	1887.88	1940.93	0.356	0.3762	0.3859	0.3954
1495.0	0.66	1384.93	0.3538	2044.85	1827.58	1876.73	1929.78	0.3538	0.3758	0.3855	0.3951
1370.0	0.67	1329.12	0.4146	2102.27	2149.3	2198.71	2251.46	0.4146	0.3867	0.3964	0.4059
1375.0	0.67	1331.74	0.4118	2099.81	2134.88	2184.28	2237.03	0.4118	0.3862	0.3959	0.4054
1380.0	0.67	1334.32	0.4091	2097.38	2120.62	2170.01	2222.78	0.4091	0.3857	0.3955	0.405
1385.0	0.67	1336.87	0.4065	2094.97	2106.51	2155.89	2208.67	0.4065	0.3853	0.395	0.4045
1390.0	0.67	1339.39	0.4039	2092.58	2092.57	2141.94	2194.73	0.4039	0.3848	0.3945	0.4041
1395.0	0.67	1341.88	0.4013	2090.22	2078.79	2128.15	2180.95	0.4013	0.3844	0.3941	0.4036
1400.0	0.67	1344.34	0.3987	2087.88	2065.16	2114.51	2167.32	0.3987	0.3839	0.3937	0.4032
1405.0	0.67	1346.76	0.3961	2085.56	2051.67	2101.01	2153.84	0.3961	0.3835	0.3932	0.4027
1410.0	0.67	1349.16	0.3936	2083.26	2038.34	2087.67	2140.51	0.3936	0.3831	0.3928	0.4023
1415.0	0.67	1351.52	0.3911	2080.98	2025.16	2074.48	2127.33	0.3911	0.3826	0.3924	0.4019
1420.0	0.67	1353.86	0.3887	2078.73	2012.12	2061.43	2114.29	0.3887	0.3822	0.3919	0.4015
1425.0	0.67	1356.16	0.3862	2076.5	1999.22	2048.51	2101.39	0.3862	0.3818	0.3915	0.401
1430.0	0.67	1358.44	0.3838	2074.28	1986.46	2035.75	2088.63	0.3838	0.3814	0.3911	0.4006
1435.0	0.67	1360.69	0.3814	2072.09	1973.84	2023.11	2076.01	0.3814	0.381	0.3907	0.4002
1440.0	0.67	1362.91	0.3791	2069.92	1961.35	2010.62	2063.53	0.3791	0.3806	0.3903	0.3998
1445.0	0.67	1365.11	0.3768	2067.77	1948.99	1998.25	2051.17	0.3768	0.3802	0.3899	0.3994
1450.0	0.67	1367.28	0.3745	2065.64	1936.77	1986.01	2038.95	0.3745	0.3797	0.3895	0.399
1455.0	0.67	1369.42	0.3722	2063.52	1924.67	1973.91	2026.86	0.3722	0.3793	0.3891	0.3986
1460.0	0.67	1371.54	0.3699	2061.43	1912.71	1961.93	2014.9	0.3699	0.379	0.3887	0.3982
1465.0	0.67	1373.63	0.3677	2059.35	1900.86	1950.08	2003.05	0.3677	0.3786	0.3883	0.3978
1470.0	0.67	1375.7	0.3655	2057.3	1889.14	1938.35	1991.33	0.3655	0.3782	0.3879	0.3974
1475.0	0.67	1377.75	0.3633	2055.26	1877.55	1926.74	1979.74	0.3633	0.3778	0.3875	0.397

1480.0	0.67	1379.77	0.3611	2053.24	1866.07	1915.25	1968.26	0.3611	0.3774	0.3871	0.3967
1485.0	0.67	1381.77	0.359	2051.24	1854.71	1903.88	1956.91	0.359	0.377	0.3868	0.3963
1490.0	0.67	1383.74	0.3568	2049.26	1843.46	1892.62	1945.66	0.3568	0.3767	0.3864	0.3959
1495.0	0.67	1385.69	0.3547	2047.29	1832.33	1881.48	1934.53	0.3547	0.3763	0.386	0.3955
1500.0	0.67	1387.62	0.3527	2045.34	1821.31	1870.45	1923.52	0.3527	0.3759	0.3856	0.3952
1375.0	0.68	1332.92	0.4126	2102.4	2138.88	2188.28	2241.03	0.4126	0.3867	0.3964	0.4059
1380.0	0.68	1335.49	0.4099	2099.96	2124.63	2174.03	2226.79	0.4099	0.3862	0.3959	0.4055
1385.0	0.68	1338.03	0.4072	2097.54	2110.56	2159.94	2212.72	0.4072	0.3858	0.3955	0.405
1390.0	0.68	1340.53	0.4046	2095.15	2096.64	2146.01	2198.8	0.4046	0.3853	0.395	0.4046
1395.0	0.68	1343.0	0.402	2092.77	2082.87	2132.23	2185.03	0.402	0.3849	0.3946	0.4041
1400.0	0.68	1345.44	0.3995	2090.42	2069.26	2118.62	2171.43	0.3995	0.3844	0.3941	0.4037
1405.0	0.68	1347.85	0.3969	2088.1	2055.8	2105.15	2157.97	0.3969	0.384	0.3937	0.4032
1410.0	0.68	1350.23	0.3944	2085.79	2042.49	2091.83	2144.66	0.3944	0.3835	0.3933	0.4028
1415.0	0.68	1352.57	0.3919	2083.5	2029.32	2078.65	2131.49	0.3919	0.3831	0.3928	0.4024
1420.0	0.68	1354.89	0.3895	2081.24	2016.3	2065.61	2118.47	0.3895	0.3827	0.3924	0.4019
1425.0	0.68	1357.19	0.387	2079.0	2003.42	2052.72	2105.6	0.387	0.3823	0.392	0.4015
1430.0	0.68	1359.45	0.3846	2076.78	1990.68	2039.97	2092.86	0.3846	0.3818	0.3916	0.4011
1435.0	0.68	1361.68	0.3822	2074.58	1978.07	2027.35	2080.25	0.3822	0.3814	0.3912	0.4007
1440.0	0.68	1363.89	0.3799	2072.4	1965.6	2014.87	2067.78	0.3799	0.381	0.3907	0.4003
1445.0	0.68	1366.07	0.3776	2070.24	1953.26	2002.53	2055.45	0.3776	0.3806	0.3903	0.3999
1450.0	0.68	1368.23	0.3753	2068.1	1941.06	1990.31	2043.24	0.3753	0.3802	0.3899	0.3995
1455.0	0.68	1370.36	0.373	2065.97	1928.97	1978.21	2031.16	0.373	0.3798	0.3895	0.3991
1460.0	0.68	1372.46	0.3707	2063.87	1917.02	1966.25	2019.21	0.3707	0.3794	0.3891	0.3987
1465.0	0.68	1374.54	0.3685	2061.79	1905.2	1954.42	2007.38	0.3685	0.379	0.3887	0.3983
1470.0	0.68	1376.6	0.3663	2059.73	1893.49	1942.7	1995.68	0.3663	0.3786	0.3884	0.3979
1475.0	0.68	1378.63	0.3641	2057.68	1881.91	1931.11	1984.1	0.3641	0.3782	0.388	0.3975
1480.0	0.68	1380.64	0.3619	2055.65	1870.44	1919.63	1972.63	0.3619	0.3779	0.3876	0.3971
1485.0	0.68	1382.62	0.3598	2053.64	1859.09	1908.27	1961.29	0.3598	0.3775	0.3872	0.3967
1490.0	0.68	1384.59	0.3577	2051.65	1847.86	1897.03	1950.06	0.3577	0.3771	0.3868	0.3964
1495.0	0.68	1386.52	0.3556	2049.68	1836.74	1885.9	1938.94	0.3556	0.3767	0.3865	0.396
1500.0	0.68	1388.44	0.3535	2047.72	1825.73	1874.88	1927.94	0.3535	0.3764	0.3861	0.3956
1505.0	0.68	1390.34	0.3514	2045.78	1814.83	1863.97	1917.04	0.3514	0.376	0.3857	0.3952
1380.0	0.69	1336.74	0.4106	2102.49	2128.27	2177.67	2230.43	0.4106	0.3867	0.3964	0.4059
1385.0	0.69	1339.25	0.4079	2100.06	2114.22	2163.6	2216.37	0.4079	0.3862	0.396	0.4055
1390.0	0.69	1341.74	0.4053	2097.65	2100.32	2149.7	2202.48	0.4053	0.3858	0.3955	0.405
1395.0	0.69	1344.19	0.4027	2095.27	2086.59	2135.95	2188.75	0.4027	0.3853	0.3951	0.4046
1400.0	0.69	1346.61	0.4002	2092.91	2073.0	2122.36	2175.16	0.4002	0.3849	0.3946	0.4041
1405.0	0.69	1349.01	0.3976	2090.58	2059.56	2108.9	2161.72	0.3976	0.3845	0.3942	0.4037
1410.0	0.69	1351.37	0.3951	2088.26	2046.27	2095.61	2148.44	0.3951	0.384	0.3937	0.4033
1415.0	0.69	1353.7	0.3926	2085.97	2033.13	2082.45	2135.3	0.3926	0.3836	0.3933	0.4028
1420.0	0.69	1356.01	0.3902	2083.7	2020.13	2069.44	2122.3	0.3902	0.3832	0.3929	0.4024
1425.0	0.69	1358.28	0.3878	2081.45	2007.26	2056.57	2109.44	0.3878	0.3827	0.3924	0.402
1430.0	0.69	1360.53	0.3854	2079.22	1994.54	2043.84	2096.72	0.3854	0.3823	0.392	0.4016
1435.0	0.69	1362.75	0.383	2077.01	1981.96	2031.24	2084.14	0.383	0.3819	0.3916	0.4011
1440.0	0.69	1364.94	0.3806	2074.82	1969.51	2018.78	2071.69	0.3806	0.3815	0.3912	0.4007
1445.0	0.69	1367.11	0.3783	2072.65	1957.19	2006.45	2059.37	0.3783	0.3811	0.3908	0.4003
1450.0	0.69	1369.25	0.376	2070.5	1944.99	1994.25	2047.18	0.376	0.3807	0.3904	0.3999
1455.0	0.69	1371.36	0.3737	2068.37	1932.93	1982.18	2035.12	0.3737	0.3803	0.39	0.3995
1460.0	0.69	1373.46	0.3715	2066.26	1921.0	1970.23	2023.19	0.3715	0.3799	0.3896	0.3991
1465.0	0.69	1375.52	0.3692	2064.17	1909.19	1958.41	2011.38	0.3692	0.3795	0.3892	0.3987
1470.0	0.69	1377.56	0.367	2062.1	1897.5	1946.71	1999.69	0.367	0.3791	0.3888	0.3983
1475.0	0.69	1379.58	0.3649	2060.04	1885.93	1935.13	1988.12	0.3649	0.3787	0.3884	0.3979
1480.0	0.69	1381.58	0.3627	2058.01	1874.48	1923.67	1976.67	0.3627	0.3783	0.388	0.3976

1485.0	0.69	1383.55	0.3606	2055.99	1863.15	1912.33	1965.34	0.3606	0.3779	0.3876	0.3972
1490.0	0.69	1385.5	0.3584	2053.99	1851.93	1901.1	1954.13	0.3584	0.3776	0.3873	0.3968
1495.0	0.69	1387.42	0.3563	2052.01	1840.82	1889.98	1943.02	0.3563	0.3772	0.3869	0.3964
1500.0	0.69	1389.33	0.3543	2050.04	1829.83	1878.98	1932.03	0.3543	0.3768	0.3865	0.3961
1505.0	0.69	1391.21	0.3522	2048.1	1818.95	1868.09	1921.15	0.3522	0.3764	0.3862	0.3957
1510.0	0.69	1393.07	0.3502	2046.17	1808.17	1857.3	1910.38	0.3502	0.3761	0.3858	0.3953
1385.0	0.7	1340.55	0.4086	2102.52	2117.52	2166.9	2219.67	0.4086	0.3867	0.3964	0.4059
1390.0	0.7	1343.02	0.4059	2100.1	2103.65	2153.03	2205.81	0.4059	0.3862	0.396	0.4055
1395.0	0.7	1345.45	0.4034	2097.71	2089.94	2139.31	2192.1	0.4034	0.3858	0.3955	0.405
1400.0	0.7	1347.86	0.4008	2095.35	2076.37	2125.73	2178.54	0.4008	0.3854	0.3951	0.4046
1405.0	0.7	1350.23	0.3983	2093.0	2062.96	2112.31	2165.13	0.3983	0.3849	0.3946	0.4042
1410.0	0.7	1352.58	0.3958	2090.68	2049.7	2099.04	2151.87	0.3958	0.3845	0.3942	0.4037
1415.0	0.7	1354.9	0.3933	2088.38	2036.58	2085.91	2138.75	0.3933	0.384	0.3938	0.4033
1420.0	0.7	1357.18	0.3908	2086.1	2023.6	2072.92	2125.77	0.3908	0.3836	0.3933	0.4028
1425.0	0.7	1359.44	0.3884	2083.84	2010.76	2060.07	2112.94	0.3884	0.3832	0.3929	0.4024
1430.0	0.7	1361.67	0.386	2081.6	1998.07	2047.36	2100.24	0.386	0.3828	0.3925	0.402
1435.0	0.7	1363.88	0.3837	2079.39	1985.5	2034.79	2087.68	0.3837	0.3823	0.3921	0.4016
1440.0	0.7	1366.06	0.3813	2077.19	1973.07	2022.35	2075.25	0.3813	0.3819	0.3916	0.4012
1445.0	0.7	1368.21	0.379	2075.01	1960.77	2010.04	2062.95	0.379	0.3815	0.3912	0.4008
1450.0	0.7	1370.33	0.3767	2072.86	1948.6	1997.86	2050.79	0.3767	0.3811	0.3908	0.4004
1455.0	0.7	1372.44	0.3744	2070.72	1936.56	1985.81	2038.75	0.3744	0.3807	0.3904	0.3999
1460.0	0.7	1374.51	0.3722	2068.6	1924.65	1973.88	2026.83	0.3722	0.3803	0.39	0.3996
1465.0	0.7	1376.56	0.3699	2066.5	1912.85	1962.08	2015.04	0.3699	0.3799	0.3896	0.3992
1470.0	0.7	1378.59	0.3677	2064.42	1901.18	1950.4	2003.37	0.3677	0.3795	0.3892	0.3988
1475.0	0.7	1380.59	0.3656	2062.36	1889.63	1938.84	1991.82	0.3656	0.3791	0.3888	0.3984
1480.0	0.7	1382.57	0.3634	2060.32	1878.2	1927.39	1980.39	0.3634	0.3787	0.3885	0.398
1485.0	0.7	1384.53	0.3613	2058.29	1866.88	1916.07	1969.08	0.3613	0.3784	0.3881	0.3976
1490.0	0.7	1386.47	0.3592	2056.28	1855.68	1904.85	1957.87	0.3592	0.378	0.3877	0.3972
1495.0	0.7	1388.38	0.3571	2054.29	1844.59	1893.75	1946.79	0.3571	0.3776	0.3873	0.3969
1500.0	0.7	1390.27	0.355	2052.32	1833.61	1882.77	1935.82	0.355	0.3772	0.387	0.3965
1505.0	0.7	1392.14	0.3529	2050.37	1822.75	1871.89	1924.95	0.3529	0.3769	0.3866	0.3961
1510.0	0.7	1393.99	0.3509	2048.43	1811.99	1861.12	1914.19	0.3509	0.3765	0.3862	0.3957
1515.0	0.7	1395.82	0.3489	2046.51	1801.33	1850.45	1903.54	0.3489	0.3761	0.3859	0.3954

Table 4.2: ab -model results

Startup values			Using $b_{p_{ab,out}}$ as input				Using $a_{p_{ab,out}}$ as input		
$a_{p_{ab,in}}$	$b_{p_{ab,in}}$	$a_{p_{ab,out}}$	a_{p_+}	a_{p_-}	$b_{p_{ab,out}}$	b_{p_-}	b_p	b_{p_+}	
1005.0	0.25	2078.35	2246.06	2193.31	2143.9	0.4135	0.4014	0.3919	0.3821
1025.0	0.25	2078.35	2246.05	2193.3	2143.89	0.4135	0.4014	0.3919	0.3821
1045.0	0.25	2077.9	2252.09	2199.35	2149.94	0.4147	0.4013	0.3918	0.3821
1065.0	0.25	2078.04	2250.26	2197.51	2148.1	0.4143	0.4013	0.3918	0.3821
1085.0	0.25	2078.14	2248.84	2196.1	2146.69	0.4141	0.4013	0.3918	0.3821
1105.0	0.25	2078.22	2247.79	2195.05	2145.64	0.4139	0.4014	0.3918	0.3821
1125.0	0.25	2078.27	2247.06	2194.31	2144.91	0.4137	0.4014	0.3918	0.3821
1145.0	0.25	2078.31	2246.58	2193.83	2144.43	0.4136	0.4014	0.3919	0.3821
1165.0	0.25	2078.33	2246.29	2193.55	2144.14	0.4136	0.4014	0.3919	0.3821
1185.0	0.25	2078.35	2246.05	2193.3	2143.89	0.4135	0.4014	0.3919	0.3821
1205.0	0.25	2077.89	2252.2	2199.46	2150.04	0.4147	0.4013	0.3918	0.3821
1225.0	0.25	2078.03	2250.34	2197.6	2148.19	0.4143	0.4013	0.3918	0.3821
1245.0	0.25	2078.13	2248.91	2196.17	2146.76	0.4141	0.4013	0.3918	0.3821
1265.0	0.25	2078.21	2247.85	2195.1	2145.69	0.4139	0.4014	0.3918	0.3821

1285.0	0.25	2078.27	2247.1	2194.35	2144.95	0.4137	0.4014	0.3918	0.3821
1305.0	0.25	2078.31	2246.61	2193.86	2144.45	0.4136	0.4014	0.3919	0.3821
1325.0	0.25	2078.33	2246.3	2193.56	2144.15	0.4136	0.4014	0.3919	0.3821
1345.0	0.25	2078.34	2246.14	2193.4	2143.99	0.4136	0.4014	0.3919	0.3821
1365.0	0.25	2077.65	2255.77	2203.03	2153.62	0.4154	0.4013	0.3917	0.382
1385.0	0.25	2077.89	2252.15	2199.41	2150.0	0.4147	0.4013	0.3918	0.3821
1405.0	0.25	2078.18	2248.29	2195.54	2146.14	0.414	0.4014	0.3918	0.3821
1425.0	0.25	2078.34	2246.14	2193.4	2143.99	0.4136	0.4014	0.3919	0.3821
1445.0	0.25	2078.35	2246.07	2193.32	2143.91	0.4135	0.4014	0.3919	0.3821
1465.0	0.25	2077.89	2252.24	2199.5	2150.08	0.4147	0.4013	0.3918	0.3821
1485.0	0.25	2078.18	2248.34	2195.59	2146.18	0.414	0.4014	0.3918	0.3821
1505.0	0.25	2078.31	2246.54	2193.79	2144.39	0.4136	0.4014	0.3919	0.3821
1525.0	0.25	2077.51	2257.31	2204.57	2155.15	0.4157	0.4012	0.3917	0.382
1545.0	0.25	2078.31	2246.55	2193.8	2144.39	0.4136	0.4014	0.3919	0.3821
1565.0	0.25	2077.5	2257.42	2204.68	2155.27	0.4157	0.4012	0.3917	0.382
1585.0	0.25	2078.35	2246.04	2193.3	2143.89	0.4135	0.4014	0.3919	0.3821
1605.0	0.25	2078.26	2247.25	2194.5	2145.09	0.4138	0.4014	0.3918	0.3821
1625.0	0.25	2078.35	2246.03	2193.28	2143.88	0.4135	0.4014	0.3919	0.3821
1645.0	0.25	2078.32	2246.4	2193.66	2144.25	0.4136	0.4014	0.3919	0.3821
1665.0	0.25	2076.38	2272.56	2219.83	2170.41	0.4185	0.401	0.3915	0.3818
1685.0	0.25	2078.02	2250.52	2197.77	2148.36	0.4144	0.4013	0.3918	0.3821
1705.0	0.25	2078.08	2249.6	2196.86	2147.45	0.4142	0.4013	0.3918	0.3821
1725.0	0.25	2088.21	2108.73	2055.86	2006.56	0.3876	0.4032	0.3937	0.384
1745.0	0.25	2112.27	1775.2	1721.95	1672.96	0.3247	0.4078	0.3983	0.3885
1765.0	0.25	2121.21	1651.7	1598.27	1549.43	0.3013	0.4095	0.3999	0.3902
1785.0	0.25	2135.74	1451.23	1397.43	1348.89	0.2635	0.4122	0.4027	0.393
1805.0	0.25	2138.49	1413.53	1359.65	1311.17	0.2564	0.4127	0.4032	0.3935
1005.0	0.3	2078.19	2248.11	2195.36	2145.95	0.4139	0.4014	0.3918	0.3821
1025.0	0.3	2078.26	2247.28	2194.53	2145.12	0.4138	0.4014	0.3918	0.3821
1045.0	0.3	2078.3	2246.72	2193.97	2144.56	0.4137	0.4014	0.3919	0.3821
1065.0	0.3	2078.32	2246.37	2193.62	2144.22	0.4136	0.4014	0.3919	0.3821
1085.0	0.3	2078.34	2246.18	2193.43	2144.02	0.4136	0.4014	0.3919	0.3821
1105.0	0.3	2078.35	2246.04	2193.29	2143.89	0.4135	0.4014	0.3919	0.3821
1125.0	0.3	2077.99	2250.92	2198.18	2148.77	0.4145	0.4013	0.3918	0.3821
1145.0	0.3	2078.1	2249.35	2196.61	2147.2	0.4142	0.4013	0.3918	0.3821
1165.0	0.3	2078.19	2248.17	2195.43	2146.02	0.4139	0.4014	0.3918	0.3821
1185.0	0.3	2078.25	2247.32	2194.57	2145.17	0.4138	0.4014	0.3918	0.3821
1205.0	0.3	2078.29	2246.75	2194.0	2144.59	0.4137	0.4014	0.3919	0.3821
1225.0	0.3	2078.32	2246.39	2193.64	2144.23	0.4136	0.4014	0.3919	0.3821
1245.0	0.3	2078.34	2246.18	2193.44	2144.03	0.4136	0.4014	0.3919	0.3821
1265.0	0.3	2078.34	2246.09	2193.34	2143.93	0.4135	0.4014	0.3919	0.3821
1285.0	0.3	2078.35	2246.04	2193.3	2143.89	0.4135	0.4014	0.3919	0.3821
1305.0	0.3	2078.1	2249.32	2196.58	2147.17	0.4142	0.4013	0.3918	0.3821
1325.0	0.3	2078.28	2246.93	2194.18	2144.78	0.4137	0.4014	0.3919	0.3821
1345.0	0.3	2078.34	2246.09	2193.34	2143.93	0.4135	0.4014	0.3919	0.3821
1365.0	0.3	2078.35	2246.04	2193.3	2143.89	0.4135	0.4014	0.3919	0.3821
1385.0	0.3	2078.1	2249.38	2196.64	2147.23	0.4142	0.4013	0.3918	0.3821
1405.0	0.3	2078.28	2246.96	2194.21	2144.8	0.4137	0.4014	0.3918	0.3821
1425.0	0.3	2078.34	2246.13	2193.39	2143.98	0.4136	0.4014	0.3919	0.3821
1445.0	0.3	2078.28	2246.96	2194.21	2144.81	0.4137	0.4014	0.3918	0.3821
1465.0	0.3	2078.34	2246.13	2193.39	2143.98	0.4136	0.4014	0.3919	0.3821
1485.0	0.3	2078.34	2246.1	2193.36	2143.95	0.4135	0.4014	0.3919	0.3821
1505.0	0.3	2078.35	2246.03	2193.28	2143.88	0.4135	0.4014	0.3919	0.3821

1525.0	0.3	2078.35	2246.03	2193.28	2143.88	0.4135	0.4014	0.3919	0.3821
1545.0	0.3	2077.4	2258.83	2206.09	2156.67	0.4159	0.4012	0.3917	0.382
1565.0	0.3	2078.15	2248.64	2195.9	2146.49	0.414	0.4014	0.3918	0.3821
1585.0	0.3	2078.16	2248.61	2195.87	2146.46	0.414	0.4014	0.3918	0.3821
1605.0	0.3	2078.34	2246.1	2193.36	2143.95	0.4135	0.4014	0.3919	0.3821
1625.0	0.3	2089.82	2086.36	2033.47	1984.18	0.3834	0.4036	0.394	0.3843
1645.0	0.3	2099.58	1950.92	1897.89	1848.72	0.3578	0.4054	0.3959	0.3861
1665.0	0.3	2115.02	1736.95	1683.64	1634.7	0.3174	0.4083	0.3988	0.3891
1685.0	0.3	2118.47	1689.47	1636.1	1587.21	0.3085	0.409	0.3994	0.3897
1705.0	0.3	2120.86	1656.36	1602.94	1554.09	0.3022	0.4094	0.3999	0.3902
1725.0	0.3	2122.67	1631.48	1578.02	1529.21	0.2975	0.4097	0.4002	0.3905
1745.0	0.3	2124.11	1611.66	1558.16	1509.37	0.2938	0.41	0.4005	0.3908
1765.0	0.3	2125.31	1595.07	1541.55	1492.78	0.2907	0.4102	0.4007	0.391
1785.0	0.3	2126.35	1580.7	1527.16	1478.41	0.2879	0.4104	0.4009	0.3912
1805.0	0.3	2127.28	1567.91	1514.34	1465.61	0.2855	0.4106	0.4011	0.3914
1005.0	0.35	2078.35	2246.04	2193.3	2143.89	0.4135	0.4014	0.3919	0.3821
1025.0	0.35	2077.94	2251.55	2198.81	2149.4	0.4146	0.4013	0.3918	0.3821
1045.0	0.35	2078.07	2249.84	2197.09	2147.68	0.4143	0.4013	0.3918	0.3821
1065.0	0.35	2078.16	2248.53	2195.79	2146.38	0.414	0.4014	0.3918	0.3821
1085.0	0.35	2078.23	2247.58	2194.83	2145.42	0.4138	0.4014	0.3918	0.3821
1105.0	0.35	2078.28	2246.91	2194.17	2144.76	0.4137	0.4014	0.3919	0.3821
1125.0	0.35	2078.31	2246.49	2193.74	2144.33	0.4136	0.4014	0.3919	0.3821
1145.0	0.35	2078.33	2246.24	2193.49	2144.09	0.4136	0.4014	0.3919	0.3821
1165.0	0.35	2078.34	2246.11	2193.36	2143.96	0.4135	0.4014	0.3919	0.3821
1185.0	0.35	2078.35	2246.05	2193.31	2143.9	0.4135	0.4014	0.3919	0.3821
1205.0	0.35	2078.01	2250.62	2197.88	2148.47	0.4144	0.4013	0.3918	0.3821
1225.0	0.35	2078.24	2247.52	2194.77	2145.37	0.4138	0.4014	0.3918	0.3821
1245.0	0.35	2078.34	2246.11	2193.37	2143.96	0.4135	0.4014	0.3919	0.3821
1265.0	0.35	2078.35	2246.05	2193.31	2143.9	0.4135	0.4014	0.3919	0.3821
1285.0	0.35	2078.0	2250.7	2197.96	2148.55	0.4144	0.4013	0.3918	0.3821
1305.0	0.35	2078.23	2247.56	2194.81	2145.4	0.4138	0.4014	0.3918	0.3821
1325.0	0.35	2078.33	2246.29	2193.54	2144.13	0.4136	0.4014	0.3919	0.3821
1345.0	0.35	2078.23	2247.56	2194.82	2145.41	0.4138	0.4014	0.3918	0.3821
1365.0	0.35	2078.33	2246.29	2193.54	2144.13	0.4136	0.4014	0.3919	0.3821
1385.0	0.35	2078.01	2250.57	2197.83	2148.42	0.4144	0.4013	0.3918	0.3821
1405.0	0.35	2078.35	2246.03	2193.29	2143.88	0.4135	0.4014	0.3919	0.3821
1425.0	0.35	2078.34	2246.11	2193.37	2143.96	0.4135	0.4014	0.3919	0.3821
1445.0	0.35	2078.05	2250.1	2197.36	2147.95	0.4143	0.4013	0.3918	0.3821
1465.0	0.35	2076.11	2276.3	2223.58	2174.15	0.4192	0.401	0.3914	0.3817
1485.0	0.35	2077.95	2250.65	2197.91	2148.49	0.4144	0.4013	0.3918	0.3821
1505.0	0.35	2086.72	2129.07	2076.22	2026.9	0.3915	0.403	0.3934	0.3837
1525.0	0.35	2093.01	2041.93	1988.99	1939.74	0.375	0.4042	0.3946	0.3849
1545.0	0.35	2097.33	1982.08	1929.08	1879.88	0.3637	0.405	0.3954	0.3857
1565.0	0.35	2100.41	1939.42	1886.37	1837.21	0.3557	0.4055	0.396	0.3863
1585.0	0.35	2102.73	1907.28	1854.2	1805.07	0.3496	0.406	0.3965	0.3867
1605.0	0.35	2104.57	1881.76	1828.65	1779.54	0.3448	0.4063	0.3968	0.3871
1625.0	0.35	2106.1	1860.55	1807.42	1758.34	0.3408	0.4066	0.3971	0.3874
1645.0	0.35	2107.42	1842.29	1789.13	1740.07	0.3373	0.4069	0.3973	0.3876
1665.0	0.35	2108.59	1826.08	1772.9	1723.85	0.3343	0.4071	0.3976	0.3878
1685.0	0.35	2109.65	1811.37	1758.17	1709.14	0.3315	0.4073	0.3978	0.388
1705.0	0.35	2110.63	1797.8	1744.58	1695.56	0.3289	0.4075	0.398	0.3882
1725.0	0.35	2078.29	2246.83	2194.08	2144.68	0.4137	0.4014	0.3919	0.3821
1745.0	0.35	2078.28	2246.93	2194.18	2144.77	0.4137	0.4014	0.3919	0.3821

1765.0	0.35	2078.27	2247.02	2194.28	2144.87	0.4137	0.4014	0.3918	0.3821
1785.0	0.35	2078.27	2247.13	2194.39	2144.98	0.4137	0.4014	0.3918	0.3821
1805.0	0.35	2078.26	2247.24	2194.49	2145.08	0.4138	0.4014	0.3918	0.3821
1005.0	0.4	2078.27	2247.11	2194.36	2144.95	0.4137	0.4014	0.3918	0.3821
1025.0	0.4	2078.3	2246.61	2193.86	2144.46	0.4136	0.4014	0.3919	0.3821
1045.0	0.4	2078.33	2246.31	2193.56	2144.15	0.4136	0.4014	0.3919	0.3821
1065.0	0.4	2078.34	2246.14	2193.4	2143.99	0.4136	0.4014	0.3919	0.3821
1085.0	0.4	2078.35	2246.07	2193.32	2143.91	0.4135	0.4014	0.3919	0.3821
1105.0	0.4	2077.89	2252.22	2199.47	2150.06	0.4147	0.4013	0.3918	0.3821
1125.0	0.4	2078.18	2248.32	2195.58	2146.17	0.414	0.4014	0.3918	0.3821
1145.0	0.4	2078.34	2246.15	2193.4	2143.99	0.4136	0.4014	0.3919	0.3821
1165.0	0.4	2078.34	2246.07	2193.32	2143.92	0.4135	0.4014	0.3919	0.3821
1185.0	0.4	2078.35	2246.04	2193.29	2143.88	0.4135	0.4014	0.3919	0.3821
1205.0	0.4	2078.17	2248.37	2195.62	2146.21	0.414	0.4014	0.3918	0.3821
1225.0	0.4	2078.31	2246.56	2193.81	2144.4	0.4136	0.4014	0.3919	0.3821
1245.0	0.4	2077.49	2257.63	2204.89	2155.48	0.4157	0.4012	0.3917	0.382
1265.0	0.4	2078.31	2246.56	2193.81	2144.4	0.4136	0.4014	0.3919	0.3821
1285.0	0.4	2077.48	2257.75	2205.01	2155.59	0.4157	0.4012	0.3917	0.382
1305.0	0.4	2078.35	2246.06	2193.31	2143.91	0.4135	0.4014	0.3919	0.3821
1325.0	0.4	2078.35	2246.03	2193.28	2143.88	0.4135	0.4014	0.3919	0.3821
1345.0	0.4	2078.25	2247.32	2194.58	2145.17	0.4138	0.4014	0.3918	0.3821
1365.0	0.4	2078.75	2240.39	2187.64	2138.24	0.4125	0.4015	0.3919	0.3822
1385.0	0.4	2080.24	2219.64	2166.87	2117.49	0.4086	0.4017	0.3922	0.3825
1405.0	0.4	2082.02	2194.86	2142.07	2092.7	0.4039	0.4021	0.3926	0.3828
1425.0	0.4	2083.77	2170.53	2117.72	2068.37	0.3993	0.4024	0.3929	0.3832
1445.0	0.4	2085.38	2148.12	2095.29	2045.95	0.3951	0.4027	0.3932	0.3835
1465.0	0.4	2086.85	2127.75	2074.9	2025.58	0.3912	0.403	0.3935	0.3837
1485.0	0.4	2088.19	2109.14	2056.27	2006.96	0.3877	0.4032	0.3937	0.384
1505.0	0.4	2089.42	2091.92	2039.03	1989.74	0.3844	0.4035	0.394	0.3842
1525.0	0.4	2090.58	2075.83	2022.93	1973.65	0.3814	0.4037	0.3942	0.3845
1545.0	0.4	2091.68	2060.63	2007.72	1958.45	0.3785	0.4039	0.3944	0.3847
1565.0	0.4	2092.72	2046.17	1993.24	1943.99	0.3758	0.4041	0.3946	0.3849
1585.0	0.4	2093.71	2032.33	1979.38	1930.14	0.3732	0.4043	0.3948	0.385
1605.0	0.4	2094.67	2018.99	1966.03	1916.8	0.3707	0.4045	0.3949	0.3852
1625.0	0.4	2077.29	2260.39	2207.65	2158.23	0.4162	0.4012	0.3917	0.3819
1645.0	0.4	2077.16	2262.01	2209.28	2159.86	0.4165	0.4012	0.3916	0.3819
1665.0	0.4	2077.04	2263.71	2210.98	2161.56	0.4169	0.4011	0.3916	0.3819
1685.0	0.4	2076.91	2265.42	2212.69	2163.27	0.4172	0.4011	0.3916	0.3819
1705.0	0.4	2076.78	2267.23	2214.5	2165.08	0.4175	0.4011	0.3916	0.3818
1725.0	0.4	2076.64	2269.04	2216.32	2166.89	0.4179	0.4011	0.3915	0.3818
1745.0	0.4	2076.51	2270.92	2218.19	2168.77	0.4182	0.401	0.3915	0.3818
1765.0	0.4	2076.36	2272.86	2220.14	2170.71	0.4186	0.401	0.3915	0.3818
1785.0	0.4	2076.22	2274.8	2222.08	2172.65	0.419	0.401	0.3915	0.3817
1805.0	0.4	2076.07	2276.82	2224.1	2174.67	0.4193	0.401	0.3914	0.3817
1005.0	0.45	2078.35	2246.05	2193.3	2143.89	0.4135	0.4014	0.3919	0.3821
1025.0	0.45	2078.1	2249.36	2196.62	2147.21	0.4142	0.4013	0.3918	0.3821
1045.0	0.45	2078.28	2246.95	2194.2	2144.79	0.4137	0.4014	0.3918	0.3821
1065.0	0.45	2078.34	2246.09	2193.34	2143.93	0.4135	0.4014	0.3919	0.3821
1085.0	0.45	2078.35	2246.05	2193.3	2143.89	0.4135	0.4014	0.3919	0.3821
1105.0	0.45	2078.1	2249.42	2196.68	2147.27	0.4142	0.4013	0.3918	0.3821
1125.0	0.45	2078.28	2246.98	2194.23	2144.82	0.4137	0.4014	0.3918	0.3821
1145.0	0.45	2078.34	2246.14	2193.39	2143.98	0.4136	0.4014	0.3919	0.3821
1165.0	0.45	2078.28	2246.98	2194.24	2144.83	0.4137	0.4014	0.3918	0.3821

1185.0	0.45	2078.34	2246.14	2193.39	2143.98	0.4136	0.4014	0.3919	0.3821
1205.0	0.45	2078.34	2246.13	2193.39	2143.98	0.4136	0.4014	0.3919	0.3821
1225.0	0.45	2074.25	2302.98	2250.28	2200.84	0.4243	0.4006	0.3911	0.3814
1245.0	0.45	2076.4	2272.97	2220.24	2170.82	0.4186	0.401	0.3915	0.3818
1265.0	0.45	2075.48	2285.83	2233.11	2183.68	0.421	0.4008	0.3913	0.3816
1285.0	0.45	2074.51	2299.51	2246.8	2197.36	0.4236	0.4007	0.3911	0.3814
1305.0	0.45	2073.84	2308.8	2256.1	2206.65	0.4254	0.4005	0.391	0.3813
1325.0	0.45	2073.58	2312.46	2259.77	2210.32	0.4261	0.4005	0.391	0.3812
1345.0	0.45	2073.67	2311.21	2258.51	2209.06	0.4258	0.4005	0.391	0.3813
1365.0	0.45	2074.03	2306.24	2253.54	2204.09	0.4249	0.4006	0.391	0.3813
1385.0	0.45	2074.57	2298.66	2245.96	2196.51	0.4235	0.4007	0.3912	0.3814
1405.0	0.45	2075.24	2289.3	2236.58	2187.15	0.4217	0.4008	0.3913	0.3816
1425.0	0.45	2076.0	2278.75	2226.03	2176.6	0.4197	0.4009	0.3914	0.3817
1445.0	0.45	2076.81	2267.42	2214.69	2165.27	0.4176	0.4011	0.3916	0.3819
1465.0	0.45	2077.66	2255.6	2202.86	2153.45	0.4153	0.4013	0.3917	0.382
1485.0	0.45	2078.53	2243.49	2190.74	2141.33	0.4131	0.4014	0.3919	0.3822
1505.0	0.45	2079.41	2231.21	2178.45	2129.05	0.4107	0.4016	0.3921	0.3823
1525.0	0.45	2078.34	2246.19	2193.44	2144.04	0.4136	0.4014	0.3919	0.3821
1545.0	0.45	2078.32	2246.37	2193.63	2144.22	0.4136	0.4014	0.3919	0.3821
1565.0	0.45	2078.3	2246.63	2193.88	2144.48	0.4136	0.4014	0.3919	0.3821
1585.0	0.45	2078.28	2246.96	2194.21	2144.8	0.4137	0.4014	0.3918	0.3821
1605.0	0.45	2078.25	2247.35	2194.6	2145.2	0.4138	0.4014	0.3918	0.3821
1625.0	0.45	2078.22	2247.81	2195.07	2145.66	0.4139	0.4014	0.3918	0.3821
1645.0	0.45	2078.18	2248.34	2195.59	2146.19	0.414	0.4014	0.3918	0.3821
1665.0	0.45	2078.13	2248.93	2196.19	2146.78	0.4141	0.4013	0.3918	0.3821
1685.0	0.45	2078.08	2249.59	2196.84	2147.43	0.4142	0.4013	0.3918	0.3821
1705.0	0.45	2078.03	2250.31	2197.56	2148.15	0.4143	0.4013	0.3918	0.3821
1725.0	0.45	2077.97	2251.07	2198.33	2148.92	0.4145	0.4013	0.3918	0.3821
1745.0	0.45	2077.91	2251.92	2199.17	2149.76	0.4146	0.4013	0.3918	0.3821
1765.0	0.45	2077.85	2252.8	2200.06	2150.65	0.4148	0.4013	0.3918	0.3821
1785.0	0.45	2077.78	2253.75	2201.01	2151.59	0.415	0.4013	0.3918	0.382
1805.0	0.45	2077.7	2254.75	2202.01	2152.6	0.4152	0.4013	0.3917	0.382
1005.0	0.5	2078.0	2250.75	2198.01	2148.6	0.4144	0.4013	0.3918	0.3821
1025.0	0.5	2078.23	2247.58	2194.84	2145.43	0.4138	0.4014	0.3918	0.3821
1045.0	0.5	2078.33	2246.29	2193.55	2144.14	0.4136	0.4014	0.3919	0.3821
1065.0	0.5	2078.23	2247.59	2194.85	2145.44	0.4138	0.4014	0.3918	0.3821
1085.0	0.5	2078.33	2246.3	2193.55	2144.14	0.4136	0.4014	0.3919	0.3821
1105.0	0.5	2078.0	2250.78	2198.04	2148.63	0.4144	0.4013	0.3918	0.3821
1125.0	0.5	2077.01	2264.06	2211.33	2161.91	0.4169	0.4011	0.3916	0.3819
1145.0	0.5	2078.13	2248.96	2196.21	2146.81	0.4141	0.4013	0.3918	0.3821
1165.0	0.5	2078.03	2250.35	2197.61	2148.2	0.4143	0.4013	0.3918	0.3821
1185.0	0.5	2077.9	2252.13	2199.39	2149.98	0.4147	0.4013	0.3918	0.3821
1205.0	0.5	2074.27	2302.64	2249.94	2200.49	0.4242	0.4006	0.3911	0.3814
1225.0	0.5	2062.99	2460.21	2407.62	2358.08	0.4539	0.3985	0.389	0.3792
1245.0	0.5	2062.17	2471.72	2419.15	2369.59	0.4561	0.3983	0.3888	0.3791
1265.0	0.5	2061.76	2477.48	2424.9	2375.35	0.4572	0.3983	0.3887	0.379
1285.0	0.5	2061.68	2478.6	2426.03	2376.47	0.4574	0.3982	0.3887	0.379
1305.0	0.5	2061.85	2476.13	2423.56	2374.01	0.457	0.3983	0.3888	0.379
1325.0	0.5	2062.23	2470.96	2418.38	2368.83	0.456	0.3983	0.3888	0.3791
1345.0	0.5	2062.74	2463.75	2411.17	2361.62	0.4546	0.3984	0.3889	0.3792
1365.0	0.5	2063.37	2455.03	2402.44	2352.9	0.453	0.3986	0.389	0.3793
1385.0	0.5	2064.07	2445.21	2392.61	2343.08	0.4511	0.3987	0.3892	0.3795
1405.0	0.5	2076.75	2268.1	2215.38	2165.95	0.4177	0.4011	0.3916	0.3818

1425.0	0.5	2076.91	2265.91	2213.18	2163.76	0.4173	0.4011	0.3916	0.3819
1445.0	0.5	2077.07	2263.68	2210.95	2161.53	0.4169	0.4011	0.3916	0.3819
1465.0	0.5	2077.23	2261.48	2208.74	2159.32	0.4164	0.4012	0.3917	0.3819
1485.0	0.5	2077.38	2259.34	2206.61	2157.19	0.416	0.4012	0.3917	0.382
1505.0	0.5	2077.53	2257.31	2204.57	2155.16	0.4157	0.4012	0.3917	0.382
1525.0	0.5	2077.67	2255.41	2202.67	2153.25	0.4153	0.4013	0.3917	0.382
1545.0	0.5	2077.8	2253.65	2200.91	2151.5	0.415	0.4013	0.3918	0.382
1565.0	0.5	2077.91	2252.05	2199.31	2149.9	0.4147	0.4013	0.3918	0.3821
1585.0	0.5	2078.01	2250.63	2197.89	2148.48	0.4144	0.4013	0.3918	0.3821
1605.0	0.5	2078.1	2249.39	2196.64	2147.23	0.4142	0.4013	0.3918	0.3821
1625.0	0.5	2074.36	2301.65	2248.95	2199.51	0.424	0.4006	0.3911	0.3814
1645.0	0.5	2075.22	2289.61	2236.9	2187.47	0.4218	0.4008	0.3913	0.3816
1665.0	0.5	2076.08	2277.68	2224.96	2175.53	0.4195	0.401	0.3914	0.3817
1685.0	0.5	2076.92	2265.86	2213.13	2163.71	0.4173	0.4011	0.3916	0.3819
1705.0	0.5	2077.76	2254.16	2201.42	2152.01	0.4151	0.4013	0.3918	0.382
1725.0	0.5	2078.6	2242.58	2189.83	2140.43	0.4129	0.4014	0.3919	0.3822
1745.0	0.5	2079.42	2231.13	2178.37	2128.98	0.4107	0.4016	0.3921	0.3823
1765.0	0.5	2078.34	2246.18	2193.43	2144.02	0.4136	0.4014	0.3919	0.3821
1785.0	0.5	2094.31	2023.96	1971.01	1921.77	0.3716	0.4044	0.3949	0.3852
1805.0	0.5	2098.54	1965.24	1912.22	1863.04	0.3605	0.4052	0.3957	0.386
1005.0	0.55	2077.2	2261.59	2208.86	2159.44	0.4165	0.4012	0.3916	0.3819
1025.0	0.55	2072.82	2322.87	2270.18	2220.72	0.428	0.4003	0.3908	0.3811
1045.0	0.55	2071.15	2346.18	2293.51	2244.04	0.4324	0.4	0.3905	0.3808
1065.0	0.55	2068.82	2378.74	2326.1	2276.6	0.4386	0.3996	0.3901	0.3803
1085.0	0.55	2066.33	2413.36	2360.75	2311.23	0.4451	0.3991	0.3896	0.3799
1105.0	0.55	2064.08	2444.89	2392.29	2342.76	0.4511	0.3987	0.3892	0.3795
1125.0	0.55	2062.23	2470.71	2418.13	2368.58	0.4559	0.3983	0.3888	0.3791
1145.0	0.55	2060.85	2490.01	2437.44	2387.88	0.4596	0.3981	0.3886	0.3788
1165.0	0.55	2049.91	2643.15	2590.68	2541.04	0.4885	0.396	0.3865	0.3768
1185.0	0.55	2059.35	2510.9	2458.35	2408.78	0.4635	0.3978	0.3883	0.3786
1205.0	0.55	2077.29	2260.29	2207.56	2158.14	0.4162	0.4012	0.3917	0.3819
1225.0	0.55	2077.29	2260.26	2207.53	2158.11	0.4162	0.4012	0.3917	0.3819
1245.0	0.55	2059.37	2510.65	2458.1	2408.52	0.4635	0.3978	0.3883	0.3786
1265.0	0.55	2059.76	2505.18	2452.62	2403.05	0.4624	0.3979	0.3884	0.3786
1285.0	0.55	2060.28	2497.94	2445.38	2395.81	0.4611	0.398	0.3885	0.3787
1305.0	0.55	2060.9	2489.31	2436.74	2387.18	0.4594	0.3981	0.3886	0.3789
1325.0	0.55	2061.59	2479.61	2427.04	2377.48	0.4576	0.3982	0.3887	0.379
1345.0	0.55	2062.34	2469.08	2416.5	2366.95	0.4556	0.3984	0.3888	0.3791
1365.0	0.55	2063.14	2457.91	2405.33	2355.79	0.4535	0.3985	0.389	0.3793
1385.0	0.55	2063.98	2446.27	2393.67	2344.14	0.4513	0.3987	0.3892	0.3794
1405.0	0.55	2064.84	2434.26	2381.65	2332.12	0.449	0.3988	0.3893	0.3796
1425.0	0.55	2065.72	2421.98	2369.37	2319.85	0.4467	0.399	0.3895	0.3798
1445.0	0.55	2066.61	2409.51	2356.89	2307.38	0.4444	0.3992	0.3896	0.3799
1465.0	0.55	2067.51	2396.92	2344.29	2294.79	0.442	0.3993	0.3898	0.3801
1485.0	0.55	2075.12	2290.68	2237.97	2188.53	0.422	0.4008	0.3913	0.3815
1505.0	0.55	2075.37	2287.24	2234.53	2185.09	0.4213	0.4008	0.3913	0.3816
1525.0	0.55	2075.61	2283.89	2231.18	2181.74	0.4207	0.4009	0.3913	0.3816
1545.0	0.55	2075.84	2280.65	2227.93	2178.5	0.4201	0.4009	0.3914	0.3817
1565.0	0.55	2076.07	2277.51	2224.79	2175.36	0.4195	0.401	0.3914	0.3817
1585.0	0.55	2076.29	2274.5	2221.78	2172.35	0.4189	0.401	0.3915	0.3818
1605.0	0.55	2076.5	2271.63	2218.9	2169.48	0.4184	0.401	0.3915	0.3818
1625.0	0.55	2076.69	2268.88	2216.16	2166.73	0.4178	0.4011	0.3916	0.3818
1645.0	0.55	2076.88	2266.29	2213.56	2164.14	0.4174	0.4011	0.3916	0.3819

1665.0	0.55	2083.72	2171.16	2118.35	2068.99	0.3994	0.4024	0.3929	0.3832
1685.0	0.55	2086.98	2125.81	2072.96	2023.64	0.3908	0.403	0.3935	0.3838
1705.0	0.55	2090.47	2077.34	2024.44	1975.16	0.3817	0.4037	0.3941	0.3844
1725.0	0.55	2094.02	2028.12	1975.17	1925.94	0.3724	0.4043	0.3948	0.3851
1745.0	0.55	2097.51	1979.58	1926.58	1877.39	0.3632	0.405	0.3955	0.3858
1765.0	0.55	2100.9	1932.58	1879.53	1830.38	0.3544	0.4056	0.3961	0.3864
1785.0	0.55	2104.15	1887.5	1834.4	1785.29	0.3459	0.4063	0.3967	0.387
1805.0	0.55	2107.26	1844.5	1791.34	1742.28	0.3377	0.4068	0.3973	0.3876
1005.0	0.6	2078.34	2246.15	2193.4	2143.99	0.4136	0.4014	0.3919	0.3821
1025.0	0.6	2078.2	2248.0	2195.26	2145.85	0.4139	0.4014	0.3918	0.3821
1045.0	0.6	2078.12	2249.08	2196.34	2146.93	0.4141	0.4013	0.3918	0.3821
1065.0	0.6	2078.05	2250.05	2197.31	2147.9	0.4143	0.4013	0.3918	0.3821
1085.0	0.6	2078.0	2250.79	2198.05	2148.64	0.4144	0.4013	0.3918	0.3821
1105.0	0.6	2077.96	2251.29	2198.55	2149.14	0.4145	0.4013	0.3918	0.3821
1125.0	0.6	2077.94	2251.53	2198.79	2149.38	0.4146	0.4013	0.3918	0.3821
1145.0	0.6	2077.94	2251.57	2198.83	2149.42	0.4146	0.4013	0.3918	0.3821
1165.0	0.6	2077.95	2251.42	2198.67	2149.26	0.4145	0.4013	0.3918	0.3821
1185.0	0.6	2077.97	2251.12	2198.38	2148.97	0.4145	0.4013	0.3918	0.3821
1205.0	0.6	2078.0	2250.73	2197.99	2148.58	0.4144	0.4013	0.3918	0.3821
1225.0	0.6	2078.04	2250.26	2197.51	2148.1	0.4143	0.4013	0.3918	0.3821
1245.0	0.6	2078.07	2249.75	2197.0	2147.59	0.4142	0.4013	0.3918	0.3821
1265.0	0.6	2078.11	2249.22	2196.48	2147.07	0.4141	0.4013	0.3918	0.3821
1285.0	0.6	2078.15	2248.7	2195.95	2146.55	0.414	0.4014	0.3918	0.3821
1305.0	0.6	2078.19	2248.2	2195.45	2146.04	0.4139	0.4014	0.3918	0.3821
1325.0	0.6	2078.22	2247.72	2194.98	2145.57	0.4139	0.4014	0.3918	0.3821
1345.0	0.6	2078.34	2246.16	2193.42	2144.01	0.4136	0.4014	0.3919	0.3821
1365.0	0.6	2078.34	2246.15	2193.4	2143.99	0.4136	0.4014	0.3919	0.3821
1385.0	0.6	2077.8	2253.48	2200.74	2151.33	0.4149	0.4013	0.3918	0.382
1405.0	0.6	2077.87	2252.53	2199.79	2150.38	0.4148	0.4013	0.3918	0.3821
1425.0	0.6	2077.93	2251.65	2198.91	2149.5	0.4146	0.4013	0.3918	0.3821
1445.0	0.6	2077.99	2250.82	2198.07	2148.66	0.4144	0.4013	0.3918	0.3821
1465.0	0.6	2078.22	2247.74	2195.0	2145.59	0.4139	0.4014	0.3918	0.3821
1485.0	0.6	2078.23	2247.58	2194.83	2145.43	0.4138	0.4014	0.3918	0.3821
1505.0	0.6	2078.24	2247.42	2194.67	2145.27	0.4138	0.4014	0.3918	0.3821
1525.0	0.6	2078.26	2247.28	2194.53	2145.12	0.4138	0.4014	0.3918	0.3821
1545.0	0.6	2078.27	2247.14	2194.4	2144.99	0.4137	0.4014	0.3918	0.3821
1565.0	0.6	2077.57	2256.93	2204.2	2154.78	0.4156	0.4012	0.3917	0.382
1585.0	0.6	2080.04	2222.41	2169.64	2120.25	0.4091	0.4017	0.3922	0.3825
1605.0	0.6	2082.91	2182.5	2129.69	2080.33	0.4015	0.4022	0.3927	0.383
1625.0	0.6	2086.01	2139.39	2086.55	2037.22	0.3934	0.4028	0.3933	0.3836
1645.0	0.6	2089.21	2094.84	2041.96	1992.67	0.385	0.4034	0.3939	0.3842
1665.0	0.6	2092.43	2050.09	1997.16	1947.91	0.3766	0.404	0.3945	0.3848
1685.0	0.6	2095.62	2005.93	1952.96	1903.74	0.3682	0.4046	0.3951	0.3854
1705.0	0.6	2098.72	1962.88	1909.86	1860.68	0.3601	0.4052	0.3957	0.386
1725.0	0.6	2101.72	1921.2	1868.14	1818.99	0.3522	0.4058	0.3963	0.3866
1745.0	0.6	2104.62	1881.06	1827.95	1778.85	0.3447	0.4063	0.3968	0.3871
1765.0	0.6	2107.41	1842.48	1789.33	1740.26	0.3374	0.4069	0.3973	0.3876
1785.0	0.6	2110.08	1805.5	1752.29	1703.27	0.3304	0.4074	0.3978	0.3881
1805.0	0.6	2078.28	2246.95	2194.21	2144.8	0.4137	0.4014	0.3918	0.3821
1005.0	0.65	2078.34	2246.12	2193.38	2143.97	0.4136	0.4014	0.3919	0.3821
1025.0	0.65	2078.34	2246.13	2193.39	2143.98	0.4136	0.4014	0.3919	0.3821
1045.0	0.65	2078.34	2246.14	2193.39	2143.98	0.4136	0.4014	0.3919	0.3821
1065.0	0.65	2078.34	2246.14	2193.39	2143.98	0.4136	0.4014	0.3919	0.3821

1085.0	0.65	2078.34	2246.13	2193.39	2143.98	0.4136	0.4014	0.3919	0.3821
1105.0	0.65	2078.34	2246.13	2193.38	2143.98	0.4136	0.4014	0.3919	0.3821
1125.0	0.65	2078.34	2246.12	2193.38	2143.97	0.4136	0.4014	0.3919	0.3821
1145.0	0.65	2076.92	2265.3	2212.57	2163.15	0.4172	0.4011	0.3916	0.3819
1165.0	0.65	2076.99	2264.31	2211.58	2162.16	0.417	0.4011	0.3916	0.3819
1185.0	0.65	2077.08	2263.22	2210.49	2161.07	0.4168	0.4011	0.3916	0.3819
1205.0	0.65	2077.16	2262.08	2209.35	2159.93	0.4166	0.4012	0.3916	0.3819
1225.0	0.65	2077.25	2260.9	2208.16	2158.75	0.4163	0.4012	0.3917	0.3819
1245.0	0.65	2077.34	2259.7	2206.96	2157.55	0.4161	0.4012	0.3917	0.382
1265.0	0.65	2078.33	2246.22	2193.47	2144.06	0.4136	0.4014	0.3919	0.3821
1285.0	0.65	2078.34	2246.19	2193.45	2144.04	0.4136	0.4014	0.3919	0.3821
1305.0	0.65	2078.34	2246.17	2193.43	2144.02	0.4136	0.4014	0.3919	0.3821
1325.0	0.65	2078.34	2246.16	2193.41	2144.0	0.4136	0.4014	0.3919	0.3821
1345.0	0.65	2078.34	2246.14	2193.39	2143.98	0.4136	0.4014	0.3919	0.3821
1365.0	0.65	2078.34	2246.12	2193.38	2143.97	0.4136	0.4014	0.3919	0.3821
1385.0	0.65	2076.96	2264.81	2212.08	2162.66	0.4171	0.4011	0.3916	0.3819
1405.0	0.65	2077.07	2263.3	2210.57	2161.15	0.4168	0.4011	0.3916	0.3819
1425.0	0.65	2077.18	2261.84	2209.1	2159.69	0.4165	0.4012	0.3916	0.3819
1445.0	0.65	2077.28	2260.44	2207.71	2158.29	0.4163	0.4012	0.3917	0.3819
1465.0	0.65	2071.5	2341.47	2288.79	2239.32	0.4315	0.4001	0.3906	0.3809
1485.0	0.65	2073.41	2314.85	2262.16	2212.7	0.4265	0.4005	0.3909	0.3812
1505.0	0.65	2075.77	2281.91	2229.2	2179.77	0.4203	0.4009	0.3914	0.3817
1525.0	0.65	2078.47	2244.37	2191.62	2142.22	0.4132	0.4014	0.3919	0.3822
1545.0	0.65	2081.38	2203.87	2151.09	2101.71	0.4056	0.402	0.3924	0.3827
1565.0	0.65	2084.4	2161.78	2108.97	2059.62	0.3976	0.4025	0.393	0.3833
1585.0	0.65	2087.47	2119.13	2066.27	2016.95	0.3896	0.4031	0.3936	0.3839
1605.0	0.65	2090.52	2076.63	2023.73	1974.45	0.3816	0.4037	0.3942	0.3844
1625.0	0.65	2093.54	2034.8	1981.86	1932.62	0.3737	0.4043	0.3947	0.385
1645.0	0.65	2096.48	1993.95	1940.97	1891.76	0.366	0.4048	0.3953	0.3856
1665.0	0.65	2099.34	1954.28	1901.25	1852.08	0.3585	0.4053	0.3958	0.3861
1685.0	0.65	2102.11	1915.89	1862.82	1813.68	0.3512	0.4059	0.3963	0.3866
1705.0	0.65	2075.68	2282.14	2229.42	2179.99	0.4203	0.4009	0.3914	0.3816
1725.0	0.65	2078.32	2246.47	2193.72	2144.31	0.4136	0.4014	0.3919	0.3821
1745.0	0.65	2078.3	2246.66	2193.91	2144.51	0.4137	0.4014	0.3919	0.3821
1765.0	0.65	2078.28	2246.9	2194.16	2144.75	0.4137	0.4014	0.3919	0.3821
1785.0	0.65	2078.26	2247.2	2194.45	2145.04	0.4138	0.4014	0.3918	0.3821
1805.0	0.65	2078.23	2247.56	2194.82	2145.41	0.4138	0.4014	0.3918	0.3821

Chapter 5

Summary and conclusion

5.1 Summary and future work

In the first project, we show the effects of velocity models on seismic traveltimes and derive a relationship between the linear inhomogeneity and anisotropy parameters in an equivalent TI medium. We derive expressions for model parameters of a homogeneous TI medium that is long-wave equivalent to a stack of thin isotropic layers. As a future study, we plan to apply the Backus average on a stack of transversely isotropic layers to examine the linear inhomogeneity and anisotropy relationship.

In the second project, we review the forward-modeling expression for seismic traveltimes on a vertically inhomogeneous and isotropic medium. We develop a 1-D traveltime tomography method and apply it to VSP data to obtain a velocity model. Through synthetic experiments, we show the sensitivity of the inversion method to the initial model parameters. We calculate the linear inhomogeneity parameters using 1-D tomography and two-parameter methods. For future work, we wish to extend the tomography method for 2-D velocity model, which can be used to obtain inhomogeneities along both horizontal and

vertical directions.

In the third project, we use the works of the first two projects and obtain the inhomogeneity parameters for a specific region from an analytical relationship.

5.2 Significant findings

The stack of shale layers is intrinsically anisotropic. Using the wave speeds from a vertical well log, we cannot use the Backus average on a stack of isotropic layers to obtain that anisotropy.

The linear inhomogeneity parameters calculated from both 1-D tomography and *ab* methods support the analytical relationship between anisotropy and inhomogeneity.

To our knowledge, this is the only study since that of Adamus et al. [2018] to develop a formulation relating inhomogeneity and anisotropy parameters in equivalent TI media. In the current thesis, we extend that work to a nonalternating stack of isotropic layers. Also, we broaden the scope by including the application of the analytical relationship to the field data.

Overall Bibliography

M. Abu Sayed and T. Stanoev. On relations of anisotropy and linear inhomogeneity using Backus average. arXiv [physics.geo-ph], 1906.10196, 2019.

F. P. Adamus, M. A. Slawinski, and T. Stanoev. On effects of inhomogeneity on anisotropy in Backus average. arXiv [physics.geo-ph], 1802.04075, 2018.

M. Al-Chalabi. Instantaneous slownessversus depth functions. *Geophysics*, 62:270–273, 1997a.

M. Al-Chalabi. Parameter non-uniqueness in velocity versus depth functions. *Geophysics*, 62:970–979, 1997b.

D. L. Anderson. Elastic wave propagation in layered anisotropic media. *Journal of Geophysical Research*, 66(9):2953–2963, 1961.

G. E. Backus. Long-wave elastic anisotropy produced by horizontal layering. *Journal of Geophysical Research*, 67(11):4427–4440, 1962.

L. P. Bos, D. R. Dalton, M. A. Slawinski, and T. Stanoev. On Backus average for generally anisotropic layers. *Journal of Elasticity*, 127(2):179–196, 2017.

C-NLOPB. Canada-Newfoundland & Labrador Offshore Petroleum Board website.
<https://www.cnlopb.ca>.

- V. Červený. *Seismic ray theory*. Cambridge university press, 2001.
- C. Chapman. Seismic wave propagation course, 2014, 2014. URL <https://www.esc.cam.ac.uk/directory/chris-chapman>.
- C.H. Chapman and H. Keers. Application of the maslov seismogram method in three dimensions. *Studia Geophysica et Geodetica*, 46:615–649, 2002.
- D. R. Dalton and M. A. Slawinski. On Backus average for oblique incidence. arXiv [physics.geo-ph], 1601.02966, 2016.
- C. Hewitt Dix. Seismic velocities from surface measurements. *Geophysics*, XX(1):68–86, 1955.
- M. E. Enachescu. Petroleum exploration opportunities in area “C” - Flemish pass/North Central Ridge: Calls for bids NL11-02. URL: https://www.nr.gov.nl.ca/nr/invest/enachescu_NL1102Flemish.pdf, 2011.
- M. Epstein and M. A. Slawinski. On raytracing in constant velocity-gradient media: Geometrical approach. *Canadian Journal of Exploration Geophysics*, 35(1/2):1–6, 1999.
- L.Y. Faust. Seismic velocity as a function of depth and geologic time. *Geophysics*, 16: 192–206, 1951.
- L.Y. Faust. A velocity function including lithologic variation. *Geophysics*, 18:271–288, 1953.
- N. A. Haskell. The dispersion of surface waves on multilayered media. *Bulletin of the Seismological Society of America*, 43(1):17–34, 1953.
- M. T. Heath. *Scientific Computing*. The McGraw-Hill Companies, 2nd edition, July 2002.

K. Helbig. Elastische wellen in anisotropen medien. *Gerlands Beitr'age zur Geophysik*, 67: 177–211, 1958.

Ikon Science and Nalcor Energy. Regional rock physics analysis of offshore Newfoundland and Labrador: Unlocking the shelf-to-deep-transition. <http://exploration.nalcorenergy.com/wp-content/uploads/2017/01/RockPhysics.pdf>, 2016.

D. Kumar. Applying backus averaging for deriving seismic anisotropy of a longwavelength equivalent medium from well-log data. *Journal of Geophysics and Engineering*, 10, 2013.

K. Levenberg. A method for the solution of certain non-linear problems in least squares. *American Mathematical Society*, II(2), 1944.

G. F. Margrave and M. P. Lamoureux. *Numerical Methods of Exploration Seismology: With Algorithms in MATLAB*. Cambridge University Press, 2019.

D. W. Marquardt. An algorithm for least-squares estimation of nonlinear parameters. *J. Soc. Indust. Appl. Math.*, II(2), 1963.

M. Muskat. A note on propagation of seismic waves. *Geophysics*, 2(4):319–328, 1937.

G. W. Postma. Wave propagation in a stratified medium. *Geophysics*, 20(4):780–806, 1955.

J. Pujol. The solution of nonlinear inverse problems and the Levenberg-Marquardt method. *Geophysics*, 72(4), August 2007.

J. Pujol, R. Burridge, and S. B. Smithson. Velocity determination from offset vertical seismic profiling data. *Journal of Geophysical Research*, 90(B2):1871–1880, 1985.

I. Ravve and Z. Koren. Exponential asymptotically bounded velocity model: Part i- effective models and velocity transformations. *Geophysics*, 71:T67–T85, 2006a.

- I. Ravve and Z. Koren. Exponential asymptotically bounded velocity model: Part ii- ray tracing. *Geophysics*, 71(T67-T85), 2006b.
- Y. V. Riznichenko. On seismic anisotropy. *Izvestiia Akademii nauk SSSR. Seria biologicheskaiia*, 13(6):518–544, 1949.
- Y. Rogister and M. A. Slawinski. Analytic solution of ray-tracing equations for a linearly inhomogeneous and elliptically anisotropic velocity model. *Geophysics*, 70(5):D37–D41, 2005.
- M. P. Rudzki. Parametrische darstellung der elastischen welle in anisotropen medien. *Anzeiger der Akademie der Wissenschaften, Krakau*, pages 503–536, 1911.
- M. P. Rudzki. Parametric representation of the elastic wave in anisotropic media. *Journal of Applied Geophysics*, 54(3):165–183, 2003.
- S. M. Rytov. The acoustical properties of a thinly laminated medium. *Soviet Physical Acoustics*, 2:68–80, 1956.
- M. Schoenberg and F. Muir. A calculus for finely layered anisotropic media. *Geophysics*, 54:581–589, 1989.
- M. A. Slawinski. *Waves and rays in elastic continua*. World Scientific, 3rd edition, 2015.
- M. A. Slawinski. *Waves and rays in seismology: Answers to unasked questions*. World Scientific, 2nd edition, 2018.
- M. A. Slawinski, C. J. Wheaton, and M. Powojowski. VSP travelttime inversion for linear inhomogeneity and elliptical anisotropy. *Geophysics*, 69(2):373–377, 2004.
- R. A. Slawinski and M. A. Slawinski. On raytracing in constant velocity-gradient media: Calculus approach. *Canadian Journal of Exploration Geophysics*, 35(1/2):24–27, 1999.

M. M. Slotnick. On seismic computations, with applications, I. *Society of Exploration Geophysicists*, 1:1–169, 1936.

L. Thomsen. Weak elastic anisotropy. *Geophysics*, 51(10):1954–1966, 1986.

I. Tsvankin. *Seismic Signatures and Analysis of Reflection Data in Anisotropic Media*, volume 29. Pergamon, 1st edition, 2001.

J. E. White and F. A. Angona. Elastic wave velocities in laminated media. *J. Acoust. Soc. Am.*, 27:310–317, 1955.

C.A. Zelt and R.B. Smith. Seismic traveltimes inversion for 2-D crustal velocity structure. *Geophys. J. Int.*, 108:16–34, 1992.

M. S. Zhdanov. *Geophysical inverse theory and regularization problems*. Elsevier, 2002.

Appendix A

Data: Mizzen O-16

A.1 Traveltime data [C-NLOPB]

Geophone	Depth (m)	Traveltime (s)	Geophone	Depth (m)	Traveltime (s)	Geophone	Depth (m)	Traveltime (s)
1	1849.0	1.143	19	2121.0	1.271	37	2393.0	1.391
2	1864.0	1.149	20	2136.0	1.278	38	2408.0	1.398
3	1879.0	1.157	21	2151.0	1.285	39	2424.0	1.404
4	1894.0	1.165	22	2166.0	1.291	40	2439.0	1.411
5	1909.0	1.173	23	2182.0	1.298	41	2454.0	1.418
6	1924.0	1.18	24	2197.0	1.305	42	2469.0	1.425
7	1940.0	1.188	25	2212.0	1.312	43	2484.0	1.431
8	1955.0	1.195	26	2227.0	1.319	44	2499.0	1.438
9	1970.0	1.202	27	2242.0	1.325	45	2514.0	1.445
10	1985.0	1.208	28	2257.0	1.332	46	2529.0	1.451
11	2000.0	1.215	29	2272.0	1.338	47	2544.0	1.458
12	2015.0	1.222	30	2287.0	1.345	48	2560.0	1.465
13	2030.0	1.229	31	2302.0	1.352	49	2575.0	1.471
14	2046.0	1.236	32	2318.0	1.358	50	2590.0	1.478
15	2061.0	1.243	33	2333.0	1.365	51	2605.0	1.485
16	2076.0	1.25	34	2348.0	1.371	52	2620.0	1.491
17	2091.0	1.257	35	2363.0	1.378	53	2635.0	1.498
18	2106.0	1.264	36	2378.0	1.385	54	2650.0	1.504

A.2 Well log data [Enachescu, 2011]

No.	d(m)	$v_p(\text{ms}^{-1})$	$v_s(\text{ms}^{-1})$	No.	d(m)	$v_p(\text{ms}^{-1})$	$v_s(\text{ms}^{-1})$	No.	d(m)	$v_p(\text{ms}^{-1})$	$v_s(\text{ms}^{-1})$	No.	d(m)	$v_p(\text{ms}^{-1})$	$v_s(\text{ms}^{-1})$
1.0	1865.0	2119.92	736.306	81.0	1873.0	2045.62	725.142	161.0	1881.0	2023.88	649.699	241.0	1889.0	2054.45	715.154
2.0	1865.1	2116.85	731.924	82.0	1873.1	2044.15	720.288	162.0	1881.1	2032.52	653.36	242.0	1889.1	2051.68	708.433
3.0	1865.2	2110.6	728.209	83.0	1873.2	2042.69	717.586	163.0	1881.2	2041.23	658.321	243.0	1889.2	2056.19	701.506
4.0	1865.3	2101.28	735.677	84.0	1873.3	2047.08	717.586	164.0	1881.3	2047.08	664.418	244.0	1889.3	2065.21	695.836
5.0	1865.4	2092.05	734.108	85.0	1873.4	2051.49	720.288	165.0	1881.4	2047.08	670.107	245.0	1889.4	2072.83	690.256
6.0	1865.5	2085.94	729.134	86.0	1873.5	2052.97	724.837	166.0	1881.5	2045.62	674.835	246.0	1889.5	2081.98	690.81
7.0	1865.6	2067.82	723.618	87.0	1873.6	2052.97	730.062	167.0	1881.6	2044.15	680.167	247.0	1889.6	2085.14	693.035
8.0	1865.7	2060.35	718.785	88.0	1873.7	2054.44	732.547	168.0	1881.7	2042.69	684.744	248.0	1889.7	2085.26	697.244
9.0	1865.8	2049.9	713.424	89.0	1873.8	2054.44	730.991	169.0	1881.8	2042.69	690.453	249.0	1889.8	2085.39	698.376
10.0	1865.9	2049.9	709.894	90.0	1873.9	2047.08	727.593	170.0	1881.9	2048.55	695.422	250.0	1889.9	2088.55	699.795
11.0	1866.0	2049.9	708.725	91.0	1874.0	2035.42	724.837	171.0	1882.0	2051.49	701.311	251.0	1890.0	2088.66	701.22
12.0	1866.1	2049.82	707.269	92.0	1874.1	2019.61	720.59	172.0	1882.1	2052.97	706.439	252.0	1890.1	2087.21	704.956
13.0	1866.2	2049.69	706.399	93.0	1874.2	2021.08	714.608	173.0	1882.2	2055.93	710.773	253.0	1890.2	2087.21	707.855
14.0	1866.3	2051.03	704.952	94.0	1874.3	2026.84	707.56	174.0	1882.3	2061.86	711.654	254.0	1890.3	2085.7	711.642
15.0	1866.4	2055.36	704.376	95.0	1874.4	2024.02	700.935	175.0	1882.4	2063.23	712.833	255.0	1890.4	2087.21	714.86
16.0	1866.5	2059.67	704.952	96.0	1874.5	2018.36	694.993	176.0	1882.5	2072.32	713.719	256.0	1890.5	2094.78	717.219
17.0	1866.6	2061.03	707.269	97.0	1874.6	2011.34	688.6	177.0	1882.6	2079.87	714.608	257.0	1890.6	2102.41	718.404
18.0	1866.7	2063.85	710.773	98.0	1874.7	2007.17	683.136	178.0	1882.7	2084.42	728.825	258.0	1890.7	2091.75	719.593
19.0	1866.8	2065.2	714.905	99.0	1874.8	2003.04	676.75	179.0	1882.8	2085.94	742.015	259.0	1890.8	2079.69	720.189
20.0	1866.9	2075.54	719.085	100.0	1874.9	1997.54	673.866	180.0	1882.9	2088.99	743.296	260.0	1890.9	2073.71	718.998
21.0	1867.0	2084.49	722.707	101.0	1875.0	1994.84	672.563	181.0	1883.0	2090.52	740.741	261.0	1891.0	2070.73	714.566
22.0	1867.1	2096.66	727.286	102.0	1875.1	1994.91	671.274	182.0	1883.1	2090.59	732.547	262.0	1891.1	2064.81	709.61
23.0	1867.2	2104.38	730.991	103.0	1875.2	1994.99	670.253	183.0	1883.2	2090.71	723.618	263.0	1891.2	2055.98	703.866
24.0	1867.3	2112.16	735.362	104.0	1875.3	1999.21	670.265	184.0	1883.3	2092.36	719.987	264.0	1891.3	2057.45	698.214
25.0	1867.4	2113.72	740.104	105.0	1875.4	2009.07	670.279	185.0	1883.4	2090.97	716.69	265.0	1891.4	2069.25	691.826
26.0	1867.5	2118.42	748.069	106.0	1875.5	2020.47	678.703	186.0	1883.5	2083.49	714.905	266.0	1891.5	2058.91	685.284
27.0	1867.6	2124.72	750.328	107.0	1875.6	2029.13	686.261	187.0	1883.6	2074.6	712.538	267.0	1891.6	2054.52	679.898
28.0	1867.7	2131.06	752.601	108.0	1875.7	2040.8	693.424	188.0	1883.7	2067.27	727.593	268.0	1891.7	2047.23	673.515
29.0	1867.8	2132.65	754.56	109.0	1875.8	2049.7	694.552	189.0	1883.8	2060.01	734.421	269.0	1891.8	2039.99	672.463
30.0	1867.9	2123.14	757.189	110.0	1875.9	2055.71	703.001	190.0	1883.9	2052.78	727.901	270.0	1891.9	2032.81	679.362
31.0	1868.0	2121.16	779.65	111.0	1876.0	2061.79	711.654	191.0	1884.0	2045.56	723.01	271.0	1892.0	2025.67	689.905
32.0	1868.1	2099.74	780.004	112.0	1876.1	2067.77	714.626	192.0	1884.1	2036.87	717.305	272.0	1892.1	2020.06	690.458
33.0	1868.2	2088.99	769.246	113.0	1876.2	2073.73	717.935	193.0	1884.2	2028.19	711.703	273.0	1892.2	2017.34	685.829
34.0	1868.3	2076.84	760.5	114.0	1876.3	2075.23	720.666	194.0	1884.3	2022.45	707.078	274.0	1892.3	2016.01	682.054
35.0	1868.4	2073.83	751.301	115.0	1876.4	2075.25	724.641	195.0	1884.4	2016.74	701.665	275.0	1892.4	2014.7	678.573
36.0	1868.5	2066.33	747.098	116.0	1876.5	2079.77	728.968	196.0	1884.5	2011.06	697.164	276.0	1892.5	2017.63	681.518
37.0	1868.6	2060.37	742.943	117.0	1876.6	2082.8	730.542	197.0	1884.6	2001.2	693.265	277.0	1892.6	2020.56	686.114
38.0	1868.7	2052.97	738.834	118.0	1876.7	2082.83	727.181	198.0	1884.7	1995.61	688.853	278.0	1892.7	2022.09	689.953
39.0	1868.8	2047.08	735.048	119.0	1876.8	2082.85	723.85	199.0	1884.8	1985.9	677.265	279.0	1892.8	2025.06	692.175
40.0	1868.9	2041.23	728.209	120.0	1876.9	2087.43	721.148	200.0	1884.9	1976.28	669.697	280.0	1892.9	2030.91	694.416
41.0	1869.0	2036.87	722.707	121.0	1877.0	2090.51	719.071	201.0	1885.0	1977.65	661.301	281.0	1893.0	2038.27	696.392
42.0	1869.1	2035.5	716.112	122.0	1877.1	2088.99	725.142	202.0	1885.1	1979.07	658.058	282.0	1893.1	2045.62	698.943
43.0	1869.2	2034.19	710.524	123.0	1877.2	2084.42	735.991	203.0	1885.2	1981.88	664.608	283.0	1893.2	2052.97	701.22
44.0	1869.3	2031.45	704.45	124.0	1877.3	2081.38	736.621	204.0	1885.3	1987.47	660.315	284.0	1893.3	2055.92	703.225
45.0	1869.4	2030.16	698.196	125.0	1877.4	2076.84	730.062	205.0	1885.4	1993.07	655.32	285.0	1893.4	2060.37	705.53
46.0	1869.5	2033.18	692.883	126.0	1877.5	2072.32	723.618	206.0	1885.5	1997.29	651.619	286.0	1893.5	2069.25	708.142
47.0	1869.6	2039.14	687.379	127.0	1877.6	2066.33	722.707	207.0	1885.6	2004.32	651.623	287.0	1893.6	2070.73	710.187
48.0	1869.7	2046.57	684.671	128.0	1877.7	2058.9	726.672	208.0	1885.7	2011.38	654.088	288.0	1893.7	2075.2	713.98
49.0	1869.8	2054.08	681.72	129.0	1877.8	2051.57	734.108	209.0	1885.8	2015.66	658.318	289.0	1893.8	2084.19	723.183
50.0	1869.9	2063.14	680.671	130.0	1877.9	2051.58	740.741	210.0	1885.9	2018.53	662.662	290.0	1893.9	2085.7	731.395
51.0	1870.0	2069.25	680.962	131.0	1878.0	2051.59	741.379	211.0	1886.0	2021.4	668.023	291.0	1894.0	2087.21	735.727
52.0	1870.1	2073.83	682.865	132.0	1878.1	2048.76	741.06	212.0	1886.1	2024.31	672.463	292.0	1894.1	2091.77	736.678
53.0	1870.2	2078.35	687.775	133.0	1878.2	2047.44	736.306	213.0	1886.2	2030.12	677.757	293.0	1894.2	2093.31	734.211
54.0	1870.3	2079.87	694.432	134.0	1878.3	2051.94	733.795	214.0	1886.3	2035.98	682.594	294.0	1894.3	2093.35	728.073
55.0	1870.4	2079.87	701.506	135.0	1878.4	2056.49	735.677	215.0	1886.4	2040.44	687.994	295.0	1894.4	2085.79	721.123
56.0	1870.5	2079.87	707.56	136.0	1878.5	2061.06	734.421	216.0	1886.5	2046.37	692.653	296.0	1894.5	2076.76	714.586
57.0	1870.6	2085.94	713.719	137.0	1878.6	2068.61	738.517	217.0	1886.6	2055.3	700.464	297.0	1894.6	2076.78	712.235
58.0	1870.7	2093.58	718.185	138.0	1878.7	2076.23	743.591	218.0	1886.7	2064.3	705.007	298.0	1894.7	2078.3	713.413
59.0	1870.8	2098.2	723.618	139.0	1878.8	2082.38	740.741	219.0	1886.8	2068.91	710.189	299.0	1894.8	2084.37	714.894

No.	d(m)	$v_p(\text{ms}^{-1})$	$v_s(\text{ms}^{-1})$	No.	d(m)	$v_p(\text{ms}^{-1})$	$v_s(\text{ms}^{-1})$	No.	d(m)	$v_p(\text{ms}^{-1})$	$v_s(\text{ms}^{-1})$	No.	d(m)	$v_p(\text{ms}^{-1})$	$v_s(\text{ms}^{-1})$
321.0	1897.0	2055.92	706.979	401.0	1905.0	2100.83	739.468	481.0	1913.0	2053.05	718.107	561.0	1921.0	2016.76	740.741
322.0	1897.1	2051.49	704.664	402.0	1905.1	2099.36	739.152	482.0	1913.1	2058.91	717.515	562.0	1921.1	1998.4	731.302
323.0	1897.2	2044.15	700.935	403.0	1905.2	2096.31	738.204	483.0	1913.2	2067.82	716.332	563.0	1921.2	1981.77	721.798
324.0	1897.3	2042.69	697.527	404.0	1905.3	2090.23	737.261	484.0	1913.3	2076.84	735.105	564.0	1921.3	1966.76	714.015
325.0	1897.4	2039.78	693.593	405.0	1905.4	2084.19	736.322	485.0	1913.4	2078.35	722.282	565.0	1921.4	1960.02	704.952
326.0	1897.5	2039.78	690.256	406.0	1905.5	2082.69	735.7	486.0	1913.5	2076.84	740.11	566.0	1921.5	1960.02	696.68
327.0	1897.6	2041.23	690.256	407.0	1905.6	2076.69	735.704	487.0	1913.6	2070.82	742.978	567.0	1921.6	1955.99	688.325
328.0	1897.7	2047.08	690.81	408.0	1905.7	2072.22	735.71	488.0	1913.7	2070.82	745.552	568.0	1921.7	1954.65	684.766
329.0	1897.8	2057.4	692.477	409.0	1905.8	2072.22	735.715	489.0	1913.8	2067.82	747.819	569.0	1921.8	1955.99	685.038
330.0	1897.9	2063.33	692.477	410.0	1905.9	2067.77	736.656	490.0	1913.9	2066.33	748.795	570.0	1921.9	1968.12	686.404
331.0	1898.0	2070.73	692.477	411.0	1906.0	2064.81	737.598	491.0	1914.0	2063.34	738.225	571.0	1922.0	1983.14	689.98
332.0	1898.1	2078.19	692.199	412.0	1906.1	2064.81	738.225	492.0	1914.1	2060.38	736.974	572.0	1922.1	2005.41	694.152
333.0	1898.2	2084.19	693.314	413.0	1906.2	2066.29	739.167	493.0	1914.2	2057.44	732.319	573.0	1922.2	2029.63	697.527
334.0	1898.3	2084.19	694.993	414.0	1906.3	2070.76	739.481	494.0	1914.3	2053.03	727.723	574.0	1922.3	2054.44	701.792
335.0	1898.4	2072.22	695.836	415.0	1906.4	2076.75	738.539	495.0	1914.4	2047.18	723.484	575.0	1922.4	2079.87	705.53
336.0	1898.5	2042.78	696.68	416.0	1906.5	2084.3	736.974	496.0	1914.5	2039.89	722.883	576.0	1922.5	2092.05	706.689
337.0	1898.6	2044.25	702.078	417.0	1906.6	2087.35	735.727	497.0	1914.6	2039.87	722.883	577.0	1922.6	2095.12	713.128
338.0	1898.7	2045.72	714.86	418.0	1906.7	2085.86	735.727	498.0	1914.7	2047.13	722.883	578.0	1922.7	2084.42	745.841
339.0	1898.8	2034.17	714.273	419.0	1906.8	2087.4	736.974	499.0	1914.8	2048.58	722.883	579.0	1922.8	2075.33	752.958
340.0	1898.9	2017.12	707.56	420.0	1906.9	2090.48	744.907	500.0	1914.9	2042.72	723.484	580.0	1922.9	2067.82	759.863
341.0	1899.0	2017.16	701.22	421.0	1907.0	2090.51	751.081	501.0	1915.0	2033.98	724.388	581.0	1923.0	2060.37	759.842
342.0	1899.1	2021.41	700.08	422.0	1907.1	2090.52	755.034	502.0	1915.1	2032.52	725.588	582.0	1923.1	2052.97	757.189
343.0	1899.2	2022.83	697.527	423.0	1907.2	2088.99	754.372	503.0	1915.2	2032.52	725.878	583.0	1923.2	2045.62	751.95
344.0	1899.3	2021.41	695.836	424.0	1907.3	2085.94	742.658	504.0	1915.3	2041.23	726.775	584.0	1923.3	2036.87	738.834
345.0	1899.4	2018.59	694.432	425.0	1907.4	2082.9	740.422	505.0	1915.4	2041.23	727.371	585.0	1923.4	2026.75	738.834
346.0	1899.5	2017.18	693.035	426.0	1907.5	2078.35	744.585	506.0	1915.5	2047.08	727.971	586.0	1923.5	2011.06	738.517
347.0	1899.6	2021.41	691.643	427.0	1907.6	2070.82	742.639	507.0	1915.6	2055.92	728.571	587.0	1923.6	2001.2	737.884
348.0	1899.7	2024.25	690.81	428.0	1907.7	2061.86	742.639	508.0	1915.7	2058.88	729.481	588.0	1923.7	2001.2	734.421
349.0	1899.8	2028.52	692.477	429.0	1907.8	2048.68	742.322	509.0	1915.8	2063.34	730.088	589.0	1923.8	2005.41	728.517
350.0	1899.9	2032.81	694.152	430.0	1907.9	2037.11	739.481	510.0	1915.9	2067.82	730.695	590.0	1923.9	2008.23	725.753
351.0	1900.0	2035.67	695.836	431.0	1908.0	2082.52	734.794	511.0	1916.0	2075.33	732.239	591.0	1924.0	2009.65	728.517
352.0	1900.1	2038.55	697.527	432.0	1908.1	2072.09	733.245	512.0	1916.1	2085.94	733.795	592.0	1924.1	2012.48	737.884
353.0	1900.2	2038.55	700.935	433.0	1908.2	2029.95	732.936	513.0	1916.2	2096.66	735.048	593.0	1924.2	2015.32	737.568
354.0	1900.3	2034.24	712.225	434.0	1908.3	2034.24	728.332	514.0	1916.3	2110.6	736.306	594.0	1924.3	2021.02	731.924
355.0	1900.4	2034.24	723.183	435.0	1908.4	2035.67	721.983	515.0	1916.4	2123.14	737.884	595.0	1924.4	2026.75	737.252
356.0	1900.5	2029.95	710.77	436.0	1908.5	2037.11	716.628	516.0	1916.5	2123.14	739.151	596.0	1924.5	2031.08	737.778
357.0	1900.6	2021.41	711.642	437.0	1908.6	2039.99	712.225	517.0	1916.6	2123.14	740.741	597.0	1924.6	2032.52	738.305
358.0	1900.7	2017.18	716.332	438.0	1908.7	2042.88	717.515	518.0	1916.7	2121.57	742.018	598.0	1924.7	2033.97	738.834
359.0	1900.8	2014.36	704.376	439.0	1908.8	2042.88	726.81	519.0	1916.8	2116.85	746.198	599.0	1924.8	2032.52	736.936
360.0	1900.9	2010.15	698.943	440.0	1908.9	2044.33	734.484	520.0	1916.9	2115.28	753.711	600.0	1924.9	2023.88	734.735
361.0	1901.0	2008.75	696.962	441.0	1909.0	2048.68	734.794	521.0	1917.0	2112.16	754.703	601.0	1925.0	2015.32	735.991
362.0	1901.1	2011.55	696.962	442.0	1909.1	2052.97	735.105	522.0	1917.1	2105.93	755.696	602.0	1925.1	2011.06	751.938
363.0	1901.2	2015.77	697.527	443.0	1909.2	2057.22	735.105	523.0	1917.2	2101.28	755.696	603.0	1925.2	2008.23	751.593
364.0	1901.3	2017.18	698.943	444.0	1909.3	2061.48	735.105	524.0	1917.3	2098.2	755.034	604.0	1925.3	2001.2	740.741
365.0	1901.4	2022.83	700.649	445.0	1909.4	2061.32	736.038	525.0	1917.4	2092.05	754.703	605.0	1925.4	1992.83	738.517
366.0	1901.5	2031.38	702.364	446.0	1909.5	2058.25	737.599	526.0	1917.5	2085.94	761.377	606.0	1925.5	1987.28	733.17
367.0	1901.6	2041.44	704.088	447.0	1909.6	2055.16	737.599	527.0	1917.6	2078.35	767.144	607.0	1925.6	1981.77	726.979
368.0	1901.7	2051.59	705.53	448.0	1909.7	2053.56	736.35	528.0	1917.7	2070.82	739.468	608.0	1925.7	1977.65	721.495
369.0	1901.8	2060.38	707.269	449.0	1909.8	2050.49	732.936	529.0	1917.8	2061.86	739.151	609.0	1925.8	1972.19	716.094
370.0	1901.9	2066.33	709.017	450.0	1909.9	2047.43	729.554	530.0	1917.9	2052.97	738.517	610.0	1925.9	1966.76	714.905
371.0	1902.0	2073.83	710.77	451.0	1910.0	2045.84	728.943	531.0	1918.0	2050.02	734.735	611.0	1926.0	1961.36	713.719
372.0	1902.1	2081.38	714.86	452.0	1910.1	2042.88	728.943	532.0	1918.1	2050.02	728.209	612.0	1926.1	1957.33	712.538
373.0	1902.2	2090.52	718.998	453.0	1910.2	2042.88	729.248	533.0	1918.2	2050.02	727.707	613.0	1926.2	1954.65	711.36
374.0	1902.3	2093.58	722.583	454.0	1910.3	2044.33	730.78	534.0	1918.3	2050.02	716.989	614.0	1926.3	1954.65	709.601
375.0	1902.4	2095.12	726.507	455.0	1910.4	2044.33	732.628	535.0	1918.4	2058.88	716.989	615.0	1926.4	1955.99	707.269
376.0	1902.5	2095.12	728.637	456.0	1910.5	2048.68	734.174	536.0	1918.5	2061.86	717.885	616.0	1926.5	1955.99	704.952
377.0	1902.6	2088.99	729.248	457.0	1910.6	2053.05	736.038	537.0	1918.6	2070.82	720.288	617.0	1926.6	1955.99	704.088
378.0	1902.7	2081.38	728.332	458.0	1910.7	2058.91	736.662	538.0	1918.7	2075.33	723.922	618.0	1926.7	1954.65	703.8
379.0	1902.8	2073.83	725.9	459.0	1910.8	2064.84	736.038	539.0	1918.8	2084.42	727.901	619.0</			

No.	$d(\text{m})$	$v_p(\text{ms}^{-1})$	$v_s(\text{ms}^{-1})$												
641.0	1929.0	1929.57	698.093	721.0	1937.0	1951.98	703.8	801.0	1945.0	2008.23	718.107	881.0	1953.0	2075.33	739.167
642.0	1929.1	1929.49	697.527	722.0	1937.1	1953.32	702.066	802.0	1945.1	2013.9	718.404	882.0	1953.1	2072.23	739.795
643.0	1929.2	1928.07	697.244	723.0	1937.2	1954.65	700.621	803.0	1945.2	2022.45	718.701	883.0	1953.2	2069.08	739.734
644.0	1929.3	1925.33	697.527	724.0	1937.3	1957.33	699.183	804.0	1945.3	2028.19	718.701	884.0	1953.3	2067.45	742.875
645.0	1929.4	1923.9	698.659	725.0	1937.4	1960.02	697.753	805.0	1945.4	2029.63	718.998	885.0	1953.4	2070.28	743.795
646.0	1929.5	1923.78	699.227	726.0	1937.5	1962.71	697.739	806.0	1945.5	2026.75	722.583	886.0	1953.5	2076.15	744.08
647.0	1929.6	1924.94	699.511	727.0	1937.6	1965.41	698.567	807.0	1945.6	2018.16	725.295	887.0	1953.6	2089.68	744.37
648.0	1929.7	1926.12	698.943	728.0	1937.7	1965.41	698.268	808.0	1945.7	2005.41	725.295	888.0	1953.7	2106.46	744.656
649.0	1929.8	1928.58	698.943	729.0	1937.8	1965.41	698.816	809.0	1945.8	1991.44	722.282	889.0	1953.8	2126.68	746.861
650.0	1929.9	1933.67	699.511	730.0	1937.9	1966.76	700.49	810.0	1945.9	1979.02	717.811	890.0	1953.9	2140.88	749.084
651.0	1930.0	1937.48	700.08	731.0	1938.0	1966.76	701.887	811.0	1946.0	1970.83	712.517	891.0	1954.0	2158.5	751.965
652.0	1930.1	1938.74	700.935	732.0	1938.1	1970.83	702.728	812.0	1946.1	1958.67	707.589	892.0	1954.1	2168.16	754.549
653.0	1930.2	1941.37	703.225	733.0	1938.2	1974.92	704.151	813.0	1946.2	1951.98	703.012	893.0	1954.2	2179.56	757.492
654.0	1930.3	1945.34	710.48	734.0	1938.3	1977.65	706.152	814.0	1946.3	1945.34	701.594	894.0	1954.3	2189.44	765.838
655.0	1930.4	1949.32	712.517	735.0	1938.4	1985.9	708.742	815.0	1946.4	1944.01	700.182	895.0	1954.4	2195.99	776.486
656.0	1930.5	1949.32	709.017	736.0	1938.5	1992.83	710.189	816.0	1946.5	1944.01	698.495	896.0	1954.5	2199.19	781.774
657.0	1930.6	1949.32	704.664	737.0	1938.6	1999.8	716.037	817.0	1946.6	1942.69	697.095	897.0	1954.6	2202.43	788.217
658.0	1930.7	1950.65	700.935	738.0	1938.7	2011.06	719.295	818.0	1946.7	1941.37	695.701	898.0	1954.7	2202.26	794.033
659.0	1930.8	1951.98	703.225	739.0	1938.8	2018.16	721.683	819.0	1946.8	1942.69	695.701	899.0	1954.8	2197.0	800.679
660.0	1930.9	1953.32	704.376	740.0	1938.9	2022.45	723.484	820.0	1946.9	1945.34	695.701	900.0	1954.9	2191.79	807.438
661.0	1931.0	1953.32	706.979	741.0	1939.0	2028.19	725.295	821.0	1947.0	1946.66	695.701	901.0	1955.0	2184.91	808.956
662.0	1931.1	1955.99	709.894	742.0	1939.1	2032.52	724.992	822.0	1947.1	1949.32	695.701	902.0	1955.1	2179.84	809.336
663.0	1931.2	1957.33	712.809	743.0	1939.2	2032.52	727.418	823.0	1947.2	1955.99	696.258	903.0	1955.2	2176.52	810.094
664.0	1931.3	1960.02	715.154	744.0	1939.3	2031.08	734.484	824.0	1947.3	1972.19	698.495	904.0	1955.3	2173.2	809.717
665.0	1931.4	1962.71	716.923	745.0	1939.4	2028.19	738.539	825.0	1947.4	1981.77	701.029	905.0	1955.4	2169.9	806.304
666.0	1931.5	1965.41	718.107	746.0	1939.5	2025.32	732.011	826.0	1947.5	1994.22	703.012	906.0	1955.5	2169.9	802.545
667.0	1931.6	1966.76	719.891	747.0	1939.6	2019.59	729.248	827.0	1947.6	1998.4	705.579	907.0	1955.6	2171.55	799.193
668.0	1931.7	1970.83	721.384	748.0	1939.7	2012.48	729.248	828.0	1947.7	1999.8	707.877	908.0	1955.7	2174.86	797.342
669.0	1931.8	1973.55	723.183	749.0	1939.8	2008.23	731.395	829.0	1947.8	1998.4	708.742	909.0	1955.8	2181.5	795.133
670.0	1931.9	1976.28	725.295	750.0	1939.9	2005.41	731.395	830.0	1947.9	1994.22	708.454	910.0	1955.9	2186.51	792.571
671.0	1932.0	1981.77	727.723	751.0	1940.0	2002.6	729.86	831.0	1948.0	1990.05	707.589	911.0	1956.0	2194.91	789.663
672.0	1932.1	1990.05	729.854	752.0	1940.1	1999.8	729.86	832.0	1948.1	1985.9	706.439	912.0	1956.1	2196.6	787.135
673.0	1932.2	1995.61	732.614	753.0	1940.2	1997.0	729.554	833.0	1948.2	1980.39	705.293	913.0	1956.2	2196.6	784.625
674.0	1932.3	1995.61	735.714	754.0	1940.3	1995.61	729.86	834.0	1948.3	1977.65	704.436	914.0	1956.3	2191.54	781.42
675.0	1932.4	1990.05	737.274	755.0	1940.4	1994.22	730.78	835.0	1948.4	1973.55	703.297	915.0	1956.4	2181.5	777.187
676.0	1932.5	1981.77	738.529	756.0	1940.5	1997.0	731.703	836.0	1948.5	1968.12	702.161	916.0	1956.5	2169.9	774.042
677.0	1932.6	1974.92	739.474	757.0	1940.6	2004.01	731.088	837.0	1948.6	1966.76	701.311	917.0	1956.6	2163.33	771.96
678.0	1932.7	1970.83	740.423	758.0	1940.7	2008.23	730.167	838.0	1948.7	1966.76	700.746	918.0	1956.7	2155.17	766.12
679.0	1932.8	1966.76	740.423	759.0	1940.8	2015.32	729.554	839.0	1948.8	1965.41	700.746	919.0	1956.8	2145.46	761.041
680.0	1932.9	1962.71	740.105	760.0	1940.9	2022.45	736.35	840.0	1948.9	1966.76	701.311	920.0	1956.9	2137.44	758.025
681.0	1933.0	1955.99	738.834	761.0	1941.0	2022.45	748.713	841.0	1949.0	1969.47	703.866	921.0	1957.0	2129.47	755.696
682.0	1933.1	1950.65	737.568	762.0	1941.1	2023.88	746.143	842.0	1949.1	1973.48	706.996	922.0	1957.1	2123.14	754.042
683.0	1933.2	1950.65	736.306	763.0	1941.2	2022.45	747.011	843.0	1949.2	1982.92	709.277	923.0	1957.2	2116.85	752.065
684.0	1933.3	1947.99	734.108	764.0	1941.3	2022.45	739.889	844.0	1949.3	1992.48	712.442	924.0	1957.3	2112.16	749.446
685.0	1933.4	1949.32	729.443	765.0	1941.4	2018.16	739.669	845.0	1949.4	2003.5	715.341	925.0	1957.4	2104.38	747.494
686.0	1933.5	1949.32	723.314	766.0	1941.5	2015.32	737.454	846.0	1949.5	2013.25	717.676	926.0	1957.5	2099.74	746.198
687.0	1933.6	1950.65	721.495	767.0	1941.6	2012.48	734.003	847.0	1949.6	2024.51	717.94	927.0	1957.6	2098.2	747.17
688.0	1933.7	1953.32	717.885	768.0	1941.7	2009.65	733.97	848.0	1949.7	2040.28	718.506	928.0	1957.7	2099.74	748.144
689.0	1933.8	1957.33	715.202	769.0	1941.8	2006.82	733.938	849.0	1949.8	2048.91	718.475	929.0	1957.8	2104.38	748.795
690.0	1933.9	1962.71	713.719	770.0	1941.9	2004.01	731.134	850.0	1949.9	2048.75	718.448	930.0	1957.9	2107.48	750.099
691.0	1934.0	1969.47	713.424	771.0	1942.0	2001.2	727.128	851.0	1950.0	2039.84	740.422	931.0	1958.0	2113.72	751.081
692.0	1934.1	1973.63	712.831	772.0	1942.1	1992.83	722.883	852.0	1950.1	2033.97	741.698	932.0	1958.1	2123.14	752.387
693.0	1934.2	1975.14	712.24	773.0	1942.2	1984.52	736.974	853.0	1950.2	2035.42	743.62	933.0	1958.2	2131.06	753.69
694.0	1934.3	1976.63	711.651	774.0	1942.3	1980.39	736.038	854.0	1950.3	2054.44	739.167	934.0	1958.3	2142.25	755.657
695.0	1934.4	1979.51	713.119	775.0	1942.4	1983.14	728.332	855.0	1950.4	2051.49	737.286	935.0	1958.4	2150.31	758.627
696.0	1934.5	1986.53	715.476	776.0	1942.5	1985.9	721.983	856.0	1950.5	2044.15	734.174	936.0	1958.5	2155.17	763.968
697.0	1934.6	1992.22	718.141	777.0	1942.6	1990.05	714.566	857.0	1950.6	2036.87	731.088	937.0	1958.6	2161.69	768.696
698.0	1934.7	1992.34	720.223	778.0	1942.7	1994.22	713.394	858.0	1950.7	2028.19	728.027	938.0	1958.7	2164.97	773.468
699.0	1934.8	1995.27	722.312	779.0	1942.8	1994.22	720.189								

No.	$d(\text{m})$	$v_p(\text{ms}^{-1})$	$v_s(\text{ms}^{-1})$												
961.0	1961.0	2032.52	729.248	1041.0	1969.0	2127.89	760.494	1121.0	1977.0	2199.98	799.193	1201.0	1985.0	2213.61	816.627
962.0	1961.1	2022.43	725.9	1042.0	1969.1	2121.57	759.847	1122.0	1977.1	2208.48	803.669	1202.0	1985.1	2217.05	815.876
963.0	1961.2	2013.82	721.983	1043.0	1969.2	2115.28	759.865	1123.0	1977.2	2217.05	806.682	1203.0	1985.2	2220.5	815.519
964.0	1961.3	2008.1	719.593	1044.0	1969.3	2109.04	759.221	1124.0	1977.3	2227.37	808.576	1204.0	1985.3	2225.68	815.939
965.0	1961.4	2006.63	717.515	1045.0	1969.4	2101.28	756.919	1125.0	1977.4	2239.47	812.364	1205.0	1985.4	2229.16	816.74
966.0	1961.5	2012.25	715.743	1046.0	1969.5	2093.58	754.625	1126.0	1977.5	2241.21	816.177	1206.0	1985.5	2234.39	816.773
967.0	1961.6	2022.23	713.687	1047.0	1969.6	2085.94	752.669	1127.0	1977.6	2241.21	818.867	1207.0	1985.6	2239.64	816.807
968.0	1961.7	2029.42	712.809	1048.0	1969.7	2078.35	752.025	1128.0	1977.7	2239.47	820.412	1208.0	1985.7	2239.64	817.22
969.0	1961.8	2033.76	713.98	1049.0	1969.8	2067.82	751.382	1129.0	1977.8	2230.81	821.963	1209.0	1985.8	2239.64	816.1
970.0	1961.9	2033.73	718.998	1050.0	1969.9	2063.34	750.74	1130.0	1977.9	2229.09	823.13	1210.0	1985.9	2239.64	815.367
971.0	1962.0	2038.1	724.087	1051.0	1970.0	2061.86	750.422	1131.0	1978.0	2225.65	823.13	1211.0	1986.0	2239.64	814.632
972.0	1962.1	2045.45	728.943	1052.0	1970.1	2063.43	749.753	1132.0	1978.1	2222.22	823.13	1212.0	1986.1	2239.74	813.885
973.0	1962.2	2051.39	733.555	1053.0	1970.2	2063.57	749.723	1133.0	1978.2	2218.77	823.52	1213.0	1986.2	2239.88	813.124
974.0	1962.3	2054.37	738.539	1054.0	1970.3	2066.7	750.342	1134.0	1978.3	2215.33	823.13	1214.0	1986.3	2240.05	812.364
975.0	1962.4	2052.88	745.875	1055.0	1970.4	2069.84	752.608	1135.0	1978.4	2211.9	821.575	1215.0	1986.4	2236.72	811.227
976.0	1962.5	2052.88	751.081	1056.0	1970.5	2075.96	755.545	1136.0	1978.5	2203.37	819.639	1216.0	1986.5	2229.91	811.227
977.0	1962.6	2046.93	751.081	1057.0	1970.6	2089.69	758.504	1137.0	1978.6	2201.67	818.096	1217.0	1986.6	2224.91	811.227
978.0	1962.7	2041.03	742.639	1058.0	1970.7	2108.19	760.82	1138.0	1978.7	2203.37	816.943	1218.0	1986.7	2218.14	811.227
979.0	1962.8	2041.03	741.372	1059.0	1970.8	2120.73	763.149	1139.0	1978.8	2201.67	816.56	1219.0	1986.8	2213.13	811.227
980.0	1962.9	2036.62	741.372	1060.0	1970.9	2130.23	775.134	1140.0	1978.9	2199.98	816.943	1220.0	1986.9	2206.41	811.227
981.0	1963.0	2033.69	741.372	1061.0	1971.0	2131.89	776.851	1141.0	1979.0	2203.37	817.327	1221.0	1987.0	2201.4	811.985
982.0	1963.1	2033.62	742.005	1062.0	1971.1	2135.13	777.899	1142.0	1979.1	2208.48	818.121	1222.0	1987.1	2201.47	812.744
983.0	1963.2	2033.5	739.481	1063.0	1971.2	2136.78	781.42	1143.0	1979.2	2215.33	818.54	1223.0	1987.2	2201.47	813.504
984.0	1963.3	2034.85	736.662	1064.0	1971.3	2136.86	787.135	1144.0	1979.3	2218.77	818.966	1224.0	1987.3	2206.62	814.266
985.0	1963.4	2037.65	734.484	1065.0	1971.4	2133.77	789.663	1145.0	1979.4	2222.22	819.778	1225.0	1987.4	2211.8	814.266
986.0	1963.5	2037.52	733.555	1066.0	1971.5	2130.67	789.663	1146.0	1979.5	2225.67	820.974	1226.0	1987.5	2211.8	815.411
987.0	1963.6	2034.49	732.936	1067.0	1971.6	2126.01	784.625	1147.0	1979.6	2227.4	821.403	1227.0	1987.6	2218.74	816.56
988.0	1963.7	2028.57	731.703	1068.0	1971.7	2123.5	778.945	1148.0	1979.7	2229.13	821.055	1228.0	1987.7	2223.93	816.943
989.0	1963.8	2024.14	730.167	1069.0	1971.8	2116.71	771.96	1149.0	1979.8	2229.14	821.09	1229.0	1987.8	2234.27	817.712
990.0	1963.9	2021.17	729.554	1070.0	1971.9	2112.09	769.889	1150.0	1979.9	2229.15	821.13	1230.0	1987.9	2237.73	819.639
991.0	1964.0	2028.24	729.554	1071.0	1972.0	2110.57	769.889	1151.0	1980.0	2225.68	820.009	1231.0	1988.0	2244.69	821.187
992.0	1964.1	2033.97	730.149	1072.0	1972.1	2109.04	767.829	1152.0	1980.1	2223.95	819.252	1232.0	1988.1	2255.33	823.13
993.0	1964.2	2041.23	723.268	1073.0	1972.2	2107.48	768.857	1153.0	1980.2	2220.5	819.252	1233.0	1988.2	2262.56	825.083
994.0	1964.3	2050.02	733.786	1074.0	1972.3	2104.38	770.923	1154.0	1980.3	2217.05	820.025	1234.0	1988.3	2268.08	826.651
995.0	1964.4	2057.4	734.994	1075.0	1972.4	2102.83	769.889	1155.0	1980.4	2217.05	821.575	1235.0	1988.4	2271.84	828.226
996.0	1964.5	2063.34	734.961	1076.0	1972.5	2104.38	768.857	1156.0	1980.5	2217.05	822.741	1236.0	1988.5	2273.8	829.411
997.0	1964.6	2067.82	735.866	1077.0	1972.6	2105.93	768.171	1157.0	1980.6	2220.5	824.3	1237.0	1988.6	2270.41	830.996
998.0	1964.7	2073.83	738.02	1078.0	1972.7	2107.48	767.487	1158.0	1980.7	2223.95	826.258	1238.0	1988.7	2267.0	832.986
999.0	1964.8	2078.35	751.409	1079.0	1972.8	2110.6	766.461	1159.0	1980.8	2227.42	828.621	1239.0	1988.8	2258.32	834.986
1000.0	1964.9	2081.38	754.703	1080.0	1972.9	2112.16	765.439	1160.0	1980.9	2230.9	831.393	1240.0	1988.9	2251.46	836.19
1001.0	1965.0	2082.9	755.034	1081.0	1973.0	2113.72	764.442	1161.0	1981.0	2239.64	835.387	1241.0	1989.0	2248.11	837.398
1002.0	1965.1	2082.9	754.372	1082.0	1973.1	2115.28	763.065	1162.0	1981.1	2248.56	838.61	1242.0	1989.1	2242.95	838.604
1003.0	1965.2	2082.9	753.711	1083.0	1973.2	2116.85	761.714	1163.0	1981.2	2259.41	842.265	1243.0	1989.2	2239.47	837.379
1004.0	1965.3	2079.87	756.36	1084.0	1973.3	2119.99	760.369	1164.0	1981.3	2270.35	844.719	1244.0	1989.3	2239.47	836.561
1005.0	1965.4	2073.83	762.727	1085.0	1973.4	2124.72	759.698	1165.0	1981.4	2281.41	846.776	1245.0	1989.4	2239.47	836.548
1006.0	1965.5	2073.83	766.461	1086.0	1973.5	2127.89	759.028	1166.0	1981.5	2290.75	848.015	1246.0	1989.5	2241.21	836.131
1007.0	1965.6	2070.82	764.081	1087.0	1973.6	2131.06	759.363	1167.0	1981.6	2294.6	849.257	1247.0	1989.6	2241.21	835.309
1008.0	1965.7	2069.32	751.737	1088.0	1973.7	2135.84	760.369	1168.0	1981.7	2298.48	850.087	1248.0	1989.7	2241.21	834.49
1009.0	1965.8	2067.82	759.028	1089.0	1973.8	2137.44	762.389	1169.0	1981.8	2300.52	850.503	1249.0	1989.8	2242.95	834.475
1010.0	1965.9	2064.84	766.461	1090.0	1973.9	2137.44	765.099	1170.0	1981.9	2300.69	851.336	1250.0	1989.9	2241.21	834.863
1011.0	1966.0	2063.34	765.78	1091.0	1974.0	2140.64	767.829	1171.0	1982.0	2297.18	851.336	1251.0	1990.0	2242.95	835.255
1012.0	1966.1	2061.86	760.051	1092.0	1974.1	2143.85	770.558	1172.0	1982.1	2293.58	850.503	1252.0	1990.1	2248.3	835.249
1013.0	1966.2	2060.37	756.028	1093.0	1974.2	2145.46	773.001	1173.0	1982.2	2289.9	850.087	1253.0	1990.2	2251.97	835.249
1014.0	1966.3	2057.4	737.912	1094.0	1974.3	2148.69	775.437	1174.0	1982.3	2284.41	850.919	1254.0	1990.3	2253.92	834.844
1015.0	1966.4	2054.44	731.088	1095.0	1974.4	2156.8	777.889	1175.0	1982.4	2277.13	850.919	1255.0	1990.4	2255.84	832.422
1016.0	1966.5	2050.02	721.683	1096.0	1974.5	2164.97	781.065	1176.0	1982.5	2268.09	850.087	1256.0	1990.5	2256.02	830.415
1017.0	1966.6	2045.62	716.628	1097.0	1974.6	2176.52	784.982	1177.0	1982.6	2260.91	849.257	1257.0	1990.6	2256.21	829.215
1018.0	1966.7	2045.62	712.225	1098.0	1974.7	2183.17	788.578</td								

No.	$d(\text{m})$	$v_p(\text{ms}^{-1})$	$v_s(\text{ms}^{-1})$												
1281.0	1993.0	2216.4	803.358	1361.0	2001.0	2239.28	796.745	1441.0	2009.0	2218.77	832.189	1521.0	2017.0	2246.94	815.411
1282.0	1993.1	2210.05	801.502	1362.0	2001.1	2251.02	800.032	1442.0	2009.1	2218.67	832.986	1522.0	2017.1	2241.59	823.91
1283.0	1993.2	2205.01	799.28	1363.0	2001.2	2262.95	802.987	1443.0	2009.2	2223.67	832.986	1523.0	2017.2	2232.75	829.411
1284.0	1993.3	2194.79	797.066	1364.0	2001.3	2275.04	805.218	1444.0	2009.3	2228.72	833.385	1524.0	2017.3	2222.22	826.258
1285.0	1993.4	2189.82	795.226	1365.0	2001.4	2283.69	807.461	1445.0	2009.4	2237.26	834.185	1525.0	2017.4	2215.4	821.963
1286.0	1993.5	2186.58	794.481	1366.0	2001.5	2288.83	809.717	1446.0	2009.5	2244.1	832.189	1526.0	2017.5	2206.93	817.327
1287.0	1993.6	2183.32	793.736	1367.0	2001.6	2295.81	812.008	1447.0	2009.6	2245.71	829.411	1527.0	2017.6	2198.52	813.504
1288.0	1993.7	2183.5	792.627	1368.0	2001.7	2302.81	815.083	1448.0	2009.7	2247.29	825.866	1528.0	2017.7	2191.84	811.606
1289.0	1993.8	2183.68	792.976	1369.0	2001.8	2302.62	818.571	1449.0	2009.8	2250.64	822.352	1529.0	2017.8	2188.52	811.606
1290.0	1993.9	2188.95	793.689	1370.0	2001.9	2302.46	822.088	1450.0	2009.9	2257.6	819.252	1530.0	2017.9	2186.86	811.227
1291.0	1994.0	2194.28	792.577	1371.0	2002.0	2302.27	824.45	1451.0	2010.0	2260.98	821.963	1531.0	2018.0	2188.52	810.849
1292.0	1994.1	2199.62	791.842	1372.0	2002.1	2296.59	826.024	1452.0	2010.1	2264.49	827.438	1532.0	2018.1	2191.94	810.094
1293.0	1994.2	2206.72	790.751	1373.0	2002.2	2292.63	827.989	1453.0	2010.2	2268.09	829.411	1533.0	2018.2	2193.78	809.336
1294.0	1994.3	2210.36	789.663	1374.0	2002.3	2288.75	828.765	1454.0	2010.3	2266.29	830.203	1534.0	2018.3	2193.93	808.956
1295.0	1994.4	2210.53	788.217	1375.0	2002.4	2284.82	828.747	1455.0	2010.4	2260.91	827.438	1535.0	2018.4	2197.45	809.717
1296.0	1994.5	2210.7	786.416	1376.0	2002.5	2280.91	827.933	1456.0	2010.5	2253.78	820.025	1536.0	2018.5	2202.65	809.717
1297.0	1994.6	2210.84	784.267	1377.0	2002.6	2278.83	827.123	1457.0	2010.6	2244.92	811.606	1537.0	2018.6	2207.86	809.336
1298.0	1994.7	2211.02	783.91	1378.0	2002.7	2273.18	827.104	1458.0	2010.7	2236.14	810.094	1538.0	2018.7	2213.12	810.094
1299.0	1994.8	2212.95	783.553	1379.0	2002.8	2272.81	827.483	1459.0	2010.8	2227.42	807.438	1539.0	2018.8	2216.69	811.606
1300.0	1994.9	2214.86	783.553	1380.0	2002.9	2272.5	827.464	1460.0	2010.9	2217.05	804.42	1540.0	2018.9	2220.26	820.799
1301.0	1995.0	2216.81	783.197	1381.0	2003.0	2275.65	827.051	1461.0	2011.0	2208.48	803.294	1541.0	2019.0	2222.15	831.791
1302.0	1995.1	2220.44	782.857	1382.0	2003.1	2278.76	826.651	1462.0	2011.1	2201.57	801.798	1542.0	2019.1	2222.32	838.199
1303.0	1995.2	2220.44	782.881	1383.0	2003.2	2283.65	826.651	1463.0	2011.2	2198.03	800.307	1543.0	2019.2	2224.26	838.188
1304.0	1995.3	2220.44	783.619	1384.0	2003.3	2288.63	826.258	1464.0	2011.3	2201.24	800.307	1544.0	2019.3	2222.66	833.344
1305.0	1995.4	2218.66	785.424	1385.0	2003.4	2293.6	825.866	1465.0	2011.4	2201.06	799.935	1545.0	2019.4	2219.42	829.343
1306.0	1995.5	2216.89	790.113	1386.0	2003.5	2296.8	825.866	1466.0	2011.5	2199.21	799.564	1546.0	2019.5	2214.48	828.528
1307.0	1995.6	2215.12	793.026	1387.0	2003.6	2296.45	825.474	1467.0	2011.6	2197.34	798.081	1547.0	2019.6	2206.17	826.923
1308.0	1995.7	2213.35	796.69	1388.0	2003.7	2296.03	825.474	1468.0	2011.7	2197.19	796.236	1548.0	2019.7	2199.62	820.616
1309.0	1995.8	2213.35	800.377	1389.0	2003.8	2295.62	824.691	1469.0	2011.8	2198.7	794.399	1549.0	2019.8	2194.77	814.392
1310.0	1995.9	2215.12	803.349	1390.0	2003.9	2295.27	824.3	1470.0	2011.9	2191.91	793.301	1550.0	2019.9	2191.61	809.773
1311.0	1996.0	2216.89	804.843	1391.0	2004.0	2293.03	824.691	1471.0	2012.0	2201.75	790.751	1551.0	2020.0	2190.1	808.98
1312.0	1996.1	2220.44	806.712	1392.0	2004.1	2290.88	825.083	1472.0	2012.1	2199.88	788.217	1552.0	2020.1	2186.93	808.211
1313.0	1996.2	2222.22	807.836	1393.0	2004.2	2287.03	825.474	1473.0	2012.2	2196.32	785.34	1553.0	2020.2	2185.4	807.836
1314.0	1996.3	2227.27	808.587	1394.0	2004.3	2283.16	825.474	1474.0	2012.3	2191.11	782.485	1554.0	2020.3	2183.88	806.712
1315.0	1996.4	2237.43	808.963	1395.0	2004.4	2279.31	826.258	1475.0	2012.4	2184.24	780.004	1555.0	2020.4	2182.34	805.964
1316.0	1996.5	2245.97	808.587	1396.0	2004.5	2275.48	826.651	1476.0	2012.5	2179.09	778.593	1556.0	2020.5	2182.48	806.338
1317.0	1996.6	2258.03	808.963	1397.0	2004.6	2275.28	826.258	1477.0	2012.6	2177.25	776.486	1557.0	2020.6	2184.25	807.461
1318.0	1996.7	2263.24	810.098	1398.0	2004.7	2273.25	826.258	1478.0	2012.7	2178.73	774.042	1558.0	2020.7	2184.39	808.587
1319.0	1996.8	2268.47	811.243	1399.0	2004.8	2269.46	827.044	1479.0	2012.8	2176.92	771.635	1559.0	2020.8	2189.52	810.861
1320.0	1996.9	2270.22	812.391	1400.0	2004.9	2269.26	828.226	1480.0	2012.9	2176.75	766.871	1560.0	2020.9	2199.77	812.391
1321.0	1997.0	2275.49	813.543	1401.0	2005.0	2270.8	829.807	1481.0	2013.0	2171.64	760.832	1561.0	2021.0	2211.82	813.543
1322.0	1997.1	2277.25	814.309	1402.0	2005.1	2275.48	830.996	1482.0	2013.1	2166.55	760.832	1562.0	2021.1	2223.97	815.083
1323.0	1997.2	2279.01	814.305	1403.0	2005.2	2280.07	832.189	1483.0	2013.2	2159.9	765.858	1563.0	2021.2	2230.99	815.469
1324.0	1997.3	2277.25	814.684	1404.0	2005.3	2284.56	831.791	1484.0	2013.3	2159.79	767.548	1564.0	2021.3	2238.05	818.571
1325.0	1997.4	2268.47	813.912	1405.0	2005.4	2287.4	831.393	1485.0	2013.4	2161.32	770.951	1565.0	2021.4	2238.05	828.816
1326.0	1997.5	2261.5	812.76	1406.0	2005.5	2288.32	830.996	1486.0	2013.5	2164.47	774.042	1566.0	2021.5	2239.82	838.095
1327.0	1997.6	2252.84	811.614	1407.0	2005.6	2289.25	830.203	1487.0	2013.6	2167.64	777.889	1567.0	2021.6	2243.37	840.55
1328.0	1997.7	2244.25	810.853	1408.0	2005.7	2286.68	829.807	1488.0	2013.7	2170.8	779.297	1568.0	2021.7	2245.15	828.417
1329.0	1997.8	2235.73	810.095	1409.0	2005.8	2282.19	829.411	1489.0	2013.8	2170.68	782.841	1569.0	2021.8	2248.72	828.417
1330.0	1997.9	2225.58	806.712	1410.0	2005.9	2275.92	828.621	1490.0	2013.9	2175.5	788.217	1570.0	2021.9	2248.72	827.223
1331.0	1998.0	2218.66	802.987	1411.0	2006.0	2269.79	827.438	1491.0	2014.0	2183.6	792.936	1571.0	2022.0	2243.37	825.241
1332.0	1998.1	2209.72	798.929	1412.0	2006.1	2265.55	825.843	1492.0	2014.1	2186.76	798.452	1572.0	2022.1	2238.05	822.874
1333.0	1998.2	2200.79	793.824	1413.0	2006.2	2259.77	824.633	1493.0	2014.2	2193.23	803.294	1573.0	2022.2	2243.51	820.13
1334.0	1998.3	2197.17	788.783	1414.0	2006.3	2248.66	821.864	1494.0	2014.3	2199.77	806.682	1574.0	2022.3	2230.99	816.242
1335.0	1998.4	2191.82	784.868	1415.0	2006.4	2239.37	819.5	1495.0	2014.4	2206.32	810.094	1575.0	2022.4	2230.99	813.927
1336.0	1998.5	2188.25	779.94	1416.0	2006.5	2231.95	817.918	1496.0	2014.5	2216.31	813.885	1576.0	2022.5	2230.99	812.008
1337.0	1998.6	2188.1	775.419	1417.0	2006.6	2222.77	817.115	1497.0	2014.6	2222.99	818.096	1577.0	2022.6	2232.75	808.211
1338.0	1998.7	2187.96</													

No.	$d(\text{m})$	$v_p(\text{ms}^{-1})$	$v_s(\text{ms}^{-1})$												
1601.0	2025.0	2270.38	806.665	1681.0	2033.0	2203.19	792.739	1761.0	2041.0	2225.65	802.634	1841.0	2049.0	2163.33	770.609
1602.0	2025.1	2255.9	800.307	1682.0	2033.1	2204.9	796.733	1762.0	2041.1	2232.44	802.246	1842.0	2049.1	2166.61	768.566
1603.0	2025.2	2243.37	801.425	1683.0	2033.2	2203.18	800.769	1763.0	2041.2	2235.74	801.876	1843.0	2049.2	2169.9	766.871
1604.0	2025.3	2232.75	804.796	1684.0	2033.3	2203.18	802.246	1764.0	2041.3	2235.59	801.876	1844.0	2049.3	2174.86	765.521
1605.0	2025.4	2225.72	807.817	1685.0	2033.4	2203.18	802.246	1765.0	2041.4	2235.43	802.617	1845.0	2049.4	2181.5	763.84
1606.0	2025.5	2222.22	803.294	1686.0	2033.5	2203.18	802.246	1766.0	2041.5	2231.78	803.729	1846.0	2049.5	2186.51	763.169
1607.0	2025.6	2220.5	796.604	1687.0	2033.6	2206.62	802.246	1767.0	2041.6	2231.64	806.712	1847.0	2049.6	2193.22	764.848
1608.0	2025.7	2223.97	794.399	1688.0	2033.7	2213.53	802.246	1768.0	2041.7	2231.46	809.717	1848.0	2049.7	2199.98	766.871
1609.0	2025.8	2227.47	796.604	1689.0	2033.8	2217.0	801.876	1769.0	2041.8	2229.56	812.008	1849.0	2049.8	2208.48	777.152
1610.0	2025.9	2227.47	801.425	1690.0	2033.9	2217.0	802.246	1770.0	2041.9	2229.41	815.083	1850.0	2049.9	2206.77	793.1
1611.0	2026.0	2227.47	805.549	1691.0	2034.0	2220.48	802.617	1771.0	2042.0	2229.23	818.96	1851.0	2050.0	2201.67	809.717
1612.0	2026.1	2227.47	810.471	1692.0	2034.1	2223.95	802.987	1772.0	2042.1	2229.16	821.696	1852.0	2050.1	2193.22	813.925
1613.0	2026.2	2225.72	813.124	1693.0	2034.2	2229.16	802.987	1773.0	2042.2	2229.16	825.636	1853.0	2050.2	2184.84	813.537
1614.0	2026.3	2222.22	807.817	1694.0	2034.3	2229.16	800.769	1774.0	2042.3	2230.9	829.615	1854.0	2050.3	2174.86	809.717
1615.0	2026.4	2217.05	802.92	1695.0	2034.4	2229.16	800.032	1775.0	2042.4	2232.64	832.02	1855.0	2050.4	2163.33	806.338
1616.0	2026.5	2213.61	807.06	1696.0	2034.5	2229.16	805.591	1776.0	2042.5	2237.89	833.632	1856.0	2050.5	2155.17	801.876
1617.0	2026.6	2211.9	808.956	1697.0	2034.6	2227.42	810.098	1777.0	2042.6	2248.45	834.035	1857.0	2050.6	2145.46	795.276
1618.0	2026.7	2213.61	809.336	1698.0	2034.7	2222.22	812.391	1778.0	2042.7	2235.78	833.228	1858.0	2050.7	2139.04	791.296
1619.0	2026.8	2217.05	809.336	1699.0	2034.8	2215.26	807.461	1779.0	2042.8	2257.34	831.217	1859.0	2050.8	2135.84	788.069
1620.0	2026.9	2222.22	810.094	1700.0	2034.9	2210.07	803.358	1780.0	2042.9	2257.34	830.816	1860.0	2050.9	2135.84	786.643
1621.0	2027.0	2225.72	810.094	1701.0	2035.0	2203.18	798.563	1781.0	2043.0	2257.34	833.228	1861.0	2051.0	2135.84	785.577
1622.0	2027.1	2227.47	809.336	1702.0	2035.1	2196.34	793.462	1782.0	2043.1	2255.55	835.655	1862.0	2051.1	2137.44	783.792
1623.0	2027.2	2227.47	808.956	1703.0	2035.2	2189.54	789.5	1783.0	2043.2	2255.55	837.28	1863.0	2051.2	2139.04	782.353
1624.0	2027.3	2227.47	810.849	1704.0	2035.3	2182.78	786.287	1784.0	2043.3	2253.78	837.28	1864.0	2051.3	2140.64	780.569
1625.0	2027.4	2230.99	815.411	1705.0	2035.4	2179.42	783.453	1785.0	2043.4	2250.23	837.687	1865.0	2051.4	2145.46	778.785
1626.0	2027.5	2234.51	813.124	1706.0	2035.5	2181.1	782.044	1786.0	2043.5	2250.23	835.655	1866.0	2051.5	2148.69	776.658
1627.0	2027.6	2236.28	807.06	1707.0	2035.6	2184.47	782.044	1787.0	2043.6	2241.4	830.015	1867.0	2051.6	2153.55	774.89
1628.0	2027.7	2236.28	807.06	1708.0	2035.7	2187.85	783.101	1788.0	2043.7	2234.39	825.636	1868.0	2051.7	2158.43	773.125
1629.0	2027.8	2230.99	808.576	1709.0	2035.8	2191.24	784.868	1789.0	2043.8	2229.16	820.13	1869.0	2051.8	2163.33	772.745
1630.0	2027.9	2227.47	808.956	1710.0	2035.9	2196.34	786.643	1790.0	2043.9	2220.5	817.793	1870.0	2051.9	2174.86	772.371
1631.0	2028.0	2223.97	808.576	1711.0	2036.0	2201.47	787.712	1791.0	2044.0	2211.9	817.793	1871.0	2052.0	2179.84	772.679
1632.0	2028.1	2222.22	807.06	1712.0	2036.1	2204.91	789.5	1792.0	2044.1	2206.77	817.793	1872.0	2052.1	2186.51	774.739
1633.0	2028.2	2217.05	804.796	1713.0	2036.2	2210.09	790.936	1793.0	2044.2	2206.77	818.182	1873.0	2052.2	2193.22	776.836
1634.0	2028.3	2210.19	802.172	1714.0	2036.3	2215.28	793.1	1794.0	2044.3	2206.77	818.182	1874.0	2052.3	2196.6	777.889
1635.0	2028.4	2205.07	799.193	1715.0	2036.4	2220.48	795.64	1795.0	2044.4	2206.77	818.571	1875.0	2052.4	2198.29	778.945
1636.0	2028.5	2199.98	797.342	1716.0	2036.5	2220.49	797.464	1796.0	2044.5	2210.19	818.571	1876.0	2052.5	2199.98	782.841
1637.0	2028.6	2194.91	795.868	1717.0	2036.6	2220.49	798.563	1797.0	2044.6	2211.9	818.182	1877.0	2052.6	2205.07	789.301
1638.0	2028.7	2194.91	792.936	1718.0	2036.7	2220.49	799.297	1798.0	2044.7	2217.05	816.63	1878.0	2052.7	2210.19	801.425
1639.0	2028.8	2194.91	791.114	1719.0	2036.8	2220.49	799.664	1799.0	2044.8	2218.77	815.469	1879.0	2052.8	2215.33	813.504
1640.0	2028.9	2196.6	790.025	1720.0	2036.9	2218.77	800.032	1800.0	2044.9	2223.95	814.312	1880.0	2052.9	2217.05	816.177
1641.0	2029.0	2199.98	790.025	1721.0	2037.0	2218.77	800.032	1801.0	2045.0	2230.9	813.543	1881.0	2053.0	2218.77	818.481
1642.0	2029.1	2206.77	790.025	1722.0	2037.1	2217.15	798.929	1802.0	2045.1	2236.03	813.54	1882.0	2053.1	2218.77	821.575
1643.0	2029.2	2221.19	790.388	1723.0	2037.2	2205.32	797.464	1803.0	2045.2	2244.65	813.537	1883.0	2053.2	2218.77	823.91
1644.0	2029.3	2213.61	790.025	1724.0	2037.3	2195.26	796.369	1804.0	2045.3	2244.47	813.533	1884.0	2053.3	2220.5	826.258
1645.0	2029.4	2217.05	789.663	1725.0	2037.4	2192.03	796.004	1805.0	2045.4	2244.28	819.314	1885.0	2053.4	2225.65	827.832
1646.0	2029.5	2222.22	790.025	1726.0	2037.5	2188.8	795.64	1806.0	2045.5	2244.12	828.33	1886.0	2053.5	2229.09	828.226
1647.0	2029.6	2223.97	790.025	1727.0	2037.6	2183.9	796.004	1807.0	2045.6	2243.93	837.929	1887.0	2053.6	2230.81	828.621
1648.0	2029.7	2227.47	789.663	1728.0	2037.7	2180.66	796.369	1808.0	2045.7	2243.77	837.903	1888.0	2053.7	2232.54	830.203
1649.0	2029.8	2222.22	789.663	1729.0	2037.8	2182.47	797.099	1809.0	2045.8	2240.07	836.257	1889.0	2053.8	2239.47	833.385
1650.0	2029.9	2220.5	789.301	1730.0	2037.9	2185.97	797.83	1810.0	2045.9	2231.14	834.621	1890.0	2053.9	2244.69	837.398
1651.0	2030.0	2213.61	788.578	1731.0	2038.0	2187.78	798.196	1811.0	2046.0	2225.76	832.995	1891.0	2054.0	2248.19	840.636
1652.0	2030.1	2208.48	787.127	1732.0	2038.1	2189.46	798.929	1812.0	2046.1	2218.77	829.411	1892.0	2054.1	2249.85	844.309
1653.0	2030.2	2203.37	786.038	1733.0	2038.2	2191.01	799.664	1813.0	2046.2	2206.77	823.91	1893.0	2054.2	2247.96	841.857
1654.0	2030.3	2196.6	783.883	1734.0	2038.3	2194.27	800.769	1814.0	2046.3	2203.37	818.867	1894.0	2054.3	2239.06	823.91
1655.0	2030.4	2194.91	781.391	1735.0	2038.4	2202.63	801.138	1815.0	2046.4	2203.37	813.504	1895.0	2054.4	2233.68	808.576
1656.0	2030.5	2194.91	778.92	1736.0	2038.5	2207.63	800.4	1816.0	2046.5	2205.07	808.204	1896.0	2054.5	2226.61	805.926
1657.0	2030.6	2191.54	776.819	1737.0	2038.6	2210.89	801.876	1817.0	2046.6	2205.07	805.568	1897.0	2054.6	2216.09	803.669
1658.0	2030.7	2186.51	775.078	17											

No.	$d(\text{m})$	$v_p(\text{ms}^{-1})$	$v_s(\text{ms}^{-1})$												
1921.0	2057.0	2203.37	802.545	2001.0	2065.0	2176.59	792.384	2081.0	2073.0	2147.07	777.889	2161.0	2081.0	2199.98	814.695
1922.0	2057.1	2196.6	796.951	2002.0	2065.1	2178.17	788.069	2082.0	2073.1	2145.46	778.945	2162.0	2081.1	2198.29	814.697
1923.0	2057.2	2189.86	794.706	2003.0	2065.2	2179.84	783.101	2083.0	2073.2	2148.69	779.297	2163.0	2081.2	2194.91	815.083
1924.0	2057.3	2184.84	791.022	2004.0	2065.3	2183.17	778.195	2084.0	2073.3	2153.55	780.711	2164.0	2081.3	2189.86	813.927
1925.0	2057.4	2176.52	786.288	2005.0	2065.4	2186.51	775.419	2085.0	2073.4	2160.06	782.841	2165.0	2081.4	2184.84	809.34
1926.0	2057.5	2169.9	780.547	2006.0	2065.5	2188.18	773.694	2086.0	2073.5	2164.97	784.982	2166.0	2081.5	2181.5	802.246
1927.0	2057.6	2169.9	776.993	2007.0	2065.6	2186.51	773.347	2087.0	2073.6	2171.55	787.856	2167.0	2081.6	2178.17	797.099
1928.0	2057.7	2169.9	774.162	2008.0	2065.7	2186.51	773.347	2088.0	2073.7	2147.86	791.478	2168.0	2081.7	2173.2	797.464
1929.0	2057.8	2173.2	771.717	2009.0	2065.8	2184.84	781.693	2089.0	2073.8	2178.17	799.935	2169.0	2081.8	2166.61	797.83
1930.0	2057.9	2174.86	770.655	2010.0	2065.9	2183.17	782.396	2090.0	2073.9	2178.17	807.06	2170.0	2081.9	2163.33	798.929
1931.0	2058.0	2181.5	770.625	2011.0	2066.0	2184.84	738.853	2091.0	2074.0	2178.17	811.606	2171.0	2082.0	2163.33	799.664
1932.0	2058.1	2188.18	771.292	2012.0	2066.1	2186.51	705.293	2092.0	2074.1	2176.62	811.607	2172.0	2082.1	2164.97	800.786
1933.0	2058.2	2196.6	771.977	2013.0	2066.2	2189.86	715.743	2093.0	2074.2	2175.11	811.609	2173.0	2082.2	2166.61	801.551
1934.0	2058.3	2198.29	772.663	2014.0	2066.3	2196.6	732.319	2094.0	2074.3	2173.63	806.689	2174.0	2082.3	2171.55	801.581
1935.0	2058.4	2198.29	773.35	2015.0	2066.4	2206.77	798.196	2095.0	2074.4	2172.15	799.6	2175.0	2082.4	2176.52	800.871
1936.0	2058.5	2194.91	777.187	2016.0	2066.5	2217.05	793.1	2096.0	2074.5	2167.36	793.738	2176.0	2082.5	2179.84	804.245
1937.0	2058.6	2191.54	793.667	2017.0	2066.6	2223.95	782.044	2097.0	2074.6	2159.34	787.258	2177.0	2082.6	2188.18	817.578
1938.0	2058.7	2188.18	780.711	2018.0	2066.7	2232.64	778.892	2098.0	2074.7	2152.98	782.307	2178.0	2082.7	2193.22	821.871
1939.0	2058.8	2183.17	768.226	2019.0	2066.8	2252.0	779.94	2099.0	2074.8	2148.3	782.331	2179.0	2082.8	2194.91	819.569
1940.0	2058.9	2176.52	767.887	2020.0	2066.9	2273.5	782.044	2100.0	2074.9	2145.24	782.36	2180.0	2082.9	2198.29	814.984
1941.0	2059.0	2169.9	765.858	2021.0	2067.0	2280.76	785.222	2101.0	2075.0	2145.39	784.149	2181.0	2083.0	2199.98	812.728
1942.0	2059.1	2163.33	763.84	2022.0	2067.1	2257.31	788.783	2102.0	2075.1	2147.07	785.563	2182.0	2083.1	2198.29	812.767
1943.0	2059.2	2156.8	762.166	2023.0	2067.2	2244.89	791.656	2103.0	2075.2	2147.07	786.609	2183.0	2083.2	2196.6	812.801
1944.0	2059.3	2151.93	762.166	2024.0	2067.3	2227.41	793.1	2104.0	2075.3	2148.69	787.657	2184.0	2083.3	2194.91	806.401
1945.0	2059.4	2156.8	762.166	2025.0	2067.4	2213.61	793.1	2105.0	2075.4	2148.69	787.992	2185.0	2083.4	2189.86	799.699
1946.0	2059.5	2155.17	762.166	2026.0	2067.5	2193.22	792.739	2106.0	2075.5	2153.55	787.973	2186.0	2083.5	2181.5	794.566
1947.0	2059.6	2158.43	762.166	2027.0	2067.6	2176.52	796.369	2107.0	2075.6	2160.06	788.31	2187.0	2083.6	2174.86	790.954
1948.0	2059.7	2160.06	765.184	2028.0	2067.7	2174.86	801.876	2108.0	2075.7	2168.26	789.008	2188.0	2083.7	2174.86	789.536
1949.0	2059.8	2166.61	766.871	2029.0	2067.8	2164.97	802.617	2109.0	2075.8	2178.17	791.159	2189.0	2083.8	2171.55	790.3
1950.0	2059.9	2174.86	774.39	2030.0	2067.9	2151.93	799.297	2110.0	2075.9	2189.86	795.887	2190.0	2083.9	2168.26	792.521
1951.0	2060.0	2179.84	779.65	2031.0	2068.0	2139.04	797.099	2111.0	2076.0	2198.29	802.175	2191.0	2084.0	2168.26	794.382
1952.0	2060.1	2186.51	782.841	2032.0	2068.1	2127.89	794.549	2112.0	2076.1	2198.29	810.094	2192.0	2084.1	2168.26	796.604
1953.0	2060.2	2191.54	785.699	2033.0	2068.2	2121.57	792.377	2113.0	2076.2	2198.29	813.504	2193.0	2084.2	2166.61	797.712
1954.0	2060.3	2201.67	788.939	2034.0	2068.3	2116.85	788.426	2114.0	2076.3	2198.29	811.227	2194.0	2084.3	2166.61	799.193
1955.0	2060.4	2211.9	791.842	2035.0	2068.4	2113.72	784.514	2115.0	2076.4	2189.86	808.576	2195.0	2084.4	2171.55	801.798
1956.0	2060.5	2222.22	796.604	2036.0	2068.5	2113.72	781.342	2116.0	2076.5	2186.51	803.669	2196.0	2084.5	2174.86	802.172
1957.0	2060.6	2232.54	801.798	2037.0	2068.6	2116.85	777.499	2117.0	2076.6	2183.17	796.973	2197.0	2084.6	2179.84	802.92
1958.0	2060.7	2242.95	807.438	2038.0	2068.7	2124.72	774.039	2118.0	2076.7	2179.84	791.114	2198.0	2084.7	2183.17	810.094
1959.0	2060.8	2253.46	820.412	2039.0	2068.8	2131.06	775.419	2119.0	2076.8	2174.86	787.496	2199.0	2084.8	2186.51	820.025
1960.0	2060.9	2256.98	825.387	2040.0	2068.9	2135.84	785.222	2120.0	2076.9	2168.26	785.34	2200.0	2084.9	2186.51	828.621
1961.0	2061.0	2256.98	843.081	2041.0	2069.0	2142.25	794.549	2121.0	2077.0	2163.33	783.197	2201.0	2085.0	2188.18	829.016
1962.0	2061.1	2253.46	843.081	2042.0	2069.1	2148.69	803.354	2122.0	2077.1	2155.17	781.065	2202.0	2085.1	2189.86	821.963
1963.0	2061.2	2249.94	841.857	2043.0	2069.2	2155.17	799.281	2123.0	2077.2	2147.07	779.65	2203.0	2085.2	2191.54	813.885
1964.0	2061.3	2241.21	829.016	2044.0	2069.3	2161.69	796.7	2124.0	2077.3	2143.85	779.297	2204.0	2085.3	2193.22	807.817
1965.0	2061.4	2234.27	821.575	2045.0	2069.4	2166.61	796.687	2125.0	2077.4	2143.85	779.297	2205.0	2085.4	2193.22	807.817
1966.0	2061.5	2229.09	824.691	2046.0	2069.5	2169.9	796.675	2126.0	2077.5	2143.85	778.945	2206.0	2085.5	2189.86	807.06
1967.0	2061.6	2223.93	832.189	2047.0	2069.6	2171.55	796.295	2127.0	2077.6	2145.46	779.297	2207.0	2085.6	2184.84	808.956
1968.0	2061.7	2220.48	836.19	2048.0	2069.7	2171.55	796.283	2128.0	2077.7	2148.69	781.42	2208.0	2085.7	2181.5	811.606
1969.0	2061.8	2211.82	824.3	2049.0	2069.8	2171.55	796.268	2129.0	2077.8	2158.43	783.91	2209.0	2085.8	2176.52	808.576
1970.0	2061.9	2203.21	814.647	2050.0	2069.9	2171.55	799.578	2130.0	2077.9	2166.61	786.776	2210.0	2085.9	2174.86	805.926
1971.0	2062.0	2194.65	823.52	2051.0	2070.0	2171.55	798.087	2131.0	2078.0	2178.17	790.025	2211.0	2086.0	2174.86	803.294
1972.0	2062.1	2194.55	833.376	2052.0	2070.1	2171.52	794.399	2132.0	2078.1	2188.18	792.936	2212.0	2086.1	2174.86	803.294
1973.0	2062.2	2194.4	803.622	2053.0	2070.2	2169.82	791.478	2133.0	2078.2	2198.29	794.033	2213.0	2086.2	2178.17	803.294
1974.0	2062.3	2195.97	796.176	2054.0	2070.3	2169.77	787.496	2134.0	2078.3	2203.37	801.798	2214.0	2086.3	2181.5	803.294
1975.0	2062.4	2195.82	807.31	2055.0	2070.4	2169.72	786.416	2135.0	2078.4	2208.48	812.364	2215.0	2086.4	2181.5	803.294
1976.0	2062.5	2195.67	818.731	2056.0	2070.5	2166.37	786.416	2136.0	2078.5	2210.19	821.575	2216.0	2086.5	2186.51	809.336
1977.0	2062.6	2197.24	817.93	2057.0	2070.6	2163.01	787.135	2137.0	2078.6	2208.48	821.187	2217.0	2086.6	2191.54	806.682
1978.0	2062.7	2198.79	814.045	2058.0											

No.	$d(\text{m})$	$v_p(\text{ms}^{-1})$	$v_s(\text{ms}^{-1})$												
2241.0	2089.0	2201.67	808.587	2321.0	2097.0	2181.5	799.193	2401.0	2105.0	2213.61	830.21	2481.0	2113.0	2194.21	820.412
2242.0	2089.1	2201.67	808.609	2322.0	2097.1	2181.5	802.92	2402.0	2105.1	2208.48	827.821	2482.0	2113.1	2192.74	818.867
2243.0	2089.2	2201.67	808.647	2323.0	2097.2	2181.5	807.817	2403.0	2105.2	2203.37	821.922	2483.0	2113.2	2192.9	816.943
2244.0	2089.3	2201.67	807.551	2324.0	2097.3	2183.17	808.956	2404.0	2105.3	2198.29	812.273	2484.0	2113.3	2199.97	814.266
2245.0	2089.4	2193.22	806.46	2325.0	2097.4	2188.18	808.956	2405.0	2105.4	2188.18	807.687	2485.0	2113.4	2200.16	819.252
2246.0	2089.5	2171.55	803.874	2326.0	2097.5	2188.18	808.956	2406.0	2105.5	2176.52	803.901	2486.0	2113.5	2202.04	832.189
2247.0	2089.6	2173.2	802.411	2327.0	2097.6	2191.54	823.13	2407.0	2105.6	2164.97	798.677	2487.0	2113.6	2209.18	831.791
2248.0	2089.7	2178.17	800.583	2328.0	2097.7	2196.6	837.802	2408.0	2105.7	2158.43	790.996	2488.0	2113.7	2212.83	828.621
2249.0	2089.8	2179.84	796.548	2329.0	2097.8	2199.98	838.61	2409.0	2105.8	2151.93	783.831	2489.0	2113.8	2214.76	825.474
2250.0	2089.9	2178.17	793.636	2330.0	2097.9	2201.67	838.61	2410.0	2105.9	2147.07	794.943	2490.0	2113.9	2214.95	822.741
2251.0	2090.0	2168.26	791.106	2331.0	2098.0	2199.98	836.995	2411.0	2106.0	2143.85	801.891	2491.0	2114.0	2213.36	819.639
2252.0	2090.1	2158.43	790.751	2332.0	2098.1	2199.98	835.387	2412.0	2106.1	2140.64	799.664	2492.0	2114.1	2213.54	818.096
2253.0	2090.2	2155.17	791.478	2333.0	2098.2	2198.29	833.385	2413.0	2106.2	2140.64	782.396	2493.0	2114.2	2213.7	817.327
2254.0	2090.3	2155.17	792.936	2334.0	2098.3	2196.6	831.791	2414.0	2106.3	2139.04	781.342	2494.0	2114.3	2212.14	815.794
2255.0	2090.4	2161.69	794.766	2335.0	2098.4	2196.6	829.807	2415.0	2106.4	2140.64	783.453	2495.0	2114.4	2207.09	812.364
2256.0	2090.5	2166.61	798.081	2336.0	2098.5	2193.22	828.226	2416.0	2106.5	2143.85	789.858	2496.0	2114.5	2203.78	807.06
2257.0	2090.6	2169.9	801.052	2337.0	2098.6	2189.86	826.258	2417.0	2106.6	2150.31	791.656	2497.0	2114.6	2198.77	802.545
2258.0	2090.7	2178.17	804.42	2338.0	2098.7	2188.18	824.691	2418.0	2106.7	2158.43	794.187	2498.0	2114.7	2195.5	804.796
2259.0	2090.8	2186.51	806.682	2339.0	2098.8	2186.51	823.52	2419.0	2106.8	2168.26	802.913	2499.0	2114.8	2193.94	805.549
2260.0	2090.9	2191.54	808.956	2340.0	2098.9	2181.5	820.799	2420.0	2106.9	2178.17	822.481	2500.0	2114.9	2194.12	806.304
2261.0	2091.0	2191.54	813.885	2341.0	2099.0	2176.52	815.029	2421.0	2107.0	2186.51	822.481	2501.0	2115.0	2192.56	807.438
2262.0	2091.1	2189.86	823.52	2342.0	2099.1	2173.3	808.956	2422.0	2107.1	2191.62	822.874	2502.0	2115.1	2192.54	808.576
2263.0	2091.2	2188.18	831.393	2343.0	2099.2	2180.09	804.804	2423.0	2107.2	2195.12	823.662	2503.0	2115.2	2194.08	808.576
2264.0	2091.3	2186.51	831.393	2344.0	2099.3	2181.93	804.059	2424.0	2107.3	2203.76	824.056	2504.0	2115.3	2193.93	810.094
2265.0	2091.4	2184.84	829.807	2345.0	2099.4	2182.11	804.065	2425.0	2107.4	2210.77	824.056	2505.0	2115.4	2197.19	811.985
2266.0	2091.5	2181.5	824.691	2346.0	2099.5	2182.26	803.697	2426.0	2107.5	2214.36	825.241	2506.0	2115.5	2200.46	814.266
2267.0	2091.6	2176.52	821.575	2347.0	2099.6	2185.77	802.958	2427.0	2107.6	2216.26	826.826	2507.0	2115.6	2203.77	815.411
2268.0	2091.7	2171.55	817.327	2348.0	2099.7	2190.95	803.336	2428.0	2107.7	2216.41	828.816	2508.0	2115.7	2205.32	817.712
2269.0	2091.8	2166.61	813.124	2349.0	2099.8	2196.19	804.087	2429.0	2107.8	2213.13	830.816	2509.0	2115.8	2206.88	821.187
2270.0	2091.9	2161.69	811.227	2350.0	2099.9	2201.44	805.212	2430.0	2107.9	2204.69	832.422	2510.0	2115.9	2210.18	833.785
2271.0	2092.0	2160.06	810.094	2351.0	2100.0	2206.7	806.336	2431.0	2108.0	2197.98	834.44	2511.0	2116.0	2210.02	833.785
2272.0	2092.1	2153.55	809.717	2352.0	2100.1	2213.61	807.086	2432.0	2108.1	2189.54	836.467	2512.0	2116.1	2208.01	833.785
2273.0	2092.2	2148.69	809.336	2353.0	2100.2	2218.77	812.391	2433.0	2108.2	2182.78	830.415	2513.0	2116.2	2205.92	832.587
2274.0	2092.3	2145.46	807.438	2354.0	2100.3	2223.94	827.621	2434.0	2108.3	2181.1	822.088	2514.0	2116.3	2205.63	830.599
2275.0	2092.4	2140.64	799.564	2355.0	2100.4	2229.11	838.503	2435.0	2108.4	2179.42	815.083	2515.0	2116.4	2205.28	828.226
2276.0	2092.5	2137.44	792.206	2356.0	2100.5	2230.85	839.73	2436.0	2108.5	2177.74	812.775	2516.0	2116.5	2204.94	825.474
2277.0	2092.6	2135.84	786.416	2357.0	2100.6	2229.13	838.912	2437.0	2108.6	2176.06	813.543	2517.0	2116.6	2204.65	823.13
2278.0	2092.7	2139.04	779.65	2358.0	2100.7	2223.95	837.28	2438.0	2108.7	2172.72	815.083	2518.0	2116.7	2200.86	821.575
2279.0	2092.8	2147.07	778.945	2359.0	2100.8	2218.77	834.844	2439.0	2108.8	2172.72	818.571	2519.0	2116.8	2197.1	817.327
2280.0	2092.9	2153.55	778.945	2360.0	2100.9	2211.9	834.035	2440.0	2108.9	2172.72	834.44	2520.0	2116.9	2196.77	813.504
2281.0	2093.0	2153.55	782.485	2361.0	2101.0	2203.37	833.228	2441.0	2109.0	2109.0	836.873	2521.0	2117.0	2194.78	810.849
2282.0	2093.1	2156.8	790.025	2362.0	2101.1	2194.91	832.422	2442.0	2109.1	2186.46	834.035	2522.0	2117.1	2192.84	808.196
2283.0	2093.2	2161.69	795.5	2363.0	2101.2	2188.18	831.618	2443.0	2109.2	2192.07	830.816	2523.0	2117.2	2190.96	805.926
2284.0	2093.3	2164.97	799.935	2364.0	2101.3	2181.5	829.215	2444.0	2109.3	2195.93	828.019	2524.0	2117.3	2189.11	804.42
2285.0	2093.4	2169.9	798.822	2365.0	2101.4	2178.17	818.182	2445.0	2109.4	2199.88	824.845	2525.0	2117.4	2188.94	804.42
2286.0	2093.5	2173.2	798.081	2366.0	2101.5	2171.55	811.625	2446.0	2109.5	2202.13	823.662	2526.0	2117.5	2193.85	805.549
2287.0	2093.6	2173.2	795.868	2367.0	2101.6	2164.97	807.461	2447.0	2109.6	2200.88	820.13	2527.0	2117.6	2197.11	807.06
2288.0	2093.7	2171.55	790.025	2368.0	2101.7	2161.69	804.473	2448.0	2109.7	2201.42	815.856	2528.0	2117.7	2202.06	809.717
2289.0	2093.8	2169.9	781.42	2369.0	2101.8	2158.43	801.507	2449.0	2109.8	2198.53	811.625	2529.0	2117.8	2203.59	811.985
2290.0	2093.9	2168.26	774.042	2370.0	2101.9	2155.17	799.297	2450.0	2109.9	2193.87	810.098	2530.0	2117.9	2210.3	813.124
2291.0	2094.0	2164.97	769.246	2371.0	2102.0	2160.06	797.099	2451.0	2110.0	2189.31	808.963	2531.0	2118.0	2213.61	821.963
2292.0	2094.1	2163.43	769.246	2372.0	2102.1	2164.97	805.218	2452.0	2110.1	2184.57	807.482	2532.0	2118.1	2218.63	830.996
2293.0	2094.2	2160.33	769.246	2373.0	2102.2	2169.9	815.083	2453.0	2110.2	2177.99	806.019	2533.0	2118.2	2223.65	836.19
2294.0	2094.3	2160.47	773.694	2374.0	2102.3	2171.55	807.461	2454.0	2110.3	2169.82	804.928	2534.0	2118.3	2226.92	835.788
2295.0	2094.4	2160.65	778.241	2375.0	2102.4	2176.52	795.276	2455.0	2110.4	2165.01	803.096	2535.0	2118.4	2228.45	835.387
2296.0	2094.5	2160.82	782.13	2376.0	2102.5	2183.17	793.462	2456.0	2110.5	2160.2	798.314	2536.0	2118.5	2229.98	834.585
2297.0	2094.6	2160.96	786.776	2377.0	2102.6	2188.18	802.617	2457.0	2110.6	2153.79	794.303	2537.0	2118.6	2229.82	834.585
2298.0	2094.7	2162.77	791.114	2											

No.	$d(\text{m})$	$v_p(\text{ms}^{-1})$	$v_s(\text{ms}^{-1})$												
2561.0	2121.0	2211.88	820.416	2641.0	2129.0	2213.7	828.807	2721.0	2137.0	2143.85	797.83	2801.0	2145.0	2243.16	847.601
2562.0	2121.1	2203.09	816.56	2642.0	2129.1	2213.8	821.319	2722.0	2137.1	2143.85	794.913	2802.0	2145.1	2241.4	845.539
2563.0	2121.2	2201.24	813.504	2643.0	2129.2	2210.57	814.365	2723.0	2137.2	2143.85	796.004	2803.0	2145.2	2239.64	843.482
2564.0	2121.3	2201.08	811.227	2644.0	2129.3	2203.94	807.177	2724.0	2137.3	2145.46	806.712	2804.0	2145.3	2234.39	841.022
2565.0	2121.4	2197.51	809.717	2645.0	2129.4	2204.1	801.238	2725.0	2137.4	2150.31	816.242	2805.0	2145.4	2230.9	838.977
2566.0	2121.5	2195.68	809.717	2646.0	2129.5	2202.56	800.158	2726.0	2137.5	2158.43	811.625	2806.0	2145.5	2227.42	836.94
2567.0	2121.6	2195.53	809.717	2647.0	2129.6	2192.6	800.924	2727.0	2137.6	2163.33	804.845	2807.0	2145.6	2223.95	833.7
2568.0	2121.7	2198.79	810.094	2648.0	2129.7	2186.06	802.443	2728.0	2137.7	2168.26	798.563	2808.0	2145.7	2220.5	830.079
2569.0	2121.8	2202.04	811.227	2649.0	2129.8	2177.88	800.981	2729.0	2137.8	2174.86	797.464	2809.0	2145.8	2220.5	826.089
2570.0	2121.9	2203.58	813.504	2650.0	2129.9	2168.09	798.045	2730.0	2137.9	2179.84	813.158	2810.0	2145.9	2220.5	826.461
2571.0	2122.0	2211.97	815.794	2651.0	2130.0	2163.28	793.659	2731.0	2138.0	2184.84	818.96	2811.0	2146.0	2220.5	828.824
2572.0	2122.1	2222.12	816.177	2652.0	2130.1	2158.43	788.939	2732.0	2138.1	2189.86	820.521	2812.0	2146.1	2220.5	831.217
2573.0	2122.2	2230.55	814.266	2653.0	2130.2	2155.17	784.982	2733.0	2138.2	2198.29	827.223	2813.0	2146.2	2220.5	833.632
2574.0	2122.3	2232.09	811.985	2654.0	2130.3	2153.55	783.553	2734.0	2138.3	2208.48	832.825	2814.0	2146.3	2222.2	836.467
2575.0	2122.4	2233.65	820.412	2655.0	2130.4	2155.17	783.197	2735.0	2138.4	2213.61	826.826	2815.0	2146.4	2223.95	841.783
2576.0	2122.5	2235.2	833.785	2656.0	2130.5	2156.8	784.267	2736.0	2138.5	2213.61	813.158	2816.0	2146.5	2227.42	845.088
2577.0	2122.6	2235.04	837.802	2657.0	2130.6	2160.06	786.416	2737.0	2138.6	2213.61	813.158	2817.0	2146.6	2232.64	848.002
2578.0	2122.7	2233.12	839.419	2658.0	2130.7	2163.33	790.751	2738.0	2138.7	2213.61	818.182	2818.0	2146.7	2237.89	850.919
2579.0	2122.8	2229.51	839.419	2659.0	2130.8	2173.2	799.564	2739.0	2138.8	2215.33	823.268	2819.0	2146.8	2241.4	854.263
2580.0	2122.9	2222.46	837.398	2660.0	2130.9	2179.84	802.545	2740.0	2138.9	2215.33	827.621	2820.0	2146.9	2246.69	857.633
2581.0	2123.0	2218.82	836.995	2661.0	2131.0	2188.18	805.926	2741.0	2139.0	2213.61	830.816	2821.0	2147.0	2252.0	860.604
2582.0	2123.1	2213.33	836.19	2662.0	2131.1	2194.82	809.717	2742.0	2139.1	2211.9	833.632	2822.0	2147.1	2257.34	881.99
2583.0	2123.2	2207.85	835.387	2663.0	2131.2	2203.12	812.744	2743.0	2139.2	2211.9	836.06	2823.0	2147.2	2257.34	882.885
2584.0	2123.3	2202.36	834.986	2664.0	2131.3	2206.38	816.177	2744.0	2139.3	2210.19	838.912	2824.0	2147.3	2253.78	877.982
2585.0	2123.4	2200.31	834.185	2665.0	2131.4	2202.83	816.943	2745.0	2139.4	2211.9	841.783	2825.0	2147.4	2246.69	871.821
2586.0	2123.5	2200.02	833.785	2666.0	2131.5	2204.37	816.943	2746.0	2139.5	2211.9	842.607	2826.0	2147.5	2239.64	864.884
2587.0	2123.6	2197.98	830.996	2667.0	2131.6	2207.62	815.794	2747.0	2139.6	2213.61	845.503	2827.0	2147.6	2232.64	857.21
2588.0	2123.7	2195.95	827.832	2668.0	2131.7	2207.46	814.647	2748.0	2139.7	2211.9	850.093	2828.0	2147.7	2225.68	852.588
2589.0	2123.8	2199.06	816.56	2669.0	2131.8	2203.92	825.083	2749.0	2139.8	2215.33	857.698	2829.0	2147.8	2218.77	850.503
2590.0	2123.9	2198.72	818.096	2670.0	2131.9	2197.06	814.266	2750.0	2139.9	2218.77	858.561	2830.0	2147.9	2213.61	849.672
2591.0	2124.0	2200.13	818.481	2671.0	2132.0	2188.58	803.669	2751.0	2140.0	2222.22	856.01	2831.0	2148.0	2205.07	846.335
2592.0	2124.1	2201.57	816.56	2672.0	2132.1	2186.94	799.564	2752.0	2140.1	2225.68	854.314	2832.0	2148.1	2198.29	841.372
2593.0	2124.2	2201.39	814.647	2673.0	2132.2	2187.06	801.052	2753.0	2140.2	2229.15	851.778	2833.0	2148.2	2194.91	836.873
2594.0	2124.3	2202.94	813.124	2674.0	2132.3	2188.86	807.06	2754.0	2140.3	2230.88	850.096	2834.0	2148.3	2193.22	833.632
2595.0	2124.4	2209.57	816.56	2675.0	2132.4	2194.01	808.956	2755.0	2140.4	2230.87	848.007	2835.0	2148.4	2193.22	831.217
2596.0	2124.5	2216.27	833.385	2676.0	2132.5	2200.86	810.471	2756.0	2140.5	2229.13	847.592	2836.0	2148.5	2188.18	828.417
2597.0	2124.6	2221.25	836.593	2677.0	2132.6	2209.49	813.124	2757.0	2140.6	2227.39	847.594	2837.0	2148.6	2184.84	826.429
2598.0	2124.7	2226.29	838.205	2678.0	2132.7	2213.05	816.177	2758.0	2140.7	2227.39	846.354	2838.0	2148.7	2184.84	845.845
2599.0	2124.8	2231.32	839.014	2679.0	2132.8	2218.36	820.025	2759.0	2140.8	2223.94	848.426	2839.0	2148.8	2186.51	823.662
2600.0	2124.9	2229.39	840.23	2680.0	2132.9	2227.19	827.438	2760.0	2140.9	2218.77	848.427	2840.0	2148.9	2191.54	823.268
2601.0	2125.0	2227.5	840.23	2681.0	2133.0	2232.57	833.385	2761.0	2141.0	2215.33	848.428	2841.0	2149.0	2198.29	824.45
2602.0	2125.1	2227.42	840.23	2682.0	2133.1	2239.55	839.419	2762.0	2141.1	2210.19	846.364	2842.0	2149.1	2208.48	825.231
2603.0	2125.2	2227.43	840.23	2683.0	2133.2	2246.44	842.265	2763.0	2141.2	2205.07	844.309	2843.0	2149.2	2217.05	826.403
2604.0	2125.3	2225.69	839.824	2684.0	2133.3	2249.85	868.974	2764.0	2141.3	2199.98	841.857	2844.0	2149.3	2223.97	828.368
2605.0	2125.4	2220.5	838.61	2685.0	2133.4	2253.26	870.732	2765.0	2141.4	2196.6	840.636	2845.0	2149.4	2234.51	831.137
2606.0	2125.5	2220.5	825.866	2686.0	2133.5	2253.1	871.613	2766.0	2141.5	2196.6	841.043	2846.0	2149.5	2243.37	834.726
2607.0	2125.6	2217.05	816.56	2687.0	2133.6	2252.95	865.044	2767.0	2141.6	2198.29	849.257	2847.0	2149.6	2248.72	841.596
2608.0	2125.7	2211.9	815.794	2688.0	2133.7	2249.24	888.251	2768.0	2141.7	2199.98	856.013	2848.0	2149.7	2250.51	850.238
2609.0	2125.8	2205.07	816.943	2689.0	2133.8	2249.09	889.168	2769.0	2141.8	2199.98	858.574	2849.0	2149.8	2250.51	872.986
2610.0	2125.9	2196.6	817.712	2690.0	2133.9	2245.36	887.335	2770.0	2141.9	2205.07	858.574	2850.0	2149.9	2248.72	878.304
2611.0	2126.0	2189.86	816.177	2691.0	2134.0	2243.44	882.333	2771.0	2142.0	2208.48	857.718	2851.0	2150.0	2245.15	878.289
2612.0	2126.1	2184.94	814.266	2692.0	2134.1	2236.37	876.048	2772.0	2142.1	2220.39	857.718	2852.0	2150.1	2241.59	872.055
2613.0	2126.2	2186.76	812.744	2693.0	2134.2	2231.26	871.172	2773.0	2142.2	2233.66	857.718	2853.0	2150.2	2236.28	866.786
2614.0	2126.3	2191.97	812.744	2694.0	2134.3	2226.15	863.742	2774.0	2142.3	2226.94	857.718	2854.0	2150.3	2225.72	860.72
2615.0	2126.4	2202.29	812.744	2695.0	2134.4	2221.12	858.146	2775.0	2142.4	2226.77	857.718	2855.0	2150.4	2217.05	854.738
2616.0	2126.5	2207.55	812.744	2696.0	2134.5	2217.87	858.574	2776.0	2142.5	2233.52	857.718	2856.0	2150.5	2208.48	852.199
2617.0	2126.6	2209.44	815.029	2697.0	2134.6	2214.6	859.431	2777.0	2142.6	2238.6	858.146	2857.0	2150.6	2199.98	852.199
2618.0	2126.7	2211.3	820.412	2698.											

No.	$d(\text{m})$	$v_p(\text{ms}^{-1})$	$v_s(\text{ms}^{-1})$	No.	$d(\text{m})$	$v_p(\text{ms}^{-1})$	$v_s(\text{ms}^{-1})$	No.	$d(\text{m})$	$v_p(\text{ms}^{-1})$	$v_s(\text{ms}^{-1})$	No.	$d(\text{m})$	$v_p(\text{ms}^{-1})$	$v_s(\text{ms}^{-1})$
2881.0	2153.0	2229.23	859.86	2961.0	2161.0	2252.0	867.667	3041.0	2169.0	2230.9	849.276	3121.0	2177.0	2257.34	875.603
2882.0	2153.1	2230.99	856.438	2962.0	2161.1	2251.89	861.993	3042.0	2169.1	2234.29	853.937	3122.0	2177.1	2246.69	871.172
2883.0	2153.2	2234.51	862.013	2963.0	2161.2	2249.93	857.239	3043.0	2169.2	2237.65	857.806	3123.0	2177.2	2237.89	866.35
2884.0	2153.3	2238.05	880.528	2964.0	2161.3	2246.24	852.522	3044.0	2169.3	2240.99	857.806	3124.0	2177.3	2225.68	860.72
2885.0	2153.4	2243.37	880.528	2965.0	2161.4	2239.01	852.481	3045.0	2169.4	2242.59	854.366	3125.0	2177.4	2215.4	854.314
2886.0	2153.5	2248.72	878.731	2966.0	2161.5	2230.09	856.707	3046.0	2169.5	2242.45	849.257	3126.0	2177.5	2203.56	848.42
2887.0	2153.6	2254.1	876.94	2967.0	2161.6	2228.2	860.545	3047.0	2169.6	2242.29	845.088	3127.0	2177.6	2195.17	843.433
2888.0	2153.7	2259.5	875.603	2968.0	2161.7	2228.02	860.945	3048.0	2169.7	2242.14	840.14	3128.0	2177.7	2193.51	837.687
2889.0	2153.8	2263.12	873.825	2969.0	2161.8	2227.83	860.917	3049.0	2169.8	2236.67	839.321	3129.0	2177.8	2195.17	834.44
2890.0	2153.9	2268.56	876.494	2970.0	2161.9	2232.9	860.884	3050.0	2169.9	2232.97	838.503	3130.0	2177.9	2196.85	830.816
2891.0	2154.0	2274.03	877.835	2971.0	2162.0	2237.97	860.851	3051.0	2170.0	2227.55	838.503	3131.0	2178.0	2205.24	827.621
2892.0	2154.1	2272.18	877.37	2972.0	2162.1	2239.64	860.838	3052.0	2170.1	2222.22	839.321	3132.0	2178.1	2215.4	824.845
2893.0	2154.2	2268.48	876.447	2973.0	2162.2	2243.16	866.088	3053.0	2170.2	2222.22	841.783	3133.0	2178.2	2225.68	825.241
2894.0	2154.3	2264.82	875.977	2974.0	2162.3	2246.69	872.74	3054.0	2170.3	2222.22	843.433	3134.0	2178.3	2234.39	827.621
2895.0	2154.4	2262.97	875.948	2975.0	2162.4	2250.23	875.43	3055.0	2170.4	2222.22	847.168	3135.0	2178.4	2243.16	830.015
2896.0	2154.5	2257.53	875.033	2976.0	2162.5	2253.78	876.33	3056.0	2170.5	2233.97	849.678	3136.0	2178.5	2250.23	835.249
2897.0	2154.6	2252.13	874.126	2977.0	2162.6	2255.55	876.781	3057.0	2170.6	2233.97	852.636	3137.0	2178.6	2262.7	846.751
2898.0	2154.7	2246.77	872.778	2978.0	2162.7	2257.34	868.737	3058.0	2170.7	2233.97	855.183	3138.0	2178.7	2271.69	862.013
2899.0	2154.8	2244.98	865.353	2979.0	2162.8	2257.34	865.648	3059.0	2170.8	2225.72	856.456	3139.0	2178.8	2271.69	875.603
2900.0	2154.9	2241.43	859.769	2980.0	2162.9	2255.55	861.709	3060.0	2170.9	2227.47	856.876	3140.0	2178.9	2271.69	877.387
2901.0	2155.0	2237.89	855.526	2981.0	2163.0	2252.0	857.374	3061.0	2171.0	2232.75	862.45	3141.0	2179.0	2273.5	879.629
2902.0	2155.1	2232.65	850.895	2982.0	2163.1	2248.45	853.937	3062.0	2171.1	2241.59	869.413	3142.0	2179.1	2269.89	878.282
2903.0	2155.2	2229.17	846.272	2983.0	2163.2	2239.64	850.953	3063.0	2171.2	2248.72	877.835	3143.0	2179.2	2268.09	868.535
2904.0	2155.3	2227.43	845.408	2984.0	2163.3	2227.42	849.257	3064.0	2171.3	2259.5	876.94	3144.0	2179.3	2264.49	863.742
2905.0	2155.4	2225.7	845.369	2985.0	2163.4	2218.77	848.838	3065.0	2171.4	2268.56	871.613	3145.0	2179.4	2259.12	864.176
2906.0	2155.5	2225.7	850.733	2986.0	2163.5	2210.19	845.088	3066.0	2171.5	2272.21	867.223	3146.0	2179.5	2257.34	865.479
2907.0	2155.6	2227.45	855.325	2987.0	2163.6	2203.37	839.73	3067.0	2171.6	2272.21	867.223	3147.0	2179.6	2253.78	869.413
2908.0	2155.7	2229.2	855.711	2988.0	2163.7	2198.29	834.844	3068.0	2171.7	2270.38	867.223	3148.0	2179.7	2253.78	874.269
2909.0	2155.8	2230.96	857.8	2989.0	2163.8	2193.22	834.844	3069.0	2171.8	2268.56	865.044	3149.0	2179.8	2253.78	878.282
2910.0	2155.9	2241.57	857.769	2990.0	2163.9	2188.18	834.44	3070.0	2171.9	2266.74	864.61	3150.0	2179.9	2253.78	883.239
2911.0	2156.0	2246.92	857.734	2991.0	2164.0	2188.18	833.228	3071.0	2172.0	2266.74	863.309	3151.0	2180.0	2253.78	884.6
2912.0	2156.1	2246.94	858.146	2992.0	2164.1	2189.86	832.422	3072.0	2172.1	2264.93	862.013	3152.0	2180.1	2255.53	883.239
2913.0	2156.2	2246.94	858.574	2993.0	2164.2	2194.91	829.215	3073.0	2172.2	2259.5	860.72	3153.0	2180.2	2255.5	880.528
2914.0	2156.3	2246.94	859.002	2994.0	2164.3	2196.6	826.033	3074.0	2172.3	2254.1	859.431	3154.0	2180.3	2257.25	878.282
2915.0	2156.4	2250.51	857.718	2995.0	2164.4	2201.67	823.662	3075.0	2172.4	2254.1	858.146	3155.0	2180.4	2258.99	873.382
2916.0	2156.5	2248.72	853.044	2996.0	2164.5	2210.19	823.662	3076.0	2172.5	2250.51	854.738	3156.0	2180.5	2260.73	867.66
2917.0	2156.6	2248.72	848.428	2997.0	2164.6	2217.05	823.662	3077.0	2172.6	2241.59	850.515	3157.0	2180.6	2264.25	862.013
2918.0	2156.7	2246.94	847.601	2998.0	2164.7	2225.68	835.655	3078.0	2172.7	2236.28	847.168	3158.0	2180.7	2265.99	865.013
2919.0	2156.8	2245.15	860.29	2999.0	2164.8	2234.39	853.083	3079.0	2172.8	2229.23	828.816	3159.0	2180.8	2265.95	850.936
2920.0	2156.9	2243.37	860.29	3000.0	2164.9	2241.4	853.083	3080.0	2172.9	2222.22	826.826	3160.0	2180.9	2265.91	847.585
2921.0	2157.0	2245.15	844.309	3001.0	2165.0	2246.69	850.528	3081.0	2173.0	2215.4	824.845	3161.0	2181.0	2262.31	846.335
2922.0	2157.1	2245.14	848.015	3002.0	2165.1	2246.69	848.002	3082.0	2173.1	2213.7	823.268	3162.0	2181.1	2256.98	845.503
2923.0	2157.2	2246.92	855.162	3003.0	2165.2	2246.69	845.503	3083.0	2173.2	2215.4	834.035	3163.0	2181.2	2251.7	844.674
2924.0	2157.3	2248.65	859.431	3004.0	2165.3	2246.69	845.503	3084.0	2173.3	2215.4	836.974	3164.0	2181.3	2242.95	844.226
2925.0	2157.4	2252.19	861.581	3005.0	2165.4	2243.16	868.737	3085.0	2173.4	2217.1	868.974	3165.0	2181.4	2236.0	845.503
2926.0	2157.5	2255.74	862.877	3006.0	2165.5	2243.16	864.769	3086.0	2173.5	2223.97	869.852	3166.0	2181.5	2234.27	848.838
2927.0	2157.6	2261.09	864.176	3007.0	2165.6	2237.89	856.512	3087.0	2173.6	2230.99	869.852	3167.0	2181.6	2230.81	856.013
2928.0	2157.7	2268.25	864.176	3008.0	2165.7	2229.16	848.002	3088.0	2173.7	2236.28	868.097	3168.0	2181.7	2223.93	860.72
2929.0	2157.8	2273.63	867.048	3009.0	2165.8	2225.68	847.168	3089.0	2173.8	2236.28	866.35	3169.0	2181.8	2217.05	864.176
2930.0	2157.9	2275.39	887.793	3010.0	2165.9	2239.95	848.838	3090.0	2173.9	2238.05	865.044	3170.0	2181.9	2210.19	868.974
2931.0	2158.0	2277.15	887.793	3011.0	2166.0	2222.22	850.953	3091.0	2174.0	2239.82	863.309	3171.0	2182.0	2211.9	874.269
2932.0	2158.1	2278.94	885.055	3012.0	2166.1	2218.67	852.659	3092.0	2174.1	2214.69	861.851	3172.0	2182.1	2215.33	877.396
2933.0	2158.2	2282.58	881.43	3013.0	2166.2	2218.49	853.51	3093.0	2174.2	2214.83	859.431	3173.0	2182.2	2218.77	883.254
2934.0	2158.3	2282.58	878.282	3014.0	2166.3	2220.06	853.937	3094.0	2174.3	2242.0	855.162	3174.0	2182.3	2230.81	888.263
2935.0	2158.4	2278.94	876.494	3015.0	2166.4	2219.89	852.229	3095.0	2174.4	2242.17	852.621	3175.0	2182.4	2244.69	894.248
2936.0	2158.5	2275.31	872.497	3016.0	2166.5	2219.71	848.002	3096.0	2174.5	2244.08	852.621	3176.0	2182.5	2258.75	897.044
2937.0	2158.6	2271.69	868.097	3017.0	2166.6	2226.46	843.002	3097.0	2174.6	2237.18	850.936	3177.0	2182.6	2272.98	879.98
2938.0	2158.7	2266.29	863.309	3018.0</											

No.	$d(\text{m})$	$v_p(\text{ms}^{-1})$	$v_s(\text{ms}^{-1})$												
3201.0	2185.0	2293.58	885.583	3281.0	2193.0	2225.68	877.835	3361.0	2201.0	2266.37	894.228	3441.0	2209.0	2225.65	852.199
3202.0	2185.1	2297.27	889.205	3282.0	2193.1	2222.22	877.835	3362.0	2201.1	2262.72	894.713	3442.0	2209.1	2225.65	863.309
3203.0	2185.2	2297.27	891.484	3283.0	2193.2	2220.5	878.282	3363.0	2201.2	2260.97	895.178	3443.0	2209.2	2225.66	864.176
3204.0	2185.3	2297.27	891.484	3284.0	2193.3	2217.05	878.731	3364.0	2201.3	2259.22	895.644	3444.0	2209.3	2225.66	864.61
3205.0	2185.4	2293.58	889.205	3285.0	2193.4	2217.05	877.835	3365.0	2201.4	2255.68	895.178	3445.0	2209.4	2225.66	865.044
3206.0	2185.5	2288.07	887.39	3286.0	2193.5	2215.33	865.044	3366.0	2201.5	2252.14	894.248	3446.0	2209.5	2227.39	861.15
3207.0	2185.6	2278.94	885.132	3287.0	2193.6	2217.05	857.718	3367.0	2201.6	2250.39	892.857	3447.0	2209.6	2227.4	853.467
3208.0	2185.7	2268.09	883.334	3288.0	2193.7	2220.5	847.601	3368.0	2201.7	2248.63	891.009	3448.0	2209.7	2229.13	844.627
3209.0	2185.8	2260.91	881.543	3289.0	2193.8	2225.68	839.419	3369.0	2201.8	2248.66	887.793	3449.0	2209.8	2230.88	844.627
3210.0	2185.9	2253.78	876.213	3290.0	2193.9	2232.64	839.419	3370.0	2201.9	2250.47	885.51	3450.0	2209.9	2236.11	844.627
3211.0	2186.0	2252.0	870.076	3291.0	2194.0	2237.89	839.419	3371.0	2202.0	2248.71	884.146	3451.0	2210.0	2241.39	847.568
3212.0	2186.1	2248.45	870.076	3292.0	2194.1	2246.69	841.445	3372.0	2202.1	2243.37	882.786	3452.0	2210.1	2246.69	848.386
3213.0	2186.2	2244.92	870.076	3293.0	2194.2	2252.0	843.9	3373.0	2202.2	2234.51	881.43	3453.0	2210.2	2250.23	849.193
3214.0	2186.3	2243.16	869.206	3294.0	2194.3	2257.34	846.776	3374.0	2202.3	2255.72	879.629	3454.0	2210.3	2252.0	851.253
3215.0	2186.4	2244.92	866.607	3295.0	2194.4	2262.7	849.257	3375.0	2202.4	2239.7	876.494	3455.0	2210.4	2252.0	852.904
3216.0	2186.5	2248.45	864.884	3296.0	2194.5	2266.29	851.778	3376.0	2202.5	2222.22	869.852	3456.0	2210.5	2252.0	853.718
3217.0	2186.6	2248.45	864.454	3297.0	2194.6	2271.69	854.738	3377.0	2202.6	2220.51	863.742	3457.0	2210.6	2252.0	854.53
3218.0	2186.7	2248.45	863.167	3298.0	2194.7	2273.5	856.013	3378.0	2202.7	2215.4	863.309	3458.0	2210.7	2253.78	886.839
3219.0	2186.8	2252.0	862.311	3299.0	2194.8	2273.5	860.29	3379.0	2202.8	2212.0	862.445	3459.0	2210.8	2253.78	887.293
3220.0	2186.9	2259.12	861.883	3300.0	2194.9	2273.5	866.786	3380.0	2202.9	2212.0	862.013	3460.0	2210.9	2252.0	884.07
3221.0	2187.0	2264.49	864.884	3301.0	2195.0	2273.5	872.939	3381.0	2203.0	2212.0	862.877	3461.0	2211.0	2252.0	881.776
3222.0	2187.1	2268.09	869.217	3302.0	2195.1	2273.53	877.843	3382.0	2203.1	2212.0	864.176	3462.0	2211.1	2252.0	879.95
3223.0	2187.2	2271.69	874.492	3303.0	2195.2	2273.58	883.254	3383.0	2203.2	2212.0	863.742	3463.0	2211.2	2250.23	879.042
3224.0	2187.3	2273.5	878.947	3304.0	2195.3	2270.02	888.263	3384.0	2203.3	2213.7	856.438	3464.0	2211.3	2246.69	879.496
3225.0	2187.4	2273.5	883.01	3305.0	2195.4	2264.65	891.935	3385.0	2203.4	2215.4	849.257	3465.0	2211.4	2244.92	879.95
3226.0	2187.5	2271.69	882.147	3306.0	2195.5	2257.5	890.1	3386.0	2203.5	2218.8	843.433	3466.0	2211.5	2243.16	879.95
3227.0	2187.6	2268.09	879.934	3307.0	2195.6	2250.39	887.366	3387.0	2203.6	2218.8	848.842	3467.0	2211.6	2243.16	879.042
3228.0	2187.7	2260.91	877.732	3308.0	2195.7	2248.63	883.752	3388.0	2203.7	2220.51	859.002	3468.0	2211.7	2241.4	877.684
3229.0	2187.8	2257.34	877.317	3309.0	2195.8	2250.44	879.282	3389.0	2203.8	2222.22	868.097	3469.0	2211.8	2239.64	877.684
3230.0	2187.9	2250.23	878.237	3310.0	2195.9	2250.47	875.308	3390.0	2203.9	2222.22	874.269	3470.0	2211.9	2239.64	878.136
3231.0	2188.0	2241.4	878.717	3311.0	2196.0	2250.5	872.687	3391.0	2204.0	2239.97	874.269	3471.0	2212.0	2237.89	878.589
3232.0	2188.1	2232.65	870.305	3312.0	2196.1	2261.31	870.076	3392.0	2204.1	2229.33	874.269	3472.0	2212.1	2236.14	879.042
3233.0	2188.2	2235.95	862.925	3313.0	2196.2	2281.37	866.607	3393.0	2204.2	2234.78	874.269	3473.0	2212.2	2237.91	879.042
3234.0	2188.3	2220.5	856.103	3314.0	2196.3	2328.32	862.738	3394.0	2204.3	2238.45	874.713	3474.0	2212.3	2241.45	879.496
3235.0	2188.4	2218.78	852.339	3315.0	2196.4	2336.01	739.151	3395.0	2204.4	2245.7	874.269	3475.0	2212.4	2243.24	880.859
3236.0	2188.5	2217.07	852.38	3316.0	2196.5	2343.75	739.151	3396.0	2204.5	2245.86	874.269	3476.0	2212.5	2246.8	882.227
3237.0	2188.6	2217.08	853.255	3317.0	2196.6	2351.54	663.139	3397.0	2204.6	2246.46	873.825	3477.0	2212.6	2257.54	882.684
3238.0	2188.7	2217.08	860.07	3318.0	2196.7	2351.54	686.095	3398.0	2204.7	2240.86	873.825	3478.0	2212.7	2270.21	884.058
3239.0	2188.8	2218.8	868.281	3319.0	2196.8	2351.54	730.371	3399.0	2204.8	2234.0	873.382	3479.0	2212.8	2275.73	884.976
3240.0	2188.9	2223.97	871.352	3320.0	2196.9	2351.54	891.484	3400.0	2204.9	2227.17	871.172	3480.0	2212.9	2275.78	884.058
3241.0	2189.0	2229.22	872.249	3321.0	2197.0	2343.75	892.399	3401.0	2205.0	2218.73	868.535	3481.0	2213.0	2274.01	883.599
3242.0	2189.1	2234.61	867.065	3322.0	2197.1	2337.94	894.248	3402.0	2205.1	2217.1	866.359	3482.0	2213.1	2274.28	884.495
3243.0	2189.2	2240.08	854.271	3323.0	2197.2	2330.23	896.111	3403.0	2205.2	2215.4	863.332	3483.0	2213.2	2274.75	884.914
3244.0	2189.3	2245.54	843.846	3324.0	2197.3	2320.68	895.178	3404.0	2205.3	2212.0	861.182	3484.0	2213.3	2273.33	885.338
3245.0	2189.4	2251.05	840.14	3325.0	2197.4	2309.31	895.178	3405.0	2205.4	2205.24	861.194	3485.0	2213.4	2271.98	885.297
3246.0	2189.5	2251.2	853.865	3326.0	2197.5	2298.05	895.644	3406.0	2205.5	2200.2	859.91	3486.0	2213.5	2270.57	882.98
3247.0	2189.6	2253.12	864.544	3327.0	2197.6	2286.9	895.644	3407.0	2205.6	2196.85	859.059	3487.0	2213.6	2269.24	881.58
3248.0	2189.7	2255.06	865.423	3328.0	2197.7	2275.86	895.178	3408.0	2205.7	2195.17	859.5	3488.0	2213.7	2266.12	879.736
3249.0	2189.8	2253.43	858.551	3329.0	2197.8	2268.56	894.248	3409.0	2205.8	2195.17	860.81	3489.0	2213.8	2262.96	877.909
3250.0	2189.9	2253.56	851.774	3330.0	2197.9	2264.93	891.484	3410.0	2205.9	2196.85	861.69	3490.0	2213.9	2261.66	875.642
3251.0	2190.0	2251.93	843.846	3331.0	2198.0	2263.12	888.297	3411.0	2206.0	2200.2	863.012	3491.0	2214.0	2262.07	874.278
3252.0	2190.1	2248.45	842.611	3332.0	2198.1	2257.7	885.583	3412.0	2206.1	2203.56	863.911	3492.0	2214.1	2258.75	874.269
3253.0	2190.2	2241.4	844.267	3333.0	2198.2	2254.1	882.885	3413.0	2206.2	2206.93	864.812	3493.0	2214.2	2256.98	874.269
3254.0	2190.3	2234.39	845.928	3334.0	2198.3	2250.51	881.99	3414.0	2206.3	2210.31	864.841	3494.0	2214.3	2251.7	874.269
3255.0	2190.4	2230.9	848.423	3335.0	2198.4	2246.94	881.543	3415.0	2206.4	2212.0	864.433	3495.0	2214.4	2246.44	874.269
3256.0	2190.5	2227.42	850.936	3336.0	2198.5	2241.59	879.759	3416.0	2206.5	2215.4	860.547	3496.0	2214.5	2241.21	874.713
3257.0	2190.6	2225.68	853.467	3337.0	2198.6	2238.05	877.539	3417.0	2206.6	2217.1	857.995	3497.0	2214.6	2236.0	874.713
3258.0	2190.7	2227.42	855.587	3338.0	2198.7	2236.28</td									

No.	$d(\text{m})$	$v_p(\text{ms}^{-1})$	$v_s(\text{ms}^{-1})$												
3521.0	2217.0	2249.94	849.257	3601.0	2225.0	2206.54	865.044	3681.0	2233.0	2289.9	904.568	3761.0	2241.0	2290.63	944.212
3522.0	2217.1	2253.46	856.013	3602.0	2225.1	2209.96	864.176	3682.0	2233.1	2295.38	906.021	3762.0	2241.1	2296.18	947.778
3523.0	2217.2	2256.98	857.291	3603.0	2225.2	2213.26	862.877	3683.0	2233.2	2300.84	906.033	3763.0	2241.2	2305.54	948.802
3524.0	2217.3	2256.98	858.574	3604.0	2225.3	2213.08	862.013	3684.0	2233.3	2304.46	906.526	3764.0	2241.3	2313.08	948.802
3525.0	2217.4	2256.98	866.786	3605.0	2225.4	2212.9	861.15	3685.0	2233.4	2309.94	907.98	3765.0	2241.4	2316.87	949.315
3526.0	2217.5	2258.75	890.548	3606.0	2225.5	2212.74	860.29	3686.0	2233.5	2315.44	908.958	3766.0	2241.5	2314.98	949.828
3527.0	2217.6	2258.75	893.32	3607.0	2225.6	2212.56	859.431	3687.0	2233.6	2320.96	910.91	3767.0	2241.6	2313.08	950.342
3528.0	2217.7	2256.98	894.248	3608.0	2225.7	2212.4	858.574	3688.0	2233.7	2328.37	913.359	3768.0	2241.7	2318.77	951.372
3529.0	2217.8	2256.98	894.248	3609.0	2225.8	2212.22	857.291	3689.0	2233.8	2332.03	916.812	3769.0	2241.8	2320.68	951.372
3530.0	2217.9	2256.98	894.248	3610.0	2225.9	2210.31	856.438	3690.0	2233.9	2331.92	921.293	3770.0	2241.9	2324.49	953.437
3531.0	2218.0	2256.98	892.857	3611.0	2226.0	2210.15	855.162	3691.0	2234.0	2331.8	928.343	3771.0	2242.0	2330.23	956.032
3532.0	2218.1	2257.0	891.47	3612.0	2226.1	2211.5	854.314	3692.0	2234.1	2333.7	940.138	3772.0	2242.1	2334.12	958.641
3533.0	2218.2	2257.04	888.251	3613.0	2226.2	2210.97	853.89	3693.0	2234.2	2333.82	941.176	3773.0	2242.2	2338.05	960.738
3534.0	2218.3	2258.84	882.786	3614.0	2226.3	2210.52	851.778	3694.0	2234.3	2335.84	941.176	3774.0	2242.3	2340.05	962.317
3535.0	2218.4	2257.11	876.94	3615.0	2226.4	2209.99	848.411	3695.0	2234.4	2330.27	938.068	3775.0	2242.4	2343.98	965.491
3536.0	2218.5	2253.6	871.613	3616.0	2226.5	2209.46	841.292	3696.0	2234.5	2328.5	936.008	3776.0	2242.5	2349.86	967.086
3537.0	2218.6	2251.86	872.497	3617.0	2226.6	2212.45	822.217	3697.0	2234.6	2326.73	934.981	3777.0	2242.6	2353.8	968.152
3538.0	2218.7	2251.9	890.548	3618.0	2226.7	2213.64	822.217	3698.0	2234.7	2326.83	934.981	3778.0	2242.7	2355.81	969.22
3539.0	2218.8	2251.93	891.47	3619.0	2226.8	2216.55	824.205	3699.0	2234.8	2325.05	934.981	3779.0	2242.8	2357.81	970.291
3540.0	2218.9	2251.95	892.394	3620.0	2226.9	2219.54	825.802	3700.0	2234.9	2321.39	936.522	3780.0	2242.9	2357.86	970.827
3541.0	2219.0	2251.98	892.394	3621.0	2227.0	2225.88	827.808	3701.0	2235.0	2321.49	937.552	3781.0	2243.0	2359.86	973.517
3542.0	2219.1	2250.21	892.857	3622.0	2227.1	2229.09	829.419	3702.0	2235.1	2323.42	938.585	3782.0	2243.1	2361.83	976.766
3543.0	2219.2	2250.18	892.857	3623.0	2227.2	2230.81	832.254	3703.0	2235.2	2325.31	939.62	3783.0	2243.2	2365.74	980.035
3544.0	2219.3	2250.15	891.932	3624.0	2227.3	2236.0	835.928	3704.0	2235.3	2329.1	940.138	3784.0	2243.3	2369.67	982.777
3545.0	2219.4	2250.12	890.088	3625.0	2227.4	2239.47	839.221	3705.0	2235.4	2341.0	930.387	3785.0	2243.4	2371.64	984.981
3546.0	2219.5	2250.09	887.793	3626.0	2227.5	2239.47	845.885	3706.0	2235.5	2334.81	920.339	3786.0	2243.5	2369.67	986.087
3547.0	2219.6	2248.31	884.6	3627.0	2227.6	2242.95	858.574	3707.0	2235.6	2336.72	909.049	3787.0	2243.6	2367.7	987.196
3548.0	2219.7	2248.28	880.528	3628.0	2227.7	2249.94	869.413	3708.0	2235.7	2338.63	899.454	3788.0	2243.7	2365.74	986.641
3549.0	2219.8	2241.25	868.974	3629.0	2227.8	2249.94	876.048	3709.0	2235.8	2340.55	898.506	3789.0	2243.8	2363.79	984.981
3550.0	2219.9	2234.28	875.291	3630.0	2227.9	2251.7	879.179	3710.0	2235.9	2342.47	921.334	3790.0	2243.9	2359.88	981.679
3551.0	2220.0	2229.09	861.15	3631.0	2228.0	2251.7	880.528	3711.0	2236.0	2342.47	949.828	3791.0	2244.0	2357.93	978.398
3552.0	2220.1	2225.75	861.581	3632.0	2228.1	2253.36	881.881	3712.0	2236.1	2342.47	985.534	3792.0	2244.1	2355.99	975.702
3553.0	2220.2	2224.48	862.013	3633.0	2228.2	2253.17	881.881	3713.0	2236.2	2338.63	984.981	3793.0	2244.2	2355.99	973.572
3554.0	2220.3	2222.67	862.013	3634.0	2228.3	2253.02	881.881	3714.0	2236.3	2334.81	976.223	3794.0	2244.3	2354.05	972.521
3555.0	2220.4	2221.12	861.15	3635.0	2228.4	2252.83	882.333	3715.0	2236.4	2329.1	964.96	3795.0	2244.4	2355.99	972.555
3556.0	2220.5	2219.55	860.72	3636.0	2228.5	2250.89	882.786	3716.0	2236.5	2323.42	956.032	3796.0	2244.5	2354.05	972.588
3557.0	2220.6	2219.74	859.431	3637.0	2228.6	2248.95	883.239	3717.0	2236.6	2319.65	945.737	3797.0	2244.6	2352.11	972.617
3558.0	2220.7	2219.89	838.844	3638.0	2228.7	2248.8	883.239	3718.0	2236.7	2319.65	937.552	3798.0	2244.7	2355.99	972.651
3559.0	2220.8	2220.08	833.932	3639.0	2228.8	2243.37	883.692	3719.0	2236.8	2315.89	936.008	3799.0	2244.8	2355.99	972.142
3560.0	2220.9	2220.26	831.062	3640.0	2228.9	2237.97	883.239	3720.0	2236.9	2312.14	937.552	3800.0	2244.9	2354.05	972.171
3561.0	2221.0	2220.42	831.043	3641.0	2229.0	2237.81	881.843	3721.0	2237.0	2310.27	940.138	3801.0	2245.0	2355.99	971.119
3562.0	2221.1	2222.33	831.037	3642.0	2229.1	2237.64	879.629	3722.0	2237.1	2306.54	940.138	3802.0	2245.1	2356.08	968.952
3563.0	2221.2	2222.51	832.661	3643.0	2229.2	2235.74	878.282	3723.0	2237.2	2304.68	935.965	3803.0	2245.2	2356.22	967.311
3564.0	2221.3	2226.09	837.16	3644.0	2229.3	2232.13	876.048	3724.0	2237.3	2304.68	926.845	3804.0	2245.3	2356.35	966.211
3565.0	2221.4	2229.71	840.048	3645.0	2229.4	2230.22	872.055	3725.0	2237.4	2304.68	923.831	3805.0	2245.4	2356.5	966.184
3566.0	2221.5	2233.34	842.54	3646.0	2229.5	2230.05	868.535	3726.0	2237.5	2304.68	923.831	3806.0	2245.5	2356.65	967.231
3567.0	2221.6	2236.96	859.86	3647.0	2229.6	2229.9	866.335	3727.0	2237.6	2304.68	928.866	3807.0	2245.6	2356.78	968.274
3568.0	2221.7	2240.61	877.387	3648.0	2229.7	2226.27	865.479	3728.0	2237.7	2304.68	930.387	3808.0	2245.7	2356.93	967.71
3569.0	2221.8	2244.28	880.528	3649.0	2229.8	2226.64	863.742	3729.0	2237.8	2304.68	931.404	3809.0	2245.8	2355.13	966.085
3570.0	2221.9	2244.44	881.881	3650.0	2229.9	2224.48	861.581	3730.0	2237.9	2304.68	932.933	3810.0	2245.9	2357.21	964.465
3571.0	2222.0	2244.62	882.333	3651.0	2230.0	2222.3	857.718	3731.0	2238.0	2304.68	933.444	3811.0	2246.0	2357.36	962.326
3572.0	2222.1	2244.69	883.239	3652.0	2230.1	2222.22	853.044	3732.0	2238.1	2304.68	933.956	3812.0	2246.1	2357.42	960.213
3573.0	2222.2	2241.21	881.881	3653.0	2230.2	2222.22	848.834	3733.0	2238.2	2304.68	933.956	3813.0	2246.2	2355.46	958.118
3574.0	2222.3	2237.73	882.333	3654.0	2230.3	2222.22	847.146	3734.0	2238.3	2302.82	934.981	3814.0	2246.3	2355.46	956.553
3575.0	2222.4	2232.54	880.979	3655.0	2230.4	2220.5	844.627	3735.0	2238.4	2304.68	935.494	3815.0	2246.4	2355.46	956.032
3576.0	2222.5	2232.54	879.629	3656.0	2230.5	2220.5	841.707	3736.0	2238.5	2304.68	934.468	3816.0	2246.5	2355.46	957.074
3577.0	2222.6	2232.54	877.835	3657.0	2230.6	2223.95	836.338	3737.0	2238.6	2302.82	934.981	3817.0	2246.6	2357.42	958.641
3578.0	2222.7	2232.54	874.2												

No.	$d(\text{m})$	$v_p(\text{ms}^{-1})$	$v_s(\text{ms}^{-1})$												
3841.0	2249.0	2354.05	958.118	3921.0	2257.0	2334.81	940.159	4001.0	2265.0	2302.82	901.652	4081.0	2273.0	2319.69	919.562
3842.0	2249.1	2350.18	954.482	3922.0	2257.1	2329.1	937.119	4002.0	2265.1	2299.0	899.297	4082.0	2273.1	2319.65	917.112
3843.0	2249.2	2348.24	951.904	3923.0	2257.2	2323.42	934.601	4003.0	2265.2	2295.12	896.938	4083.0	2273.2	2317.77	915.649
3844.0	2249.3	2348.24	950.366	3924.0	2257.3	2323.42	932.097	4004.0	2265.3	2293.11	894.119	4084.0	2273.3	2310.27	913.221
3845.0	2249.4	2348.24	950.376	3925.0	2257.4	2321.53	929.606	4005.0	2265.4	2287.41	891.308	4085.0	2273.4	2308.4	911.288
3846.0	2249.5	2348.24	951.418	3926.0	2257.5	2323.42	927.622	4006.0	2265.5	2283.56	890.351	4086.0	2273.5	2306.54	908.403
3847.0	2249.6	2348.24	951.429	3927.0	2257.6	2327.21	927.128	4007.0	2265.6	2283.4	888.934	4087.0	2273.6	2300.97	905.536
3848.0	2249.7	2350.18	950.92	3928.0	2257.7	2322.91	927.622	4008.0	2265.7	2283.21	887.979	4088.0	2273.7	2297.27	902.215
3849.0	2249.8	2350.18	949.894	3929.0	2257.8	2338.63	928.613	4009.0	2265.8	2281.2	887.034	4089.0	2273.8	2295.42	898.917
3850.0	2249.9	2350.18	950.941	3930.0	2257.9	2338.63	929.606	4010.0	2265.9	2275.58	888.353	4090.0	2273.9	2293.58	896.11
3851.0	2250.0	2348.24	951.147	3931.0	2258.0	2346.32	933.097	4011.0	2266.0	2279.02	891.962	4091.0	2274.0	2289.9	893.784
3852.0	2250.1	2348.24	951.475	3932.0	2258.1	2355.99	937.625	4012.0	2266.1	2286.24	895.644	4092.0	2274.1	2284.41	892.857
3853.0	2250.2	2348.24	950.955	3933.0	2258.2	2357.93	942.722	4013.0	2266.2	2293.58	886.034	4093.0	2274.2	2278.94	892.857
3854.0	2250.3	2350.18	950.955	3934.0	2258.3	2359.88	948.435	4014.0	2266.3	2295.42	870.947	4094.0	2274.3	2275.31	891.484
3855.0	2250.4	2348.24	950.435	3935.0	2258.4	2367.7	954.217	4015.0	2266.4	2299.11	862.311	4095.0	2274.4	2269.89	889.205
3856.0	2250.5	2348.24	949.397	3936.0	2258.5	2373.61	957.401	4016.0	2266.5	2302.82	862.311	4096.0	2274.5	2266.29	888.297
3857.0	2250.6	2344.39	947.329	3937.0	2258.6	2375.58	961.142	4017.0	2266.6	2308.4	865.314	4097.0	2274.6	2271.69	890.115
3858.0	2250.7	2338.63	944.242	3938.0	2258.7	2379.54	963.293	4018.0	2266.7	2312.14	873.572	4098.0	2274.7	2275.31	892.399
3859.0	2250.8	2323.42	940.662	3939.0	2258.8	2377.56	963.293	4019.0	2266.8	2317.77	885.132	4099.0	2274.8	2271.69	893.784
3860.0	2250.9	2314.01	939.123	3940.0	2258.9	2373.61	963.293	4020.0	2266.9	2319.65	893.32	4100.0	2274.9	2271.69	891.941
3861.0	2251.0	2306.54	938.611	3941.0	2259.0	2367.7	963.293	4021.0	2267.0	2321.53	925.493	4101.0	2275.0	2273.5	889.205
3862.0	2251.1	2302.87	936.569	3942.0	2259.1	2361.83	963.293	4022.0	2267.1	2325.31	938.1	4102.0	2275.1	2280.8	886.938
3863.0	2251.2	2299.24	932.006	3943.0	2259.2	2357.93	960.605	4023.0	2267.2	2329.1	932.511	4103.0	2275.2	2290.02	881.096
3864.0	2251.3	2297.46	739.795	3944.0	2259.3	2354.05	956.868	4024.0	2267.3	2323.91	927.987	4104.0	2275.3	2295.61	906.967
3865.0	2251.4	2303.12	731.088	3945.0	2259.4	2354.05	953.16	4025.0	2267.4	2340.55	922.518	4105.0	2275.4	2304.99	908.403
3866.0	2251.5	2308.81	675.365	3946.0	2259.5	2350.18	950.005	4026.0	2267.5	2342.47	917.112	4106.0	2275.5	2310.69	909.362
3867.0	2251.6	2318.32	660.848	3947.0	2259.6	2346.32	947.913	4027.0	2267.6	2342.47	917.112	4107.0	2275.6	2314.54	910.805
3868.0	2251.7	2327.94	662.628	3948.0	2259.7	2346.32	947.913	4028.0	2267.7	2338.63	921.037	4108.0	2275.7	2314.64	912.737
3869.0	2251.8	2335.71	674.043	3949.0	2259.8	2342.47	946.35	4029.0	2267.8	2332.91	934.028	4109.0	2275.8	2318.53	914.191
3870.0	2251.9	2345.51	682.862	3950.0	2259.9	2338.63	944.274	4030.0	2267.9	2327.21	947.329	4110.0	2275.9	2322.42	915.649
3871.0	2252.0	2351.48	658.321	3951.0	2260.0	2338.63	942.722	4031.0	2268.0	2327.21	948.362	4111.0	2276.0	2322.53	917.601
3872.0	2252.1	2359.42	658.336	3952.0	2260.1	2338.71	941.691	4032.0	2268.1	2327.21	948.358	4112.0	2276.1	2324.49	919.562
3873.0	2252.2	2365.38	741.372	3953.0	2260.2	2338.82	940.159	4033.0	2268.2	2325.31	946.804	4113.0	2276.2	2326.4	921.037
3874.0	2252.3	2377.32	949.01	3954.0	2260.3	2338.95	938.637	4034.0	2268.3	2321.53	945.259	4114.0	2276.3	2330.23	922.518
3875.0	2252.4	2385.34	942.89	3955.0	2260.4	2337.16	939.144	4035.0	2268.4	2319.65	945.254	4115.0	2276.4	2330.23	924.499
3876.0	2252.5	2385.37	967.599	3956.0	2260.5	2337.27	940.159	4036.0	2268.5	2321.53	945.25	4116.0	2276.5	2332.16	927.487
3877.0	2252.6	2387.39	968.194	3957.0	2260.6	2337.4	940.159	4037.0	2268.6	2327.21	946.782	4117.0	2276.6	2336.01	928.989
3878.0	2252.7	2389.42	970.404	3958.0	2260.7	2337.51	939.651	4038.0	2268.7	2325.31	947.288	4118.0	2276.7	2343.75	930.998
3879.0	2252.8	2387.44	974.266	3959.0	2260.8	2339.57	938.637	4039.0	2268.8	2321.53	946.77	4119.0	2276.8	2347.64	933.522
3880.0	2252.9	2385.46	978.16	3960.0	2260.9	2341.64	937.625	4040.0	2268.9	2321.53	944.217	4120.0	2276.9	2347.64	935.551
3881.0	2253.0	2381.51	981.522	3961.0	2261.0	2339.82	935.607	4041.0	2269.0	2317.77	942.187	4121.0	2277.0	2349.59	937.078
3882.0	2253.1	2375.58	980.993	3962.0	2261.1	2332.16	932.097	4042.0	2269.1	2310.22	939.605	4122.0	2277.1	2351.58	939.123
3883.0	2253.2	2369.67	980.44	3963.0	2261.2	2324.49	928.613	4043.0	2269.2	2300.8	936.485	4123.0	2277.2	2355.55	940.149
3884.0	2253.3	2363.79	978.785	3964.0	2261.3	2320.68	925.647	4044.0	2269.3	2296.98	931.878	4124.0	2277.3	2357.55	940.662
3885.0	2253.4	2357.93	967.352	3965.0	2261.4	2322.58	922.211	4045.0	2269.4	2295.03	925.813	4125.0	2277.4	2359.57	941.686
3886.0	2253.5	2350.18	960.938	3966.0	2261.5	2322.58	918.801	4046.0	2269.5	2294.92	919.826	4126.0	2277.5	2361.58	941.686
3887.0	2253.6	2340.55	955.133	3967.0	2261.6	2318.77	915.416	4047.0	2269.6	2292.95	917.82	4127.0	2277.6	2357.71	940.662
3888.0	2253.7	2336.72	952.517	3968.0	2261.7	2314.98	912.534	4048.0	2269.7	2289.15	915.33	4128.0	2277.7	2355.81	939.636
3889.0	2253.8	2332.91	948.362	3969.0	2261.8	2309.31	911.099	4049.0	2269.8	2285.34	911.885	4129.0	2277.8	2353.92	938.611
3890.0	2253.9	2329.1	945.269	3970.0	2261.9	2305.54	909.67	4050.0	2269.9	2279.7	909.915	4130.0	2277.9	2353.97	938.611
3891.0	2254.0	2325.31	943.73	3971.0	2262.0	2301.79	908.719	4051.0	2270.0	2275.92	907.945	4131.0	2278.0	2352.09	937.078
3892.0	2254.1	2321.53	941.686	3972.0	2262.1	2299.98	907.297	4052.0	2270.1	2270.38	906.49	4132.0	2278.1	2348.24	935.043
3893.0	2254.2	2319.65	940.159	3973.0	2262.2	2298.22	906.824	4053.0	2270.2	2268.56	905.536	4133.0	2278.2	2342.47	932.511
3894.0	2254.3	2315.89	939.144	3974.0	2262.3	2300.18	906.351	4054.0	2270.3	2266.74	904.585	4134.0	2278.3	2336.72	930.998
3895.0	2254.4	2314.01	936.615	3975.0	2262.4	2300.3	906.351	4055.0	2270.4	2259.5	903.161	4135.0	2278.4	2327.21	928.989
3896.0	2254.5	2315.89	936.615	3976.0	2262.5	2298.55	905.879	4056.0	2270.5	2257.7	900.327	4136.0	2278.5	2323.42	925.991
3897.0	2254.6	2315.89	936.615	3977.0	2262.6	2302.36	905.408	4057.0	2270.6	2264.93	896.11	4137.0	2278.6	2321.53	923.012
3898.0	2254.7	2319.65													

No.	$d(\text{m})$	$v_p(\text{ms}^{-1})$	$v_s(\text{ms}^{-1})$												
4161.0	2281.0	2321.53	932.511	4241.0	2289.0	2403.41	938.13	4321.0	2297.0	2343.75	942.164	4401.0	2305.0	2323.42	908.698
4162.0	2281.1	2319.65	930.998	4242.0	2289.1	2401.46	934.628	4322.0	2297.1	2339.91	938.613	4402.0	2305.1	2323.42	904.466
4163.0	2281.2	2319.65	929.992	4243.0	2289.2	2399.44	931.659	4323.0	2297.2	2338.04	935.053	4403.0	2305.2	2325.31	899.786
4164.0	2281.3	2315.89	928.488	4244.0	2289.3	2399.44	928.212	4324.0	2297.3	2336.19	931.526	4404.0	2305.3	2331.0	896.077
4165.0	2281.4	2312.14	926.489	4245.0	2289.4	2397.43	926.762	4325.0	2297.4	2332.43	927.038	4405.0	2305.4	2338.63	895.155
4166.0	2281.5	2308.4	922.024	4246.0	2289.5	2393.4	926.794	4326.0	2297.5	2328.68	922.603	4406.0	2305.5	2342.47	934.601
4167.0	2281.6	2306.54	920.545	4247.0	2289.6	2381.39	924.849	4327.0	2297.6	2324.95	920.168	4407.0	2305.6	2340.55	936.615
4168.0	2281.7	2302.82	920.545	4248.0	2289.7	2369.53	922.41	4328.0	2297.7	2323.13	918.239	4408.0	2305.7	2338.63	937.625
4169.0	2281.8	2302.82	923.012	4249.0	2289.8	2361.72	919.494	4329.0	2297.8	2323.22	916.807	4409.0	2305.8	2338.63	936.11
4170.0	2281.9	2302.82	922.518	4250.0	2289.9	2352.03	916.104	4330.0	2297.9	2321.42	916.344	4410.0	2305.9	2338.63	933.097
4171.0	2282.0	2304.68	919.562	4251.0	2290.0	2342.44	914.666	4331.0	2298.0	2323.38	914.923	4411.0	2306.0	2336.72	934.601
4172.0	2282.1	2302.82	916.136	4252.0	2290.1	2334.81	913.706	4332.0	2298.1	2323.48	911.577	4412.0	2306.1	2340.55	934.103
4173.0	2282.2	2300.97	915.163	4253.0	2290.2	2327.21	912.737	4333.0	2298.2	2323.58	906.351	4413.0	2306.2	2340.55	933.61
4174.0	2282.3	2300.97	915.163	4254.0	2290.3	2323.42	912.253	4334.0	2298.3	2331.3	899.786	4414.0	2306.3	2340.55	933.117
4175.0	2282.4	2299.11	913.706	4255.0	2290.4	2321.53	912.737	4335.0	2298.4	2333.33	897.465	4415.0	2306.4	2342.47	932.627
4176.0	2282.5	2297.27	910.805	4256.0	2290.5	2321.53	912.737	4336.0	2298.5	2337.27	898.392	4416.0	2306.5	2342.47	931.64
4177.0	2282.6	2295.42	908.403	4257.0	2290.6	2321.53	914.676	4337.0	2298.6	2343.18	901.185	4417.0	2306.6	2342.47	930.658
4178.0	2282.7	2295.42	906.49	4258.0	2290.7	2323.42	918.091	4338.0	2298.7	2345.24	903.526	4418.0	2306.7	2344.39	929.681
4179.0	2282.8	2293.58	905.536	4259.0	2290.8	2327.21	902.012	4339.0	2298.8	2345.38	910.146	4419.0	2306.8	2352.11	928.214
4180.0	2282.9	2297.27	906.013	4260.0	2290.9	2332.91	927.987	4340.0	2298.9	2345.51	934.099	4420.0	2306.9	2355.99	926.266
4181.0	2283.0	2297.27	906.967	4261.0	2291.0	2340.55	932.511	4341.0	2299.0	2349.53	940.159	4421.0	2307.0	2359.88	922.389
4182.0	2283.1	2299.17	907.445	4262.0	2291.1	2344.46	937.591	4342.0	2299.1	2355.46	947.24	4422.0	2307.1	2359.88	915.676
4183.0	2283.2	2301.13	908.403	4263.0	2291.2	2346.52	940.15	4343.0	2299.2	2361.36	953.377	4423.0	2307.2	2357.93	907.174
4184.0	2283.3	2303.08	908.882	4264.0	2291.3	2352.48	941.686	4344.0	2299.3	2365.31	957.504	4424.0	2307.3	2359.88	924.911
4185.0	2283.4	2306.89	908.882	4265.0	2291.4	2354.55	942.196	4345.0	2299.4	2371.26	959.565	4425.0	2307.4	2359.88	940.852
4186.0	2283.5	2316.3	907.445	4266.0	2291.5	2356.65	942.707	4346.0	2299.5	2375.24	961.116	4426.0	2307.5	2361.83	941.926
4187.0	2283.6	2323.88	902.215	4267.0	2291.6	2354.83	942.707	4347.0	2299.6	2377.24	959.498	4427.0	2307.6	2357.93	941.971
4188.0	2283.7	2329.61	896.577	4268.0	2291.7	2349.13	940.666	4348.0	2299.7	2377.24	958.413	4428.0	2307.7	2357.93	942.024
4189.0	2283.8	2331.58	896.577	4269.0	2291.8	2345.37	936.098	4349.0	2299.8	2379.24	956.798	4429.0	2307.8	2357.93	943.613
4190.0	2283.9	2333.53	905.006	4270.0	2291.9	2341.63	931.585	4350.0	2299.9	2381.24	952.572	4430.0	2307.9	2355.99	944.691
4191.0	2284.0	2337.39	916.136	4271.0	2292.0	2337.88	926.627	4351.0	2300.0	2377.24	948.899	4431.0	2308.0	2348.24	944.22
4192.0	2284.1	2339.28	927.487	4272.0	2292.1	2334.12	921.264	4352.0	2300.1	2359.39	943.761	4432.0	2308.1	2342.47	943.218
4193.0	2284.2	2339.21	932.511	4273.0	2292.2	2330.35	915.949	4353.0	2300.2	2359.49	939.223	4433.0	2308.2	2334.81	941.686
4194.0	2284.3	2341.05	935.551	4274.0	2292.3	2320.9	910.747	4354.0	2300.3	2343.75	934.712	4434.0	2308.3	2327.21	936.615
4195.0	2284.4	2337.17	936.569	4275.0	2292.4	2311.53	907.464	4355.0	2300.4	2332.16	928.248	4435.0	2308.4	2321.53	933.097
4196.0	2284.5	2337.1	937.589	4276.0	2292.5	2306.0	905.625	4356.0	2300.5	2326.4	922.351	4436.0	2308.5	2317.77	928.613
4197.0	2284.6	2335.13	939.636	4277.0	2292.6	2398.64	899.114	4357.0	2300.6	2322.58	918.463	4437.0	2308.6	2314.01	919.287
4198.0	2284.7	2335.06	940.662	4278.0	2292.7	2387.67	889.932	4358.0	2300.7	2318.77	916.056	4438.0	2308.7	2314.01	915.898
4199.0	2284.8	2336.89	941.176	4279.0	2292.8	2282.3	889.974	4359.0	2300.8	2314.98	914.621	4439.0	2308.8	2314.01	914.934
4200.0	2284.9	2336.82	941.176	4280.0	2292.9	2308.59	890.024	4360.0	2300.9	2311.19	913.675	4440.0	2308.9	2314.01	913.013
4201.0	2285.0	2334.85	941.176	4281.0	2293.0	2280.72	890.066	4361.0	2301.0	2313.08	908.876	4441.0	2309.0	2314.01	912.055
4202.0	2285.1	2331.0	941.176	4282.0	2293.1	2280.76	890.089	4362.0	2301.1	2315.03	896.603	4442.0	2309.1	2315.89	911.577
4203.0	2285.2	2329.1	941.176	4283.0	2293.2	2282.58	892.395	4363.0	2301.2	2317.02	886.097	4443.0	2309.2	2315.89	911.577
4204.0	2285.3	2329.1	941.176	4284.0	2293.3	2286.24	897.002	4364.0	2301.3	2320.89	894.826	4444.0	2309.3	2314.01	911.577
4205.0	2285.4	2331.0	942.707	4285.0	2293.4	2289.9	901.185	4365.0	2301.4	2328.6	916.712	4445.0	2309.4	2319.65	912.534
4206.0	2285.5	2331.0	944.242	4286.0	2293.5	2297.27	905.408	4366.0	2301.5	2334.42	913.045	4446.0	2309.5	2319.65	912.534
4207.0	2285.6	2334.81	944.242	4287.0	2293.6	2306.54	910.146	4367.0	2301.6	2336.4	926.571	4447.0	2309.6	2321.53	913.013
4208.0	2285.7	2336.72	943.73	4288.0	2293.7	2312.14	917.831	4368.0	2301.7	2344.17	919.212	4448.0	2309.7	2323.42	913.972
4209.0	2285.8	2336.63	943.218	4289.0	2293.8	2319.65	926.124	4369.0	2301.8	2348.1	926.104	4449.0	2309.8	2325.31	916.863
4210.0	2285.9	2338.63	943.218	4290.0	2293.9	2331.0	933.097	4370.0	2301.9	2348.16	937.114	4450.0	2309.9	2329.1	919.287
4211.0	2286.0	2334.81	942.196	4291.0	2294.0	2338.63	938.637	4371.0	2302.0	2348.22	938.129	4451.0	2310.0	2332.91	922.211
4212.0	2286.1	2331.0	940.663	4292.0	2294.1	2350.18	945.269	4372.0	2302.1	2348.24	938.13	4452.0	2310.1	2336.72	925.647
4213.0	2286.2	2325.31	938.615	4293.0	2294.2	2359.88	950.435	4373.0	2302.2	2350.18	938.13	4453.0	2310.2	2338.63	928.613
4214.0	2286.3	2323.42	935.058	4294.0	2294.3	2367.7	955.133	4374.0	2302.3	2348.24	937.625	4454.0	2310.3	2342.47	932.097
4215.0	2286.4	2321.53	931.034	4295.0	2294.4	2373.61	957.236	4375.0	2302.4	2344.39	936.615	4455.0	2310.4	2342.47	935.607
4216.0	2286.5	2319.65	927.053	4296.0	2294.5	2375.58	957.763	4376.0	2302.5	2338.63	934.099	4456.0	2310.5	2344.39	937.625
4217.0	2286.6	2314.01	924.097	4297.0	2294.6	2373.61	957.763	4377.0	2302.6	2336.72	931.597	4457.0	2310.6	2346.32	939.144
4218.0	2286.7	2310.27													

No.	$d(\text{m})$	$v_p(\text{ms}^{-1})$	$v_s(\text{ms}^{-1})$												
4481.0	2313.0	2323.42	918.294	4561.0	2321.0	2340.55	934.535	4641.0	2329.0	2322.58	930.998	4721.0	2337.0	2314.98	932.511
4482.0	2313.1	2321.53	918.316	4562.0	2321.1	2340.55	936.572	4642.0	2329.1	2328.36	931.502	4722.0	2337.1	2309.31	928.989
4483.0	2313.2	2321.53	919.287	4563.0	2321.2	2340.55	938.104	4643.0	2329.2	2332.28	932.511	4723.0	2337.2	2309.31	925.493
4484.0	2313.3	2323.42	918.316	4564.0	2321.3	2344.39	939.64	4644.0	2329.3	2334.27	933.016	4724.0	2337.3	2309.31	924.499
4485.0	2313.4	2319.65	916.38	4565.0	2321.4	2344.39	939.641	4645.0	2329.4	2334.34	933.522	4725.0	2337.4	2314.98	924.499
4486.0	2313.5	2315.89	914.934	4566.0	2321.5	2342.47	940.153	4646.0	2329.5	2334.42	934.028	4726.0	2337.5	2322.58	924.499
4487.0	2313.6	2314.01	913.013	4567.0	2321.6	2340.55	940.665	4647.0	2329.6	2336.41	936.06	4727.0	2337.6	2328.32	924.996
4488.0	2313.7	2312.14	911.099	4568.0	2321.7	2340.55	941.176	4648.0	2329.7	2338.39	938.611	4728.0	2337.7	2336.01	927.487
4489.0	2313.8	2310.27	909.194	4569.0	2321.8	2340.55	942.186	4649.0	2329.8	2338.47	936.569	4729.0	2337.8	2341.81	934.028
4490.0	2313.9	2310.27	907.771	4570.0	2321.9	2344.39	944.72	4650.0	2329.9	2338.54	937.078	4730.0	2337.9	2345.69	938.611
4491.0	2314.0	2304.68	904.936	4571.0	2322.0	2344.39	948.29	4651.0	2330.0	2338.6	938.611	4731.0	2338.0	2345.69	943.73
4492.0	2314.1	2299.11	902.588	4572.0	2322.1	2346.32	949.315	4652.0	2330.1	2338.7	940.149	4732.0	2338.1	2345.69	948.362
4493.0	2314.2	2300.97	902.588	4573.0	2322.2	2352.11	949.315	4653.0	2330.2	2338.83	941.676	4733.0	2338.2	2345.69	950.435
4494.0	2314.3	2302.82	899.786	4574.0	2322.3	2352.11	949.315	4654.0	2330.3	2338.95	942.677	4734.0	2338.3	2345.69	950.955
4495.0	2314.4	2304.68	894.694	4575.0	2322.4	2354.05	950.342	4655.0	2330.4	2337.16	943.68	4735.0	2338.4	2345.69	950.955
4496.0	2314.5	2306.54	888.751	4576.0	2322.5	2352.11	951.372	4656.0	2330.5	2335.35	943.178	4736.0	2338.5	2347.64	950.435
4497.0	2314.6	2308.4	880.65	4577.0	2322.6	2352.11	950.857	4657.0	2330.6	2335.48	943.178	4737.0	2338.6	2345.69	948.879
4498.0	2314.7	2308.4	874.891	4578.0	2322.7	2354.05	948.29	4658.0	2330.7	2335.6	946.197	4738.0	2338.7	2345.69	947.845
4499.0	2314.8	2312.14	874.891	4579.0	2322.8	2354.05	945.228	4659.0	2330.8	2339.57	947.713	4739.0	2338.8	2345.69	946.813
4500.0	2314.9	2319.65	877.097	4580.0	2322.9	2350.18	943.705	4660.0	2330.9	2345.51	949.235	4740.0	2338.9	2345.69	945.783
4501.0	2315.0	2325.31	880.204	4581.0	2323.0	2344.39	941.176	4661.0	2331.0	2349.53	951.271	4741.0	2339.0	2345.69	944.755
4502.0	2315.1	2331.0	884.682	4582.0	2323.1	2340.55	937.119	4662.0	2331.1	2355.46	953.805	4742.0	2339.1	2343.79	943.73
4503.0	2315.2	2334.81	904.466	4583.0	2323.2	2336.72	934.099	4663.0	2331.2	2359.39	955.313	4743.0	2339.2	2341.91	943.218
4504.0	2315.3	2338.63	936.11	4584.0	2323.3	2329.1	930.103	4664.0	2331.3	2361.36	955.273	4744.0	2339.3	2340.05	943.73
4505.0	2315.4	2344.39	944.242	4585.0	2323.4	2323.42	926.14	4665.0	2331.4	2363.33	955.75	4745.0	2339.4	2342.05	945.783
4506.0	2315.5	2350.18	946.813	4586.0	2323.5	2317.77	923.191	4666.0	2331.5	2363.33	956.233	4746.0	2339.5	2344.04	948.362
4507.0	2315.6	2354.05	946.813	4587.0	2323.6	2314.01	920.26	4667.0	2331.6	2361.36	956.194	4747.0	2339.6	2351.86	951.475
4508.0	2315.7	2354.05	946.298	4588.0	2323.7	2312.14	917.831	4668.0	2331.7	2359.39	955.125	4748.0	2339.7	2357.76	954.085
4509.0	2315.8	2354.05	945.269	4589.0	2323.8	2310.27	914.453	4669.0	2331.8	2363.33	954.049	4749.0	2339.8	2363.68	956.709
4510.0	2315.9	2352.11	943.73	4590.0	2323.9	2308.4	912.534	4670.0	2331.9	2363.33	952.974	4750.0	2339.9	2365.68	960.407
4511.0	2316.0	2352.11	942.196	4591.0	2324.0	2304.68	913.013	4671.0	2332.0	2359.39	950.876	4751.0	2340.0	2365.72	962.533
4512.0	2316.1	2350.18	940.667	4592.0	2324.1	2304.68	914.453	4672.0	2332.1	2353.5	948.29	4752.0	2340.1	2365.74	962.001
4513.0	2316.2	2348.24	938.637	4593.0	2324.2	2306.54	894.234	4673.0	2332.2	2347.64	946.247	4753.0	2340.2	2365.74	962.001
4514.0	2316.3	2346.32	935.607	4594.0	2324.3	2310.27	874.713	4674.0	2332.3	2339.87	943.705	4754.0	2340.3	2365.74	960.938
4515.0	2316.4	2340.55	932.097	4595.0	2324.4	2312.14	873.825	4675.0	2332.4	2336.01	941.176	4755.0	2340.4	2363.79	958.819
4516.0	2316.5	2331.0	928.613	4596.0	2324.5	2314.01	877.835	4676.0	2332.5	2334.08	937.589	4756.0	2340.5	2359.88	954.085
4517.0	2316.6	2331.0	925.647	4597.0	2324.6	2317.77	876.974	4677.0	2332.6	2332.16	934.028	4757.0	2340.6	2354.05	948.362
4518.0	2316.7	2331.0	921.723	4598.0	2324.7	2319.65	878.731	4678.0	2332.7	2326.4	931.502	4758.0	2340.7	2348.24	943.218
4519.0	2316.8	2329.11	918.801	4599.0	2324.8	2323.42	885.51	4679.0	2332.8	2324.49	927.987	4759.0	2340.8	2334.81	938.637
4520.0	2316.9	2329.11	919.287	4600.0	2324.9	2329.1	896.077	4680.0	2332.9	2322.58	926.988	4760.0	2340.9	2323.42	934.601
4521.0	2317.0	2331.0	919.773	4601.0	2325.0	2329.1	906.351	4681.0	2333.0	2326.4	926.988	4761.0	2341.0	2319.65	931.099
4522.0	2317.1	2327.21	919.789	4602.0	2325.1	2336.79	918.303	4682.0	2333.1	2328.32	926.988	4762.0	2341.1	2314.01	927.128
4523.0	2317.2	2325.31	920.306	4603.0	2325.2	2340.75	920.306	4683.0	2333.2	2322.16	928.488	4763.0	2341.2	2310.27	924.172
4524.0	2317.3	2323.42	921.309	4604.0	2325.3	2340.86	941.176	4684.0	2333.3	2340.86	930.495	4764.0	2341.3	2310.27	922.211
4525.0	2317.4	2327.21	922.321	4605.0	2325.4	2335.23	942.186	4685.0	2333.4	2341.81	932.511	4765.0	2341.4	2310.27	920.747
4526.0	2317.5	2329.11	925.805	4606.0	2325.5	2325.81	941.681	4686.0	2333.5	2347.64	935.551	4766.0	2341.5	2312.14	920.747
4527.0	2317.6	2332.91	928.321	4607.0	2325.6	2324.02	940.665	4687.0	2333.6	2353.5	938.1	4767.0	2341.6	2314.01	921.723
4528.0	2317.7	2340.55	931.362	4608.0	2325.7	2322.21	939.641	4688.0	2333.7	2349.59	939.123	4768.0	2341.7	2321.53	923.681
4529.0	2317.8	2340.55	932.915	4609.0	2325.8	2320.42	939.128	4689.0	2333.8	2347.64	940.149	4769.0	2341.8	2325.31	926.14
4530.0	2317.9	2338.63	933.964	4610.0	2325.9	2316.73	939.638	4690.0	2333.9	2351.54	941.681	4770.0	2341.9	2327.21	928.613
4531.0	2318.0	2336.72	934.516	4611.0	2326.0	2313.05	934.538	4691.0	2334.0	2349.59	942.186	4771.0	2342.0	2334.81	932.597
4532.0	2318.1	2336.72	933.522	4612.0	2326.1	2311.19	932.511	4692.0	2334.1	2347.73	942.186	4772.0	2342.1	2340.55	936.615
4533.0	2318.2	2334.81	932.511	4613.0	2326.2	2307.42	930.495	4693.0	2334.2	2339.98	942.186	4773.0	2342.2	2348.24	941.176
4534.0	2318.3	2332.91	931.502	4614.0	2326.3	2305.54	928.989	4694.0	2334.3	2338.12	942.186	4774.0	2342.3	2352.11	945.269
4535.0	2318.4	2331.0	930.998	4615.0	2326.4	2305.54	927.987	4695.0	2334.4	2336.26	940.662	4775.0	2342.4	2355.99	948.879
4536.0	2318.5	2327.21	928.488	4616.0	2326.5	2305.54	929.49	4696.0	2334.5	2330.59	938.611	4776.0	2342.5	2355.99	950.955
4537.0	2318.6	2323.42	925.991	4617.0	2326.6	2311.19	932.006	4697.0	2334.6	2326.85	936.06	4777.0	2342.6	2352.11	951.996
4538.0	2318.7	2323.42	92												

No.	$d(\text{m})$	$v_p(\text{ms}^{-1})$	$v_s(\text{ms}^{-1})$												
4801.0	2345.0	2323.42	936.615	4881.0	2353.0	2310.27	918.801	4961.0	2361.0	2323.42	927.144	5041.0	2369.0	2321.53	703.581
4802.0	2345.1	2321.53	934.099	4882.0	2353.1	2306.54	914.453	4962.0	2361.1	2323.42	927.128	5042.0	2369.1	2315.89	898.804
4803.0	2345.2	2317.77	932.097	4883.0	2353.2	2300.97	911.099	4963.0	2361.2	2321.53	927.622	5043.0	2369.2	2310.27	929.016
4804.0	2345.3	2317.77	931.099	4884.0	2353.3	2300.97	909.194	4964.0	2361.3	2323.42	929.109	5044.0	2369.3	2306.54	930.945
4805.0	2345.4	2321.53	930.6	4885.0	2353.4	2299.11	906.824	4965.0	2361.4	2325.31	930.6	5045.0	2369.4	2308.4	928.388
4806.0	2345.5	2329.1	930.103	4886.0	2353.5	2299.11	904.466	4966.0	2361.5	2331.0	932.097	5046.0	2369.5	2308.4	922.396
4807.0	2345.6	2331.0	934.601	4887.0	2353.6	2299.11	902.12	4967.0	2361.6	2336.72	933.097	5047.0	2369.6	2306.54	906.851
4808.0	2345.7	2332.91	935.607	4888.0	2353.7	2299.11	893.775	4968.0	2361.7	2336.72	921.723	5048.0	2369.7	2308.4	900.153
4809.0	2345.8	2338.63	935.607	4889.0	2353.8	2300.97	878.764	4969.0	2361.8	2344.39	907.771	5049.0	2369.8	2312.14	910.039
4810.0	2345.9	2338.63	901.185	4890.0	2353.9	2304.68	867.257	4970.0	2361.9	2352.11	903.526	5050.0	2369.9	2317.77	921.627
4811.0	2346.0	2338.63	903.996	4891.0	2354.0	2308.4	879.186	4971.0	2362.0	2355.99	902.588	5051.0	2370.0	2321.53	927.02
4812.0	2346.1	2342.47	905.408	4892.0	2354.1	2310.27	908.245	4972.0	2362.1	2363.79	902.618	5052.0	2370.1	2325.25	928.989
4813.0	2346.2	2346.32	903.526	4893.0	2354.2	2312.14	918.801	4973.0	2362.2	2369.67	944.353	5053.0	2370.2	2328.93	929.992
4814.0	2346.3	2346.32	903.057	4894.0	2354.3	2314.01	921.723	4974.0	2362.3	2369.67	949.07	5054.0	2370.3	2326.92	928.488
4815.0	2346.4	2342.47	942.196	4895.0	2354.4	2319.65	923.681	4975.0	2362.4	2367.7	954.885	5055.0	2370.4	2324.92	926.489
4816.0	2346.5	2344.39	940.667	4896.0	2354.5	2319.65	925.647	4976.0	2362.5	2369.67	960.227	5056.0	2370.5	2321.07	924.996
4817.0	2346.6	2346.32	939.144	4897.0	2354.6	2321.53	926.634	4977.0	2362.6	2375.58	962.927	5057.0	2370.6	2315.35	923.012
4818.0	2346.7	2340.55	937.625	4898.0	2354.7	2323.42	929.606	4978.0	2362.7	2381.52	960.292	5058.0	2370.7	2315.25	922.024
4819.0	2346.8	2338.63	938.637	4899.0	2354.8	2325.31	930.103	4979.0	2362.8	2389.49	932.477	5059.0	2370.8	2317.02	920.545
4820.0	2346.9	2340.55	941.686	4900.0	2354.9	2327.21	930.6	4980.0	2362.9	2395.5	924.105	5060.0	2370.9	2316.92	919.071
4821.0	2347.0	2336.72	941.686	4901.0	2355.0	2327.21	930.6	4981.0	2363.0	2401.54	942.174	5061.0	2371.0	2316.82	918.091
4822.0	2347.1	2334.81	938.13	4902.0	2355.1	2327.21	930.6	4982.0	2363.1	2409.64	960.938	5062.0	2371.1	2313.07	917.112
4823.0	2347.2	2332.91	935.104	4903.0	2355.2	2329.1	929.606	4983.0	2363.2	2415.75	962.533	5063.0	2371.2	2309.36	917.112
4824.0	2347.3	2336.72	933.598	4904.0	2355.3	2327.21	927.622	4984.0	2363.3	2417.79	966.277	5064.0	2371.3	2307.52	917.112
4825.0	2347.4	2338.63	933.598	4905.0	2355.4	2325.31	927.128	4985.0	2363.4	2419.84	971.676	5065.0	2371.4	2305.67	917.112
4826.0	2347.5	2340.55	934.099	4906.0	2355.5	2323.42	925.155	4986.0	2363.5	2415.75	980.993	5066.0	2371.5	2296.5	917.601
4827.0	2347.6	2338.63	935.607	4907.0	2355.6	2317.77	923.681	4987.0	2363.6	2409.64	989.364	5067.0	2371.6	2296.5	739.795
4828.0	2347.7	2338.63	937.625	4908.0	2355.7	2315.89	921.723	4988.0	2363.7	2399.52	989.927	5068.0	2371.7	2298.33	666.123
4829.0	2347.8	2342.47	939.651	4909.0	2355.8	2314.01	921.234	4989.0	2363.8	2389.49	989.927	5069.0	2371.8	2303.83	680.457
4830.0	2347.9	2348.24	942.196	4910.0	2355.9	2315.89	921.723	4990.0	2363.9	2385.5	985.999	5070.0	2371.9	2309.36	698.495
4831.0	2348.0	2352.11	943.73	4911.0	2356.0	2317.77	922.701	4991.0	2364.0	2383.51	974.944	5071.0	2372.0	2316.78	717.515
4832.0	2348.1	2357.93	946.298	4912.0	2356.1	2319.65	924.201	4992.0	2364.1	2375.58	966.277	5072.0	2372.1	2326.12	743.591
4833.0	2348.2	2361.83	948.879	4913.0	2356.2	2323.42	925.236	4993.0	2364.2	2363.79	958.819	5073.0	2372.2	2337.42	855.945
4834.0	2348.3	2363.79	950.435	4914.0	2356.3	2323.42	925.28	4994.0	2364.3	2352.11	951.475	5074.0	2372.3	2345.02	891.484
4835.0	2348.4	2363.79	951.475	4915.0	2356.4	2321.53	925.824	4995.0	2364.4	2344.39	946.298	5075.0	2372.4	2346.93	921.53
4836.0	2348.5	2357.93	950.435	4916.0	2356.5	2325.31	925.875	4996.0	2364.5	2340.55	941.176	5076.0	2372.5	2346.93	938.1
4837.0	2348.6	2355.99	947.329	4917.0	2356.6	2327.21	925.919	4997.0	2364.6	2383.63	936.06	5077.0	2372.6	2348.84	939.636
4838.0	2348.7	2350.18	943.73	4918.0	2356.7	2329.1	926.464	4998.0	2364.7	2334.81	930.998	5078.0	2372.7	2352.67	941.686
4839.0	2348.8	2342.47	940.667	4919.0	2356.8	2325.31	926.516	4999.0	2364.8	2331.0	915.163	5079.0	2372.8	2354.59	943.218
4840.0	2348.9	2336.72	937.119	4920.0	2356.9	2327.21	925.574	5000.0	2364.9	2329.1	915.163	5080.0	2372.9	2356.51	947.845
4841.0	2349.0	2331.0	932.597	4921.0	2357.0	2331.0	926.612	5001.0	2365.0	2332.91	918.091	5081.0	2373.0	2354.59	949.397
4842.0	2349.1	2323.42	928.117	4922.0	2357.1	2334.81	928.613	5002.0	2365.1	2334.81	918.566	5082.0	2373.1	2350.72	950.408
4843.0	2349.2	2317.77	924.663	4923.0	2357.2	2338.63	930.6	5003.0	2365.2	2338.63	921.975	5083.0	2373.2	2346.83	950.369
4844.0	2349.3	2314.01	920.747	4924.0	2357.3	2336.72	931.099	5004.0	2365.3	2342.47	928.394	5084.0	2373.3	2337.24	950.324
4845.0	2349.4	2312.14	918.316	4925.0	2357.4	2332.91	931.099	5005.0	2365.4	2344.39	936.404	5085.0	2373.4	2329.59	949.764
4846.0	2349.5	2315.89	917.347	4926.0	2357.5	2331.0	930.103	5006.0	2365.5	2346.32	941.96	5086.0	2373.5	2323.87	947.639
4847.0	2349.6	2317.77	916.38	4927.0	2357.6	2331.0	928.613	5007.0	2365.6	2350.18	942.936	5087.0	2373.6	2314.41	943.97
4848.0	2349.7	2315.89	915.416	4928.0	2357.7	2331.0	927.622	5008.0	2365.7	2352.11	942.882	5088.0	2373.7	2308.74	939.314
4849.0	2349.8	2315.89	914.934	4929.0	2357.8	2331.0	926.634	5009.0	2365.8	2350.18	941.808	5089.0	2373.8	2304.92	934.708
4850.0	2349.9	2315.89	914.453	4930.0	2357.9	2331.0	926.14	5010.0	2365.9	2346.32	939.725	5090.0	2373.9	2304.82	929.658
4851.0	2350.0	2319.65	915.416	4931.0	2358.0	2331.0	926.634	5011.0	2366.0	2344.39	937.14	5091.0	2374.0	2302.87	927.144
4852.0	2350.1	2323.42	917.831	4932.0	2358.1	2339.1	927.128	5012.0	2366.1	2342.47	935.104	5092.0	2374.1	2300.97	924.653
4853.0	2350.2	2325.31	898.856	4933.0	2358.2	2329.1	928.117	5013.0	2366.2	2340.55	939.097	5093.0	2374.2	2300.97	924.638
4854.0	2350.3	2331.0	887.843	4934.0	2358.3	2327.21	929.109	5014.0	2366.3	2334.81	930.6	5094.0	2374.3	2299.11	924.621
4855.0	2350.4	2336.72	932.097	4935.0	2358.4	2327.21	929.606	5015.0	2366.4	2331.0	928.117	5095.0	2374.4	2299.11	924.111
4856.0	2350.5	2340.55	932.097	4936.0	2358.5	2327.21	931.099	5016.0	2366.5	2327.21	926.14	5096.0	2374.5	2293.58	922.127
4857.0	2350.6	2340.55	936.111	4937.0	2358.6	2329.1	931.597	5017.0	2366.6	2325.31	924.172	5097.0	2374.6	2289.9	920.144
4858.0	2350.7	2340.55	937.625	4938.0											

No.	$d(\text{m})$	$v_p(\text{ms}^{-1})$	$v_s(\text{ms}^{-1})$												
5121.0	2377.0	2285.58	915.649	5201.0	2385.0	2319.65	930.103	5281.0	2393.0	2337.42	973.297	5361.0	2401.0	2322.37	950.525
5122.0	2377.1	2283.71	913.208	5202.0	2385.1	2325.31	930.103	5282.0	2393.1	2339.32	974.398	5362.0	2401.1	2316.78	950.529
5123.0	2377.2	2279.97	910.775	5203.0	2385.2	2331.0	933.598	5283.0	2393.2	2341.21	975.491	5363.0	2401.2	2313.07	950.529
5124.0	2377.3	2278.05	908.841	5204.0	2385.3	2338.63	940.667	5284.0	2393.3	2345.02	977.135	5364.0	2401.3	2313.07	950.529
5125.0	2377.4	2277.92	907.392	5205.0	2385.4	2344.39	946.35	5285.0	2393.4	2346.93	979.888	5365.0	2401.4	2311.21	950.529
5126.0	2377.5	2277.79	906.425	5206.0	2385.5	2346.32	955.806	5286.0	2393.5	2348.84	982.101	5366.0	2401.5	2313.07	953.16
5127.0	2377.6	2277.68	906.888	5207.0	2385.6	2350.18	959.0	5287.0	2393.6	2348.84	984.882	5367.0	2401.6	2313.07	955.806
5128.0	2377.7	2277.55	907.823	5208.0	2385.7	2352.11	959.0	5288.0	2393.7	2346.93	987.118	5368.0	2401.7	2314.92	952.633
5129.0	2377.8	2279.23	908.758	5209.0	2385.8	2352.11	962.216	5289.0	2393.8	2350.75	990.491	5369.0	2401.8	2320.51	952.106
5130.0	2377.9	2280.94	909.695	5210.0	2385.9	2352.11	966.537	5290.0	2393.9	2348.84	994.456	5370.0	2401.9	2327.99	950.005
5131.0	2378.0	2278.99	911.108	5211.0	2386.0	2352.11	968.713	5291.0	2394.0	2346.93	997.908	5371.0	2402.0	2329.87	951.58
5132.0	2378.1	2282.58	912.055	5212.0	2386.1	2352.11	970.35	5292.0	2394.1	2346.93	1001.97	5372.0	2402.1	2327.99	953.712
5133.0	2378.2	2284.41	913.492	5213.0	2386.2	2352.11	971.994	5293.0	2394.2	2346.93	1005.48	5373.0	2402.2	2327.99	954.805
5134.0	2378.3	2288.07	914.934	5214.0	2386.3	2350.18	973.093	5294.0	2394.3	2346.93	1007.84	5374.0	2402.3	2326.12	955.374
5135.0	2378.4	2291.74	917.831	5215.0	2386.4	2348.24	974.194	5295.0	2394.4	2345.02	1007.84	5375.0	2402.4	2324.24	955.943
5136.0	2378.5	2293.58	921.234	5216.0	2386.5	2348.24	974.745	5296.0	2394.5	2345.02	1007.25	5376.0	2402.5	2324.24	955.978
5137.0	2378.6	2297.27	926.14	5217.0	2386.6	2348.24	975.297	5297.0	2394.6	2346.93	1006.07	5377.0	2402.6	2318.64	955.49
5138.0	2378.7	2304.68	933.598	5218.0	2386.7	2348.24	975.297	5298.0	2394.7	2346.93	1004.31	5378.0	2402.7	2314.92	953.952
5139.0	2378.8	2308.4	941.176	5219.0	2386.8	2346.32	973.643	5299.0	2394.8	2348.84	1002.56	5379.0	2402.8	2313.07	951.895
5140.0	2378.9	2312.14	938.13	5220.0	2386.9	2344.39	970.898	5300.0	2394.9	2354.59	1000.81	5380.0	2402.9	2311.21	951.417
5141.0	2379.0	2308.4	935.104	5221.0	2387.0	2344.39	968.168	5301.0	2395.0	2360.36	999.647	5381.0	2403.0	2311.21	950.934
5142.0	2379.1	2306.54	933.598	5222.0	2387.1	2342.47	964.912	5302.0	2395.1	2366.26	997.942	5382.0	2403.1	2309.36	950.955
5143.0	2379.2	2302.82	932.097	5223.0	2387.2	2340.55	962.754	5303.0	2395.2	2370.29	997.992	5383.0	2403.2	2307.52	950.955
5144.0	2379.3	2299.11	930.6	5224.0	2387.3	2338.63	961.142	5304.0	2395.3	2382.23	1000.94	5384.0	2403.3	2305.67	950.955
5145.0	2379.4	2297.27	928.613	5225.0	2387.4	2336.72	963.293	5305.0	2395.4	2382.41	1005.65	5385.0	2403.4	2307.52	950.955
5146.0	2379.5	2297.27	927.128	5226.0	2387.5	2336.72	965.453	5306.0	2395.5	2384.55	1011.58	5386.0	2403.5	2305.67	950.955
5147.0	2379.6	2297.27	926.14	5227.0	2387.6	2338.63	967.624	5307.0	2395.6	2384.73	1017.57	5387.0	2403.6	2303.83	950.955
5148.0	2379.7	2295.42	924.172	5228.0	2387.7	2338.63	969.258	5308.0	2395.7	2384.89	1020.6	5388.0	2403.7	2309.36	949.397
5149.0	2379.8	2295.42	922.701	5229.0	2387.8	2334.81	971.445	5309.0	2395.8	2381.11	1024.26	5389.0	2403.8	2309.36	945.269
5150.0	2379.9	2295.42	921.234	5230.0	2387.9	2334.81	972.543	5310.0	2395.9	2377.33	1026.71	5390.0	2403.9	2307.52	934.099
5151.0	2380.0	2295.42	922.211	5231.0	2388.0	2331.0	972.543	5311.0	2396.0	2375.5	1027.34	5391.0	2404.0	2309.36	925.647
5152.0	2380.1	2295.42	923.681	5232.0	2388.1	2329.03	972.543	5312.0	2396.1	2369.67	1027.35	5392.0	2404.1	2318.6	926.634
5153.0	2380.2	2295.42	925.155	5233.0	2388.2	2328.93	971.994	5313.0	2396.2	2369.67	1027.96	5393.0	2404.2	2337.31	933.598
5154.0	2380.3	2297.27	925.155	5234.0	2388.3	2326.92	970.35	5314.0	2396.3	2367.7	1027.96	5394.0	2404.3	2358.3	937.625
5155.0	2380.4	2297.27	924.663	5235.0	2388.4	2323.04	968.713	5315.0	2396.4	2357.93	1027.35	5395.0	2404.4	2366.02	940.667
5156.0	2380.5	2300.97	923.681	5236.0	2388.5	2322.94	967.08	5316.0	2396.5	2350.18	1026.14	5396.0	2404.5	2373.8	955.133
5157.0	2380.6	2302.82	924.663	5237.0	2388.6	2320.95	966.537	5317.0	2396.6	2348.24	1024.33	5397.0	2404.6	2379.66	989.364
5158.0	2380.7	2304.68	927.128	5238.0	2388.7	2322.74	965.453	5318.0	2396.7	2346.32	1020.12	5398.0	2404.7	2381.62	994.456
5159.0	2380.8	2304.68	930.103	5239.0	2388.8	2324.5	964.372	5319.0	2396.8	2340.55	1014.76	5399.0	2404.8	2385.55	994.456
5160.0	2380.9	2306.54	932.097	5240.0	2388.9	2324.39	963.832	5320.0	2396.9	2348.81	1010.64	5400.0	2404.9	2381.56	994.456
5161.0	2381.0	2310.27	935.104	5241.0	2389.0	2322.42	962.754	5321.0	2397.0	2329.1	1004.8	5401.0	2405.0	2373.62	992.753
5162.0	2381.1	2310.27	938.637	5242.0	2389.1	2322.37	961.679	5322.0	2397.1	2317.77	999.6	5402.0	2405.1	2363.79	992.753
5163.0	2381.2	2312.14	941.691	5243.0	2389.2	2324.24	961.142	5323.0	2397.2	2314.01	993.888	5403.0	2405.2	2354.05	991.056
5164.0	2381.3	2317.77	944.274	5244.0	2389.3	2326.12	960.07	5324.0	2397.3	2312.14	992.753	5404.0	2405.3	2350.18	988.24
5165.0	2381.4	2317.77	945.31	5245.0	2389.4	2329.87	959.0	5325.0	2397.4	2312.14	992.753	5405.0	2405.4	2344.39	984.325
5166.0	2381.5	2317.77	947.913	5246.0	2389.5	2331.76	958.466	5326.0	2397.5	2310.27	992.753	5406.0	2405.5	2336.72	979.888
5167.0	2381.6	2317.77	949.481	5247.0	2389.6	2329.87	959.0	5327.0	2397.6	2312.14	993.32	5407.0	2405.6	2319.65	977.684
5168.0	2381.7	2314.01	948.958	5248.0	2389.7	2327.99	961.679	5328.0	2397.7	2312.14	992.753	5408.0	2405.7	2300.97	973.852
5169.0	2381.8	2312.14	948.958	5249.0	2389.8	2324.24	961.142	5329.0	2397.8	2312.14	993.888	5409.0	2405.8	2300.97	969.509
5170.0	2381.9	2312.14	947.913	5250.0	2389.9	2322.37	960.605	5330.0	2397.9	2310.27	993.888	5410.0	2405.9	2300.97	964.669
5171.0	2382.0	2312.14	945.83	5251.0	2390.0	2320.51	961.142	5331.0	2398.0	2310.27	991.621	5411.0	2406.0	2304.68	960.938
5172.0	2382.1	2312.14	946.35	5252.0	2390.1	2318.64	957.933	5332.0	2398.1	2310.27	988.802	5412.0	2406.1	2302.82	958.819
5173.0	2382.2	2310.27	946.35	5253.0	2390.2	2316.78	957.933	5333.0	2398.2	2310.27	987.679	5413.0	2406.2	2302.82	956.709
5174.0	2382.3	2310.27	944.792	5254.0	2390.3	2318.64	957.933	5334.0	2398.3	2310.27	987.118	5414.0	2406.3	2308.4	954.085
5175.0	2382.4	2308.4	944.274	5255.0	2390.4	2318.64	956.868	5335.0	2398.4	2310.27	987.118	5415.0	2406.4	2314.01	951.996
5176.0	2382.5	2312.14	943.756	5256.0	2390.5	2316.78	956.337	5336.0	2398.5	2314.01	986.558	5416.0	2406.5	2321.53	951.996
5177.0	2382.6	2312.14	942.722	5257.0	2390.6	2313.07	956.337	5337.0	2398.6	2317.77	985.44	5417.0	2406.6	2331.0	951.475
5178.0	2382.7	2310.27	941.69												

No.	$d(\text{m})$	$v_p(\text{ms}^{-1})$	$v_s(\text{ms}^{-1})$												
5441.0	2409.0	2361.83	976.586	5521.0	2417.0	2281.97	908.882	5601.0	2425.0	2280.76	914.944	5681.0	2433.0	2300.16	925.511
5442.0	2409.1	2357.93	976.038	5522.0	2417.1	2280.17	907.924	5602.0	2425.1	2282.58	912.534	5682.0	2433.1	2300.16	925.493
5443.0	2409.2	2355.99	975.491	5523.0	2417.2	2276.57	906.49	5603.0	2425.2	2284.41	909.67	5683.0	2433.2	2300.16	925.991
5444.0	2409.3	2354.05	974.944	5524.0	2417.3	2274.77	905.06	5604.0	2425.3	2286.24	906.824	5684.0	2433.3	2301.99	927.487
5445.0	2409.4	2354.05	972.219	5525.0	2417.4	2271.19	904.11	5605.0	2425.4	2288.07	903.996	5685.0	2433.4	2300.16	929.49
5446.0	2409.5	2354.05	969.509	5526.0	2417.5	2271.19	904.585	5606.0	2425.5	2288.07	903.526	5686.0	2433.5	2300.16	930.998
5447.0	2409.6	2352.11	966.814	5527.0	2417.6	2272.98	904.11	5607.0	2425.6	2286.24	903.057	5687.0	2433.6	2301.99	930.998
5448.0	2409.7	2352.11	964.669	5528.0	2417.7	2269.41	902.688	5608.0	2425.7	2286.24	901.652	5688.0	2433.7	2300.16	930.495
5449.0	2409.8	2352.11	962.001	5529.0	2417.8	2267.62	900.327	5609.0	2425.8	2286.24	897.928	5689.0	2433.8	2300.16	929.49
5450.0	2409.9	2348.24	958.819	5530.0	2417.9	2269.41	899.387	5610.0	2425.9	2282.58	890.548	5690.0	2433.9	2301.99	929.49
5451.0	2410.0	2346.32	954.608	5531.0	2418.0	2269.41	898.917	5611.0	2426.0	2277.13	891.009	5691.0	2434.0	2303.83	929.49
5452.0	2410.1	2342.47	949.397	5532.0	2418.1	2271.19	899.387	5612.0	2426.1	2273.5	892.857	5692.0	2434.1	2303.82	929.467
5453.0	2410.2	2336.72	944.242	5533.0	2418.2	2271.19	899.857	5613.0	2426.2	2271.69	894.234	5693.0	2434.2	2305.65	929.432
5454.0	2410.3	2332.91	940.159	5534.0	2418.3	2267.62	898.917	5614.0	2426.3	2273.5	892.857	5694.0	2434.3	2307.49	929.892
5455.0	2410.4	2329.1	938.13	5535.0	2418.4	2271.19	899.387	5615.0	2426.4	2269.89	891.932	5695.0	2434.4	2307.48	930.853
5456.0	2410.5	2323.42	938.13	5536.0	2418.5	2278.37	900.798	5616.0	2426.5	2268.09	888.709	5696.0	2434.5	2309.34	930.817
5457.0	2410.6	2323.42	939.651	5537.0	2418.6	2283.78	903.161	5617.0	2426.6	2268.09	883.692	5697.0	2434.6	2309.33	931.275
5458.0	2410.7	2321.53	940.159	5538.0	2418.7	2291.03	906.49	5618.0	2426.7	2268.09	876.494	5698.0	2434.7	2309.33	931.733
5459.0	2410.8	2321.53	940.667	5539.0	2418.8	2294.67	908.403	5619.0	2426.8	2284.41	867.66	5699.0	2434.8	2313.08	933.702
5460.0	2410.9	2321.53	939.651	5540.0	2418.9	2294.67	909.843	5620.0	2426.9	2319.65	860.29	5700.0	2434.9	2316.86	935.669
5461.0	2411.0	2321.53	939.651	5541.0	2419.0	2292.85	909.843	5621.0	2427.0	2377.56	880.528	5701.0	2435.0	2316.87	937.141
5462.0	2411.1	2319.65	941.176	5542.0	2419.1	2290.96	909.843	5622.0	2427.1	2401.54	891.009	5702.0	2435.1	2316.87	939.144
5463.0	2411.2	2315.89	942.196	5543.0	2419.2	2289.04	909.843	5623.0	2427.2	2413.71	900.718	5703.0	2435.2	2316.87	940.667
5464.0	2411.3	2314.01	942.707	5544.0	2419.3	2287.1	909.843	5624.0	2427.3	2419.84	909.194	5704.0	2435.3	2318.77	942.196
5465.0	2411.4	2314.01	943.218	5545.0	2419.4	2286.98	911.288	5625.0	2427.4	2430.13	934.601	5705.0	2435.4	2322.58	942.196
5466.0	2411.5	2314.01	943.218	5546.0	2419.5	2286.88	915.163	5626.0	2427.5	2430.13	953.688	5706.0	2435.5	2324.49	942.196
5467.0	2411.6	2312.14	944.755	5547.0	2419.6	2286.76	919.562	5627.0	2427.6	2435.9	962.216	5707.0	2435.6	2324.49	942.196
5468.0	2411.7	2310.27	946.298	5548.0	2419.7	2286.63	922.518	5628.0	2427.7	2417.79	971.445	5708.0	2435.7	2320.68	942.196
5469.0	2411.8	2306.54	945.269	5549.0	2419.8	2282.88	924.996	5629.0	2427.8	2415.75	976.958	5709.0	2435.8	2316.87	942.196
5470.0	2411.9	2304.68	943.73	5550.0	2419.9	2277.31	925.493	5630.0	2427.9	2407.61	975.85	5710.0	2435.9	2320.65	942.196
5471.0	2412.0	2304.68	942.196	5551.0	2420.0	2271.75	925.493	5631.0	2428.0	2389.49	974.194	5711.0	2436.0	2322.58	942.196
5472.0	2412.1	2306.54	940.667	5552.0	2420.1	2266.29	923.507	5632.0	2428.1	2377.56	972.543	5712.0	2436.1	2324.49	944.242
5473.0	2412.2	2310.27	939.144	5553.0	2420.2	2268.09	922.024	5633.0	2428.2	2350.18	969.804	5713.0	2436.2	2324.49	946.298
5474.0	2412.3	2312.14	936.615	5554.0	2420.3	2278.94	920.053	5634.0	2428.3	2323.42	963.293	5714.0	2436.3	2328.32	946.298
5475.0	2412.4	2319.65	932.097	5555.0	2420.4	2280.76	917.112	5635.0	2428.4	2310.27	955.276	5715.0	2436.4	2332.16	946.298
5476.0	2412.5	2323.42	927.622	5556.0	2420.5	2269.89	909.843	5636.0	2428.5	2302.82	948.958	5716.0	2436.5	2332.16	946.298
5477.0	2412.6	2329.1	925.647	5557.0	2420.6	2255.55	905.06	5637.0	2428.6	2297.27	941.176	5717.0	2436.6	2334.08	946.298
5478.0	2412.7	2332.91	928.117	5558.0	2420.7	2244.92	903.635	5638.0	2428.7	2289.9	933.097	5718.0	2436.7	2334.08	946.298
5479.0	2412.8	2334.81	938.13	5559.0	2420.8	2243.16	903.635	5639.0	2428.8	2289.9	924.172	5719.0	2436.8	2334.08	946.298
5480.0	2412.9	2338.63	946.298	5560.0	2420.9	2246.69	904.585	5640.0	2428.9	2289.9	916.863	5720.0	2436.9	2332.16	946.298
5481.0	2413.0	2340.55	953.039	5561.0	2421.0	2252.0	905.06	5641.0	2429.0	2293.58	911.099	5721.0	2437.0	2334.08	944.755
5482.0	2413.1	2342.47	955.657	5562.0	2421.1	2253.78	901.736	5642.0	2429.1	2291.74	909.68	5722.0	2437.1	2334.08	945.783
5483.0	2413.2	2342.47	957.763	5563.0	2421.2	2253.78	899.377	5643.0	2429.2	2289.9	908.746	5723.0	2437.2	2334.08	946.813
5484.0	2413.3	2340.55	960.407	5564.0	2421.3	2255.55	897.499	5644.0	2429.3	2289.9	908.284	5724.0	2437.3	2332.16	947.329
5485.0	2413.4	2336.72	962.533	5565.0	2421.4	2266.29	896.098	5645.0	2429.4	2288.07	906.875	5725.0	2437.4	2330.23	948.362
5486.0	2413.5	2332.91	964.669	5566.0	2421.5	2277.13	895.168	5646.0	2429.5	2284.41	905.941	5726.0	2437.5	2326.4	946.813
5487.0	2413.6	2331.0	963.6	5567.0	2421.6	2288.07	896.092	5647.0	2429.6	2278.94	905.478	5727.0	2437.6	2322.58	944.755
5488.0	2413.7	2331.0	964.134	5568.0	2421.7	2295.42	898.877	5648.0	2429.7	2278.94	905.017	5728.0	2437.7	2322.58	943.73
5489.0	2413.8	2327.21	965.204	5569.0	2421.8	2300.97	901.674	5649.0	2429.8	2278.94	903.609	5729.0	2437.8	2324.49	943.218
5490.0	2413.9	2321.53	966.814	5570.0	2421.9	2300.97	903.072	5650.0	2429.9	2277.13	901.728	5730.0	2437.9	2322.58	942.196
5491.0	2414.0	2315.89	967.89	5571.0	2422.0	2300.97	903.531	5651.0	2430.0	2277.13	902.683	5731.0	2438.0	2320.68	941.176
5492.0	2414.1	2314.01	967.89	5572.0	2422.1	2300.97	903.526	5652.0	2430.1	2277.09	903.635	5732.0	2438.1	2318.77	940.159
5493.0	2414.2	2312.14	967.352	5573.0	2422.2	2300.97	903.526	5653.0	2430.2	2277.04	903.635	5733.0	2438.2	2316.87	939.144
5494.0	2414.3	2310.27	962.533	5574.0	2422.3	2300.97	903.526	5654.0	2430.3	2276.98	903.635	5734.0	2438.3	2316.87	938.637
5495.0	2414.4	2310.27	957.236	5575.0	2422.4	2300.97	903.996	5655.0	2430.4	2278.74	904.585	5735.0	2438.4	2316.87	937.625
5496.0	2414.5	2308.4	955.133	5576.0	2422.5	2300.97	905.408	5656.0	2430.5	2278.68	907.445	5736.0	2438.5	2314.98	936.111
5497.0	2414.6	2308.4	952.517	5577.0	2422.6	2297.27	908.719	5657.0	2430.6	2278.62	908.403	5737.0	2438.6	2311.19	934.601
5498.0	2414.7	2308.4	951												

No.	$d(\text{m})$	$v_p(\text{ms}^{-1})$	$v_s(\text{ms}^{-1})$												
5761.0	2441.0	2300.97	928.994	5841.0	2449.0	2308.4	919.549	5921.0	2457.0	2313.07	931.597	6001.0	2465.0	2174.86	830.599
5762.0	2441.1	2300.97	928.989	5842.0	2449.1	2310.27	919.071	5922.0	2457.1	2311.16	931.099	6002.0	2465.1	2166.61	823.52
5763.0	2441.2	2300.97	928.488	5843.0	2449.2	2306.54	918.58	5923.0	2457.2	2309.21	928.613	6003.0	2465.2	2160.06	817.712
5764.0	2441.3	2300.97	928.488	5844.0	2449.3	2302.82	917.601	5924.0	2457.3	2309.12	925.647	6004.0	2465.3	2153.55	810.849
5765.0	2441.4	2300.97	929.49	5845.0	2449.4	2300.97	915.163	5925.0	2457.4	2305.32	923.681	6005.0	2465.4	2147.07	805.549
5766.0	2441.5	2306.54	931.502	5846.0	2449.5	2300.97	912.737	5926.0	2457.5	2301.52	917.831	6006.0	2465.5	2181.5	801.052
5767.0	2441.6	2306.54	935.551	5847.0	2449.6	2300.97	910.805	5927.0	2457.6	2295.91	910.146	6007.0	2465.6	2203.37	792.206
5768.0	2441.7	2306.54	938.1	5848.0	2449.7	2299.11	909.843	5928.0	2457.7	2293.96	908.719	6008.0	2465.7	2193.22	784.267
5769.0	2441.8	2310.27	939.636	5849.0	2449.8	2293.58	909.362	5929.0	2457.8	2293.84	906.824	6009.0	2465.8	2171.55	777.889
5770.0	2441.9	2312.14	940.149	5850.0	2449.9	2293.58	908.403	5930.0	2457.9	2293.74	904.466	6010.0	2465.9	2135.84	769.927
5771.0	2442.0	2315.89	940.149	5851.0	2450.0	2291.74	907.445	5931.0	2458.0	2291.79	903.996	6011.0	2466.0	2124.72	765.184
5772.0	2442.1	2317.77	940.149	5852.0	2450.1	2289.9	906.49	5932.0	2458.1	2291.74	904.936	6012.0	2466.1	2123.14	761.165
5773.0	2442.2	2317.77	940.15	5853.0	2450.2	2289.9	906.013	5933.0	2458.2	2291.74	907.297	6013.0	2466.2	2126.3	757.848
5774.0	2442.3	2319.65	941.176	5854.0	2450.3	2288.07	904.585	5934.0	2458.3	2291.74	908.719	6014.0	2466.3	2124.72	754.888
5775.0	2442.4	2323.42	943.218	5855.0	2450.4	2286.24	903.635	5935.0	2458.4	2291.74	909.67	6015.0	2466.4	2123.14	752.927
5776.0	2442.5	2323.42	944.755	5856.0	2450.5	2286.24	903.635	5936.0	2458.5	2291.74	909.67	6016.0	2466.5	2123.14	750.976
5777.0	2442.6	2323.42	944.755	5857.0	2450.6	2286.24	903.161	5937.0	2458.6	2291.74	908.719	6017.0	2466.6	2123.14	749.036
5778.0	2442.7	2323.42	942.707	5858.0	2450.7	2286.24	902.215	5938.0	2458.7	2291.74	908.245	6018.0	2466.7	2123.14	748.391
5779.0	2442.8	2323.42	940.666	5859.0	2450.8	2286.24	902.688	5939.0	2458.8	2291.74	909.67	6019.0	2466.8	2126.3	762.5
5780.0	2442.9	2323.42	939.141	5860.0	2450.9	2286.24	903.161	5940.0	2458.9	2295.42	912.534	6020.0	2466.9	2132.65	769.246
5781.0	2443.0	2323.42	938.635	5861.0	2451.0	2282.58	904.11	5941.0	2459.0	2297.27	916.38	6021.0	2467.0	2135.84	770.951
5782.0	2443.1	2323.42	938.637	5862.0	2451.1	2280.76	906.49	5942.0	2459.1	2293.58	917.347	6022.0	2467.1	2139.04	773.35
5783.0	2443.2	2323.42	938.13	5863.0	2451.2	2278.94	905.536	5943.0	2459.2	2289.9	912.534	6023.0	2467.2	2140.64	775.786
5784.0	2443.3	2323.42	937.625	5864.0	2451.3	2278.94	902.688	5944.0	2459.3	2284.41	911.577	6024.0	2467.3	2142.25	777.889
5785.0	2443.4	2323.42	937.625	5865.0	2451.4	2278.94	901.27	5945.0	2459.4	2277.13	914.453	6025.0	2467.4	2142.25	778.241
5786.0	2443.5	2323.42	938.13	5866.0	2451.5	2278.94	900.327	5946.0	2459.5	2275.31	916.863	6026.0	2467.5	2142.25	778.945
5787.0	2443.6	2323.42	937.625	5867.0	2451.6	2282.58	900.327	5947.0	2459.6	2277.13	920.26	6027.0	2467.6	2140.64	779.65
5788.0	2443.7	2319.65	935.607	5868.0	2451.7	2282.58	900.327	5948.0	2459.7	2277.13	918.801	6028.0	2467.7	2142.25	780.004
5789.0	2443.8	2317.77	933.097	5869.0	2451.8	2278.94	900.798	5949.0	2459.8	2277.13	915.416	6029.0	2467.8	2142.25	779.297
5790.0	2443.9	2314.01	931.099	5870.0	2451.9	2282.58	901.742	5950.0	2459.9	2277.13	911.577	6030.0	2467.9	2142.25	778.593
5791.0	2444.0	2314.01	930.6	5871.0	2452.0	2284.41	901.27	5951.0	2460.0	2277.13	907.771	6031.0	2468.0	2140.64	778.593
5792.0	2444.1	2314.01	930.6	5872.0	2452.1	2282.58	900.798	5952.0	2460.1	2277.24	905.888	6032.0	2468.1	2137.44	778.593
5793.0	2444.2	2315.89	930.6	5873.0	2452.2	2280.76	900.798	5953.0	2460.2	2277.4	905.899	6033.0	2468.2	2135.84	778.593
5794.0	2444.3	2312.14	929.606	5874.0	2452.3	2280.76	902.215	5954.0	2460.3	2277.59	909.237	6034.0	2468.3	2137.44	777.538
5795.0	2444.4	2310.27	927.622	5875.0	2452.4	2280.76	904.585	5955.0	2460.4	2277.78	912.607	6035.0	2468.4	2140.64	776.136
5796.0	2444.5	2308.4	925.647	5876.0	2452.5	2275.31	907.924	5956.0	2460.5	2277.95	915.521	6036.0	2468.5	2143.85	774.739
5797.0	2444.6	2304.68	926.14	5877.0	2452.6	2280.76	911.288	5957.0	2460.6	2278.14	914.577	6037.0	2468.6	2145.46	774.042
5798.0	2444.7	2300.97	926.634	5878.0	2452.7	2291.74	914.191	5958.0	2460.7	2278.33	914.601	6038.0	2468.7	2145.46	767.209
5799.0	2444.8	2300.97	926.634	5879.0	2452.8	2297.27	917.112	5959.0	2460.8	2280.31	914.621	6039.0	2468.8	2150.31	754.233
5800.0	2444.9	2299.11	925.647	5880.0	2452.9	2300.97	918.58	5960.0	2460.9	2284.15	914.644	6040.0	2468.9	2155.17	755.544
5801.0	2445.0	2297.27	925.155	5881.0	2453.0	2302.82	920.053	5961.0	2461.0	2288.0	917.592	6041.0	2469.0	2160.06	776.836
5802.0	2445.1	2299.11	925.155	5882.0	2453.1	2308.4	922.518	5962.0	2461.1	2289.9	920.053	6042.0	2469.1	2164.97	792.206
5803.0	2445.2	2299.11	925.155	5883.0	2453.2	2310.27	924.499	5963.0	2461.2	2291.74	923.507	6043.0	2469.2	2171.55	804.045
5804.0	2445.3	2300.97	925.647	5884.0	2453.3	2308.4	928.989	5964.0	2461.3	2297.27	927.987	6044.0	2469.3	2179.84	807.006
5805.0	2445.4	2302.82	927.128	5885.0	2453.4	2302.82	929.992	5965.0	2461.4	2300.97	930.998	6045.0	2469.4	2186.51	794.766
5806.0	2445.5	2304.68	929.109	5886.0	2453.5	2300.97	924.499	5966.0	2461.5	2306.54	933.522	6046.0	2469.5	2194.91	780.357
5807.0	2445.6	2308.4	929.606	5887.0	2453.6	2304.68	918.091	5967.0	2461.6	2308.4	936.06	6047.0	2469.6	2203.37	774.39
5808.0	2445.7	2308.4	930.6	5888.0	2453.7	2319.65	912.737	5968.0	2461.7	2308.4	940.662	6048.0	2469.7	2210.19	775.786
5809.0	2445.8	2310.27	931.099	5889.0	2453.8	2338.63	913.706	5969.0	2461.8	2304.68	944.755	6049.0	2469.8	2215.33	828.621
5810.0	2445.9	2312.14	931.597	5890.0	2453.9	2355.99	923.507	5970.0	2461.9	2299.11	946.298	6050.0	2469.9	2220.5	837.398
5811.0	2446.0	2312.14	931.597	5891.0	2454.0	2373.61	931.502	5971.0	2462.0	2293.58	942.196	6051.0	2470.0	2223.94	840.636
5812.0	2446.1	2314.01	930.103	5892.0	2454.1	2391.49	945.2	5972.0	2462.1	2295.42	952.474	6052.0	2470.1	2227.27	843.896
5813.0	2446.2	2315.89	928.117	5893.0	2454.2	2405.58	958.589	5973.0	2462.2	2299.11	913.672	6053.0	2470.2	2230.56	847.185
5814.0	2446.3	2315.89	927.128	5894.0	2454.3	2407.61	967.551	5974.0	2462.3	2304.68	913.65	6054.0	2470.3	2239.06	853.034
5815.0	2446.4	2315.89	927.622	5895.0	2454.4	2411.67	972.36	5975.0	2462.4	2315.89	920.444	6055.0	2470.4	2244.14	858.113
5816.0	2446.5	2315.89	928.613	5896.0	2454.5	2413.71	975.051	5976.0	2462.5	2331.0	936.863	6056.0	2470.5	2247.51	860.239
5817.0	2446.6	2315.89	928.613	5897.0	2454.6	2417.79	977.759	5977.0	2462.6	2346.32	947.595	6057.0	2470.6	2249.11	862.37
5818.0	2446.7	2315.89	928.613	5898.0											

No.	$d(\text{m})$	$v_p(\text{ms}^{-1})$	$v_s(\text{ms}^{-1})$												
6081.0	2473.0	2277.13	900.722	6161.0	2481.0	2288.12	907.771	6241.0	2489.0	2248.72	867.472	6321.0	2497.0	2264.57	879.179
6082.0	2473.1	2279.05	903.496	6162.0	2481.1	2284.37	904.466	6242.0	2489.1	2264.93	864.454	6322.0	2497.1	2264.38	876.494
6083.0	2473.2	2281.06	905.807	6163.0	2481.2	2280.66	903.057	6243.0	2489.2	2283.21	866.176	6323.0	2497.2	2262.42	874.269
6084.0	2473.3	2284.87	908.596	6164.0	2481.3	2280.61	902.12	6244.0	2489.3	2292.46	873.134	6324.0	2497.3	2262.23	872.939
6085.0	2473.4	2290.56	912.359	6165.0	2481.4	2280.55	900.718	6245.0	2489.4	2296.18	903.996	6325.0	2497.4	2262.07	874.269
6086.0	2473.5	2298.12	915.197	6166.0	2481.5	2276.87	899.786	6246.0	2489.5	2292.46	913.013	6326.0	2497.5	2260.09	878.731
6087.0	2473.6	2300.14	918.529	6167.0	2481.6	2275.01	898.856	6247.0	2489.6	2288.75	914.453	6327.0	2497.6	2256.33	883.692
6088.0	2473.7	2302.18	920.43	6168.0	2481.7	2273.16	898.856	6248.0	2489.7	2283.21	907.297	6328.0	2497.7	2252.61	886.878
6089.0	2473.8	2306.09	924.291	6169.0	2481.8	2273.11	897.465	6249.0	2489.8	2277.69	905.408	6329.0	2497.8	2248.88	887.793
6090.0	2473.9	2308.12	932.665	6170.0	2481.9	2271.27	895.616	6250.0	2489.9	2277.69	903.526	6330.0	2497.9	2245.18	887.335
6091.0	2474.0	2308.32	935.63	6171.0	2482.0	2269.43	894.234	6251.0	2490.0	2272.21	901.185	6331.0	2498.0	2241.48	886.878
6092.0	2474.1	2308.35	937.625	6172.0	2482.1	2267.55	893.289	6252.0	2490.1	2263.12	897.928	6332.0	2498.1	2237.79	886.422
6093.0	2474.2	2304.55	939.144	6173.0	2482.2	2267.41	892.781	6253.0	2490.2	2255.9	894.694	6333.0	2498.2	2235.89	885.966
6094.0	2474.3	2302.61	938.13	6174.0	2482.3	2267.29	895.044	6254.0	2490.3	2246.94	890.571	6334.0	2498.3	2233.97	886.878
6095.0	2474.4	2302.52	934.601	6175.0	2482.4	2272.52	898.711	6255.0	2490.4	2239.82	886.034	6335.0	2498.4	2233.79	888.709
6096.0	2474.5	2308.0	929.109	6176.0	2482.5	2272.39	902.416	6256.0	2490.5	2232.75	867.472	6336.0	2498.5	2233.64	889.628
6097.0	2474.6	2319.08	913.492	6177.0	2482.6	2275.88	904.742	6257.0	2490.6	2223.97	843.02	6337.0	2498.6	2233.47	890.088
6098.0	2474.7	2339.73	930.103	6178.0	2482.7	2279.37	905.654	6258.0	2490.7	2218.8	840.14	6338.0	2498.7	2233.32	888.709
6099.0	2474.8	2362.66	950.435	6179.0	2482.8	2279.24	903.721	6259.0	2490.8	2217.1	839.321	6339.0	2498.8	2233.15	885.966
6100.0	2474.9	2389.93	951.475	6180.0	2482.9	2279.13	903.688	6260.0	2490.9	2217.1	845.088	6340.0	2498.9	2232.97	884.6
6101.0	2475.0	2426.1	943.218	6181.0	2483.0	2279.0	904.124	6261.0	2491.0	2217.1	844.674	6341.0	2499.0	2232.82	882.786
6102.0	2475.1	2432.2	951.475	6182.0	2483.1	2278.94	904.585	6262.0	2491.1	2217.1	841.372	6342.0	2499.1	2232.75	879.656
6103.0	2475.2	2432.2	958.819	6183.0	2483.2	2278.94	905.06	6263.0	2491.2	2217.1	838.912	6343.0	2499.2	2232.75	877.455
6104.0	2475.3	2432.2	967.352	6184.0	2483.3	2278.94	905.536	6264.0	2491.3	2217.1	837.687	6344.0	2499.3	2234.51	875.717
6105.0	2475.4	2426.01	970.591	6185.0	2483.4	2284.41	906.013	6265.0	2491.4	2217.1	834.844	6345.0	2499.4	2236.28	875.764
6106.0	2475.5	2423.95	972.219	6186.0	2483.5	2286.24	906.967	6266.0	2491.5	2215.4	830.415	6346.0	2499.5	2238.05	876.25
6107.0	2475.6	2423.95	972.219	6187.0	2483.6	2286.24	907.445	6267.0	2491.6	2212.0	828.417	6347.0	2499.6	2238.05	877.637
6108.0	2475.7	2415.75	970.591	6188.0	2483.7	2286.24	906.49	6268.0	2491.7	2210.31	828.417	6348.0	2499.7	2238.05	879.927
6109.0	2475.8	2397.54	968.429	6189.0	2483.8	2286.24	906.49	6269.0	2491.8	2208.62	830.015	6349.0	2499.8	2241.59	879.518
6110.0	2475.9	2385.53	966.277	6190.0	2483.9	2286.24	906.49	6270.0	2491.9	2205.24	827.621	6350.0	2499.9	2245.15	878.668
6111.0	2476.0	2377.57	966.277	6191.0	2484.0	2286.24	906.967	6271.0	2492.0	2205.24	817.017	6351.0	2500.0	2245.15	877.372
6112.0	2476.1	2365.65	966.814	6192.0	2484.1	2286.24	906.967	6272.0	2492.1	2206.93	810.861	6352.0	2500.1	2245.07	876.048
6113.0	2476.2	2359.66	966.814	6193.0	2484.2	2286.24	906.967	6273.0	2492.2	2208.62	810.861	6353.0	2500.2	2244.94	875.157
6114.0	2476.3	2347.9	966.277	6194.0	2484.3	2286.24	906.013	6274.0	2492.3	2210.31	832.422	6354.0	2500.3	2244.82	875.157
6115.0	2476.4	2336.29	960.407	6195.0	2484.4	2289.9	905.06	6275.0	2492.4	2225.68	844.26	6355.0	2500.4	2244.68	876.048
6116.0	2476.5	2324.82	950.435	6196.0	2484.5	2297.27	906.013	6276.0	2492.5	2246.69	855.103	6356.0	2500.5	2244.54	878.282
6117.0	2476.6	2320.59	942.707	6197.0	2484.6	2310.27	908.882	6277.0	2492.6	2268.09	860.604	6357.0	2500.6	2244.42	881.881
6118.0	2476.7	2320.86	936.111	6198.0	2484.7	2314.01	911.288	6278.0	2492.7	2286.24	877.539	6358.0	2500.7	2244.28	882.786
6119.0	2476.8	2318.88	926.14	6199.0	2484.8	2315.89	913.221	6279.0	2492.8	2302.82	891.484	6359.0	2500.8	2244.14	883.239
6120.0	2476.9	2318.78	922.211	6200.0	2484.9	2314.01	915.649	6280.0	2492.9	2308.4	941.176	6360.0	2500.9	2244.02	884.146
6121.0	2477.0	2316.82	922.211	6201.0	2485.0	2312.14	914.191	6281.0	2493.0	2312.14	943.218	6361.0	2501.1	2243.87	884.6
6122.0	2477.1	2316.73	922.201	6202.0	2485.1	2310.27	913.221	6282.0	2493.1	2314.01	943.218	6362.0	2501.1	2243.91	885.059
6123.0	2477.2	2316.63	923.653	6203.0	2485.2	2308.4	911.77	6283.0	2493.2	2310.27	928.613	6363.0	2501.2	2244.07	885.977
6124.0	2477.3	2314.69	925.609	6204.0	2485.3	2306.54	911.77	6284.0	2493.3	2302.82	916.863	6364.0	2501.3	2244.22	885.983
6125.0	2477.4	2314.6	927.574	6205.0	2485.4	2306.54	911.77	6285.0	2493.4	2297.27	905.408	6365.0	2501.4	2244.38	885.536
6126.0	2477.5	2314.5	928.059	6206.0	2485.5	2302.82	912.253	6286.0	2493.5	2293.58	894.234	6366.0	2501.5	2239.13	884.638
6127.0	2477.6	2316.29	926.554	6207.0	2485.6	2300.97	910.324	6287.0	2493.6	2286.24	887.843	6367.0	2501.6	2237.48	884.195
6128.0	2477.7	2316.2	924.555	6208.0	2485.7	2295.42	906.967	6288.0	2493.7	2277.13	884.682	6368.0	2501.7	2237.65	883.751
6129.0	2477.8	2316.1	923.057	6209.0	2485.8	2288.07	903.635	6289.0	2493.8	2267.2	881.543	6369.0	2501.8	2237.82	884.662
6130.0	2477.9	2316.02	925.515	6210.0	2485.9	2277.13	903.635	6290.0	2493.9	2248.45	878.87	6370.0	2501.9	2237.97	883.321
6131.0	2478.0	2315.93	926.496	6211.0	2486.0	2266.29	902.688	6291.0	2494.0	2234.39	875.772	6371.0	2502.0	2238.14	881.09
6132.0	2478.1	2315.89	926.47	6212.0	2486.1	2257.03	898.913	6292.0	2494.1	2234.29	870.961	6372.0	2502.1	2234.74	878.426
6133.0	2478.2	2314.01	924.942	6213.0	2486.2	2256.58	896.571	6293.0	2494.2	2234.12	866.634	6373.0	2502.2	2233.15	876.655
6134.0	2478.3	2308.4	923.423	6214.0	2486.3	2256.05	891.027	6294.0	2494.3	2232.22	861.916	6374.0	2502.3	2233.31	876.213
6135.0	2478.4	2306.54	921.916	6215.0	2486.4	2255.52	883.783	6295.0	2494.4	2239.07	860.218	6375.0	2502.4	2233.49	877.097
6136.0	2478.5	2308.4	919.435	6216.0	2486.5	2258.64	881.096	6296.0	2494.5	2249.53	867.991	6376.0	2502.5	2233.68	877.097
6137.0	2478.6	2308.4	917.457	6217.0	2486.6	2259.9	879.314	6297.0	2494.6	2256.54	876.369	6377.0	2502.6	2232.06	876.655
6138.0	2478.7	2304.68	916.464	62											

No.	$d(\text{m})$	$v_p(\text{ms}^{-1})$	$v_s(\text{ms}^{-1})$												
6401.0	2505.0	2218.73	829.215	6481.0	2513.0	2201.6	840.14	6561.0	2521.0	2253.47	877.993	6641.0	2529.0	2220.5	860.604
6402.0	2505.1	2218.91	825.636	6482.0	2513.1	2201.77	839.321	6562.0	2521.1	2258.77	879.314	6642.0	2529.1	2220.49	861.864
6403.0	2505.2	2220.77	832.825	6483.0	2513.2	2201.95	838.912	6563.0	2521.2	2264.13	883.334	6643.0	2529.2	2218.77	862.693
6404.0	2505.3	2222.66	846.335	6484.0	2513.3	2200.41	838.912	6564.0	2521.3	2269.53	890.115	6644.0	2529.3	2215.31	844.168
6405.0	2505.4	2222.85	858.056	6485.0	2513.4	2200.59	840.14	6565.0	2521.4	2274.97	896.577	6645.0	2529.4	2210.15	816.219
6406.0	2505.5	2224.78	864.024	6486.0	2513.5	2200.76	841.372	6566.0	2521.5	2275.02	897.511	6646.0	2529.5	2210.13	815.828
6407.0	2505.6	2223.21	861.456	6487.0	2513.6	2199.22	842.607	6567.0	2521.6	2275.08	896.577	6647.0	2529.6	2210.12	860.43
6408.0	2505.7	2223.36	864.024	6488.0	2513.7	2196.02	843.02	6568.0	2521.7	2273.32	893.784	6648.0	2529.7	2210.11	860.826
6409.0	2505.8	2225.3	863.595	6489.0	2513.8	2196.19	842.607	6569.0	2521.8	2269.77	889.205	6649.0	2529.8	2215.28	862.087
6410.0	2505.9	2225.49	865.745	6490.0	2513.9	2196.34	842.195	6570.0	2521.9	2262.64	884.232	6650.0	2529.9	2222.22	862.056
6411.0	2506.0	2234.44	869.206	6491.0	2514.0	2196.52	841.372	6571.0	2520.2	2257.32	880.204	6651.0	2530.0	2230.9	868.983
6412.0	2506.1	2230.99	873.572	6492.0	2514.1	2196.6	840.532	6572.0	2522.1	2248.35	875.772	6652.0	2530.1	2229.16	872.042
6413.0	2506.2	2227.47	872.696	6493.0	2514.2	2198.29	840.907	6573.0	2522.2	2241.13	871.821	6653.0	2530.2	2223.95	875.115
6414.0	2506.3	2225.72	868.772	6494.0	2514.3	2198.29	843.342	6574.0	2522.3	2233.94	866.176	6654.0	2530.3	2220.48	874.201
6415.0	2506.4	2223.97	866.176	6495.0	2514.4	2198.29	845.781	6575.0	2522.4	2233.75	860.178	6655.0	2530.4	2220.48	872.853
6416.0	2506.5	2223.97	864.024	6496.0	2514.5	2199.98	846.575	6576.0	2522.5	2228.37	855.103	6656.0	2530.5	2220.48	872.387
6417.0	2506.6	2223.97	861.883	6497.0	2514.6	2201.67	845.707	6577.0	2522.6	2219.52	849.257	6657.0	2530.6	2220.48	872.362
6418.0	2506.7	2225.72	858.904	6498.0	2514.7	2201.67	844.02	6578.0	2522.7	2215.91	844.26	6658.0	2530.7	2220.48	871.898
6419.0	2506.8	2223.97	855.103	6499.0	2514.8	2208.48	843.167	6579.0	2522.8	2212.29	840.14	6659.0	2530.8	2220.48	871.002
6420.0	2506.9	2223.97	852.157	6500.0	2514.9	2215.33	846.005	6580.0	2522.9	2212.12	836.06	6660.0	2530.9	2220.48	867.932
6421.0	2507.0	2223.97	850.919	6501.0	2515.0	2220.5	850.534	6581.0	2523.0	2211.97	832.825	6661.0	2531.0	2220.48	865.32
6422.0	2507.1	2223.97	850.087	6502.0	2515.1	2225.68	856.013	6582.0	2523.1	2212.0	832.422	6662.0	2531.1	2222.22	863.595
6423.0	2507.2	2223.97	849.672	6503.0	2515.2	2232.64	862.013	6583.0	2523.2	2212.14	833.228	6663.0	2531.2	2223.95	861.456
6424.0	2507.3	2223.97	850.919	6504.0	2515.3	2246.69	866.35	6584.0	2523.3	2212.32	834.844	6664.0	2531.3	2223.95	860.604
6425.0	2507.4	2223.97	854.263	6505.0	2515.4	2253.78	869.852	6585.0	2523.4	2212.49	836.873	6665.0	2531.4	2225.67	860.604
6426.0	2507.5	2223.97	849.257	6506.0	2515.5	2259.12	874.269	6586.0	2523.5	2212.64	838.912	6666.0	2531.5	2225.67	861.456
6427.0	2507.6	2223.97	849.257	6507.0	2515.6	2264.49	878.731	6587.0	2523.6	2214.53	842.607	6667.0	2531.6	2229.12	862.311
6428.0	2507.7	2223.97	847.585	6508.0	2515.7	2266.29	880.979	6588.0	2523.7	2214.68	845.919	6668.0	2531.7	2230.84	861.883
6429.0	2507.8	2225.72	845.088	6509.0	2515.8	2264.49	880.979	6589.0	2523.8	2218.32	848.838	6669.0	2531.8	2234.3	861.03
6430.0	2507.9	2232.75	841.372	6510.0	2515.9	2264.49	879.629	6590.0	2523.9	2220.24	851.752	6670.0	2531.9	2237.75	860.178
6431.0	2508.0	2239.82	837.687	6511.0	2516.0	2266.29	877.387	6591.0	2524.0	2220.4	854.263	6671.0	2532.0	2239.48	860.604
6432.0	2508.1	2247.03	834.426	6512.0	2516.1	2264.49	875.157	6592.0	2524.1	2220.37	857.633	6672.0	2532.1	2239.37	862.336
6433.0	2508.2	2254.34	836.422	6513.0	2516.2	2264.49	872.497	6593.0	2524.2	2220.22	861.03	6673.0	2532.2	2239.21	863.66
6434.0	2508.3	2259.86	840.878	6514.0	2516.3	2269.01	870.732	6594.0	2524.3	2220.03	864.884	6674.0	2532.3	2239.07	863.704
6435.0	2508.4	2265.42	847.856	6515.0	2516.4	2257.34	868.535	6595.0	2524.4	2219.85	868.338	6675.0	2532.4	2238.9	863.75
6436.0	2508.5	2267.37	854.094	6516.0	2516.5	2248.45	866.35	6596.0	2524.5	2221.43	870.076	6676.0	2532.5	2238.74	863.788
6437.0	2508.6	2267.49	873.465	6517.0	2516.6	2237.89	864.61	6597.0	2524.6	2221.25	872.258	6677.0	2532.6	2238.6	863.833
6438.0	2508.7	2269.44	891.015	6518.0	2516.7	2232.64	862.445	6598.0	2524.7	2222.83	875.772	6678.0	2532.7	2238.43	863.878
6439.0	2508.8	2269.58	891.934	6519.0	2516.8	2230.9	860.29	6599.0	2524.8	2234.78	881.096	6679.0	2532.8	2238.27	863.917
6440.0	2508.9	2267.89	892.857	6520.0	2516.9	2232.64	858.146	6600.0	2524.9	2246.89	888.751	6680.0	2532.9	2238.12	863.533
6441.0	2509.0	2262.64	886.425	6521.0	2517.0	2234.39	857.718	6601.0	2525.0	2257.4	898.448	6681.0	2533.0	2237.96	861.866
6442.0	2509.1	2257.36	883.239	6522.0	2517.1	2236.14	859.002	6602.0	2525.1	2273.43	909.832	6682.0	2533.1	2234.28	859.328
6443.0	2509.2	2252.05	880.078	6523.0	2517.2	2236.14	860.72	6603.0	2525.2	2282.39	912.222	6683.0	2533.2	2230.63	857.21
6444.0	2509.3	2244.98	876.94	6524.0	2517.3	2236.14	862.445	6604.0	2525.3	2291.45	913.65	6684.0	2533.3	2225.24	855.103
6445.0	2509.4	2236.19	875.603	6525.0	2517.4	2236.14	862.445	6605.0	2525.4	2296.88	914.595	6685.0	2533.4	2221.59	854.263
6446.0	2509.5	2229.19	873.382	6526.0	2517.5	2236.14	862.445	6606.0	2525.5	2291.22	914.575	6686.0	2533.5	2216.27	855.103
6447.0	2509.6	2229.2	869.852	6527.0	2517.6	2236.14	862.445	6607.0	2525.6	2291.12	914.069	6687.0	2533.6	2216.09	854.683
6448.0	2509.7	2225.71	867.223	6528.0	2517.7	2236.14	862.445	6608.0	2525.7	2287.3	912.122	6688.0	2533.7	2215.93	854.263
6449.0	2509.8	2218.8	861.15	6529.0	2517.8	2232.64	864.61	6609.0	2525.8	2285.34	909.711	6689.0	2533.8	2217.47	855.523
6450.0	2509.9	2215.39	854.314	6530.0	2517.9	2230.9	863.742	6610.0	2525.9	2281.55	906.845	6690.0	2533.9	2229.39	855.103
6451.0	2510.0	2213.69	851.357	6531.0	2518.0	2230.9	860.72	6611.0	2526.0	2275.92	901.189	6691.0	2534.0	2229.24	855.945
6452.0	2510.1	2213.7	849.282	6532.0	2518.1	2230.9	858.14	6612.0	2526.1	2270.35	895.129	6692.0	2534.1	2229.16	857.611
6453.0	2510.2	2213.7	847.666	6533.0	2518.2	2229.16	858.132	6613.0	2526.2	2263.05	890.041	6693.0	2534.2	2222.22	859.278
6454.0	2510.3	2212.0	848.947	6534.0	2518.3	2229.16	860.26	6614.0	2526.3	2257.6	887.276	6694.0	2534.3	2220.5	860.095
6455.0	2510.4	2213.7	851.5	6535.0	2518.4	2229.16	859.394	6615.0	2526.4	2246.85	883.623	6695.0	2534.4	2217.05	859.214
6456.0	2510.5	2218.8	854.908	6536.0	2518.5	2225.68	857.679	6616.0	2526.5	2241.45	880.0	6696.0	2534.5	2215.33	857.053
6457.0	2510.6	2220.51	857.907	6537.0	2518.6	2225.68	855.551	6617.0	2526.6	2229.72	876.407	6697.0	2534.6	2215.33	854.476
6458.0	2510.7	2218.8	860.925	6538.											

No.	$d(\text{m})$	$v_p(\text{ms}^{-1})$	$v_s(\text{ms}^{-1})$												
6721.0	2537.0	2225.65	852.588	6801.0	2545.0	2397.51	896.577	6881.0	2553.0	2278.37	907.924	6961.0	2561.0	2275.31	909.194
6722.0	2537.1	2232.54	855.922	6802.0	2545.1	2401.54	906.49	6882.0	2553.1	2278.37	907.924	6962.0	2561.1	2269.89	904.466
6723.0	2537.2	2237.73	864.41	6803.0	2545.2	2407.61	913.221	6883.0	2553.2	2276.57	906.013	6963.0	2561.2	2268.09	902.12
6724.0	2537.3	2246.44	873.525	6804.0	2545.3	2409.64	924.996	6884.0	2553.3	2271.19	903.161	6964.0	2561.3	2266.29	901.185
6725.0	2537.4	2251.7	881.054	6805.0	2545.4	2409.64	937.078	6885.0	2553.4	2267.62	902.688	6965.0	2561.4	2266.29	900.252
6726.0	2537.5	2256.98	883.742	6806.0	2545.5	2407.61	947.329	6886.0	2553.5	2267.62	904.11	6966.0	2561.5	2266.29	899.786
6727.0	2537.6	2262.29	885.542	6807.0	2545.6	2371.64	960.938	6887.0	2553.6	2281.97	906.013	6967.0	2561.6	2268.09	900.718
6728.0	2537.7	2262.29	885.534	6808.0	2545.7	2275.31	963.6	6888.0	2553.7	2307.52	906.49	6968.0	2561.7	2271.69	902.588
6729.0	2537.8	2260.52	885.982	6809.0	2545.8	2277.13	962.533	6889.0	2553.8	2307.52	906.49	6969.0	2561.8	2273.5	904.936
6730.0	2537.9	2260.52	885.975	6810.0	2545.9	2288.07	960.938	6890.0	2553.9	2300.16	907.445	6970.0	2561.9	2273.5	906.824
6731.0	2538.0	2258.75	884.15	6811.0	2546.0	2299.11	965.74	6891.0	2554.0	2291.03	907.445	6971.0	2562.0	2275.31	910.146
6732.0	2538.1	2255.13	881.43	6812.0	2546.1	2310.27	968.969	6892.0	2554.1	2291.07	906.967	6972.0	2562.1	2277.16	911.099
6733.0	2538.2	2253.24	879.179	6813.0	2546.2	2314.01	960.407	6893.0	2554.2	2292.96	904.11	6973.0	2562.2	2282.68	910.622
6734.0	2538.3	2249.56	877.387	6814.0	2546.3	2314.01	945.269	6894.0	2554.3	2298.53	901.27	6974.0	2562.3	2295.61	903.996
6735.0	2538.4	2245.89	875.603	6815.0	2546.4	2314.01	930.495	6895.0	2554.4	2300.44	897.044	6975.0	2562.4	2306.86	903.057
6736.0	2538.5	2238.75	873.825	6816.0	2546.5	2314.01	918.091	6896.0	2554.5	2300.52	913.706	6976.0	2562.5	2312.56	905.879
6737.0	2538.6	2233.36	872.055	6817.0	2546.6	2310.27	910.805	6897.0	2554.6	2304.3	924.996	6977.0	2562.6	2322.11	912.055
6738.0	2538.7	2229.74	867.223	6818.0	2546.7	2306.54	907.445	6898.0	2554.7	2308.1	925.991	6978.0	2562.7	2329.85	915.898
6739.0	2538.8	2217.47	862.445	6819.0	2546.8	2300.97	906.967	6899.0	2554.8	2306.32	923.012	6979.0	2562.8	2333.78	920.26
6740.0	2538.9	2201.91	856.438	6820.0	2546.9	2297.27	905.06	6900.0	2554.9	2304.56	919.071	6980.0	2562.9	2333.91	924.172
6741.0	2539.0	2198.36	851.357	6821.0	2547.0	2291.74	902.688	6901.0	2555.0	2302.79	918.091	6981.0	2563.0	2335.96	925.647
6742.0	2539.1	2198.29	848.842	6822.0	2547.1	2288.07	902.688	6902.0	2555.1	2300.92	918.091	6982.0	2563.1	2332.16	926.634
6743.0	2539.2	2199.98	849.676	6823.0	2547.2	2288.07	901.27	6903.0	2555.2	2298.99	917.601	6983.0	2563.2	2330.23	927.622
6744.0	2539.3	2205.07	851.778	6824.0	2547.3	2288.07	899.387	6904.0	2555.3	2300.75	910.805	6984.0	2563.3	2326.4	928.613
6745.0	2539.4	2210.19	854.314	6825.0	2547.4	2288.07	899.387	6905.0	2555.4	2308.09	902.688	6985.0	2563.4	2320.68	930.6
6746.0	2539.5	2213.61	856.865	6826.0	2547.5	2288.07	897.98	6906.0	2555.5	2311.71	895.644	6986.0	2563.5	2314.98	932.097
6747.0	2539.6	2217.05	858.574	6827.0	2547.6	2284.41	895.178	6907.0	2555.6	2315.34	919.071	6987.0	2563.6	2311.19	933.598
6748.0	2539.7	2222.22	859.86	6828.0	2547.7	2286.24	893.784	6908.0	2555.7	2315.25	921.037	6988.0	2563.7	2311.19	935.104
6749.0	2539.8	2225.68	860.72	6829.0	2547.8	2288.07	891.484	6909.0	2555.8	2317.01	919.562	6989.0	2563.8	2309.31	936.615
6750.0	2539.9	2229.16	862.013	6830.0	2547.9	2284.41	888.751	6910.0	2555.9	2324.39	916.136	6990.0	2563.9	2305.54	937.625
6751.0	2540.0	2229.16	863.309	6831.0	2548.0	2282.58	886.486	6911.0	2556.0	2333.69	912.737	6991.0	2564.0	2299.92	936.615
6752.0	2540.1	2229.16	864.168	6832.0	2548.1	2280.73	883.777	6912.0	2556.1	2346.93	909.362	6992.0	2564.1	2290.67	931.622
6753.0	2540.2	2229.16	863.287	6833.0	2548.2	2278.85	881.077	6913.0	2556.2	2325.67	906.49	6993.0	2564.2	2283.4	925.703
6754.0	2540.3	2229.16	864.569	6834.0	2548.3	2276.98	879.726	6914.0	2556.3	2335.53	905.536	6994.0	2564.3	2279.86	920.82
6755.0	2540.4	2229.16	864.987	6835.0	2548.4	2275.12	880.159	6915.0	2556.4	2303.83	905.536	6995.0	2564.4	2279.97	912.606
6756.0	2540.5	2229.16	865.403	6836.0	2548.5	2275.07	884.645	6916.0	2556.5	2305.67	922.024	6996.0	2564.5	2281.93	908.794
6757.0	2540.6	2229.16	866.254	6837.0	2548.6	2276.81	888.728	6917.0	2556.6	2311.76	933.016	6997.0	2564.6	2282.06	907.855
6758.0	2540.7	2229.16	867.102	6838.0	2548.7	2274.96	872.124	6918.0	2556.7	2322.37	929.992	6998.0	2564.7	2282.17	907.394
6759.0	2540.8	2229.16	867.516	6839.0	2548.8	2271.31	872.103	6919.0	2556.8	2278.37	924.996	6999.0	2564.8	2282.29	907.409
6760.0	2540.9	2229.16	866.633	6840.0	2548.9	2269.47	877.856	6920.0	2556.9	2279.28	935.551	7000.0	2564.9	2282.42	906.946
6761.0	2541.0	2229.16	866.183	6841.0	2549.0	2269.43	890.549	6921.0	2557.0	2272.98	940.662	7001.0	2565.0	2282.53	906.961
6762.0	2541.1	2227.42	866.607	6842.0	2549.1	2269.41	895.15	6922.0	2557.1	2272.91	947.778	7002.0	2565.1	2280.76	906.967
6763.0	2541.2	2225.68	867.039	6843.0	2549.2	2267.62	898.371	6923.0	2557.2	2263.85	954.474	7003.0	2565.2	2278.94	906.49
6764.0	2541.3	2227.42	868.338	6844.0	2549.3	2267.62	898.329	6924.0	2557.3	2261.94	957.596	7004.0	2565.3	2277.13	905.06
6765.0	2541.4	2237.89	869.641	6845.0	2549.4	2267.62	898.749	6925.0	2557.4	2261.8	958.118	7005.0	2565.4	2277.13	903.635
6766.0	2541.5	2243.16	870.947	6846.0	2549.5	2269.41	899.169	6926.0	2557.5	2261.67	955.512	7006.0	2565.5	2273.5	902.688
6767.0	2541.6	2243.16	870.076	6847.0	2549.6	2271.19	899.597	6927.0	2557.6	2261.52	950.857	7007.0	2565.6	2271.69	901.742
6768.0	2541.7	2241.4	868.338	6848.0	2549.7	2271.19	901.431	6928.0	2557.7	2261.38	946.247	7008.0	2565.7	2269.89	900.327
6769.0	2541.8	2237.89	866.176	6849.0	2549.8	2272.98	902.799	6929.0	2557.8	2261.25	942.186	7009.0	2565.8	2269.89	898.917
6770.0	2541.9	2234.39	865.745	6850.0	2549.9	2276.57	902.757	6930.0	2557.9	2264.68	936.06	7010.0	2565.9	2269.89	896.577
6771.0	2542.0	2234.39	863.595	6851.0	2550.0	2280.17	900.818	6931.0	2558.0	2268.15	930.495	7011.0	2566.0	2269.89	895.178
6772.0	2542.1	2230.9	855.971	6852.0	2550.1	2281.97	898.917	6932.0	2558.1	2269.89	924.499	7012.0	2566.1	2269.89	894.713
6773.0	2542.2	2229.16	847.661	6853.0	2550.2	2285.58	897.044	6933.0	2558.2	2271.69	919.071	7013.0	2566.2	2269.89	894.713
6774.0	2542.3	2229.16	840.718	6854.0	2550.3	2287.4	895.178	6934.0	2558.3	2273.5	913.706	7014.0	2566.3	2269.89	895.178
6775.0	2542.4	2229.16	853.159	6855.0	2550.4	2289.21	897.511	6935.0	2558.4	2273.5	908.882	7015.0	2566.4	2271.69	896.577
6776.0	2542.5	2227.42	856.981	6856.0	2550.5	2291.03	899.857	6936.0	2558.5	2271.69	905.06	7016.0	2566.5	2271.69	897.98
6777.0	2542.6	2227.42	858.295	6857.0	2550.6	2291.03	902.688	6937.0	2558.6	2269.89	902.688	7017.0	2566.6	2273.5	899.857
6778.0	2542.7	2222.22	859.												

No.	$d(\text{m})$	$v_p(\text{ms}^{-1})$	$v_s(\text{ms}^{-1})$												
7041.0	2569.0	2277.13	900.327	7121.0	2577.0	2314.01	939.144	7201.0	2585.0	2304.68	968.686	7281.0	2593.0	2306.54	948.362
7042.0	2569.1	2275.31	898.448	7122.0	2577.1	2313.95	940.637	7202.0	2585.1	2306.54	973.517	7282.0	2593.1	2304.68	944.242
7043.0	2569.2	2271.69	896.577	7123.0	2577.2	2313.87	942.112	7203.0	2585.2	2308.4	975.68	7283.0	2593.2	2300.97	941.176
7044.0	2569.3	2269.89	894.713	7124.0	2577.3	2317.51	941.557	7204.0	2585.3	2308.4	975.139	7284.0	2593.3	2295.42	938.637
7045.0	2569.4	2269.89	890.571	7125.0	2577.4	2321.16	940.483	7205.0	2585.4	2308.4	973.517	7285.0	2593.4	2291.74	937.625
7046.0	2569.5	2268.09	888.297	7126.0	2577.5	2321.07	940.429	7206.0	2585.5	2308.4	969.755	7286.0	2593.5	2288.07	936.615
7047.0	2569.6	2264.49	891.484	7127.0	2577.6	2319.08	939.871	7207.0	2585.6	2308.4	963.901	7287.0	2593.6	2288.07	935.104
7048.0	2569.7	2262.7	893.784	7128.0	2577.7	2320.85	939.305	7208.0	2585.7	2308.4	947.267	7288.0	2593.7	2286.24	934.601
7049.0	2569.8	2262.7	896.11	7129.0	2577.8	2317.02	938.739	7209.0	2585.8	2310.27	930.495	7289.0	2593.8	2286.24	936.11
7050.0	2569.9	2266.29	898.448	7130.0	2577.9	2316.92	937.67	7210.0	2585.9	2310.27	923.507	7290.0	2593.9	2291.74	939.144
7051.0	2570.0	2271.69	901.27	7131.0	2578.0	2316.82	936.594	7211.0	2586.0	2308.4	920.053	7291.0	2594.0	2295.42	939.651
7052.0	2570.1	2278.94	903.635	7132.0	2578.1	2316.78	935.043	7212.0	2586.1	2306.54	920.053	7292.0	2594.1	2297.27	940.19
7053.0	2570.2	2282.58	906.49	7133.0	2578.2	2316.78	934.028	7213.0	2586.2	2304.68	924.003	7293.0	2594.2	2299.11	940.745
7054.0	2570.3	2288.07	908.882	7134.0	2578.3	2314.92	933.016	7214.0	2586.3	2302.82	925.991	7294.0	2594.3	2300.97	940.29
7055.0	2570.4	2291.74	911.77	7135.0	2578.4	2314.92	932.006	7215.0	2586.4	2302.82	915.649	7295.0	2594.4	2300.97	939.316
7056.0	2570.5	2293.58	913.706	7136.0	2578.5	2314.92	931.502	7216.0	2586.5	2302.82	908.403	7296.0	2594.5	2306.54	937.843
7057.0	2570.6	2297.27	915.163	7137.0	2578.6	2314.92	931.502	7217.0	2586.6	2300.97	908.403	7297.0	2594.6	2308.4	936.363
7058.0	2570.7	2299.11	916.624	7138.0	2578.7	2313.07	931.502	7218.0	2586.7	2302.82	911.288	7298.0	2594.7	2308.4	934.387
7059.0	2570.8	2299.11	918.58	7139.0	2578.8	2311.21	931.502	7219.0	2586.8	2304.68	913.221	7299.0	2594.8	2315.89	934.427
7060.0	2570.9	2302.82	920.053	7140.0	2578.9	2309.36	931.502	7220.0	2586.9	2308.4	915.649	7300.0	2594.9	2319.65	934.474
7061.0	2571.0	2306.54	921.037	7141.0	2579.0	2309.36	930.998	7221.0	2587.0	2312.14	919.562	7301.0	2595.0	2321.53	936.038
7062.0	2571.1	2308.46	922.024	7142.0	2579.1	2309.36	930.495	7222.0	2587.1	2312.14	923.507	7302.0	2595.1	2329.1	939.636
7063.0	2571.2	2310.41	923.012	7143.0	2579.2	2311.21	930.495	7223.0	2587.2	2314.01	928.488	7303.0	2595.2	2332.91	941.681
7064.0	2571.3	2312.38	924.003	7144.0	2579.3	2311.21	930.495	7224.0	2587.3	2315.89	932.511	7304.0	2595.3	2334.81	941.681
7065.0	2571.4	2314.36	924.499	7145.0	2579.4	2311.21	930.495	7225.0	2587.4	2315.89	936.569	7305.0	2595.4	2342.47	949.315
7066.0	2571.5	2314.45	925.493	7146.0	2579.5	2311.21	930.998	7226.0	2587.5	2317.77	938.611	7306.0	2595.5	2348.24	953.955
7067.0	2571.6	2318.33	927.987	7147.0	2579.6	2307.52	930.998	7227.0	2587.6	2317.77	940.149	7307.0	2595.6	2352.11	960.213
7068.0	2571.7	2322.21	929.992	7148.0	2579.7	2305.67	930.998	7228.0	2587.7	2317.77	941.681	7308.0	2595.7	2359.88	972.44
7069.0	2571.8	2322.32	929.992	7149.0	2579.8	2305.67	930.998	7229.0	2587.8	2319.65	943.705	7309.0	2595.8	2367.7	981.679
7070.0	2571.9	2322.44	930.495	7150.0	2579.9	2305.67	930.998	7230.0	2587.9	2323.42	945.228	7310.0	2595.9	2373.61	989.42
7071.0	2572.0	2322.53	929.992	7151.0	2580.0	2305.67	929.992	7231.0	2588.0	2323.42	947.778	7311.0	2596.0	2375.58	996.736
7072.0	2572.1	2324.49	929.992	7152.0	2580.1	2305.67	928.989	7232.0	2588.1	2325.31	949.828	7312.0	2596.1	2379.52	1005.96
7073.0	2572.2	2328.32	929.49	7153.0	2580.2	2305.67	927.487	7233.0	2588.2	2325.31	951.887	7313.0	2596.2	2383.47	1011.81
7074.0	2572.3	2330.23	929.49	7154.0	2580.3	2307.52	924.003	7234.0	2588.3	2325.31	952.403	7314.0	2596.3	2391.44	1012.99
7075.0	2572.4	2330.23	930.495	7155.0	2580.4	2309.36	921.037	7235.0	2588.4	2323.42	949.315	7315.0	2596.4	2397.46	1012.4
7076.0	2572.5	2326.4	931.502	7156.0	2580.5	2307.52	927.912	7236.0	2588.5	2325.31	938.611	7316.0	2596.5	2397.45	1010.05
7077.0	2572.6	2322.58	932.006	7157.0	2580.6	2305.67	907.877	7237.0	2588.6	2325.31	930.998	7317.0	2596.6	2389.37	1007.13
7078.0	2572.7	2324.49	932.006	7158.0	2580.7	2307.52	645.838	7238.0	2588.7	2323.42	930.998	7318.0	2596.7	2385.34	1002.48
7079.0	2572.8	2324.49	932.006	7159.0	2580.8	2307.52	645.838	7239.0	2588.8	2323.42	935.043	7319.0	2596.8	2381.31	995.025
7080.0	2572.9	2322.58	932.006	7160.0	2580.9	2307.52	646.318	7240.0	2588.9	2323.42	939.123	7320.0	2596.9	2379.28	990.536
7081.0	2573.0	2322.58	932.006	7161.0	2581.0	2305.67	650.915	7241.0	2589.0	2321.53	941.176	7321.0	2597.0	2375.25	986.087
7082.0	2573.1	2318.83	932.511	7162.0	2581.1	2305.67	656.566	7242.0	2589.1	2319.65	940.662	7322.0	2597.1	2371.26	981.679
7083.0	2573.2	2313.23	933.016	7163.0	2581.2	2307.52	661.813	7243.0	2589.2	2315.89	936.569	7323.0	2597.2	2367.29	978.398
7084.0	2573.3	2313.32	933.522	7164.0	2581.3	2311.21	668.427	7244.0	2589.3	2315.89	933.016	7324.0	2597.3	2363.33	972.978
7085.0	2573.4	2309.66	935.043	7165.0	2581.4	2311.21	671.265	7245.0	2589.4	2317.77	928.989	7325.0	2597.4	2359.39	966.553
7086.0	2573.5	2307.87	936.569	7166.0	2581.5	2311.21	684.888	7246.0	2589.5	2315.89	924.996	7326.0	2597.5	2353.5	959.688
7087.0	2573.6	2307.97	938.1	7167.0	2581.6	2309.36	653.605	7247.0	2589.6	2314.01	921.037	7327.0	2597.6	2347.64	952.403
7088.0	2573.7	2308.06	940.149	7168.0	2581.7	2309.36	669.714	7248.0	2589.7	2310.27	920.053	7328.0	2597.7	2336.01	946.757
7089.0	2573.8	2304.43	941.176	7169.0	2581.8	2309.36	678.599	7249.0	2589.8	2308.4	926.489	7329.0	2597.8	2328.32	937.598
7090.0	2573.9	2304.54	941.176	7170.0	2581.9	2309.36	665.868	7250.0	2589.9	2310.27	923.006	7330.0	2597.9	2324.49	931.515
7091.0	2574.0	2304.63	940.662	7171.0	2582.0	2309.36	651.402	7251.0	2590.0	2312.14	935.043	7331.0	2598.0	2324.49	929.495
7092.0	2574.1	2304.63	939.636	7172.0	2582.1	2309.36	648.729	7252.0	2590.1	2314.13	937.589	7332.0	2598.1	2324.49	927.487
7093.0	2574.2	2304.55	938.611	7173.0	2582.2	2307.52	653.605	7253.0	2590.2	2316.17	939.636	7333.0	2598.2	2322.58	925.991
7094.0	2574.3	2306.31	938.611	7174.0	2582.3	2307.52	657.808	7254.0	2590.3	2318.25	942.186	7334.0	2598.3	2322.58	926.489
7095.0	2574.4	2304.37	939.123	7175.0	2582.4	2303.83	663.075	7255.0	2590.4	2318.43	944.212	7335.0	2598.4	2320.68	926.988
7096.0	2574.5	2304.29	939.636	7176.0	2582.5	2303.83	664.595	7256.0	2590.5	2316.75	947.267	7336.0	2598.5	2318.77	926.988
7097.0	2574.6	2304.2	940.662	7177.0	2582.6	2306.16	665.104	7257.0	2590.6	2316.95	948.29	7337.0	2598.6	2318.77	925.991
7098.0	2574.7	2305.97</													

No.	$d(\text{m})$	$v_p(\text{ms}^{-1})$	$v_s(\text{ms}^{-1})$												
7361.0	2601.0	2324.49	928.613	7441.0	2609.0	2264.97	894.694	7521.0	2617.0	2266.56	872.939	7601.0	2625.0	2303.63	887.795
7362.0	2601.1	2322.52	926.14	7442.0	2609.1	2264.77	894.694	7522.0	2617.1	2266.85	873.825	7602.0	2625.1	2301.79	873.382
7363.0	2601.2	2320.5	923.191	7443.0	2609.2	2266.3	894.234	7523.0	2617.2	2267.04	874.269	7603.0	2625.2	2301.79	873.382
7364.0	2601.3	2318.52	921.234	7444.0	2609.3	2262.41	893.775	7524.0	2617.3	2267.2	874.713	7604.0	2625.3	2299.92	875.157
7365.0	2601.4	2314.63	918.316	7445.0	2609.4	2262.12	891.932	7525.0	2617.4	2265.58	874.713	7605.0	2625.4	2301.79	876.048
7366.0	2601.5	2310.76	915.898	7446.0	2609.5	2260.0	890.548	7526.0	2617.5	2265.75	874.713	7606.0	2625.5	2301.79	876.048
7367.0	2601.6	2308.81	913.972	7447.0	2609.6	2256.1	889.168	7527.0	2617.6	2265.94	874.713	7607.0	2625.6	2299.92	874.269
7368.0	2601.7	2306.84	911.099	7448.0	2609.7	2255.79	887.793	7528.0	2617.7	2266.13	874.269	7608.0	2625.7	2299.92	871.613
7369.0	2601.8	2303.02	909.194	7449.0	2609.8	2255.48	886.422	7529.0	2617.8	2266.3	874.269	7609.0	2625.8	2303.66	870.732
7370.0	2601.9	2302.95	909.194	7450.0	2609.9	2255.21	884.6	7530.0	2617.9	2266.49	874.713	7610.0	2625.9	2307.42	874.713
7371.0	2602.0	2304.72	910.146	7451.0	2610.0	2254.9	882.786	7531.0	2618.0	2268.47	874.713	7611.0	2626.0	2309.31	880.078
7372.0	2602.1	2304.68	911.111	7452.0	2610.1	2254.96	880.528	7532.0	2618.1	2272.21	876.048	7612.0	2626.1	2309.31	886.422
7373.0	2602.2	2304.68	911.608	7453.0	2610.2	2253.48	878.282	7533.0	2618.2	2274.03	877.835	7613.0	2626.2	2311.19	891.932
7374.0	2602.3	2304.68	912.105	7454.0	2610.3	2253.78	876.94	7534.0	2618.3	2277.69	879.179	7614.0	2626.3	2314.98	896.539
7375.0	2602.4	2308.4	912.606	7455.0	2610.4	2254.13	877.387	7535.0	2618.4	2279.53	881.881	7615.0	2626.4	2314.98	898.856
7376.0	2602.5	2308.4	913.59	7456.0	2610.5	2250.83	878.282	7536.0	2618.5	2281.37	883.239	7616.0	2626.5	2314.98	899.786
7377.0	2602.6	2308.4	915.06	7457.0	2610.6	2252.95	877.835	7537.0	2618.6	2281.37	884.6	7617.0	2626.6	2314.98	900.718
7378.0	2602.7	2312.14	916.54	7458.0	2610.7	2255.11	877.387	7538.0	2618.7	2285.05	885.055	7618.0	2626.7	2314.98	901.652
7379.0	2602.8	2312.14	916.566	7459.0	2610.8	2253.64	877.835	7539.0	2618.8	2286.9	885.51	7619.0	2626.8	2314.98	901.652
7380.0	2602.9	2310.27	917.563	7460.0	2610.9	2255.75	879.179	7540.0	2618.9	2283.21	884.6	7620.0	2626.9	2314.98	902.12
7381.0	2603.0	2312.14	919.549	7461.0	2611.0	2257.92	880.078	7541.0	2619.0	2281.37	883.692	7621.0	2627.0	2314.98	902.588
7382.0	2603.1	2311.8	921.571	7462.0	2611.1	2258.17	880.528	7542.0	2619.1	2281.44	882.786	7622.0	2627.1	2314.98	903.526
7383.0	2603.2	2311.11	923.617	7463.0	2611.2	2258.36	880.979	7543.0	2619.2	2281.57	881.881	7623.0	2627.2	2314.98	903.996
7384.0	2603.3	2310.43	925.162	7464.0	2611.3	2258.53	881.143	7544.0	2619.3	2281.68	880.979	7624.0	2627.3	2314.98	903.057
7385.0	2603.4	2309.84	926.223	7465.0	2611.4	2258.72	880.979	7545.0	2619.4	2281.81	880.078	7625.0	2627.4	2314.98	903.526
7386.0	2603.5	2309.15	927.78	7466.0	2611.5	2260.73	880.979	7546.0	2619.5	2281.92	879.179	7626.0	2627.5	2314.98	903.996
7387.0	2603.6	2306.59	927.837	7467.0	2611.6	2260.89	880.078	7547.0	2619.6	2282.05	879.179	7627.0	2627.6	2314.98	903.057
7388.0	2603.7	2305.9	924.931	7468.0	2611.7	2257.44	879.629	7548.0	2619.7	2278.53	877.387	7628.0	2627.7	2314.98	903.526
7389.0	2603.8	2305.3	921.56	7469.0	2611.8	2257.63	878.731	7549.0	2619.8	2271.38	874.713	7629.0	2627.8	2316.87	904.466
7390.0	2603.9	2306.49	919.669	7470.0	2611.9	2259.61	878.282	7550.0	2619.9	2276.91	875.157	7630.0	2627.9	2320.68	905.408
7391.0	2604.0	2305.79	918.769	7471.0	2612.0	2259.81	877.387	7551.0	2620.0	2266.23	876.048	7631.0	2628.0	2322.58	906.351
7392.0	2604.1	2305.49	917.831	7472.0	2612.1	2260.08	876.494	7552.0	2620.1	2266.32	877.387	7632.0	2628.1	2324.53	907.297
7393.0	2604.2	2305.39	916.863	7473.0	2612.2	2260.42	874.713	7553.0	2620.2	2267.77	878.731	7633.0	2628.2	2326.53	908.245
7394.0	2604.3	2305.28	916.38	7474.0	2612.3	2258.89	872.939	7554.0	2620.3	2261.01	878.731	7634.0	2628.3	2328.52	910.146
7395.0	2604.4	2303.31	916.38	7475.0	2612.4	2257.42	871.613	7555.0	2620.4	2261.05	877.387	7635.0	2628.4	2330.52	912.534
7396.0	2604.5	2303.2	917.347	7476.0	2612.5	2255.95	870.732	7556.0	2620.5	2262.89	875.603	7636.0	2628.5	2330.58	914.453
7397.0	2604.6	2303.09	916.863	7477.0	2612.6	2254.43	870.291	7557.0	2620.6	2264.73	875.157	7637.0	2628.6	2330.66	915.416
7398.0	2604.7	2304.87	916.38	7478.0	2612.7	2254.78	870.291	7558.0	2620.7	2262.97	875.603	7638.0	2628.7	2332.65	915.416
7399.0	2604.8	2302.89	915.988	7479.0	2612.8	2255.12	869.852	7559.0	2620.8	2261.21	875.603	7639.0	2628.8	2332.72	914.453
7400.0	2604.9	2302.78	915.416	7480.0	2612.9	2257.21	869.413	7560.0	2620.9	2263.05	875.603	7640.0	2628.9	2330.89	914.934
7401.0	2605.0	2302.67	914.934	7481.0	2613.0	2257.55	870.291	7561.0	2621.0	2264.91	875.603	7641.0	2629.0	2330.97	915.898
7402.0	2605.1	2300.77	914.934	7482.0	2613.1	2257.83	871.172	7562.0	2621.1	2266.74	875.613	7642.0	2629.1	2331.0	917.347
7403.0	2605.2	2298.72	914.934	7483.0	2613.2	2258.05	872.055	7563.0	2621.2	2268.56	875.628	7643.0	2629.2	2331.0	919.287
7404.0	2605.3	2296.76	914.453	7484.0	2613.4	2258.25	872.497	7564.0	2621.3	2268.56	875.202	7644.0	2629.3	2331.0	920.26
7405.0	2605.4	2294.81	913.013	7485.0	2613.4	2258.48	873.825	7565.0	2621.4	2270.38	875.221	7645.0	2629.4	2331.0	921.723
7406.0	2605.5	2292.86	910.146	7486.0	2613.5	2260.52	875.157	7566.0	2621.5	2268.56	875.679	7646.0	2629.5	2331.0	921.234
7407.0	2605.6	2290.92	908.719	7487.0	2613.6	2260.72	876.048	7567.0	2621.6	2270.38	876.584	7647.0	2629.6	2332.91	920.747
7408.0	2605.7	2292.72	907.771	7488.0	2613.7	2262.77	876.94	7568.0	2621.7	2274.03	876.601	7648.0	2629.7	2331.0	920.747
7409.0	2605.8	2292.64	907.297	7489.0	2613.8	2264.83	877.835	7569.0	2621.8	2275.86	875.73	7649.0	2629.8	2331.0	920.747
7410.0	2605.9	2292.56	906.351	7490.0	2613.9	2265.03	879.179	7570.0	2621.9	2277.69	874.425	7650.0	2629.9	2332.91	921.234
7411.0	2606.0	2290.64	905.408	7491.0	2614.0	2265.27	880.078	7571.0	2622.0	2279.53	875.766	7651.0	2630.0	2334.81	921.723
7412.0	2606.1	2286.83	904.466	7492.0	2614.1	2267.4	881.436	7572.0	2622.1	2279.53	878.426	7652.0	2630.1	2336.72	921.723
7413.0	2606.2	2283.03	903.996	7493.0	2614.2	2269.57	882.802	7573.0	2622.2	2279.53	881.096	7653.0	2630.2	2338.63	923.191
7414.0	2606.3	2277.37	903.057	7494.0	2614.3	2271.69	883.263	7574.0	2622.3	2281.37	883.334	7654.0	2630.3	2338.63	925.647
7415.0	2606.4	2275.4	901.652	7495.0	2614.4	2272.02	883.273	7575.0	2622.4	2281.37	886.034	7655.0	2630.4	2338.63	927.128
7416.0	2606.5	2275.28	899.786	7496.0	2614.5	2272.35	883.283	7576.0	2622.5	2279.53	877.539	7656.0	2630.5	2340.55	928.117
7417.0	2606.6	2278.83	898.856	7497.0	2614.6	2270.8	883.292	7577.0	2622.6	2286.9	740.111	7657.0	2630.6	2338.63	929.606
7418.0	2606.7	2278.7	898.392</												

No.	$d(\text{m})$	$v_p(\text{ms}^{-1})$	$v_s(\text{ms}^{-1})$	No.	$d(\text{m})$	$v_p(\text{ms}^{-1})$	$v_s(\text{ms}^{-1})$
7681.0	2633.0	2334.81	904.466	7761.0	2641.0	2329.1	902.588
7682.0	2633.1	2334.81	902.588	7762.0	2641.1	2321.53	900.718
7683.0	2633.2	2334.81	899.786	7763.0	2641.2	2314.01	897.928
7684.0	2633.3	2338.63	897.002	7764.0	2641.3	2310.27	895.155
7685.0	2633.4	2344.39	898.856	7765.0	2641.4	2310.27	892.394
7686.0	2633.5	2348.24	902.588	7766.0	2641.5	2310.27	891.009
7687.0	2633.6	2350.18	905.408	7767.0	2641.6	2310.27	890.548
7688.0	2633.7	2350.18	906.824	7768.0	2641.7	2308.4	891.009
7689.0	2633.8	2346.32	909.194	7769.0	2641.8	2308.4	890.548
7690.0	2633.9	2346.32	912.055	7770.0	2641.9	2308.4	888.709
7691.0	2634.0	2346.32	914.934	7771.0	2642.0	2310.27	883.239
7692.0	2634.1	2346.32	917.347	7772.0	2642.1	2306.6	738.853
7693.0	2634.2	2346.32	919.773	7773.0	2642.2	2304.84	726.203
7694.0	2634.3	2346.32	921.723	7774.0	2642.3	2303.08	679.362
7695.0	2634.4	2346.32	923.681	7775.0	2642.4	2303.19	664.418
7696.0	2634.5	2342.47	926.14	7776.0	2642.5	2303.29	668.027
7697.0	2634.6	2338.63	926.634	7777.0	2642.6	2301.54	703.581
7698.0	2634.7	2334.81	926.14	7778.0	2642.7	2301.64	741.688
7699.0	2634.8	2332.91	926.14	7779.0	2642.8	2307.28	856.865
7700.0	2634.9	2331.0	925.647	7780.0	2642.9	2311.07	858.146
7701.0	2635.0	2327.21	923.681	7781.0	2643.0	2314.88	864.61
7702.0	2635.1	2321.53	919.76	7782.0	2643.1	2316.73	873.825
7703.0	2635.2	2317.77	914.896	7783.0	2643.2	2329.75	884.6
7704.0	2635.3	2315.89	909.115	7784.0	2643.3	2348.69	897.002
7705.0	2635.4	2315.89	904.339	7785.0	2643.4	2375.79	915.416
7706.0	2635.5	2317.77	902.416	7786.0	2643.5	2419.84	936.11
7707.0	2635.6	2315.89	901.912	7787.0	2643.6	2480.77	958.118
7708.0	2635.7	2315.89	901.872	7788.0	2643.7	2495.94	975.68
7709.0	2635.8	2317.77	902.776	7789.0	2643.8	2495.94	991.654
7710.0	2635.9	2321.53	903.688	7790.0	2643.9	2487.25	1005.38
7711.0	2636.0	2321.53	903.176	7791.0	2644.0	2478.62	1008.29
7712.0	2636.1	2319.65	902.688	7792.0	2644.1	2470.05	1008.29
7713.0	2636.2	2315.89	902.215	7793.0	2644.2	2459.42	999.6
7714.0	2636.3	2315.89	901.742	7794.0	2644.3	2440.51	997.307
7715.0	2636.4	2315.89	901.27	7795.0	2644.4	2417.79	986.055
7716.0	2636.5	2315.89	901.742	7796.0	2644.5	2397.51	977.776
7717.0	2636.6	2315.89	901.27	7797.0	2644.6	2375.58	971.234
7718.0	2636.7	2317.77	902.215	7798.0	2644.7	2352.11	958.939
7719.0	2636.8	2323.42	903.635	7799.0	2644.8	2334.81	941.806
7720.0	2636.9	2323.42	903.635	7800.0	2644.9	2327.21	921.789
7721.0	2637.0	2321.53	903.635	7801.0	2645.0	2325.31	914.475
7722.0	2637.1	2321.53	903.635	7802.0	2645.1	2327.21	907.297
7723.0	2637.2	2321.53	903.635	7803.0	2645.2	2331.0	902.12
7724.0	2637.3	2319.65	903.635	7804.0	2645.3	2332.91	900.252
7725.0	2637.4	2321.53	904.11	7805.0	2645.4	2332.91	900.718
7726.0	2637.5	2325.31	906.49	7806.0	2645.5	2332.91	901.652
7727.0	2637.6	2329.1	908.403	7807.0	2645.6	2332.91	903.526
7728.0	2637.7	2329.1	909.362	7808.0	2645.7	2331.0	905.879
7729.0	2637.8	2332.91	910.805	7809.0	2645.8	2331.0	910.146
7730.0	2637.9	2334.81	911.77	7810.0	2645.9	2331.0	913.972
7731.0	2638.0	2334.81	912.253	7811.0	2646.0	2332.91	918.316
7732.0	2638.1	2336.72	913.221	7812.0	2646.1	2332.91	922.211
7733.0	2638.2	2338.63	914.191	7813.0	2646.2	2336.72	927.622
7734.0	2638.3	2338.63	914.676	7814.0	2646.3	2344.39	931.597
7735.0	2638.4	2340.55	913.706	7815.0	2646.4	2346.32	933.598
7736.0	2638.5	2338.63	913.221	7816.0	2646.5	2346.32	935.104
7737.0	2638.6	2338.63	913.221	7817.0	2646.6	2346.32	937.119
7738.0	2638.7	2340.55	911.77	7818.0	2646.7	2346.32	937.625
7739.0	2638.8	2338.63	911.77	7819.0	2646.8	2348.24	940.159
7740.0	2638.9	2338.63	913.221	7820.0	2646.9	2354.05	943.218
7741.0	2639.0	2338.63	912.737	7821.0	2647.0	2354.05	943.218
7742.0	2639.1	2338.63	912.243	7822.0	2647.1	2355.99	942.707
7743.0	2639.2	2338.63	911.739	7823.0	2647.2	2357.93	942.196
7744.0	2639.3	2338.63	912.683	7824.0	2647.3	2357.93	940.159
7745.0	2639.4	2338.63	913.147	7825.0	2647.4	2354.05	939.651
7746.0	2639.5	2338.63	913.607	7826.0	2647.5	2357.93	940.159
7747.0	2639.6	2338.63	914.07	7827.0	2647.6	2359.88	941.176
7748.0	2639.7	2338.63	914.046	7828.0	2647.7	2361.83	943.218
7749.0	2639.8	2338.63	912.102	7829.0	2647.8	2361.83	947.329
7750.0	2639.9	2338.63	910.649	7830.0	2647.9	2361.83	949.397
7751.0	2640.0	2336.72	911.585	7831.0	2648.0	2359.88	949.916
7752.0	2640.1	2334.81	914.934	7832.0	2648.1	2359.88	948.879
7753.0	2640.2	2331.0	919.287	7833.0	2648.2	2361.83	946.298
7754.0	2640.3	2325.31	921.234	7834.0	2648.3	2361.83	942.707
7755.0	2640.4	2325.31	921.234	7835.0	2648.4	2361.83	939.651
7756.0	2640.5	2323.42	916.38	7836.0	2648.5	2361.83	938.13
7757.0	2640.6	2321.53	911.577	7837.0	2648.6	2361.83	936.11
7758.0	2640.7	2323.42	907.771	7838.0	2648.7	2357.93	934.099
7759.0	2640.8	2327.21	905.879	7839.0	2648.8	2354.05	932.097
7760.0	2640.9	2331.0	904.466	7840.0	2648.9	2352.11	932.097